

An innovative probabilistic approach to enhance confidence levels in energy performance projections of heterogeneous building stocks

Damien Gatt

Supervised by Prof. Ing. Charles Yousif

Co-supervised by Prof. Ing. Maurizio Cellura

Institute for Sustainable Energy

University of Malta

October, 2022

A Thesis submitted in fulfilment of the requirements for the degree of Doctor of Philosophy.



L-Università
ta' Malta

University of Malta Library – Electronic Thesis & Dissertations (ETD) Repository

The copyright of this thesis/dissertation belongs to the author. The author's rights in respect of this work are as defined by the Copyright Act (Chapter 415) of the Laws of Malta or as modified by any successive legislation.

Users may access this full-text thesis/dissertation and can make use of the information contained in accordance with the Copyright Act provided that the author must be properly acknowledged. Further distribution or reproduction in any format is prohibited without the prior permission of the copyright holder.

*To all my family especially my father Frank, my mom Mary, my twin Donovan, my
sister Donna, my Fiancée Naomi and close friends*

Thanks for your endless support

Acknowledgements

Words cannot express my gratitude to my supervisor Prof. Ing. Charles Yousif and co-supervisor Prof. Ing. Maurizio Cellura from the University of Palermo for their invaluable guidance, feedback, patience, support, and motivation to enable me to complete this research successfully.

Furthermore, this research would not have been possible without the invaluable contribution of Prof. Ing. Francesco Guarino for building energy modelling, and Prof. Liberato Camilleri and Prof. Ing. Ilenia Tinnirello for their guidance in the mathematical theory required for this research.

This endeavour would also not have been successful without the detailed and technical data kindly provided by the management of the 5-star hotels in Malta. These data were fundamental in conducting the case studies that apply the methods and concepts developed in this research. Special mention goes to Ing. Joseph Restall, Ing. James Bartolo, Ing. Anton Borg, Ing. Anthony Saliba, Ing. Adrian Busuttil and Ing. Raymond Sant.

I am also grateful to the Institute for Sustainable Energy of the University of Malta, especially to the Director, Prof. Luciano Mulé Stagno, who has encouraged me to carry out this research work.

I would also like to acknowledge the contribution of the Doctoral School at the University of Malta. The continuous professional development programme enabled me to acquire the necessary research skills and made me aware of all the state-of-the-art research tools to undertake this research work successfully.

Last but not least, I would also like to thank all my family and close friends to whom I dedicate this research, especially my parents, Frank and Mary, my twin brother Donovan, my sister Donna, and my fiancée Naomi. Their continuous motivation, support and belief in me were crucial to complete this research work.

Abstract

The EU Green deal stipulates that effective policy measures are required to significantly increase building renovation, which is one key area for achieving Europe's decarbonisation target for 2050. The established cost-optimal method of the 2010 Energy Performance of Buildings Directive (EPBD) provides a harmonised framework for EU Member States (MS) to define Energy Performance (EP) benchmarks and energy efficiency measures that will best drive buildings to Nearly Zero Energy Building (NZEB) status. However, despite the positive push, literature has identified large EP gaps in the EPBD software and benchmark divergences between MS that highlight the limitations of this tool in devising successful policy measures. These shortcomings potentially stem from '*non-calibrated and deterministic*' Reference Buildings (RBs) characterised using only single and non-calibrated parameter values and which do not take into consideration the building parameters' uncertainties and building stock diversities. This could result in a significant divergence between the cost optimal calculations and the real financially feasible determinants, especially for heterogeneous building stocks. This would ultimately lead to ineffective energy efficiency policy measures and a gradual loss of confidence in the methodology's outcomes among prospective investors and energy consumers.

This thesis has focused on proposing solutions to these limitations, through an innovative EPBD cost-optimal approach that integrates '*probabilistic Bayesian calibrated RBs*' into the current EPBD methodology. RB uncertain parameters are defined as prior distributions, and metered consumption data is utilised to calibrate the RBs model and reduce the uncertainties to narrower posterior distributions. The resulting calibrated RBs and the cost-optimal plots are then employed in an objective approach to define NZEB EP benchmarks according to four distinct levels of EP ambition. Ultimately, a probabilistic risk analysis that is propagated from the posterior parameter distributions is used to quantify the robust financial risk to reach each ambition level. The approach was optimised for heterogeneous building stocks via an innovative methodology to define RBs and by developing the '*reference zone*' concept. This concept replaces full-space models with reduced space energy models to improve the computational efficiency of calibration. The RB definition methodology was applied to a 5-star hotel building stock, followed by the validation of the proposed EPBD cost-optimal method using a derived hotel RB. For this RB, the '*reference zone*' approach successfully calibrated the model in compliance with ASHRAE [1, 2] Coefficient of the Variation of the Root Mean Square Error (CVRMSE) and Normalised Mean Bias Error (NMBE) metrics for monthly data and replicated the monthly electricity energy end-uses of the full model with a 4000 % improvement in simulation run time.

A comparison of the current EPBD cost-optimal approach with the innovative approach for the hotel RB demonstrated that non-calibrated RBs can provide a large

EP gap exceeding 30 %, which have resulted in a highly unrealistic financial feasibility and misleading EP improvement projections. Furthermore, a probabilistic risk analysis considering parameter uncertainty and diversity successfully uncovered the full associated financial risk associated with each EP ambition level and the required financial support to establish realistic benchmarks to trigger renovation. Therefore, this research provides tangible findings and insight for the eventual upgrading of the current EPBD cost-optimal approach to the proposed one to increase the chances for devising robust policy measures to meet the 2050 carbon-neutrality goals.

Keywords: EPBD cost-optimal method, reference buildings, heterogeneous buildings, uncertainty analysis, Bayesian calibration, energy renovation.

Contents

1	Introduction	1
1.1	Background to the research work	1
1.2	The aim and objectives of this research work	4
1.3	Research questions	5
1.4	Significance of the study	5
1.5	Organisation of the dissertation	6
1.6	Important notes	8
2	Literature review	9
2.1	Introduction	10
2.2	EPBD and UBEM relation	11
2.2.1	The EPBD cost-optimal method	11
2.2.2	Building stock and Urban Building Energy Modelling (UBEM)	13
2.2.3	A methodological comparison between the EPBD cost-optimal method and UBEM	15
2.3	EPBD and UBEM uncertainties	22
2.3.1	Policy uncertainties in the EPBD cost-optimal method	22
2.3.2	Factors leading to policy uncertainties in the EPBD	24
2.4	Handling EPBD-cost-optimal method uncertainties	25
2.5	Proposed EPBD cost-optimal method	29
2.5.1	Step 1: Assignment of probabilistic RB models	29
2.5.2	Step 2: Sensitivity analysis (SA) for the identification of the most significant parameters of the RB models	31
2.5.3	Step 3: Probabilistic calibration of the significant uncertainty parameters of the RB models	32

2.5.4	Step 4: Bayesian model diagnostics, posterior analysis and calibration validation	33
2.5.5	Step 5: Derivation of EP benchmarks via a global LCC cost-optimal analysis	36
2.5.6	Step 6: Risk analysis for derived EP benchmarks	37
2.6	Bayesian Calibration positive attributes and limitations	38
2.6.1	Bayesian calibration versus ' <i>frequentist</i> ' calibration approaches . . .	38
2.6.2	Meeting the main objectives of the 2018 EPBD and the Green Deal	39
2.6.3	Limitations of Bayesian calibration in UBEM	42
2.7	Conclusion	47
3	Defining reference buildings for small multi-functional building stocks - a machine learning approach	49
3.1	Introduction	50
3.1.1	Chapter Objective	50
3.1.2	Background on studying the EP of multi-functional building stocks	50
3.1.3	Tackling the challenges in studying ' <i>small</i> ' multi-functional building stocks	54
3.2	Method	54
3.2.1	Data Collection and Classification phase	56
3.2.2	Data processing phase	57
3.2.3	Data post-processing phase	60
3.3	Hotel building stock case study	61
3.4	Application of approach to the case study to define RBs	63
3.4.1	Data collection and preparation	65
3.4.2	Data Processing	69
3.4.3	Data post-processing stage	82
3.4.4	Discussion on the final RB clustering solution	84
3.5	Conclusion	87
4	Bayesian calibration of a multi-functional Reference Building - a computationally efficient approach	89
4.1	Introduction	90
4.1.1	Chapter objective	90
4.2	Bayesian calibration	91
4.3	RB building physics model simplification	94
4.4	Hotel RB case study	98

4.4.1	Hotel 3 description	98
4.4.2	Hotel 3 case study EnergyPlus (building physics) models	99
4.4.3	Sensitivity Analysis (SA)	119
4.4.4	Bayesian Calibration	123
4.5	Conclusion	148
5	Developing a probabilistic approach to establish NZEB benchmarks under uncertainty	151
5.1	Introduction and chapter objectives	152
5.2	NZEB Benchmarking and risk analysis framework	153
5.2.1	Step 5: NZEB EP benchmarking approach to different ambition levels	153
5.2.2	Step 6 : Probabilistic Risk analysis for each defined NZEB benchmark	159
5.3	Hotel RB case study	163
5.3.1	Evaluating computationally efficient RB building physics models for application to the framework	163
5.3.2	Step 5 : NZEB EP Benchmarking applied to the RB case study . . .	167
5.3.3	Step 6 : Risk analysis for each defined NZEB benchmark applied to the RB case study	178
5.3.4	A critical comparison between outcome of the deterministic and robust financial risk results	183
5.4	Comparison with asset rating NCM methodology	187
5.5	Conclusion	194
6	Conclusions	195
6.1	Achieved Aim, Objectives and Key Research Findings	195
6.2	Research value and contribution	200
6.2.1	EU energy policy	200
6.2.2	Building stock energy modelling	202
6.3	Research Limitations	203
6.4	Recommendations for Future Research	204
6.5	Final Remark	206
	Appendix A Publications by the author	209
	Appendix B GitHub Repository Folders and Files	211

Appendix C 2017 DHW Schedule A	221
References	231
Index	263

List of Figures

2.1	EPBD cost-optimal plot	13
2.2	Building stock energy modelling methods	14
2.3	Comparison between the EPBD cost-optimal method and conventional UBEM	16
2.4	Approach to define RBs in UBEM and the EPBD	17
2.5	Energy estimating and modelling methods	20
2.6	Proposed EPBD cost-optimal method update flow-chart	27
2.7	Meeting EPBD objectives process mind map	40
3.1	Flow chart depicting the method to define RBs for ' <i>small</i> ' multi-functional heterogeneous building stocks	55
3.2	Flow chart showing method used to define RBs for the hotel building stock case study	64
3.3	Visual depiction of the individual hotel building models making up the building stock under study	67
3.4	Functionality feature variables for the hotel building stock case study	68
3.5	Benchmarking EP feature variables (2017 data) Pearson correlation heat map	70
3.6	Malta 5 star hotel final RB clustering solution	83
4.1	Flow chart depicting the ' <i>reference zone</i> ' bottom-up approach concept to BEM	96
4.2	Rendered view of Hotel 3 under study	104
4.3	Hotel 3 Model D geometry plan view snapshot from DesignBuilder software	110
4.4	' <i>Reference Zones</i> ' geometry for the en-suite guest rooms	113
4.5	Results from the Morris method for the LFO annual energy end-uses output from the DHW EnergyPlus model	120
4.6	Results from the Morris method for annual electricity energy end uses output from Model D	122

4.7	The prior and resulting posterior distributions of the DHW energy model calibration parameters	126
4.8	Monthly LFO energy end-use Prior & resulting Posterior distributions box-plot	127
4.9	Annual LFO energy end-use Prior & resulting Posterior distributions	128
4.10	DHW model meta-model parameters trace plots to monitor convergence	130
4.11	DHW model meta-model parameters divergence parallel plot	130
4.12	Monthly LFO energy end-use predictive distribution box plot for the training data-set	132
4.13	Monthly LFO energy end-use predictive distribution box plot for the test data-set	134
4.14	Box plot comparing the monthly electricity energy end-use of Model A with Model D for 100 LHS sample runs from the priors	136
4.15	The prior and resulting posterior distributions of the electricity end uses energy model calibration parameters	139
4.16	Monthly electrical energy end-use consumption Prior & Posterior distributions	140
4.17	Annual electrical energy end-use consumption Prior & resulting Posterior distributions	141
4.18	Electricity energy end-uses meta-model parameters Divergence parallel plot .	143
4.19	Monthly electricity energy end-use predictive distribution for the training data-set	145
4.20	Monthly electricity energy end-use predictive distribution for the test data-set	147
5.1	Flow chart detailing the approach used to execute steps 5 and 6 of the proposed EPBD cost-optimal approach	154
5.2	Visual depiction of the multiple NZEB EP benchmarks defined in this research according to the different levels of EP ambition	158
5.3	Joint plots to analyse operational EP and financial global LCC uncertainty . .	161
5.4	Robust global LCC financial risk calculation for a defined NZEB ambition level	162
5.5	EU ETS monthly carbon PD trend	171
5.6	Regression analysis using the Degree Days modelling approach	174
5.7	The NZEB primary EP benchmark results	176
5.8	Visual depiction of the NZEB EP benchmarks derived for the hotel case study	177
5.9	Uncertainty analysis joint plots for the low ambition NZEB EP benchmark level	179
5.10	Uncertainty analysis joint plots for the medium ambition NZEB EP benchmark level	180

5.11	Uncertainty analysis joint plots for the high ambition NZEB EP benchmark level	181
5.12	Uncertainty analysis joint plots for the highest ambition NZEB EP benchmark level	182
5.13	Deterministic versus robust global LCC financial risk comparison for each NZEB EP ambition level	184
5.14	'Reference scenario' annual site energy end-use consumption breakdown comparison between the RB energy models under study	190
5.15	Comparison of NZEB EP benchmarks obtained for the different RB energy models under study	191
5.16	Financial risk comparison between the calibrated RB EnergyPlus versus the Asset SBEM-MT models	193

List of Tables

3.1	The main HVAC and DHW systems for each hotel observation	71
3.2	The functional data set classified according to the six categories for each observation	75
3.3	The clustering results obtained for the sixteen clustering approaches	78
3.4	The results from the multiple categorical data clustering algorithms applied to compare the 16 hotel clustering solutions to identify the most recurrent groups	78
3.5	The data set for regression composed of the regressor matrix X and the dependent vector, y	80
3.6	The data set for regression composed of the regressor matrix X and the dependent vector, y	81
3.7	The data set to derive the final clustering solutions showing the four and six cluster options for XC_{134}	83
3.8	Data set to facilitate the RB buildings stock clustering solution validation . . .	85
4.1	2017 monthly occupancy pattern for hotel 3	101
4.2	Definition of schedules derived from the monthly occupancy patterns in Table 4.1 for the year 2017	101
4.3	DHW uncertain parameters and corresponding prior distributions	102
4.4	Guest room occupancy pattern schedules for Hotel 3	105
4.5	Main parameter values to characterise the EnergyPlus model for electricity end-use	107
4.6	Definition of Hotel RB activities and related sub-activities for the 'reference zone' approach to modelling	111

4.7	Accuracy and computational efficiency performance of various reduced space EnergyPlus models	117
4.8	Annual energy savings comparison for space heating and cooling for different 'Reference Zone' model variants and the detailed model when considering different passive ECMs	118
4.9	Electricity end uses model parameters ranked according to the modified mean μ^* for both Model A and Model D	121
4.10	Statistical summary of the DHW model posterior distributions	125
4.11	DHW Bayesian model parameters diagnostic statistical checks	129
4.12	Calibration validation statistical indicator results for the training and testing data-set for the DHW model	133
4.13	A statistical summary of the electricity energy end-uses model posterior distributions	139
4.14	Electricity energy end uses Bayesian model parameters diagnostic statistical checks	142
4.15	Calibration validation statistical indicator results for the training and testing data-sets for the electrical energy end-uses model	144
5.1	Passive measures considered for the hotel case study	164
5.2	Comparison of the improvements between Model A and Model D for all cases of combination of passive measures	165
5.3	Building energy systems (active) measures considered for the hotel case study	168
5.4	Financial global LCC parameters for the passive ECMs considered for the hotel case study	169
5.5	Financial global LCC parameters for the building energy systems (active) ECMs considered for the hotel case study	169
5.6	Derived NZEB EP benchmarks are corresponding ECMs for the hotel case study	175
5.7	Deterministic versus robust global LCC financial risk calculation for each NZEB EP ambition level	183
5.8	EP gap comparison for the RB energy models under study	189
5.9	Comparison of the resulting NZEB EP benchmarks and corresponding COMs for the RB energy models under study	191
B.1	Description of GitHub repository folders and sub-folders for Chapter 3	213
B.2	Description of GitHub repository folders and sub-folders for Chapter 4	215
B.3	Description of GitHub repository folders and sub-folders for Chapter 4...ctd .	216

B.4	Description of GitHub repository folders and sub-folders for Chapter 5	218
B.5	Description of GitHub repository folders and sub-folders for Chapter 5...ctd .	219
B.6	Description of GitHub repository folders and sub-folders for Chapter 5...ctd .	220

List of Abbreviations

ASHRAE The American Society of Heating, Refrigerating and Air-Conditioning Engineers	34
AI Artificial Intelligence	21
ANN Artificial Neural Network	
AHC Agglomerative Hierarchical Clustering	59
ACH Air Changes per Hour	
BEM Building Energy Modelling	26
BEMs Building Energy Models	6
BOH Back of House	74
COM a package (combination) of energy efficiency measures	13
COP Coefficient of Performance	19
COMs Sets of packages (combinations) of energy efficiency measures	11
CVRMSE Coefficient of the Variation of the Root Mean Square Error	ix
DB DesignBuilder	
DHW Domestic Hot Water	65
DOAS Dedicated Outdoor Air System	99
DRs Discount Rates	152
DR Discount Rate	
DOE U.S. Department of Energy	
EC European Commission	11
ECMs Energy Conservation Measures	6
ECM Energy Conservation Measure	
EP Energy Performance	ix

EPB Energy Performance of Buildings	
EPBD Energy Performance of Buildings Directive	ix
EPC Energy Performance Certificate	
EPCs Energy Performance Certificates	17
EPI Energy Performance Indicator	
EPIs Energy Performance Indicators	2
ESCOs Energy service companies	6
ESS Effective Sample Size	129
ETS Emissions Trading System	170
EU European Union	1
EUI Energy Use Intensity	25
FAMD Factor Analysis of Mixed Data	59
FOH Front of House	74
GDP Gross Domestic Product	61
GIS Geographic Information System	18
GHG Greenhouse Gas	1
GP Gaussian Process	
GPE Gaussian Process Emulator	93
GUI Graphical User Interface	21
HDI Highest Density Interval	125
HR Heat Recovery	
HVAC Heating, Ventilation, and Air Conditioning	57
IAQ Indoor Air Quality	103
IRR Internal Rate of Return	37
ISO International Organization for Standardization	
KOH Kennedy and O'Hagan	32
KS Kolmogorov–Smirnov test	30
LEED Leadership in Energy and Environmental Design	
LCC Life-cycle Costs	11
LFO Liquid Fuel Oil	
LHS Latin Hypercube Sampling	29
LPG Liquefied petroleum gas	
LOO-CV Leave-One-Out Cross-Validation	34
MARS Multivariate Adaptive Regression Lines	43

MCA Multiple Correspondence Analysis	59
MCMC Markov chain Monte Carlo	29
MCSE Monte Carlo Standard Error	129
M-H Metropolis- Hastings	43
MLR Multiple Linear Regression	43
MS EU Member States	ix
MV Mechanically Ventilated	
NCM National Calculation Methodology	2
NMBE Normalised Mean Bias Error	ix
NPV Net Present Value	37
NZEB Nearly Zero Energy Building	ix
NUTS No-U-Turn sampler	43
NV Naturally Ventilated	
OAT One-step At a Time	92
PCA Principal Component Analysis	19
PD Price Development	152
PE Percentile Error	30
POTEnCIA Policy Oriented Tool for Energy and Climate Change Impact Assessment	170
RAR Remove And Replace	
RO Reverse Osmosis	99
RB Reference Building	
RBs Reference Buildings	ix
SA Sensitivity Analysis	12
SD Standard Deviation	92
SFP Specific Fan Power	167
SHGC Solar Heat Gain Coefficient	65
SLABE Simulation-based Large-scale uncertainty/sensitivity Analysis of Building Energy performance	25
SVR Support Vector Regression	
SRC Standardised Regression Coefficient	43
TFA Total Floor Area	111
UBEM Urban Building Energy Modelling	xi
UBEMs Urban Building Energy Models	13
UK United Kingdom	189

VAT Value Added Tax 168
VRF Variable Refrigerant Flow 57
WAIC Widely Applicable Information Criterion 34
WWR Window to Wall Ratio 109
WS Work Shops 111

Introduction

1.1 | Background to the research work

In the 2020 approved European Union (EU) Green Deal [3], the EU has set ambitious goals to reach a minimum of 55 % Greenhouse Gas (GHG) emissions reduction by 2030 when compared to 1990 levels and eventually to be carbon neutral by 2050. Given that the building sector is a key contributor to GHG emissions and is responsible for 36 % of EU emissions and 40 % of its primary energy use [4, 5], it becomes critical to implement effective measures to improve the Energy Performance (EP) of existing building stocks. Prioritising the energy renovation of existing building stocks provides the best opportunity for energy savings [6], given that about 75 % of existing buildings in Europe are not sufficiently efficient, and yet more than 85 % of the current buildings will still be operational in 2050 [4, 7]. Despite this situation, the weighted average rate of energy renovation is currently only 1% per year [4], which triggered the EU in 2020 to establish the Renovation Wave Strategy [4], which defines actions such as doubling the annual building renovation rate by 2030. Furthermore, the new 2021 Energy Performance of Buildings Directive (EPBD) [8] has mandated EU-wide minimum EP standards for the worst-performing buildings.

However, achieving EU renovation goals can only materialise in practice through the establishment of appropriate policy measures at the EU Member States (MS) level to improve the EP of their buildings but a solid understanding of the existing building stock is a prerequisite to achieve this goal. This is supported by several requirements as stipulated in the EPBD Recast 2010/31/EU [9], such as the need to define “*Reference Buildings (RBs)*” for different building categories that would represent “*the typical and average building stock in a member state*” [9].



L-Università
ta' Malta

University of Malta Library – Electronic Thesis & Dissertations (ETD) Repository

The copyright of this thesis/dissertation belongs to the author. The author's rights in respect of this work are as defined by the Copyright Act (Chapter 415) of the Laws of Malta or as modified by any successive legislation.

Users may access this full-text thesis/dissertation and can make use of the information contained in accordance with the Copyright Act provided that the author must be properly acknowledged. Further distribution or reproduction in any format is prohibited without the prior permission of the copyright holder.

The application and analysis of different combinations of measures on RBs through the National Calculation Methodology (NCM) approved simulation tools for the implementation of the EPBD cost-optimal method allows MS to establish “*cost-optimal*” and “*Nearly Zero Energy Building*” (NZEB) EP benchmarks for which the new and existing buildings that undergo major renovations had to comply with as of January 2021. One of the useful outcomes of the cost-optimal method is a clear indication of the minimum energy efficiency measures for the building envelope and building energy systems that yield the cost-optimal EP range. In turn, policy makers would be empowered to set minimum energy requirements and to devise policies and incentives to further push the transition of buildings to NZEB.

Nevertheless, a review of recent research has established limitations to its potential for enabling MS the formulation of the necessary policy measures and the definition of realistic and effective benchmarks to improve the EP of building stock and to effectively achieve carbon neutrality by 2050. In addition, shortcomings in the level of harmonisation between MS to derive EP benchmarks have also been highlighted.

This research reports an “*Energy Performance (EP) gap*” as defined in [10, 11] of more than 30 % between the measured and simulated (Asset-rated¹) EP derived from the NCM software for both non-residential buildings and residential buildings. This performance gap is identified in various studies including [13, 14, 15, 16, 17, 18, 19, 20, 21, 22, 23, 24]². Although this EP gap is critical to successful policy making [25], energy policy has not yet considered this gap [11]. Furthermore, the definition of RBs among MS varied widely in detail [26, 27], and this was also noted among the different end uses and system boundaries chosen for EP calculations [28, 29, 30]. Consequently, the EU published revised EPB standards [31] and subsequently requested MS to describe their “*NCM following the national annexes of the overarching EPB standards*” [32] to improve harmonisation. All these technical factors have contributed to substantial disagreements between MS in the Energy Performance Indicators (EPIs) ($kWh.m^{-2}.year^{-1}$) derived from the cost-optimal methodology with discrepancies of up to 100 % reported in the review of [30, 33] for regions that fall under the same climatic zone.

The potential reasons for the above shortcomings stem from the application of ‘*non-calibrated and deterministic*’ RBs to the EPBD cost-optimal methodology. A deterministic

¹The building Asset EP rating depends on the characteristics of a building and on standard occupancy, operational schedules, and indoor-outdoor climate conditions. The Asset EP rating is generally calculated from the NCM software tool. In contrast, a building’s operational rating is based on actual measured amounts of delivered and exported energy [12].

²This EP gap has been demonstrated throughout Europe including Denmark [18, 19], France [14], Switzerland [20, 21, 22, 23], Germany [16], UK [17], Italy [13] and Malta [24], and there is general consensus that buildings with a high asset EP rating have a higher operational energy consumption than expected, while buildings with a low asset EP rating have a lower metered energy consumption than expected [25].

RB³ model is defined as a building energy model with a single set of input parameter values for the envelope and technical building systems for a building stock category under study. In addition, the calibration of RB energy models with building stock metered operational EP data is not undertaken. Thus, using the current deterministic and non-calibrated approach, the validation of RBs to be truly representing existing building stocks is not facilitated. Moreover, the effect of uncertainties or diversity in the input parameters for calculating cost optimal and NZEB level benchmarks is not taken into account. As a result, this approach does not provide sufficient confidence that the proposed cost-optimal measures or the NZEB levels and the derived EPIs themselves are economically feasible and ultimately achieve the desired energy savings and carbon neutrality targets when implementing them in practice.

State-of-the-art Urban Building Energy Modelling (UBEM) techniques have applied '*probabilistic Bayesian calibrated RBs*' to replace '*non-calibrated deterministic RBs*' in order to better handle parameter uncertainty and building stock diversity. In '*probabilistic Bayesian calibrated RBs*' the uncertain parameters are defined as '*prior*' probabilistic distributions representing one's initial beliefs about the true value of the parameters. The building is then calibrated using metered operational energy performance data via a Bayesian approach to reduce uncertainties by updating the '*priors*' to narrower '*posterior*' parameter probability distributions. However, '*probabilistic Bayesian calibrated RBs*' to handle uncertainties in the EPBD cost-optimal method has not been adequately addressed in literature as detailed by the author of this thesis in [35, 36]. Therefore, no clear framework exists to effectively integrate state-of-the-art UBEM techniques incorporating '*probabilistic Bayesian calibrated*' RBs into the current EPBD cost-optimal method.

The uncertainty of defining a few '*non-calibrated deterministic RBs*' to represent an entire building stock is even more critical for the non-residential building stock, which is largely diverse and comprises multiple activities and uses [27, 37, 38]. Furthermore, the geometric and technical data required to derive RBs is limited, given that most literature publications on RBs and building stock modelling in the EU revolves around the residential building stock [27, 38], given that they make up 75 % [27] of the EU building stock and are responsible for 63 % [39] of the energy consumption of the final building stock of the EU. The application of Bayesian calibration to such non-residential, heterogeneous, multi-functional building stocks has not been adequately covered in the literature.

³In literature there is no standard methodology or a harmonised process for deriving deterministic RBs [26, 34].

1.2 | The aim and objectives of this research work

The aim of this research is to propose and validate an innovative approach to the EPBD cost-optimal method to allow policy makers to optimally handle the diversity and uncertainties of the building stock when deriving EP benchmarks for heterogeneous multi-functional building stocks under different defined ambition levels of EP rating.

The objectives of this research to achieve the aim are as follows.

- Establish a clear framework for integrating state-of-the-art Urban Building Energy Modelling (UBEM) techniques employing '*probabilistic Bayesian calibrated RBs*' into the current EPBD to address the diversity and uncertainties of the buildings' different parameters.
- Develop and apply a machine learning approach to define RBs for '*small*' ($X \gg N$)⁴ multi-functional, heterogeneous building stocks and employ the novel cost-optimal approach to a defined RB.
- Investigate and statistically validate, in terms of accuracy, innovative techniques to reduce the computational expense of the novel cost-optimal approach and facilitate its implementation.
- Develop a harmonised and ordinal scale approach to define the NZEB EP ambition levels and identify how to propagate the EP and financial uncertainty for each defined ambition level for a RB under study, ultimately leading to robust energy renovation support policies.
- To compare the novel cost-optimal approach with the current deterministic approach and establish the strengths and limitations of each approach.

The 5-star hotel building stock in Malta, consisting of ten (10) hotels, will be used as the case study multi-functional '*small*' heterogeneous building stock to demonstrate the proposed cost-optimal methodology approach. Hotel building stocks present an ideal case study to meet the objectives of this thesis given their multi-functional "*comfort or service-orientated accommodations*" [40] with significant heterogeneity [27] in terms of business size and other individual characteristics. This has been demonstrated in the literature that "*the idea of a typical hotel, as well as its respective performance remains vague*" [41], and the difficulty of identifying "*typical*" or "*reference*" hotel buildings, even for large building stocks, is not straightforward.

⁴For the scope of this research, a '*small*' building stock is one where the number of explanatory variables '*X*' impacting energy performance is greater than the number of building observations '*N*' in a population.

1.3 | Research questions

Based on the background and purpose of this study, the research questions can be summarised as follows:

- What machine learning methodology can be developed to cluster a multi-functional and heterogeneous '*small*' ($X \gg N$) building stock to define RBs?
- How does the proposed EPBD cost-optimal approach developed in this research better handle uncertainties when deriving cost-optimal NZEB measures and benchmarks versus the current EPBD approach?
- How can the proposed EPBD cost-optimal approach devise more robust energy renovation support policies under different levels of ambition to meet the required renovation targets?
- How does the proposed '*probabilistic*' cost-optimal approach compare in terms of computational expense with the current approach, and what innovative techniques can be applied to optimise its computational time and to facilitate its implementation?

1.4 | Significance of the study

This research has EU-wide significance by proposing an innovative EPBD cost-optimal approach that has the potential to allow MS to define more robust policy measures to trigger energy renovation to meet the goals of the Renovation Wave [4]. This is achieved by looking to better handle the key technical and financial uncertainties, which have been identified as the main sources of uncertainties for energy renovation [42, 43, 44] and Energy Performance contracting [45]. Specifically, taking into consideration the uncertainties of different parameters may lead to stronger long-term renovation strategies in MS. This can potentially be established via a more realistic quantification of financial support measures and the definition of more realistic and achievable EPIs given uncertainties.

Furthermore, the RB calibration process is more likely to derive EPIs between MS that are more comparable by reflecting more closely the operational EP of the buildings, thus increasing harmonisation, which is also one of the key objectives of the EPBD. Consequently, this can also accelerate the rate of renovation of buildings because investors,

including Energy service companies (ESCOs)⁵ and operators, can have a better assurance that the outcome will truly produce the expected benefits and savings.

Beneficiaries of this research also include the construction industry and building owners, who will be required to upscale their competence to meet the challenge of achieving carbon neutrality by 2050. Also, policy makers will benefit from this work as it will open new venues for matching calculated carbon reduction estimates to real carbon reduction achieved targets, especially for renovation. Tackling the main barriers to energy renovation can increase the renovation rate. However, it has to be ensured that renovation will produce the expected outcomes while providing new opportunities for jobs and investments, thus contributing to the much-needed stimulus to the economy following the COVID-19 pandemic [4]. Furthermore, renovation can achieve healthier, more productive and better indoor comfort levels for building occupants [4], reducing operational energy costs and risk exposure to energy price fluctuations and weather shocks [47]. In addition, building owners, such as hoteliers, can achieve economic value through green marketing opportunities, since a green image has a significant positive impact on the intention of the consumer to purchase a service [48, 49].

From an academic point of view, this research may also contribute to the field of UBEM by aiming to establish a method to define RB energy models or archetypes for multi-functional and heterogeneous '*small*' ($X \gg N$) building stocks. In addition, this research also strives to facilitate the application of Bayesian calibration for these building stocks by analysing innovative approaches to optimise the computational efficiency of Bayesian calibration.

1.5 | Organisation of the dissertation

The dissertation is organised as follows:

- Chapter 2 reviews the limitations of the current EPBD cost-optimal methodology and defines the link between UBEM and the EPBD cost-optimal method in terms of process similarities and common uncertainties. Moreover, the chapter critically reviews and investigates state-of-the-art UBEM studies that can address building stock uncertainty and diversity using Bayesian probability. Based on the findings from this review, a novel EPBD cost-optimal method is proposed to optimally handle the diversity and uncertainties of the building stock and meet the aim and

⁵To avoid the financial risk, when Energy Conservation Measures (ECMs) are evaluated using deterministic calibrated Building Energy Models (BEMs), Energy service companies (ESCOs) consider a rule of thumb approach to consider only between 60 % and 70 % of the deterministic prediction of energy savings [46].

objectives of this research. The subsequent chapters aim to apply the proposed novel approach to the hotel building stock and validate it by comparing its potential to the current approach in its ability to provide more robust policy measures to facilitate building stocks transition to NZEB.

- Chapter 3 tackles the first step in the novel cost-optimal approach by developing a machine learning approach to define RBs for '*small*' ($X \gg N$) heterogeneous building stocks.
- Chapter 4 addresses the steps to derive '*probabilistic Bayesian calibrated RBs*' for the proposed cost-optimal approach. The approach is applied and validated for a deterministic RB defined in Chapter 3, which represents an energy model for a cluster of the 5-star hotel buildings under study. Innovative energy modelling techniques are applied and validated to reduce the computational expense of deriving '*probabilistic Bayesian calibrated RBs*' and to facilitate the implementation of the novel approach.
- Chapter 5 addresses the final steps of the proposed cost-optimal approach to objectively derive EPIs or benchmarks for the different levels of ambition proposed, while taking into consideration the propagation of EP uncertainty and financial risk for each of them to establish robust energy renovation support policies. The '*probabilistic Bayesian calibrated RB*' developed in Chapter 4 is used as a case study to demonstrate the process. The chapter will finally perform the current cost-optimal approach using the same RB case study and the NCM software to allow a critical comparison of its outcomes with that of the innovative approach developed in this study.
- The thesis concludes by analysing the degree to which this research has met its aim and objectives.

1.6 | Important notes

- A selected list of peer-reviewed publications, book chapters, and conference proceedings by the author of this thesis, many of which are referred to in this thesis, are found in Appendix A.
- All building energy model files, JEPlus [50] files, Microsoft Excel files, and Python source code used to undertake this research are found in the following repository link.

https://drive.google.com/drive/folders/1S2Y2-TIHlwabHnlzLHHUa8n06GByf_Nd?usp=sharing.

Appendix B also provides a detailed description of all folders and files in this link, highlighting the Chapter, Section, and Footnote where each folder, file and source code is referred to in the thesis.

Literature review

Chapter Abstract : Building stock energy models are tools that can be used to extract valuable knowledge of the national building stock to assist in developing appropriate policy measures to achieve decarbonisation. In this context, the 2010 EPBD recast [9] has established a common EU approach, '*the EPBD cost-optimal methodology*', for analysing building stocks to facilitate their transition to near-zero energy status. The current Energy Performance of Buildings Directive (EPBD) cost-optimal method and the different approaches to building stock modelling, such as the Urban Building Energy Modelling (UBEM) found in literature, are reviewed to establish methodological similarities and common uncertainties. The state-of-the-art UBEM literature provides multiple techniques to better handle uncertainties and building stock diversity. Therefore, it was hypothesised, in line with the aim of this research, that the handling of building stock uncertainties and diversities in the EPBD cost-optimal could be better addressed by integrating state-of-the-art UBEM techniques employing '*probabilistic Bayesian calibrated RBs*' to the current cost optimal approach. Following the systematic review of the UBEM literature, a new cost-optimal method incorporating these techniques is proposed and conceptualised. Other research gaps that need to be addressed within the specific context of the EPBD and multi-functional buildings to meet the aim and objectives of this research are also identified. The subsequent chapters aim to validate the proposed cost-optimal method through its application to a building stock case study to accept or reject the hypothesis presented in this chapter.

2.1 | Introduction

Meeting the EU carbon reduction goals and energy renovation rate targets for buildings established in the Green Deal [3] and the renovation wave strategy [4] requires EU Member States (MS) to devise successful policy measures to improve the Energy Performance (EP) of their buildings. In this context, building stock energy models, whose general purpose is to "*quantify the energy-use as a function of different input parameters*" [51], can offer valuable knowledge of the national building stock [52], including the potential to improve its EP. Therefore, these models are key for informing, devising, and evaluating policy measures and to "*assisting with the efficient and rational implementation of policy*" [53].

Although numerous building stock energy models in the literature serve different purposes, all models should be able [51, 52] to estimate the baseline EP of a building stock cluster under study and explore the technical and economic impacts of different CO₂ abatement strategies, including the potential of applying new technologies. Furthermore, the models should also be able to evaluate potential non-energy related benefits to emission reduction strategies such as indoor environmental performance.

Within this context, and to serve the specific purpose of the EPBD for establishing '*cost-optimal*' and '*NZEB*' EP benchmarks, a common approach for MS to study the building stock termed the '*EPBD cost-optimal methodology*' was established in the 2010 EPBD recast [9]. Based on the results from the cost-optimal method, MS are to devise the required policy measures to facilitate the transition of buildings to the established EP benchmarks.

This chapter reviews the current EPBD cost-optimal method and the different approaches to building stock energy modelling found in the literature to define the link in terms of methodological similarities, uncertainties, and limitations between the EPBD cost-optimal method and these approaches. The review then focuses on techniques used in state-of-the-art building stock energy modelling studies to better handle the uncertainties and limitations of conventional modelling approaches for more robust policy making. The reviewed building stock modelling studies employ building physics energy models and are termed Urban Building Energy Modelling (UBEM) studies in this research. An analysis of such state-of-the-art techniques in UBEM, including an evaluation of their limitations, and the identification of specific research gaps that need to be addressed in the fields of uncertainty analysis and building energy modelling to serve the specific requirements of EPBD cost-optimal framework, will follow. Finally, this analysis guides the aim of this research in proposing an innovative approach to opti-

mally handle the diversity and uncertainties of the building stock within the EPBD cost-optimal method and its application to heterogeneous multi-functional building stocks.

2.2 | Relation between the EPBD cost-optimal method and conventional UBEM

This section compares the EPBD cost-optimal method to conventional UBEM approaches. The establishment of similarities between the two methods can identify whether the developed state-of-the-art UBEM mathematical techniques that address many of the limitations in conventional UBEM studies have the potential for application in the EPBD cost-optimal method to better handle building stock uncertainties and diversity.

2.2.1 | The EPBD cost-optimal method

The EPBD recast [9] cost-optimal methodology can be summarised in the following steps :

- Step 1: '*Deterministic RBs*' are defined for the different building categories defined in the directive;
- Step 2: Sets of packages (combinations) of energy efficiency measures (COMs) is applied to the defined RBs. The energy efficiency measures constitute Energy Conservation Measures (ECMs) and/or measures using renewable energy systems. ECMs include both building envelope (passive) measures and building energy systems (active) measures.
- Step 3: Primary energy consumption based on the EP¹ rating of RBs for the chosen COMs is calculated using a National Calculation Methodology (NCM) that is compliant with the requirements of the EPBD recast [9];
- Step 4: The global (life cycle)² costs (*Euro.m*⁻² of the building floor area) for any package of measures are calculated according to the EPBD recast methodology

¹The building EP rating depends on the characteristics of a building and on standard occupancy, operational schedules, and indoor outdoor climate conditions, while a building operational rating is based on measured amounts of delivered and exported renewable energy [12].

²The term '*global*' or '*Life-cycle Costs (LCC)*' (refer to EN 15459-1 [54]) used in the cost-optimal level calculations is the total combination of costs, such as capital cost, maintenance, and replacement costs, as well as operational costs, all discounted to the present value over a period of time, as stipulated in European Commission (EC) delegated regulation number 244/2012 supplementing the 2010 EPBD [55]. In the 2018 EPBD cost-optimal studies for Malta [56] this period was taken to be 20 years (for non-residential buildings) and 30 years (for residential buildings).

[9]. The global cost must be carried out from both a macroeconomic³ and financial perspective, and a Sensitivity Analysis (SA) for different price development scenarios and discount rates is mandatory;

- Step 5: The results of the energy calculation are plotted against the global costs (Euro.m^{-2} of the building floor area) for each sensitivity, as shown in Figure 2.1, and the cost-optimal and NZEB EP ranges are determined.

The cost-optimal EP *“leads to the lowest cost during the estimated economic life cycle of the building”* [9], while NZEB is a building that *“has a very high EP with a low amount of energy required covered to a very significant extent by energy from renewable sources, including energy from renewable sources produced on-site or nearby”* [9]. It must be noted that the red curve represents the Pareto front⁴. The area to the left of the cost-optimal point in Figure 2.1, represents possible NZEB solutions [59].

³For the macroeconomic cost optimum, the financial global cost calculation needs to be expanded to include the cost of GHG emissions which is defined as the monetary value of environmental damage caused by the emissions generated from the operational energy consumption of a building [55].

⁴The Pareto front is the set of optimal, non-dominated solutions where each objective is considered equally good for multi-optimisation problems, and also provides superior solutions for the search space [57, 58].

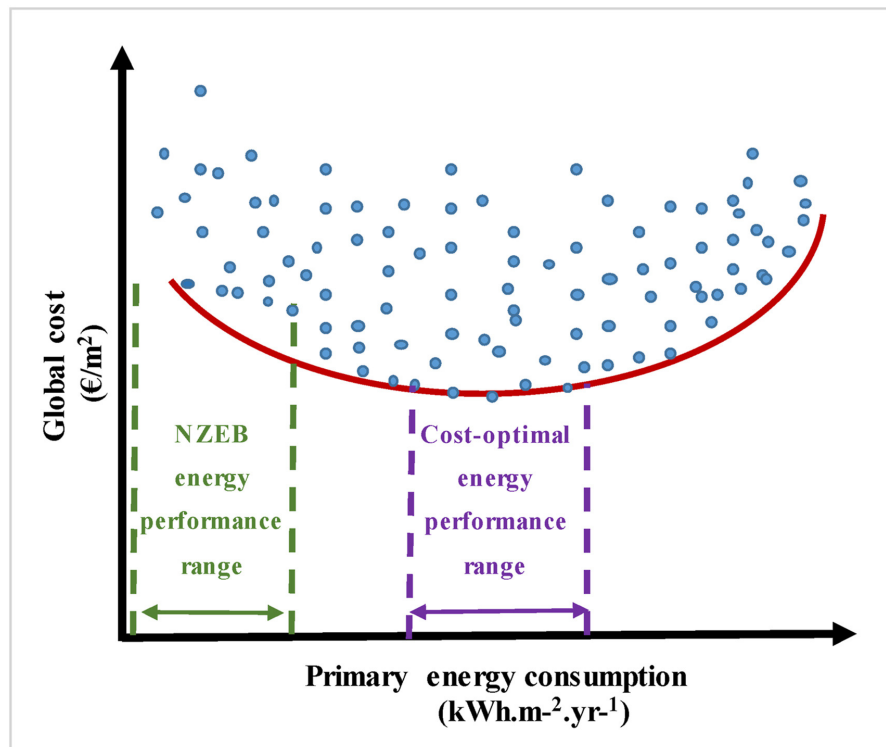


Figure 2.1: Plot showing the EPBD cost optimal and NZEB ranges where each light blue dot identifies a package (combination) of energy efficiency measures (COM), while the red curve represents the Pareto optimal solutions.

2.2.2 | Building stock and Urban Building Energy Modelling (UBEM)

In general, building stock energy modelling has been classified in three distinct approaches, namely the '*bottom-up*', the '*top-down*' and the hybrid methods, as shown in Figure 2.2, whereby the hybrid building stock energy model is a combination of the bottom-up and top-down methods [60].

The '*bottom-up*' calculates and aggregates the EP or end uses of individual buildings to represent the entire building stock under study [65]. Furthermore, it is important to distinguish between '*bottom-up*' statistical models and '*bottom-up*' engineering (or physics) building stock modelling. '*Bottom-up*' physics models make use of building energy simulation tools and are called UBEMs in this review⁵.

'*Top-down models*' are data-driven models [38] that investigate a building sector's

⁵This review adopts the classification schemes used by Swan et al. [53, 51], in which Urban Building Energy Models (UBEMs) are bottom-up engineering or bottom-up building physics models, respectively [66]. Thus, UBEMs, bottom-up engineering, and bottom-up building physics models are used interchangeably. UBEMs in this study also deal with RBs (typically archetypes) rather than distributions or samples (refer to Figure 2.2).

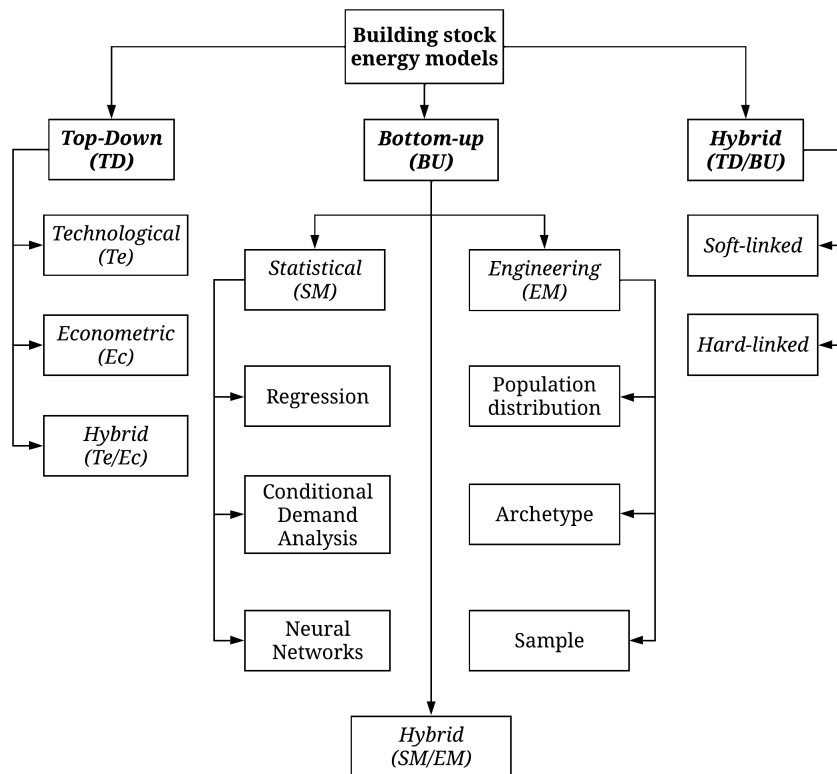


Figure 2.2: Overview of building stock modelling approaches as compiled from [61, 62, 63, 64, 53]

energy consumption or CO₂ emissions through historical databases. They evaluate the macroeconomic relationships between energy consumption and long-term changes within the existing building sector under analysis [67]. The main advantage of top-down techniques lies in their use of more easily accessible aggregate data that simplify analysis. In addition, due to the decreased need to gather in-depth descriptive data on buildings, this type of modeling is typically quicker and less expensive [62]. However, these models do not satisfy the requirements of the EPBD cost-optimal method, as they do not analyse individual building energy models, different technology options, or energy end uses.

In contrast to 'top-down models', the UBEM methodology uses building physics energy simulation tools to predict EP in an approach similar to the EPBD cost-optimal method, thus attaining more robust results and allowing for higher fine tuning to evaluate the potential of greenhouse gas avoidance in the simulation modelling, in line with the requirements of the Green Deal [3]. This is made possible because UBEMs work at

a disaggregated level and do not rely on historical data, while sharing many similarities to the EPBD cost-optimal method, such as the evaluation of the impact of different energy efficiency measures on the primary energy and CO₂ emission reductions [51, 68] and the identification of the corresponding cost-optimal levels.

2.2.3 | A methodological comparison between the EPBD cost-optimal method and UBEM

In a published paper by the author of this thesis (refer to Gatt et al. [36]), a detailed comparison was carried out between the conventional UBEM studies⁶ and the EPBD cost-optimal method and it was found that they share many methodological similarities [36], given their common objective, as depicted in Figure 2.3. For example, both approaches first require the definition of '*deterministic RBs*' to represent the building stock under study, predict the unit energy consumption of the RBs using building energy simulation tools, and model the improved EP when different energy efficiency measures are applied to the RBs.

One important difference between the two approaches is that UBEM must acquire the total EP of the building stock category by aggregating the predicted unit EP using appropriate weighting factors (for example the floor area or the number of units) for each RB before the application of measures. Aggregation enables policy makers to investigate the impact of various measures at the national or urban level.

However, in comparison to conventional UBEM and the EPBD cost-optimal method, state-of-the-art UBEM approaches probabilistically calibrate the RB parameters using metered building stock energy consumption data to enhance the confidence and validity of the defined RB energy models and realistically quantify the impact of various energy efficiency measures on the primary energy consumption. The sections that follow explain these approaches in more detail.

2.2.3.1 | Definition of deterministic Reference Buildings (RBs)

To represent the building stock under study, '*deterministic RBs*' are first defined in both conventional UBEM and the EPBD cost-optimal method. Such RBs should accurately reflect the national building stock to ensure representative calculations and benchmarking, given that the building stock division has a profound impact on the models' abilities to predict EP improvements of the proposed measures [72]. However, despite the im-

⁶Studies that explain the UBEM conventional approach process include [65, 53, 69]. Conventional UBEM studies include Mata et al. [70] and Tuominen et al. [71].

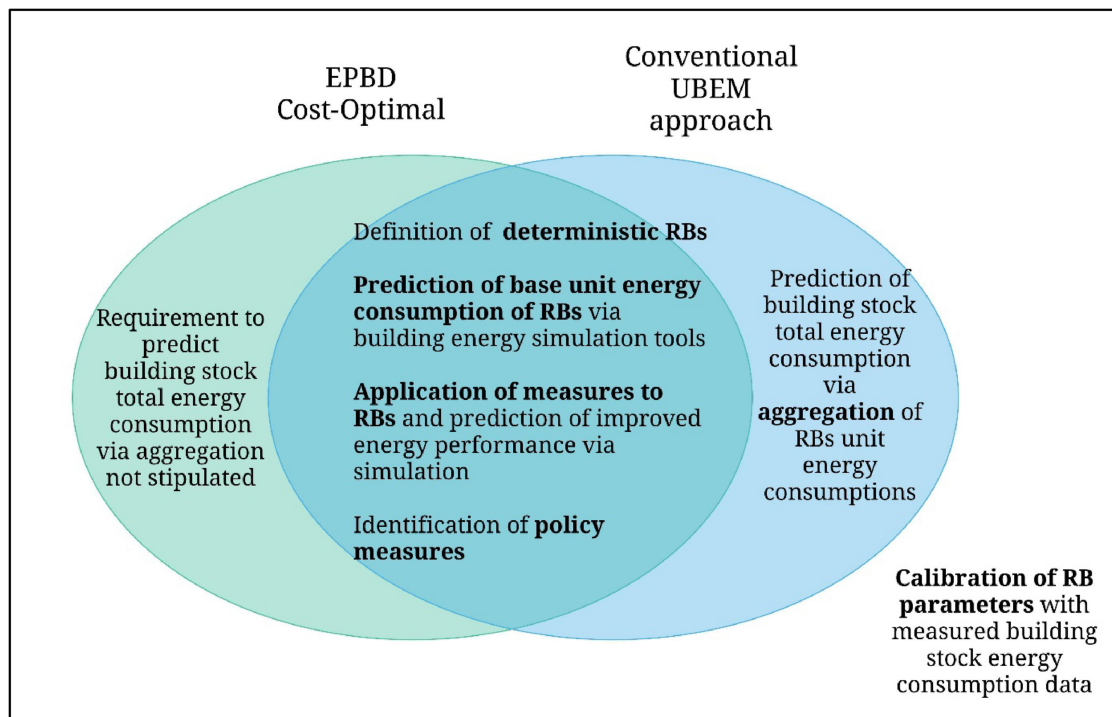


Figure 2.3: A Venn diagram showing the methodological similarities and differences between the EPBD cost-optimal method and conventional UBEM approaches

portance of correctly defining RB, their current development remains one of the biggest challenges to model building stocks [73]. First, statistically defining RBs is complex, since the process requires the collection of a significant amount of geometric, operational, and technical information [65]. Furthermore, the definition of RBs is subjective, given that the method to define them is not standardised or harmonised, as explained in Schaefer and Ghisi [34] and Corgnati et al. [26].

Despite the numerous approaches proposed in the literature for defining RBs, it can be identified that the majority of RBs have been developed conceptually using a similar two-step approach, as seen in Figure 2.4. Buildings are first classified according to one or more categories or indicators, such as usage [74] (for instance, offices, educational buildings, hotels and hospitals), location, construction period and building size plus shape [75]. Several studies of the building stock, including Aksoezen et al. [76] and Famuyibo et al. [77], applied a top-down statistical analysis of the energy consumption data of the measured building stock to verify the choice of the adopted RB classification approach and improve confidence in the selected building categories.

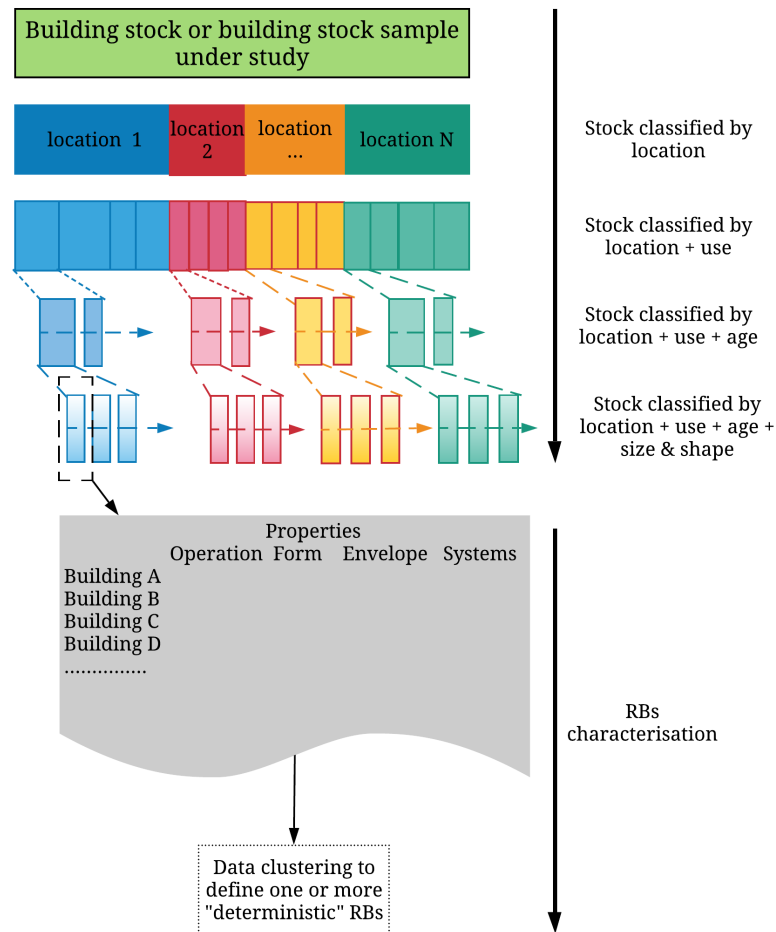


Figure 2.4: Approach generally adopted to define RBs in UBEM and the EPBD

After being classified, RBs are characterised according to all pertinent geometric and non-geometric features, including operation, form, envelope, and system data [26], using a variety of sources of information including national or local building codes and standards, national surveys results, energy audits, or other published literature. Recently, O. Pasichnyi et al. [78] developed RBs by linking Energy Performance Certificates (EPCs) and measured energy consumption data sets using statistical data techniques. The most frequently utilised characterisation approach in the literature is 'archetypes' [38], which are virtual RBs having 'a statistical composite of the features found within a category of buildings in the stock' [62]. When compared to the 'Example RB' and the 'Real (average) RB' characterisation approaches, archetypes provide the most realistic and representative method to characterise the analysed building stock sample. A downside of

archetypes is that the availability of large statistical data sets is required for their successful processing. An *'Example RB'* is developed based only on the expert's assumptions and judgement and can be a real building [75] or a virtual [79], fictional [26] building. In contrast, the *'Real (average) RB'* represents the most typical existing building in the analysed building stock sample [26], [75], [79].

Furthermore, approaches to developing RBs for *'small'* ($X \gg N$)⁷ multi-functional building stocks where the number of explanatory variables *'X'* impacting energy performance is greater than the number of building observations in a population *'N'* have not been sufficiently considered in literature⁸.

In order to make the characterisation and classification stages for defining RBs easier and less subjective, various data-driven techniques have been used in the literature. Such techniques⁹ include the use of the following:

- **Descriptive statistics.** The technique was used in a number of studies, such as Bhatnagar et al. [80] to develop office RBs for India and Streicher et al. [82] to characterise archetypes from the EPC data for a residential building stock in Switzerland;
- **Clustering analysis.** Numerous studies have employed this technique.

In Ballarini et al. [86], EPC data was used to undertake hierarchical clustering for each age class of terraced houses in Piedmont (Italy). Farrou et al. [87] employed k-means clustering for deriving EP benchmarks to enable the classification of Greek hotels. The k-means algorithm was also used by Heidarinejad et al. [81] to cluster the EP of office buildings having LEED certification. Furthermore, for Southern Brazil, Schaefer and Ghisi [34] combined hierarchical and k-means clustering to derive RBs for the low-income housing stock. More recently, Yang et al. [88] and Borges et al. [89] used k-means clustering to develop representative

⁷For the scope of this research, a *'small'* building stock is one where the number of explanatory variables *'X'* impacting EP is greater than the number of building observations *'N'* in a population or sample under study.

⁸Studies to develop RBs have generally considered building stocks with large number of observations when compared to the number of explanatory variables impacting operational energy performance. Such studies to develop RBs include Bhatnagar et al. [80] : 230 office building observations and 23 explanatory variables, Heidarinejad et al. [81] : 134 office building observations and 24 explanatory variables, Streicher et al. [82] : 25,000 residential building observations and 23 explanatory variables, and Pieri et al. [83]: who considered a sample of 35 hotels from a population of 192 hotels and 8 explanatory variables to divide the building stock into 3 groups.

⁹State-of-the-art techniques for defining RBs in UBE M include the approach by Ghiassi and Mahdavi [84], where clustering is combined with Geographic Information System (GIS) to identify representative buildings, and Tardioli et al. [85], where a novel six-step approach is proposed that includes classification and clustering to generate representative buildings.

buildings in China and Andorra, respectively. In addition, Ali et al. [90] made a comparison of different clustering techniques for an Irish EPC database when developing archetypes;

- **Regression analysis.** This technique was combined with descriptive statistics and employed by Famuyibo et al. [77] to develop archetypes for domestic dwellings in Ireland;
- **Principal Component Analysis (PCA).** PCA was combined with K-means clustering and used by Gaitani et al. [91] to identify typical school buildings in Greece and to develop a tool for their EP rating. In a similar manner, Pieri et al. [83] combined clustering and PCA for hotel buildings.

The primary constraint when defining RBs in both the conventional UBEM and the EPBD cost-optimal method is that only single parameter values are defined for each RB energy model software simulation input. Such single-parameter input values do not permit consideration of inherent randomness or diversity in the RB representing a building stock under study. For instance, when a single-parameter value for the Coefficient of Performance (COP) of a cooling system is input for a RB, one cannot propagate uncertainty and building stock diversity resulting from different COP values in the building stock for the cooling system under study. Therefore, given only single parameter values to characterise the RB, the RB model will always predict the same EP output, which makes the RB models in the conventional UBEM and the EPBD cost-optimal method '*deterministic*'. In other words, a Sensitivity Analysis (SA) is not performed for the assumed values of the energy efficiency parameters.

Although the use of classification and other statistical data-driven techniques aids in the selection and definition of '*deterministic RBs*' to better reflect the building stocks diversity, in '*deterministic RBs*' there still exists what Booth et al. [92] describe as '*heterogeneity uncertainty*' resulting from a grouping of characteristics into subsets and '*chance variability*' when single parameter values are assigned to define RBs. Consequently, even if an archetype building statistically represents the mean of all buildings in its group, each individual building will always have a different EP [74]. The following sections will describe how the definition of RBs has developed in state-of-the-art UBEM to better handle the diversity and uncertainties of the building stock.

2.2.3.2 | Predicting the EP of RBs

The EP of the derived RBs is predicted using the same approaches as those applied for both the conventional UBEM and the EPBD cost-optimal method. Figure 2.5 pro-

vides a first-hand description of the different modelling methods for predicting the EP of buildings¹⁰. In both approaches, the forward (engineering) approach is necessary to physically interpret the results to understand how the application of ECMs impacts the EP of RBs.

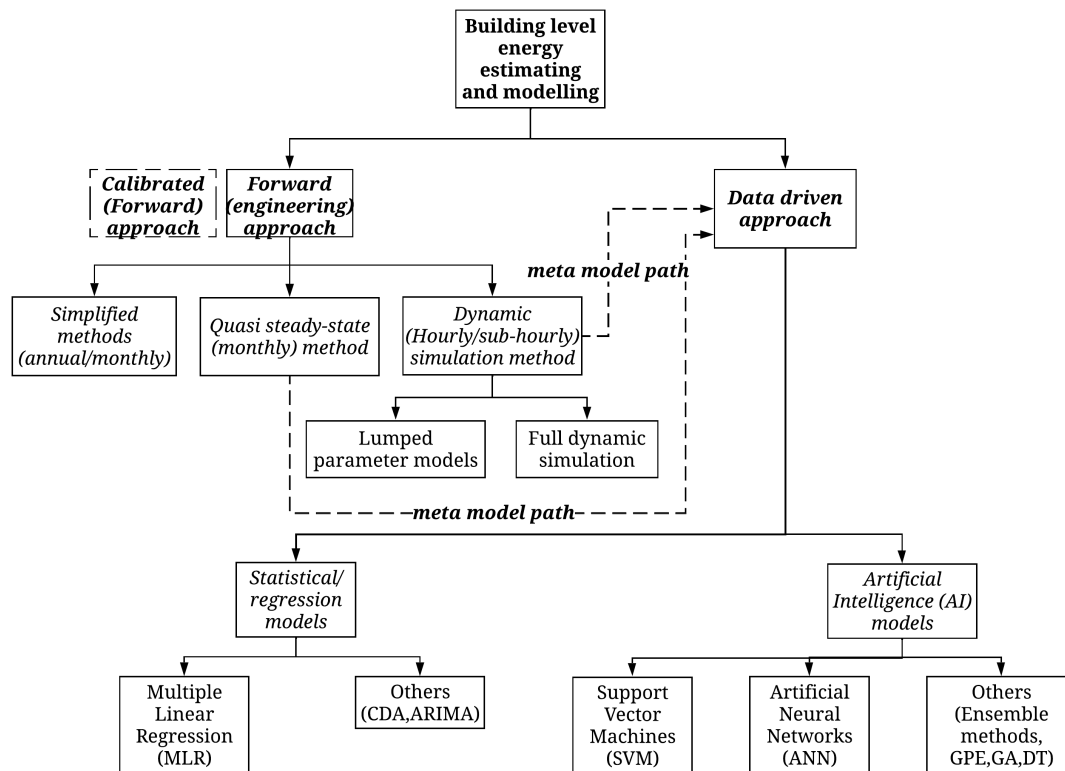


Figure 2.5: A first-hand depiction of energy estimating and modelling methods for individual buildings (RBs)

The EPBD allows MS to use forward-driven EP calculation methods for the EP analysis of RBs in the NCM. These calculation methods are to be quasi-steady-state or dynamic in compliance with ISO 52016 [108]. Most UBEM studies have also adopted these two calculation methods. Quasi-steady-state methods employ simple algebraic equations [109], require less parameter inputs, and are computationally faster than dynamic models. However, in contrast to dynamic simulation tools (which include EnergyPlus, ESP-r, and TRNSYS software [110])¹¹ that consider the transient behaviour of systems

¹⁰Recent reviews of building energy estimating and modelling methods between 2013 and 2022 in chronological order can be found in [93, 94, 95, 96, 97, 98, 99, 100, 101, 102, 103, 104, 105, 73, 1, 106, 107].

¹¹Dynamic software simulation tools have been assessed by Crawley et al. [111], and recently by Harish et al. [102] and Chalal et al.[101]. The most widely used software simulation tools, that include EnergyPlus,

and buildings, quasi-steady-state or monthly methods are not able to perform a thermal comfort assessment, model demand-based controls, perform a smart readiness assessment or track peak loads [99, 112].

Meta-models that combine (forward) engineering building simulation tools with data-driven Artificial Intelligence (AI) or statistical models have become a fundamental modelling approach in state-of-the-art UBEM studies. Meta-models are also known as surrogate models, emulators, hybrid or grey-box models. Meta-models have the advantage of reducing the simulation times of dynamic engineering models when undertaking the computationally expensive process of probabilistically calibrating RB parameters with individual building stock energy consumption data.

2.2.3.3 | Aggregating the EP of RBs

RBs in UBEM are modelled either as individual buildings, after which their EP levels are aggregated to the entire building stock under study, or the RBs in the stock are modelled collectively together [113]. The aggregation of EP and the collective modelling of RBs has recently been made easier in UBEM through integration with GIS¹². UBEM incorporating GIS allows the acquisition of the outer shell geometry of buildings in a stock but still requires one to divide the buildings into zones to comprehensively characterise non-geometric properties of the buildings such as the zone activities and their corresponding installed systems, and operational schedules. UBEM thermal models can range in complexity from contextless, single-zone, steady-state models to multi-zone dynamic models that take into account cross-shading between buildings. The impact of the urban heat island effect has also been studied by some models [115]¹³. Recently, Hong et al. [118] carried out a review of UBEM, evaluating aspects that include the available urban modelling tools and the EP calculation methods employed by the different tools.

Given that the EPBD cost-optimal method does not specify the requirement to aggregate the energy end-use (consumption) from the RBs to building stock level, the potential of GIS has not been realised. Although the aggregation of RB energy end-use (consumption) data has been a key component in conventional UBEM, only recent

ESP-r, and TRNSYS, use the multi-zone building physics model approach [94, 97]. This approach divides a building under analysis into zones and uses uniform state variables, which variables include temperature, to describe the properties defining the thermodynamic state of each thermal zone of the building [94, 97].

¹²GIS makes it easier to collect building data, facilitates the merging of data from several databases needed for engineering models, allows spatial visualisation and differentiation of results, and supplies a repository for storing and exchanging data [114, 101]. Common input variable data includes weather data, building age, physical, thermal, and occupational schedule data from buildings.

¹³State-of-the-art UBEM GIS software including CitySim [116] and CityBES [117] that combine a custom Graphical User Interface (GUI) with thermal simulation engines.

state-of-the-art UBEM studies have attempted to probabilistically calibrate RB parameters with individual measured energy consumption stock data to reduce parameter uncertainties, as discussed in the following sections.

2.3 | Uncertainties in the EPBD cost-optimal method and conventional UBEM

The methodological similarities between the conventional UBEM and the EPBD cost-optimal method result in many common uncertainties between the two processes. Uncertainties will be defined from an EPBD policy perspective before explaining the technicalities leading to such policy uncertainties.

2.3.1 | Policy uncertainties in the EPBD cost-optimal method

From a policy perspective, the EPBD cost-optimal method uncertainties have been summarised by the author of this thesis in [35, 36] as:

- The extent to which the defined '*deterministic RBs*' used to derive EP benchmarks adequately represents the diversity of the building stock under study.
- The magnitude of the '*energy performance gap*', that is, the discrepancy between the actual '*operational*' building stock (individual and aggregated) EP and the '*simulated*' EP of RBs representing the building stock calculated using NCM software tools in the EPBD cost-optimal methodology.
- The extent to which the EN 15459 [54] global Life-cycle Costs (LCC) parameters, such as the capital and maintenance costs for each defined COM¹⁴, accurately reflect the LCC parameter diversity for a building stock under study both as a result of capital costs and maintenance requirements variations between different suppliers for components having a similar function and unforeseen circumstances during the design or execution of the works.
- The difference between the actual '*operational*' versus the calculated '*simulated*' primary energy savings achieved by retrofitting a specific category of buildings to defined EP requirements. This difference leads to uncertainty as to whether measures

¹⁴While MS are to undertake SA for different price development scenarios and discount rates in the global LCC calculation for the packages of energy efficiency measure under study, other global LCC parameters are defined deterministically in the EPBD cost-optimal method.

leading to a defined EP ambition level in the simulated environment are eligible for promotion or incentive in practice.

- A quantification of the technical and economic risks associated with the defined EP benchmark for a given building stock under study.

Such uncertainties are also made evident given that an '*energy performance gap*' of more than 30 % was recorded throughout Europe, including Denmark [18, 19], France [14], Switzerland [20, 21, 22, 23], Germany [16], UK [17], Italy [13] and Malta [24]. Moreover, energy policy has not yet fully considered this critical gap [11], which impacts the success rate of energy policymaking [25]. These uncertainties and other factors led to substantial differences between MS in the EPIs ($kWh.m^{-2}.year^{-1}$) derived from the cost-optimal methodology with discrepancies of up to 100 % reported in the review of [30, 33] for regions that fall under the same climatic zone. Other factors, in addition to the above uncertainties, that can lead to these discrepancies include a lack of harmonisation in the methodology of the NCM calculation approach¹⁵ and a lack of objectivity in deriving the NZEB benchmarks between MS, as detailed in Section 2.5.5.

¹⁵RBs have been defined by MS with a significantly divergent level of detail for EPBD cost-optimal analysis [26, 27], and important discrepancies between the different end uses and the system boundaries considered for EP calculations, have been identified in [28, 30]. To counteract this harmonisation issue, the EU has published revised EPB standards [31] and requested MS in the 2018 EPBD [32] to describe their "*NCM following the national annexes of the overarching EPB standards.*"

2.3.2 | Factors leading to policy uncertainties in the EPBD

The different types of uncertainties in conventional UBEM are described in detail by Booth et al. [92], Lim and Zhai [65], Naber et al. [45], Tian et al. [119] and Pratavia et al. [120]. Given the methodological similarities between the conventional UBEM and the EPBD cost-optimal method, these uncertainty factors also lead to the EPBD policy uncertainties described above. For the purpose of this research, a simplified breakdown of uncertainties in conventional UBEM can be as follows:

1. RB energy models input parameters uncertainty
2. RB energy models technical and structural uncertainty

,as discussed in the following sections.

2.3.2.1 | RB energy models input parameters uncertainty

Building engineering simulation models are complicated even when applied to individual buildings because they require many input parameters that are variable / stochastic (aleatory uncertainty) or unknown, given a lack of knowledge (epistemic uncertainty) [119]. The problem is more pronounced in the EPBD and UBEM, since only a small number of '*deterministic RBs*' are employed to represent the whole and wide distribution of individual buildings [45]. In addition, there are also uncertainties in any measurements used or taken to define parameter input values, including the manufacturer system specifications themselves.

Furthermore, there is also an aleatory and epistemic uncertainty in the input parameters of the adopted economic model in UBEM and the LCC calculation in the EPBD cost-optimal method. These input parameters include the capital and maintenance costs of the retrofit measures under study.

2.3.2.2 | RB energy models technical and structural uncertainty

Given that it represents a simplification of the real physical process, the engineering or meta-model itself is a potential source of uncertainty and error [121]. The model will provide a difference in the outputs under study between measured and simulated results, even for exact measurements and perfectly known parameters.

2.4 | Handling of uncertainties in the EPBD-cost-optimal method

Even though the handling of uncertainties is critical for informed policy making, few attempts have been made to devise techniques to tackle the uncertainties described above for the EPBD-cost optimal approach. EPBD guidelines only require MS to perform a risk analysis on EN15459-1 [54] global life costing parameters by performing a SA to identify the impact of multiple price development scenarios and discount rates on the resulting EP benchmarks for the defined RBs.

In the literature relating to the EPBD, the Simulation-based Large-scale uncertainty/sensitivity Analysis of Building Energy performance (SLABE) approach put forward by Mauro et al. [64] enables the diversity and uncertainty of the building stock to be better tackled by replacing '*deterministic RBs*' with a representative building sample. This approach allows a simulation based uncertainty/SA in EP from the representative building sample and in life-cycle financial feasibility when ECMs are introduced and simulated. However, the SLABE process cannot aggregate and probabilistically calibrate the energy performance of the engineering model (s) with the measured energy consumption data of the building. This calibration is critical to provide confidence in the chosen representative building sample and to fully address the input parameters and structural uncertainties of the model to study the building stock¹⁶. This absence of calibration also limits the ability of SLABE to consider the '*energy performance gap*' between the simulated Energy Use Intensity (EUI) performance and the EUI operational performance.

In contrast, the literature on techniques to better handle the uncertainties and diversities of building stocks in UBEM to tackle the limitations of conventional UBEM is more comprehensive, as will be systematically reviewed in the following sections. In general, and as detailed in the following sections, state-of-the-art UBEM studies have handled uncertainties and risks by addressing the limitations of uncalibrated '*deterministic RBs*' in conventional UBEM using an approach of inverse uncertainty analysis [121]. This approach replaces '*deterministic RBs*' with '*probabilistic RBs*' and performs Bayesian inference, or more specifically, Bayesian calibration to tune the most significant input

¹⁶More recently Scarpa et al. [122] for residential buildings in Italy, not within the specific context of the EPBD cost-optimal method, used a similar approach to SLABE [64] by defining archetypes as probability distributions to consider the joint impact of uncertainty on both technical and financial aspects. However, calibration with metered energy consumption data was also not considered. Other recent studies that consider a '*probabilistic non-calibrated*' approach to the EP improvement studies in buildings include Copiello et al. [123] propagating LCC uncertainty for a housing block, Giuseppe et al [124] developing an approach to propagate EN 15459 [54] LCC uncertainty, and Tognaschi [125] who performed a joint technical and financial risk analysis for a standard seven-storey tenant office building located in Tokyo.

parameters of defined RBs with individual building stock energy consumption data¹⁷.

Given the methodological similarities and the resulting uncertainties between conventional UBEM and the EPBD cost-optimal method established in Section 2.2.3 and visualised in Figure 2.3, in line with the aim of this research, a hypothesis can be made as follows. It can be hypothesised (see Gatt [36]) that handling the uncertainties and diversities of the building stock in the EPBD cost-optimal method can be better addressed by applying state-of-the-art UBEM techniques employing '*Bayesian calibrated RBs*' to the current approach. However, to accept or reject this hypothesis, one first needs to tackle the research gap of establishing a conceptual framework to comprehensively integrate the UBEM techniques built upon '*probabilistic Bayesian calibrated RBs*' to the current cost-optimal method, given that this conceptual framework does not exist. The choice of considering '*Bayesian calibrated RBs*' versus non-calibrated probabilistic RBs and calibrated deterministic RBs using a '*frequentist*' optimisation approach are detailed in Section 2.5 and Section 2.6.1 via a review of the literature.

To address this research gap, a systematic review of the literature on how Building Energy Modelling (BEM) studies have handled the uncertainties and diversities of building stocks was carried out, as detailed in the following paragraph, and a conceptual update of the cost-optimal method is proposed to establish this framework. The proposed update to the cost-optimal method is shown in Figure 2.6 and is detailed in Section 2.5. It should be noted that the proposed update is derived on the basis of what the researcher believes is the most suitable approach to address the above hypothesis after a careful review of the literature. To answer this hypothesis, subsequent chapters will aim to validate the conceptual EPBD cost-optimal approach shown in Figure 2.6 by applying it to an actual case study of a building stock.

Furthermore, in the following chapters, each step in the proposed method will be further analysed to address the limitations of '*Bayesian calibrated RBs*' discussed below and to address the specific methodological needs of the EPBD cost-optimal method, including its application to multi-functional heterogeneous building stocks.

¹⁷'*Bayesian inference*' is "the process of fitting a probability model to a set of data and summarising the results by a probability distribution on the parameters of the model and unobserved quantities such as predictions for new observations" [126]. More specifically, for the scope of this research, Bayesian calibration starts by assigning prior probability distributions of model parameters, which defines prior expertise or knowledge independent of observations. The prior distributions of parameters are then used to characterise the building energy simulation model, for which the uncertainty in the prior distributions can be decreased to iteratively obtain posterior distributions given field observations and using Bayes rule [127].

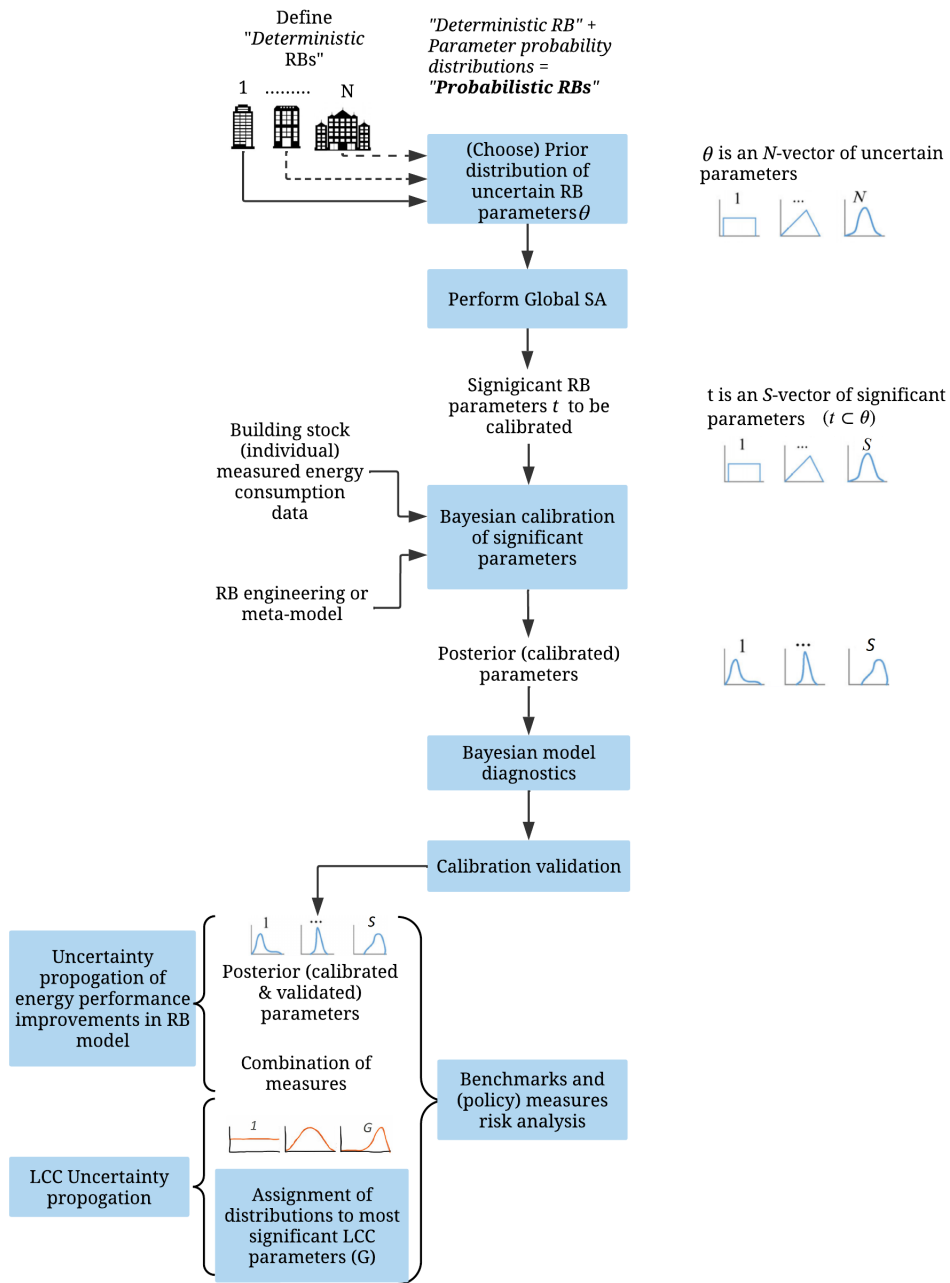


Figure 2.6: The EPBD cost-optimal method coupled with state-of-the-art UBEM techniques to handle uncertainty and allow a comprehensive risk analysis of derived EP benchmarks and (policy) measures

The literature review methodology to derive the proposed update of the EPBD cost-optimal method consisted of the following three steps:

- Step 1: Keyword search for publications in Google Scholar and the Scopus database. The search included the keywords '*Bayesian calibration*', '*Bayesian inference*', '*uncertainty quantification*', '*inverse problems*' related to Building Energy Modelling (BEM) with a focus on UBEM. Only research journals or conference papers written in English and peer-reviewed were considered relevant.
- Step 2: A review of all relevant publications. The relevant publications were reviewed in terms of the following aspects: parameter uncertainty distribution, parameter screening, parameter uncertainty propagation, Bayesian calibration of significant parameters, Bayesian model diagnostics, calibration validation, probabilistic risk analysis in the application of energy conservation measures (ECMs), strengths and limitations of Bayesian calibration, tackling the limitations of Bayesian calibration in building energy modelling.
- Step 3: A conceptual update of the proposed EPBD cost-optimal method is defined. All relevant publications were reviewed, and a conceptual update of the EPBD cost-optimal method was proposed. Methodological research gaps that are relevant to the specific needs of the EPBD cost-optimal method, and its application to multi-functional heterogeneous building stocks and so far not addressed in the UBEM literature are identified.

The next section will detail each step of the proposed update to the cost-optimal approach and, based on the reviewed UBEM literature, will attempt to justify each step in terms of allowing policy makers to better handle building stock uncertainties and diversities in the EPBD cost-optimal method. The subsequent chapters will aim to validate the proposed approach.

2.5 | Proposed EPBD cost-optimal method update

The proposed update to the cost-optimal approach is shown in Figure 2.6 and is explained in the following six steps:

- Step 1: Assignment of probabilistic RB models
- Step 2: SA for the identification of the most significant parameters of the RB models
- Step 3: Probabilistic calibration of the significant uncertainty parameters of the RB models
- Step 4: Bayesian model diagnostics, posterior analysis and calibration validation
- Step 5: Derivation of EP benchmarks via a global LCC cost-optimal analysis
- Step 6: Risk Analysis for the derived EP Benchmarks

2.5.1 | Step 1: Assignment of probabilistic RB models

Assigning '*probabilistic RBs*' is the first step in the proposed EPBD cost-optimal method depicted in Figure 2.6. '*Deterministic RBs*' used in conventional UBEM and the EPBD cost-optimal method cannot replicate the inherent diversity of buildings within a cluster of buildings under analysis. This results because each input parameter in the RB energy model is defined as a single value to predict EP [74, 128]. Therefore, to better handle the diversity and uncertainty of the parameters of the building stock that define a group of buildings, '*probabilistic RBs*' have replaced '*deterministic RBs*' in state-of-the-art UBEM studies. In '*probabilistic RBs*', an N-vector of uncertain (input) parameters θ are defined as probability distributions $p(\theta)$, representing the prior knowledge of the true values of the calibration parameters. To generate a random or near-random sample of input parameter values from the defined probability distributions statistical techniques that include Markov chain Monte Carlo (MCMC) or Latin Hypercube Sampling (LHS) are employed. This sampling allows policy makers to propagate uncertainty through variations and correlations between the input of the RB parameters and the output(s) of the RB energy model.

The drawback of '*probabilistic*' versus '*deterministic*' RBs primarily lies in the increase in the simulation time of the analysis and the need to use audit / survey data to characterise the selected RB parameters probabilistically when compared to the use of data from more readily available literature sources to define '*deterministic RBs*' [74].

2.5.1.1 | Probabilistic RBs versus deterministic RBs approach validation

Recent residential building stock UBEM studies by Cerezo et al. [74] and Sokol et al. [128] have compared the performance of the simulated Energy Use Intensity (EUI) distribution performance of both non-calibrated '*probabilistic*' archetypes and '*deterministic*' archetypes against actual measured Energy Use Intensity (EUI) distributions¹⁸. Both studies statistically proved through Kolmogorov–Smirnov test (KS) test values and maximum or mean percentile error tests that the simulated EUI distributions resulting from '*probabilistic RB*' matched more closely the annual measured EUI distributions. Yamaguchi et al. [129] for Japan's retail facilities and Tian and Choudhary [69] for campus school buildings also acknowledge the importance of using probabilistic versus deterministic energy models to capture the EUI distribution for a group of buildings.

In Bayesian UBEM calibration studies, envelope and equipment parameters were probabilistically assigned by Booth et al. [92, 130] and Booth and Choudhary [131] to a building housing stock. Operational parameters and plug loads were defined probabilistically in Cerezo et al. [72] for urban residential buildings in Kuwait. Furthermore, occupancy and envelope parameters were selected for Bayesian inference in Hedegaard et al. [132] for an urban residential neighbourhood in Denmark, while studies including Tian and Choudhary [69] for a set of campus school buildings, Cerezo et al. [74] for urban residential buildings in Kuwait, Sokol et al. [128] for residential houses in Cambridge, Kristensen et al. [113] for Danish detached single-family houses, and Prieto et al. [133] for a residential building block case study in Switzerland, defined envelope, equipment, and operational parameters as probability distributions.

While '*probabilistic RBs*' can intrinsically allow the diversity of building stocks to be represented, it does not eliminate the need to divide the building stock under study into multiple RBs using a suitable classification approach. The use of multiple '*probabilistic*' archetypes versus single '*probabilistic*' archetypes in UBEM allows policy makers to reduce the wide parameter uncertainty distributions resulting from a whole building stock. Cerezo et al. [74] and Sokol et al. [128] statistically proved, through the resulting analysis of the EUI distribution, the requirement to correctly classify the building stock and the use of multiple '*probabilistic*' archetypes to represent residential buildings in UBEM. Furthermore, Tian and Choudhary [69] also acknowledge the importance of

¹⁸Applying uncalibrated probabilistic archetypes versus deterministic archetypes, Cerezo et al. [74] showed a reduction in Percentile Error (PE) (for the 90 percentile) from 0.16 to 0.04 and an improvement in the Kolmogorov–Smirnov test (KS) test from 0.24 to 0.12 for the simulated EUI distributions compared to annual measured EUI distributions. Similarly, Sokol et al. [128] showed that the application of uncalibrated probabilistic archetypes versus deterministic archetypes achieves a reduction in the mean Percentile Error (PE) from 69 to 47 %, a decrease in CVRMSE from 78 to 69 %, and an improvement in the KS test values from 0.57 to 0.41 for the simulated EUI distributions compared to the annual measured EUI distributions.

using multiple '*probabilistic RBs*' to represent a schools' building stock. Once the building stock is divided into more than one RB, each '*probabilistic RB*' can then handle the remaining parameters (and EUI) '*natural*' variability within each cluster of buildings.

2.5.2 | Step 2: Sensitivity analysis (SA) for the identification of the most significant parameters of the RB models

Once '*probabilistic RBs*' are defined, the RB parameters must be probabilistically calibrated using individual measured energy consumption data from the building stock to improve confidence in the predictions of UBEMs and reduce the uncertainty of the RB parameters. Reduction in RB parameters uncertainty is achieved by obtaining narrower probability distributions that define the uncertainty of the parameters. Most UBEMs that employ probabilistic calibration perform a SA process to identify the S-vector of significant parameters ϕ ($\phi \subset \theta$) from the unknown parameters θ to be employed in the calibration process. Therefore, since probabilistic calibration is a computationally expensive process, SA aims to reduce the computational burden of probabilistic calibration by reducing the calibration parameters from N to S, as shown in Figure 2.6. Furthermore, calibrating a large number of parameters, which number of parameters is case-specific, can lead to identifiability problems and less precise calibrated parameters due to overparameterization [134], and this occurs because more combinations of parameters are likely to agree with the measured data.

Bayesian calibrated building energy models generally apply global versus local SA. Global SA, unlike local SA, explores the impact of uncertain parameters throughout the defined parameter range [135]. Despite being more computationally intensive than local SA, global SA can be considered a more reliable method [136]. The one-step-at-a-time (Morris) method [137] is a popular global SA method for Bayesian calibrated building energy models and has been successfully applied in various studies both for individual buildings in Heo et al. [138, 139, 140, 141] and for UBEM in Booth et al. [92, 130], Booth and Choudhary [131], and M.H. Kristensen et al. [113]. The principal advantage of the Morris method, as reviewed by Yang et al. [142] and Tian [143], is the need for less computation than the other global SA methods. The Morris method, therefore, provides a good compromise between accuracy and computational effort in BEM [134].

2.5.3 | Step 3: Probabilistic calibration of the significant uncertainty parameters of the RB models

The uncalibrated probability distributions of the S significant RB uncertain parameters t depicted in Figure 2.6 are known as '*prior distributions*' or simply '*priors*' [131]. Bayesian calibration uses Bayes' theorem, shown in Equation 2.1 [126]¹⁹, to obtain plausible distributions of the uncertain parameters referred to as '*posterior distributions*' $p(t | y)$ derived from the '*prior distributions*' $p(t)$ and the likelihood function. Given that Bayes' theorem stipulates that the posterior probability $p(t | y)$ is proportional to the likelihood function $p(y | t)$ and the prior probability, the likelihood function drives the process of updating '*prior*' distributions by evaluating how closely the model results match the measured data, y . The Markov chain Monte Carlo (MCMC) algorithms draw from the joint posterior distribution to create approximate "*posterior distributions*" to calibrate all uncertain parameters²⁰.

$$p(\phi | y) \propto p(\phi) \times p(y | t) \quad (2.1)$$

The generic approach proposed by Kennedy and O'Hagan [146] for the Bayesian calibration of computer models, as defined in Equation 2.2, has been applied both for the calibration of individual buildings and in UBEM studies to model the relationship between computer simulation η and measured data, y incorporating uncertainty of parameters, model inadequacy, and observation errors. Studies of individual buildings that employ the Kennedy and O'Hagan (KOH)[146] approach include office buildings in Heo et al. [139] and Chong and Menberg [134] and a single-family house in Denmark in Kristensen, Choudhary and Petersen [71]. RB studies in UBEM applying the Kennedy and O'Hagan [146] approach include a building housing stock in Booth et al. [92] and Danish single-family dwellings in Kristensen, Choudhary, Pedersen, et al. [147].

¹⁹Bayesian calibration was first applied to UBEM by Booth et al. [92].

²⁰While MCMC is the most widely approach to approximate the posterior distributions, '*Variational Inference*', a machine learning optimisation method, has been applied for high dimensional problems in BEM by Li et al.[144] and Cartens et al. [145].

The uncertainty in the parameters is usually explained by a meta-model (emulator) $\eta(x, t)$, which is a GPE in many studies that replaces the computationally intensive physical model [128] and fits the simulation results of the energy model through runs of the stochastic model under known conditions x and uncertain (calibration) parameters t . The (structural) inadequacy of the model is included in the bias correcting term $\delta(x)$, while $\varepsilon(x)$ accounts for observation errors.

$$y(x) = \eta(x, t) + \delta(x) + \varepsilon(x) \quad (2.2)$$

In UBEM studies employing Bayesian calibration, the heterogeneity of the archetypes was considered according to different degrees within a cluster of buildings [113]. Booth et al. [92] calibrated ‘*probabilistic*’ archetypes to average data on building stock energy consumption, thus not accounting for archetype diversity. However, in the studies by Cerezo et al. [74] and Sokol et al. [128], Bayesian inference was considered for each building energy model individually with respect to its measured energy consumption data before the data were compiled, thus accounting for archetype heterogeneity. Kristensen et al. [113] proposed an optimal solution between these two approaches to adequately account for the heterogeneity of the archetype. The solution considers a hierarchical (multilevel) Bayesian calibration approach that partially combines information from training buildings to infer uncertain parameters that are less prone to outliers.

2.5.4 | Step 4: Bayesian model diagnostics, posterior analysis and calibration validation

Once the calibration process is complete, it is crucial to assess how well the applied model fits the data to avoid misleading inferences. This will improve confidence in the resulting posterior parameter distributions. Bayesian model verification and comparison requirements are detailed in several publications, including Gelman et al. [126] and Kruschke [148]. Software packages such as ShinyStan [149], Bayesplot [150], and Arviz [151] facilitate model checking in Bayesian statistics by providing interactive plots and tables to help analyse a posterior sample.

An assessment of the representativeness, accuracy and efficiency of the MCMC sample generated from the posterior distribution is vital. This assessment should be performed by evaluating the convergence of the model, the autocorrelation in the sample chain, and the effective sample size. Statistical methods to assess model convergence include the Gelman-Rubin statistic [126], which has been used to assess convergence in Bayesian calibration of building energy models in several UBEM studies. UBEM studies

that have applied the Gelman-Rubin statistic include Kristensen, Choudhary, Pedersen et al. [113] and Kristensen et al. [147]. Furthermore, Chong and Menberg [134] applied the Gelman-Rubin statistic in an individual building study.

If the initial diagnostic inspection of convergence is satisfactory, the suitability of the applied model must be checked. Important aspects of model checking include the '*within sample*' predictive checks termed Posterior Predictive Checks (PPCs) [126] and the '*out of sample*' predictive accuracy. PPCs assess the fit of the replicated data from the model to the observed data by simulating samples from the posterior predictive distribution. They include graphical checks, such as distributions and scatter plots, or facilitate the use of test statistics that include the posterior predictive p-value [126]. Out-of-sample predictive accuracy is carried out by splitting a data set into a training set and a cross-validation (testing) test without the use of model data. The model is fitted to the training set, which is then assessed by evaluating its performance on an independent testing set through graphical checks or statistical tests. These checks have been carried out both graphically and with test statistics in the calibration of building energy models in Chong and Menberg [134] for individual buildings and in Sokol et al. [128] and Kristensen, Choudhary, Pedersen et al. [113] in UBEM. The most popular test statistics for assessing predictive precision in Bayesian calibrated of building energy models are the Normalised Mean Bias Error (NMBE) and Coefficient of the Variation of the Root Mean Square Error (CVRMSE) criteria detailed in The American Society of Heating, Refrigerating and Air-Conditioning Engineers (ASHRAE) Guideline 14 [152]. Out-of-sample tests '*without waiting*' [126], that is, '*using in sample data*' [153] which include Widely Applicable Information Criterion (WAIC), and Leave-One-Out Cross-Validation (LOO-CV), have not been applied in studies using Bayesian calibration of building energy models to the best knowledge of the researcher.

Furthermore, since multiple models may be plausible and fit the data well, verifying that the preferred model performs favourably relative to other alternatives is desirable. For this purpose, SA assesses the change in posterior inference when other reasonable probability models are used instead of the present model [126].

SA in the Bayesian calibration of building energy models has assessed the sensitivity of:

- The use of a different number of archetypes assessed in various studies, including Cerezo et al. [74] and Sokol et al. [128] for UBEM residential buildings;
- Different number of calibration parameters in Chong and Menberg [134] for an office building study;

- The extent of consideration of archetype heterogeneity in Kristensen et al. [113] for Danish detached single-family houses;
- The use of different priors, that is, different levels of parameters uncertainty in Heo, Graziano, et al. [140] and Chong and Menberg [134] for individual building studies,
- The application of different meta-models in Lim and Zhai for a medium sized office building [154] and Prieto et al. [133] for a UBEM residential building block case study in Switzerland;
- Different training set sizes to develop the emulator in Kang and Krarti [155] for an office building;
- Different data temporal resolutions analysed in various studies, including Yamaguchi et al. [129] for a UBEM supermarket study, Sokol et al. [128] for UBEM residential buildings, and Kristensen, Choudhary, and Petersen [147] for a single-family dwelling and
- The influence of error terms on the posterior predictions of calibrated model inputs in Menberg et al. [121] for a heat pump model.

2.5.4.1 | Bayesian calibration approach validation

Bayesian calibration of probabilistic RBs has been statistically proven²¹ for the UBEM of residential buildings in Cerezo et al. [74] and Sokol et al. [128] to provide closer EUI simulation predictions with measured data than EUI simulation predictions from uncalibrated probabilistic RBs, especially when RBs are calibrated with monthly versus annual energy consumption data [128]. On the downside, calibration increased the computational expense by a factor of more than six [128].

²¹By calibrating probabilistic RBs with annual measured data, Cerezo et al. [74] showed a reduction in the Percentile Error (PE) (for the 90 percentile) from 0.04 to 0.02 and an improvement in Kolmogorov–Smirnov test (KS) from 0.12 to 0.05, compared to the annual measured EUI distributions. Similarly, Sokol et al. [128] showed that when probabilistic RBs were calibrated using annual measured energy consumption data, mean PE decreased from 69 to 47 %, CVRMSE decreased from 87 to 66 %, while the KS test values improved from 0.41 to 0.21. Furthermore, probabilistic RBs calibrated with monthly energy consumption data versus annual measured data gave even closer EUI simulation predictions. The monthly calibrated probabilistic RB achieved a mean PE of 44 %, a CVRMSE of 58 %, and a KS test of 0.10.

2.5.5 | Step 5: Derivation of EP benchmarks via a global LCC cost-optimal analysis

Once the RB models are calibrated, they can better support policy decision making at the urban level. Drawing from the calibrated parameters of the resulting RB models '*posterior distributions*' in Bayesian calibration naturally allows the propagation of uncertainty and SA in the simulation output when different packages of energy conservation measures are applied to the calibrated '*probabilistic RB*' models under study [156]. This propagation of uncertainty allows for a probabilistic uncertainty analysis in predicted energy savings and associated financial risk when different ECMs are considered and applied to a building or building stock, as shown in the following studies. An energy savings probabilistic risk analysis using different retrofit measures has been performed in Booth and Choudhary [131] for a Bayesian calibrated UBEM housing stock, in Tian and Choudhary [69] for a school building stock, and in Heo et al. [157], for a case study university building. Furthermore, in UBEM studies, both Booth and Choudhary [131] and Heo et al. [157] propagated uncertainty in both the predicted energy savings of the ECMs and their capital costs to allow more accurate and reliable retrofit decision making under uncertainty. This probabilistic uncertainty and risk analysis that can lead to more reliable decision making when applying different energy efficiency measures to a building stock under study cannot be carried out by using '*deterministic RBs*' in the current EPBD cost-optimal method and in conventional UBEM.

Therefore, a more comprehensive analysis of uncertainty and financial risk would have to be carried out for the proposed EPBD cost-optimal method, that not only considers the capital costs of implementing energy efficiency measures as done in the above studies, but according to the global life-cycle cost-optimal analysis requirements stipulated by the EC [55], to enable the shift towards a probabilistic approach for deriving and analysing NZEB benchmarks. More specifically, a set of energy efficiency measures would need to be applied to '*Bayesian calibrated RBs*' to calculate primary energy consumption and global LCC for each package of energy efficiency measures (COM) and construct cost-optimal plots for determining the cost-optimal and NZEB benchmarks.

However, defining NZEB benchmarks is not straightforward even for the current '*deterministic*' EPBD cost-optimal method that uses an '*Asset rated*' approach to calculate the EP rating. This difficulty results because the EPBD does not provide objective criteria for defining NZEB benchmarks following the determination of the cost-optimal levels for different discount rates and price development scenarios. A state-of-the-art review of different NZEB definitions by Gatt [158] has concluded that while "*cost-optimal*

EP levels provide a maximum threshold for MS to define NZEB EP requirements, a clear relation and distinction between cost-optimal and NZEB EP levels has not been established at EU level". Furthermore, recent guidance from the EC in [159], only makes a generic recommendation on NZEB EP benchmark ranges for offices and single-family households under different climates.

Therefore, a methodological research gap exists in the literature for an objective and harmonised approach to enable MS to define NZEB EP benchmarks for RBs according to different defined ordinal levels of ambition. Furthermore, a gap exists in the current EPBD cost-optimal approach to account for uncertainties in predicted energy savings and life cycle financial feasibility propagated from '*probabilistic RBs*' for different ECMs.

2.5.6 | Step 6: Risk analysis for derived EP benchmarks

The last step of the proposed cost-optimal approach requires the visualisation and objective quantification of the uncertainty in predicted energy savings and the corresponding risk in life cycle financial feasibility for a RB model undergoing a major renovation.

In BEM studies that consider probabilistic approaches, operational uncertainties and financial sensitivities, a number of visualisation and statistical techniques have been used. Visualisations approaches include side-by-side univariate (box) plots for global cost uncertainty distributions comparing different ECMs in [64], Internal Rate of Return (IRR) distribution plots for ECMs in [125] and Net Present Value (NPV) impact as a function of the LCC calculation period for a NPV financial parameter under study in [122]. Furthermore, statistical risk quantification approaches include the optimal investment ratio derived based on the variance and covariance matrix of the IRR in [125] and by defining the safe and risk zones of a financial metric probability distribution in [122].

However, a probabilistic approach to risk and uncertainty analysis that considers the joint impact of technical and financial uncertainties on NZEB EP benchmarks has not been specifically developed so far. Such a framework requires the consideration of both financial and macroeconomic perspectives to LCC in order to be able to perform a SA on the impact of different price development scenarios and discount rates on the resulting EP benchmarks for a defined RB. Furthermore, the propagated uncertainty in EP improvements and LCC risks for a defined NZEB benchmark level as generated from the '*Bayesian calibrated RBs*' requires to be visualized, statistically quantified, and interpreted to produce a meaningful output that can meet the aim and objectives of this research.

2.6 | Positive attributes and limitations of Bayesian calibration in UBEM

This section discusses the potential positive attributes and limitations of applying Bayesian calibration to reduce uncertainty for BEM studies with a focus on UBEM, as explained in the literature. Furthermore, different approaches in which Bayesian calibration limitations have been counteracted in BEM studies are also reviewed, and specific literature gaps are identified to further tackle the limitations of Bayesian calibration to facilitate its implementation in the proposed EPBD cost-optimal method. The current research focus for the Bayesian calibration of building energy models is also summarised.

2.6.1 | Positive attributes to Bayesian calibration versus 'frequentist' calibration approaches

The positive attributes of applying probabilistic "*Bayesian*" calibration versus the '*frequentist*' calibration [119] approach stem naturally from the requirements of the RB models to handle the diversity of the building stock by defining and obtaining probabilistic distributions of the input parameters of the RB suitable for risk propagation. This contrasts the '*frequentist*' optimisation approach to calibration that simply aims at finding the '*best*' value of input parameters [130] by minimising the difference between observed data and the output of the model²².

More important to policy making is that prior probabilistic distributions of RB parameters allow the consideration of parameter uncertainty and evaluation of its impact via Bayesian inference in an iterative manner. Therefore, a continuous learning process can be established using the posterior parameter distribution derived as prior and inferring these distributions in light of new data or as more reliable sources of information become available [130].

Such an approach has been amply demonstrated in the literature to yield meaningful outputs. For example, Heo et al. [140] showed that Bayesian calibration for all audit levels of an individual building yielded posterior distributions that corresponded well to true values, with much reduced uncertainty compared to uncalibrated models. Furthermore, Chong and Menberg [161] also recommended the use of '*weak informative priors*' versus '*specific priors*' in case of previous knowledge, to ensure the inclusion of all sensible parameter values. Although the studies by Heo et al. [140] and Chong and

²²In [160] a state-of-the-art study employs optimisation combined with surrogate models to auto-calibrate UBEM.

Menberg [161] have not been validated in an urban context, they indicate that expensive and detailed energy audits may not be critical in defining prior distributions for RBs undertaking Bayesian calibration. Therefore, a proper SA must identify prior sensitivity before undertaking expensive data collection.

From a mathematical and EPBD policy making perspective, '*Bayesian*' versus deterministic '*frequentist*' calibration offers other advantages. Apart from the possibility of considering multiple sources of uncertainties including, model inadequacy, Bayesian calibration, unlike optimisation, aims to reduce uncertainty from all parameters to be calibrated instead of simply minimising the discrepancy between the observed data and model output. Furthermore, Bayesian calibration allows policy makers to establish quantitative confidence levels in the accuracy of calibrated models and to propagate risk via sampling from posterior distributions. The ability to probabilistically quantify parameter uncertainty and to allow for the accounting of multiple sources of uncertainties allows the '*Bayesian*' approach to providing a better framework to counteract the over-fitting and parameter identifiability issues of conventional '*frequentist*' calibration [156]²³.

2.6.2 | Meeting the main objectives of the 2018 EPBD and the Green Deal

In Gatt et al. [36], the author of this thesis explained how the proposed update of the EPBD cost-optimal method depicted in Figure 2.6 has the potential of facilitate the process for MS to meet three primary objectives of the 2018 EPBD directive (2018/844/EU) [32]. These objectives are shown in Figure 2.7. Figure 2.7 depicts a process mind map illustrating how the proposed EPBD cost-optimal method can allow MS to express comparable cross-national EP benchmarks in accordance with the EU NZEB recommendations [159], establish stronger long-term renovation strategies, and facilitate building compliance with the '*smartness indicator*' criteria introduced in the 2018 EPBD. The potential of the proposed approach to meet these objectives will be further discussed once the '*novel*' proposed EPBD cost-optimal method is validated via its application to a building stock case study in subsequent chapters.

²³Various studies have statistically, in terms of different error metrics, proven the benefits of Bayesian calibration versus conventional calibration approaches [127] including Kim et al. [162] who compared constrained optimisation versus stochastic Bayesian calibration for an existing building, Pavlak et al. [163] who compared least the squares approach to Bayesian inference for a retail building grey-box model, and more recently in Rouchier et al. [164] who compared the indoor temperatures forecast performance of an experimental test-cell using Kalman filter and Bayesian Inference.

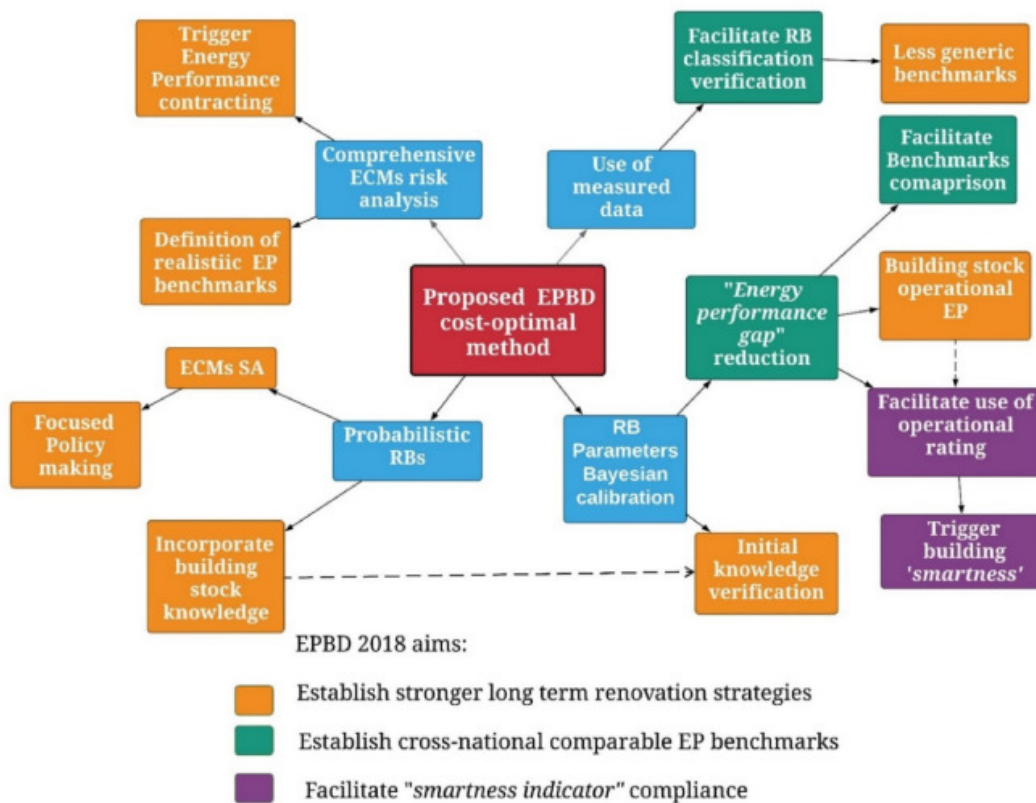


Figure 2.7: Process mind map depicting how the proposed EPBD cost-optimal method can enable MS to meet three of the main aims of the 2018 EPBD directive.

2.6.2.1 | Expressing comparable cross-national EP benchmarks

The proposed approach can make the expression of comparable benchmarks between MS easier in more than one way. First, using individual measured energy consumption data can facilitate the verification of the choice of classification of RBs and the number of RBs required to adequately represent a building stock category under study. Second, the application of the approach makes it possible to specify statistical indicators to quantify the largest variability of Energy Use Intensity (EUI) in a group of buildings that each RB should represent. Such indicators can make the RB definition process less subjective and more coherent between MS. In addition, the potential 'energy performance gap' reduction between the EUI simulated performance and EUI operational performance via the Bayesian calibration of RBs enhances confidence that the derived cost-optimal and NZEB EPIs of RBs will match more closely the improved operational EP of the building stocks under study when upgrading these stocks to comply with the cost-optimal/NZEB EPI requirements. Third, calibration of benchmarks with actual measured energy use

can facilitate the comparison of benchmarks between MS, if the energy end uses and system boundaries for the NCM are harmonised "*following the national annexes of the overarching EPB standards*" [32] and a more objective approach to define NZEB benchmarks from the resulting cost-optimal plots as detailed in Section 2.5.5 is defined.

2.6.2.2 | Enabling stronger long-term renovation strategies

The comprehensive probabilistic risk analysis framework proposed in this research can also facilitate the development of stronger long-term renovation strategies with a solid financial component aimed at "*decarbonising the national building stocks by 2050*" [3]. This framework can have a better potential to allow the definition and quantification of more robust policy and support measures to stimulate energy renovation and meet the Renovation Wave [4] goals through a better handling of uncertainties²⁴. Furthermore, quantification of uncertainties in operational energy savings and financial risks associated with different energy efficiency measures can facilitate decision-making for Energy service companies (ESCOs) [127]. This results from greater assurance that the outcome of energy efficiency measures will truly produce the anticipated benefits and savings when applied to a building stock under study. Both Deng et al. [165] and more recently Lee et al. [166] demonstrated the importance of undertaking a probabilistic approach to address uncertainty for energy performance contracting.²⁵

Such a probabilistic risk analysis framework combined with the use of measured data to verify and limit EUI variability in the selection of RBs can also lead to a less generic approach to EP benchmarking and the derivation of more ambitious but achievable benchmarks. This risks quantification can prevent the establishment of unrealistic EP benchmarks. As Galvin [168] demonstrated, unrealistic benchmarks can be counteractive to building energy renovation. Additionally, the EPBD directive (2018/844/EU) [32] also stipulates requirements that MS must have knowledge of their building stock for renovation strategies to be successful. Incorporating Bayesian calibration in the proposed approach provides the ideal framework for policy makers to incorporate knowledge, learn, and account for new information. Performing SA on building model parameters is also part of this learning process and has the potential to facilitate more targeted

²⁴This is achieved by better handling of key technical and financial uncertainties when defining EPBs and drafting policy measures, which uncertainties of which are the main barriers to energy renovation [42, 43, 44]

²⁵To avoid the financial risk, when energy efficiency measures are evaluated using deterministic calibrated building energy models (BEMs), ESCOs consider a rule of thumb approach to consider only between 60 % and 70 % of the deterministic prediction of energy savings [46]. Furthermore, given financial uncertainties, ESCOs have a problem of '*cream skimming*' [167] by funding only the "*guaranteed energy savings*" and leaving the "*shared savings*" portion to be funded by the building owner.

policy making for renovation by defining and enforcing technical requirements only for the most influential system and envelope parameters.

2.6.2.3 | Facilitating smartness indicator compliance

According to the EPBD (2018/844/EU) [32], the "*energy performance of a building shall be determined on the basis of calculated or actual energy use...*". The (asset) rating calculation approach predicts the EP of a building based on fixed schedules and set points and is independent of user behaviour, whereas operational ratings depend on actual (measured) energy consumption. Defining comfort set-point parameters for RBs probabilistically and inferring them can, in the absence of identifiability issues, allow policy makers to potentially learn about the actual operational energy use of buildings within a stock. Therefore, Bayesian calibration can better probabilistically quantify energy savings through the use of energy-efficient comfort set points and set up benchmarks that encourage energy-efficient occupant behaviour. Furthermore, an operation-dependent approach to EP can also help promote smart building energy management systems by MS to ensure better management of user behaviour in buildings. This understanding of the significance of building energy management systems can make it easier for EU buildings to comply with the '*smartness indicator*' criteria introduced in the 2018 EPBD (2018/844/EU) [32].

2.6.3 | Limitations of Bayesian calibration in UBEM

Despite its potential benefits, Bayesian calibration is highly computationally expensive. The Bayesian process becomes more computationally demanding with the addition of more input data or an increase in the number of parameters to be calibrated [169]. Furthermore, choosing poor prior distributions necessitates more iterations before reaching convergence [170]. In addition, like other calibration methods, Bayesian calibration requires measured energy consumption data from the individual buildings under study to compare model simulation outputs to. This collection of individual energy consumption data is itself a time-consuming process [170] that is not always easy to obtain [128].

Recent research on Bayesian calibration for Building Energy Models (BEMs) focuses on reducing the computational expense of Bayesian calibration by employing one or more of the following techniques:

- **Use of reduced-order models (also called simplified or grey-box models [171]) given they are more computationally efficient than dynamic (white-box) models.** This has been done in multiple studies. Heo [138] and Heo et al. [139] employ

a Quasi-steady heat balance model compliant with the CEN-ISO standards for a university building. Booth et al. [92, 130] and Booth and Choudhary [131] use an EPC quasi-steady tool compliant with CEN-ISO standards for a UBEM housing stock. Zhao et al. [172] conduct a UBEM study of offices using a physics-based reduced order normative energy model. Furthermore, Hedegaard et al. [132] apply the simple hourly method of ISO 13790 [173] to a Danish urban residential neighborhood;

- **Use of simpler and more computationally efficient meta-models including Multiple Linear Regression (MLR) to replace the GPE.** This was carried out in various studies. Tian and Choudhary [69] develop a statistical model to analyse school buildings in London using the Standardised Regression Coefficient (SRC) and Multivariate Adaptive Regression Lines (MARS). Zhao and Magoulès [93] examined various BEM meta-models. MLR was used as a meta-model for a campus building by Li, Gu, et al. [156] and Li et al. [174]. Tian et al. [175] used a retail building to combine SA, correlation, cluster analysis, and linear regression. Zhao et al. [172] used MLR as a meta-model for an office UBEM study. Lim and Zhai [154] compared the accuracy and computational time of various meta-models, including MLR, SVR, ANN and GPE, for an office building. Prieto et al. [133] also compared different emulators for a UBEM residential building block case study in Switzerland;
- **Use of information theory to select a representative subset of the entire data set for calibration.** This approach was demonstrated for a cooling system of a 10-story office building in Chong et al. [176] and for a medium-sized office building in Lim and Zhai [177];
- **Utilising the No-U-Turn sampler (NUTS) Markov chain Monte Carlo (MCMC) algorithm [178] or an improved Metropolis- Hastings (M-H) algorithm in [179].** These algorithms allow for a more efficient exploration of the posterior distribution when compared to the M-H algorithm. This was demonstrated in numerous studies, including Chong et al. [176], for the cooling system of an office building cooling system. In addition, Chong and Menberg [134] and Menberg et al. [121] utilised Stan software [180] that employs the NUTS MCMC algorithm for an office building and a heat pump, respectively;
- **Proposal of a GPE to "*simultaneously calibrate and rank input parameters for building energy simulation models*"** as shown in Yuan et al. [181] for a office building having multiple storeys and

- **Use of only a sample of the entire building stock to generate posterior distributions.** This is demonstrated in UBEM studies, including Sokol et al. [128] for residential houses in Cambridge and Kristensen et al. [113] for single and detached family houses in Denmark.
- Combining Approximate Bayesian Computation methods with machine learning techniques without computing likelihood functions to calibrate BEMs [182]

Higher computational speeds for the Bayesian BEM calibration process enable calibration at lower temporal resolutions, that is monthly, weekly, or hourly versus annually. This approach which was demonstrated in multiple studies can enhance the accuracy of both the calibrated parameters and the predictive model. Yamaguchi et al. [129] compared the weekly versus annual energy consumption calibration results for an urban-scale model of a food supermarket. Kristensen, Choudhary and Petersen [147] contrasted the calibration results for a single family home from six-hour, daily, weekly and monthly district heating temporal resolution data. In addition, Sokol et al. [128] compared monthly versus annual energy use data to calibrate residential buildings in UBEM.

The research on the Bayesian calibration of BEMs has also concentrated on the barrier to collecting observed (measured) data using the following techniques.

- Using only a sample of the whole building stock for calibration at lower temporal resolutions because fewer data are likely to be available at these temporal resolutions. Yamaguchi et al. [129] demonstrated this approach for a UBEM supermarket study;
- Combining correlation and hierarchical clustering to identify informative data to check the possibility of obtaining reliable outcomes in the event of missing data. Additionally, computational time can also be improved using informative data. Tian et al. [175] applied this approach for a retail building;
- Use of a "*hierarchical Bayesian framework for calibrating micro-level models with macro-level data*" as shown in Booth et al. [130];
- Replicating energy data of the building stock using data from energy surveys as demonstrated by Zhao et al. [172] for office buildings and
- Geometrically representing archetypes of detached single family houses as single rectangular boxes. This approach was applied in Kristensen, Choudhary, Pedersen et al. [147] and Kristensen et al. [113].

More recently, the research on Bayesian calibration has also focused on:

- Deeper analysis of model discrepancies within the Bayesian calibration framework and the identification of methods to improve model accuracy. This analysis was done in Menberg et al. [121] and Monari [183];
- Parameter identifiability concerns when undertaking Bayesian inference in BEM as analysed in Chong and Menberg [134] for an individual office building and Yi et al. [184] for a DOE RB;
- Bridging engineering simulation with demand regression using Bayesian inference to allow forecasting the energy demand of cities in Yu [185] and for residential scale space heating demand in Hedegaard et al. [132].

As detailed above, the literature has attempted to address many limitations of Bayesian calibration for BEM in terms of computational expense. However, procedures for replacing a computationally intensive building physics (RB) energy model with a more computationally efficient building physics model that retains the same dynamic nature and provides a statistically acceptable difference in simulation output have not been adequately addressed for multi-functional buildings, as explained in Gatt et al. [35]. Accurately modelling such multi-functional RBs made up of multiple activities requires thermal zones to be defined as a minimum according to the function of the space and the method used to condition the zone. This approach contrasts with more simplistic approaches to define thermal zones in UBEM, including the single zone models, one zone per floor models or multi-zone per floor models that distinguish only between perimeter and core zones [186]. These approaches do not consider or only consider in a simplified way the function diversity of the spaces. Such approaches for defining zones in BEM can be found and compared in [187, 188, 189, 190, 191, 192, 186, 1]. Accelerating simulation runs from the building physics model will reduce the computational expense of fitting the meta-model in the Bayesian calibration framework explained in Section 2.5.3.

An approach to improve the computational speed of multi-functional RB energy models to fit within the Bayesian calibration framework explained in Section 2.5.3 is conceptualised by the author of this thesis in Gatt et al. [35] and is termed the '*reference zone*' approach²⁶. In this approach, it is proposed that a full-space physical whole-

²⁶A similar but simpler concept to the '*reference zone approach*' to model school buildings in Malta was first applied by the author of this thesis in Gatt [193]. The proposed hierarchical modelling approach in this research allows policy makers to define customisable energy performance benchmarks within the framework of the EPBD cost-optimal method for school buildings having different orientations and percentage distributions of functional spaces.

building energy model composed of multiple thermal zones, with the thermal zones defined as a minimum according to the function of the space and the method used to condition the zone, is divided into a number of simplified geometric representations or building blocks, each assigned a multiplier. The building blocks are termed '*reference zones*', where each '*reference zone*' is a representative functional unit of a sub-activity. A sub-activity, a subset of an activity, must be defined for a space that offers the same service (activity) but has a different defining condition impacting EP, such as a different space conditioning system, schedule, or orientation. The '*reference zone approach*', which is detailed in Section 4.3, has been hypothesised in Gatt [35] to allow a simple and flexible aggregation of EP from the '*reference zones*', to individual buildings and even up to the urban level. This flexibility makes the approach especially suitable for modelling multi-functional heterogeneous buildings stocks to represent building stock diversity, while allowing faster computational times. However, this approach has yet to be validated in terms of simulation results accuracy for a multi-functional RB case study. It should be noted that representing the various building functions more accurately, the disadvantage of defining detailed zoning approaches, as opposed to simpler zoning approaches, such as the perimeter and core zone approach, is more detailed building information, increased user intervention to create zones, and a larger number of model parameters [1].

2.7 | Conclusion

This chapter described the current EPBD cost-optimal method and compared it methodologically to conventional urban energy modelling (UBEM) studies. Based on the similarities and differences identified between the two approaches, a link between the two methods was established, and the common uncertainties that impact policy making were defined. Although few attempts have been made to address building stock uncertainties specifically for the EPBD cost-optimal approach, the state-of-the-art UBEM literature has provided multiple techniques to better handle uncertainties and consider building stock diversity when compared to conventional UBEM studies.

Based on the link and methodological similarities between conventional UBEM and the EPBD cost-optimal method, in line with the aim of this research, a hypothesis was made as follows. It was hypothesised that the handling of the uncertainties and diversities of the building stock in the EPBD cost-optimal method can be better addressed by applying state-of-the-art UBEM techniques employing '*Bayesian calibrated RBs*' to the current approach. Based on the established link between UBEM and the EPBD cost-optimal method and a systematic literature review of UBEM studies, a novel cost-optimal method was proposed to address what the researcher believes is the best approach to address the research gap of establishing a comprehensive and conceptual framework to integrate such techniques built upon '*probabilistic Bayesian calibrated RBs*' to the current cost-optimal method to better handle building stock uncertainties and diversity and therefore to meet the aim of this research. Subsequent chapters will validate the proposed cost-optimal method through its application to a building stock case study to enable the hypothesis presented in this thesis to be accepted or rejected.

Furthermore, to address the specific methodological needs of the proposed EPBD cost-optimal method within the EC framework, including its application to '*small*' ($X \gg N$), multi-functional and heterogeneous building stocks, the other research gaps that need to be addressed to meet the specific aim and objectives of this research are summarised below.

- A machine learning methodology to define RB energy models for '*small*' ($X \gg N$), multi-functional and heterogeneous building stocks has not been developed sufficiently.
- Methodologies replacing a computationally intensive (RB) physics energy model with a more computationally efficient building physics model that retains the same dynamic nature and provides a statistically acceptable difference in simu-

lation output to reduce the computational expense of performing multiple simulation runs when employing Bayesian calibration have not been adequately addressed in the literature for multi-functional buildings.

- A harmonised and ordinal scale approach has not been established for policy makers to objectively define NZEB EP benchmarks having different levels of ambition within the EPBD cost-optimal method framework.
- A probabilistic approach to risk and uncertainty analysis that considers the joint impact of technical and financial uncertainties on NZEB EP benchmarks has not been specifically developed to comply with the EPBD framework required for the proposed approach. Such a framework requires MS to consider both a financial and macroeconomic perspective to LCC and to perform a SA on the impact of different price development scenarios and discount rates on the resulting EP benchmarks for a defined RB. Furthermore, the propagated uncertainty in EP improvements and LCC risks for a defined NZEB benchmark level as generated from the 'Bayesian calibrated RBs' requires to be visualized, statistically quantified, and interpreted to meet the aim and objectives of this research.

Defining reference buildings for small multi-functional building stocks - a machine learning approach

Chapter Abstract : Defining deterministic RBs that represent the building stock under study is the preparatory stage to execute the proposed EPBD cost-optimal method. There is, however, no standard methodology to define RBs. An approach was therefore developed to define RBs for *'small'*, multi-functional and heterogeneous building stocks, given that the heterogeneity and data-processing challenges to defining RBs for such buildings have not been adequately addressed in the literature. The approach uses unsupervised and supervised machine learning techniques to systematically combine building feature data with individual metered energy consumption data to address the high-dimensional data processing challenges inherent in such building stocks. The approach also ensures that the resulting RBs are fully characterised for bottom-up modelling and the EPBD cost-optimal method. Furthermore, a specific *'functionality feature'* is also introduced, and its data are processed to allow the RB clustering solution to better represent the diversity of the services offered by the individual buildings in a stock. The approach was successfully applied to a 5-star hotel building stock which derived statistically significant feature explanatory variables to group 10 hotel building observations under study into 6 clusters, for which a RB must be defined for each cluster. Furthermore, the RB clustering solution was shown to provide a more comprehensive approach to defining RBs when compared to clustering only on easily obtainable bench-marking variables or directly on the operational metered energy consumption. This is because the developed method can uncover building characteristics and functionalities required to successfully characterise a heterogeneous building physics RB energy model.

3.1 | Introduction

Defining deterministic RBs that are representative of the building stock under study is the first step in the current EPBD cost-optimal method, as described in Section 2.2.1. The definition of deterministic RBs is also the preparatory stage for the proposed EPBD cost-optimal method described in Figure 2.5 and forms the basis on which probabilistic RBs are developed. Furthermore, the choice of RBs has a critical impact on building stock energy modelling accuracy and the predicted EP improvement potential of a building stock resulting from implementing different energy efficiency measures for policy making [72]. Despite the importance of the correct choice of RBs to study the energy performance (EP) of a building stock, Chapter 2 identified that there is no standard methodology to define RB energy models, and their development remains a significant challenge to model building stocks [73]. To facilitate the RB definition process and make it more objective, approaches employing data-driven machine learning techniques in building stock studies have been developed [194, 195] as discussed in Section 2.2.3.1. However, the main focus of these studies was developing RBs for large population residential building stocks rather than smaller population, non-residential, multi-functional and heterogeneous building stocks. The development of RBs for these building stocks has not been appropriately addressed in the literature, as concluded in Chapter 2, and this will be further elaborated on in Section 3.1.2.

3.1.1 | Chapter Objective

The objective of this chapter is to develop a machine learning methodology to define RBs for '*small*' multi-functional, heterogeneous building stocks. For the scope of this research, a '*small*' building stock is one where the number of explanatory variables ' X ' impacting EP is greater than the number of building observations ' N ' in a population or sample under study.

3.1.2 | Background on studying the EP of multi-functional building stocks

Finding robust approaches to better study the EP of non-residential building stocks is critical given that most of the current knowledge on RBs and building stock modelling in the EU is on residential buildings [27, 38]. This results from the fact that residential buildings constitute to 75 % [196] of the EU building stock, but also due to the challenges faced when modelling the more diverse non-residential building stock, compris-

ing multiple activities and uses [27, 37, 38]. Studies of the EU building stock, including [197, 198], have recognised the vast heterogeneity of the non-residential building sector in the EU in terms of typologies, functionality, form, and size. This diversity in the building stock is also observed within a group of buildings that serve the same main function, including hotels, as detailed in [41, 27, 199] and shopping centres, as explained in [200].

Furthermore, the different services offered are an important factor that explains the diversity in energy demand, consumption, and EP of individual buildings in a non-residential building stock that serve the same main function. Given the multitude of services offered, most non-residential buildings, including hotels [27, 199] and shopping centres [200], are defined as multi-functional buildings where the space to serve the main function of the building is coupled with spaces to accommodate other functional activities [196]. For example, for a hotel, guest rooms that serve the main function of accommodation can be coupled with spaces that serve other activities, including restaurant(s), laundry, conference hall(s) and swimming pool(s). Although these activities complement the core function, they account for a significant proportion of the energy use of these buildings and often characterise the marketing differentiation strategy and business success of a commercial building. This makes the diversity of a multi-functional building stock with a large number of potential activities an unavoidable characteristic, making the process of defining a few RBs to study or derive EPIs to be representative of a whole building stock difficult, as explained by Buso et al. [27] and by the author of this thesis in Gatt et al. [35].

3.1.2.1 | Challenges in studying multi-functional building stocks

The challenges to study multi-functional building stocks can be divided into two types:

1. Building physics RB energy modelling approach challenges
2. Machine learning data processing challenges

as detailed in the following sections.

3.1.2.1.1 Building physics RB energy modelling approach challenges

The first challenge in studying multi-functional buildings lies in the RB modelling approach and the corresponding intensive data collection process required to characterise and simulate the EP of multi-functional buildings. To consider the diverse activities of such building stocks, RBs must be modelled with thermal zones defined according to the function of the space, given different schedules and internal loads, and the method

used to condition them. To develop RBs for this modelling approach requires information on the functions served by each or a sample of individual buildings in a stock to be collected. This functional information is not easy to obtain and extract, but possible sources include planning applications, energy audits, or Energy Performance Certificates (EPCs). Once collected, the data for each building must be further processed to objectively define each functional activity in terms of parameters such as floor area or volume to allow RBs to be developed and characterised.

The above modelling approach for multi-functional buildings contrasts with the simpler modelling approaches employed in the various GIS tools reviewed in [201] and the simplified Building Energy Modelling (BEM) zoning approaches explained in Chapter 2. These simpler approaches, which are more suitable for residential buildings and less diverse buildings stocks, generally consider each building observation as having only a single primary function and do not or only partly distinguish between space functionalities in the building.

3.1.2.1.2 Machine learning data processing challenges

The high-dimensional data set to define functional activity information, coupled with a large amount of data on operational and physical factors that affect the EP of such buildings, results in a high-dimensional characterisation design matrix (model) with multiple potential classification or clustering solutions to define RBs. Furthermore, using an unweighted clustering approach will give similar importance to each explanatory variable in the design matrix that shapes the clustering solution, which can dilute the impact of the most important explanatory variables that explain energy consumption or EP when defining RBs. This issue is inherent to the national typology methodologies employed, for example, by Mata et al. [202] and the TABULA project [75, 203]. These methodologies classify RBs according to standard feature classifiers and characterise them using only building feature data without considering the relative importance of different building characteristics on metered energy consumption.

One possible approach to reduce subjectivity and provide a more transparent and stable approach to defining RBs is to cluster on only the statistically significant variables that explain the operational EP of building observations in a stock [195]. This explanatory variables dimension reduction process may also facilitate the probabilistic calibration process of the proposed EPBD cost-optimal method by screening the number of parameters that need to be considered for sensitivity analysis and calibration. However, to enable the EP of RBs to be studied using a bottom-up approach, it is important that the design matrix of the retained explanatory variables or principal components that shape the clustering solution to derive and characterise RBs adequately describe

the data categories of form, envelope, equipment, and operation presented in Torcellini et al. [204]. These data categories are also called subsets of features in Corgnati et al. [26]. Therefore, retaining only one or two dominant explanatory variables that satisfactorily explain EP but only partially cover these data categories is insufficient to derive and characterise RBs. Similarly, clustering directly on individual energy consumption data will provide the best segregation of the building stock in terms of EP. However, it will fail to directly diversify the clustering solution in terms of the above data categories to characterise each RB. This characterisation is essential to define, calibrate model parameters, and apply potential energy efficiency measures to the building physics RB energy models.

A mathematical approach to identify the most important and significant explanatory variables that explain EP for the dimension reduction process is through a top-down and supervised learning regression method that uses individual metered energy consumption data as the dependent variable. Regression has been used to obtain RBs both to validate the classification of the building stock in Aksoezen et al. [76] or to identify significant variables that explain the metered energy consumption on which to apply clustering to define RBs for a large residential building stock in Ireland [77] and for office buildings in New York [205].

However, compared to residential and office buildings, heterogeneous multi-functional buildings have a larger number of potential explanatory variables explaining EP. Thus, establishing a relationship between these large number of variables and individual operational EP is challenging given that regression is more prone to multi-collinearity and over-fitting issues [206]. These issues makes it more difficult to comprehensively identify all statistically significant variables that impact EP to comprehensively define building physics RB models.

These high-dimensionality challenges become even more pronounced for a building stock having a '*small*' number of observations, where the number of explanatory variables '*X*' impacting EP is greater than the number of building observations '*N*' in a population or sample under study. These '*small*' building stocks are synonymous with a specific group of unique buildings that deserve special attention or when a '*small*' building stock sample size is chosen to represent the whole building stock from a much larger population. Choosing a '*small*' building sample size may be triggered by data collection constraints including the lack of availability of metered energy consumption data.

3.1.3 | Tackling the challenges in studying 'small' multi-functional building stocks

This chapter develops a systematic, robust, and more objective approach based on multiple machine learning techniques to tackle the above challenges in studying 'small' multi-functional building stocks. The following sections will apply and validate the approach using the 5-star hotel building stock on the island of Malta.

It must be noted that the approach developed to define RBs in this chapter is complementary to the two-stage building stock classification and characterisation approach shown in Figure 2.4, which is generally adopted to develop RBs for the EPBD cost-optimal method and UBEM studies. More specifically, the approach in this chapter details a RB characterisation stage approach for a 'small' multi-functional building stock cluster identified from the building stock classification stage of the RB definition process depicted in Figure 2.4.

3.2 | Method

The approach to develop RBs for a 'small', multi-functional building stock is shown graphically in Figure 3.1 and consists of three (3) main phases:

1. Data Collection and Classification
2. Data Processing
3. Data Post-Processing.

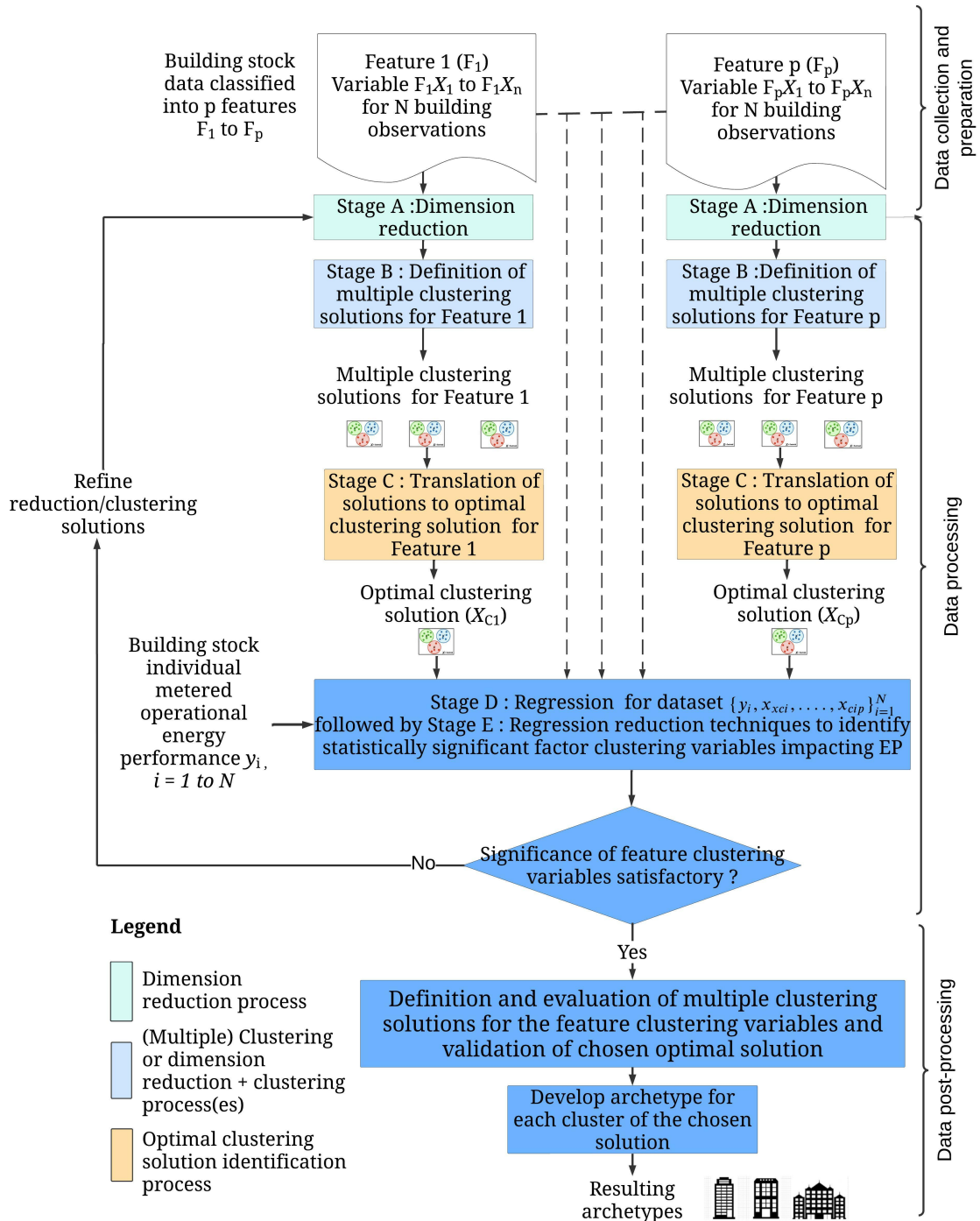


Figure 3.1: Flow chart depicting the method to define RBs for 'small' multi-functional heterogeneous building stocks

3.2.1 | Data Collection and Classification phase

This phase first involves data collection for ' N ' building observations of a building stock under study on all relevant geometric and non-geometric features, including operation, form, envelope, and system data [26]. This data can be collected from numerous sources, including EPCs and energy audits. Once the data are collected, each variable in the collected data set is classified according to ' p ' features, F_1 to F_p .

To specifically cater for the requirements of diversity in the space functionalities of multi-functional and heterogeneous building stocks, the proposed approach introduces two additional features that complement the "*operation*", "*form*", "*envelope*", and "*systems*" presented by Torcellini et al. [204] and Corgnati et al. [26] (refer to Figure 2.4 to characterise the building stock as follows:

1. **A functionality feature** : The functionality feature is comprised of variables that define and quantify the functionality, including the services offered by each individual building. Segregating these variables into a specific feature ensures that the diversity of services offered by individual buildings in a multi-functional building is well represented when deriving and characterising RBs. Furthermore, this feature may contain a large number of explanatory variables and therefore requires a specific and objective data reduction processing approach.

Unlike the majority of variables comprising the features presented by Torcellini et al. [204] and Corgnati et al. [26], the variables representing the '*functionality*' feature of a building are not a building physics model parameter that can be easily defined probabilistically, but are represented and fixed by the geometry of the RB whole-building physics model and its zoning configuration. Therefore, the functionality feature as an additional feature to those presented by Torcellini et al. [204] and Corgnati et al. [26] allows the variability in functionality to be optimised when deriving RBs in the following data-processing phases¹.

2. **A Benchmarking feature** : This feature includes normalisation variables that derive Energy Performance Indicators (EPIs) to be used for comparison of EP rating of the individual buildings according to the main service they cater for. This feature is usually characterised by one or more variables that explains a major portion

¹Defining a RB model using the hierarchical and reduced space modelling '*reference zone*' approach conceptualised by the author in Gatt et al. [35], introduced in Chapter 2 and detailed in Chapter 4, can potentially provide more flexibility to accommodate the diversity of functionality within a group of buildings under study as detailed in Chapter 4. However, this chapter will consider the more established and validated approach to BEM that defines whole-building (full-space) and multi-functional RB energy models divided according to different zones to distinguish between the various functional activities of the building.

of the building's energy consumption. Given the low data dimensionality of this feature, no or minimal further data reduction processing is required. Furthermore, given the potential dominance of the EPI normalisation variables over other explanatory variables in supervised learning machine approaches, their segregation into a specific feature allows variables from other data categories to be independently reduced and therefore better statistically represented in the RB definition process for a more comprehensive RB energy modelling characterisation.

One must note, given that RBs require to be defined probabilistically in the proposed EPBD cost-optimal method, each '*p*' feature must prioritise the inclusion of variables critical to driving the segregation of individual buildings into different clusters. Then a separate RB energy model must be defined for each cluster. More specifically, less priority should be given to parameter variables that can be easily defined probabilistically. As an example, for Heating, Ventilation, and Air Conditioning (HVAC) equipment, an important system feature variable required to cluster the building stock is the type of HVAC system equipment installed for each building observation, such as water-cooled chillers or an air-cooled Variable Refrigerant Flow (VRF) system for space cooling. Therefore, to derive RBs, the type of HVAC system for each observation must be included in the feature variables data set as input to the data processing stages in the next phases, and its variability must be fully considered to drive the final RB clustering solution. For each derived RB energy model having a specific HVAC system, the diversity of HVAC parameters such as Coefficient of Performance (COP) can then be defined probabilistically.

3.2.2 | Data processing phase

The step uses multiple machine learning techniques to reduce each feature's high-dimensional explanatory variable data set to a minimum number of regressors to perform regression with metered energy consumption data, the dependent variable. A minimum of one regressor must be retained from each defined feature to allow RB energy models to be comprehensively characterised. This step is an iterative process, and data reduction is carried out until a significant statistical relation between each regressor and the dependent variable can be defined. These significant regressors explaining the metered energy consumption make up the data set for input in the data post-processing stage. The data post-processing stage then applies additional machine learning approaches to the data set to divide the building observations into clusters, where each cluster is used to develop a RB energy model to study the building stock.

The iterative data processing stage consists of five sequential sub-stages as depicted in Figure 3.1:

1. **Stage A** : Explanatory variables dimension reduction stage for each feature separately;
2. **Stage B** : Generation of multiple potential clustering solutions on the Stage A reduced data set for each feature separately;
3. **Stage C**: Identification of an optimal clustering solution for each feature separately from the multiple clustering solutions generated in stage B;
4. **Stage D**: Regression of the clustering solution explanatory variables resulting for each feature with individual metered energy consumption data;
5. **Stage E**: Regression model reduction and regressors significance analysis;

Stage A to stage C are individual feature processing stages, and not all of these stages may be required to be performed for each feature depending on the dimensionality and the specific data processing requirements of the feature under study. This concept is shown in the case study demonstrating this approach in Section 3.4.

3.2.2.1 | Stage A : Feature explanatory variables dimension reduction stage

In this stage, various machine learning techniques and combinations of techniques are used to reduce the high dimensional data set for each feature separately. These techniques include:

- **Classification** of a feature data set into sub-features to group the data into defined classes and reduce its dimensions. Reviewing the literature and energy audits of the building typology for the building stock under study facilitates such data classification and makes it more objective, as demonstrated in the case study in Section 3.4.
- **The transformation of variables to fewer uncorrelated variables termed principal components.** The available techniques to transform the data into smaller components depend on the type of variables in the data set to be analysed are discussed in [207] and include:
 1. **Principal Component Analysis (PCA)** for continuous variables applied and reviewed in various building stock EP literature including [91, 83, 103, 1];

2. **Multiple Correspondence Analysis (MCA)** for categorical variables, as explained in [208];
3. **Factor Analysis of Mixed Data (FAMD)** when the data set contains both continuous and categorical variables, as explained in [207];

3.2.2.2 | Stage B : Generation of multiple clustering solutions for each feature

Following the explanatory variables dimension reduction process, the reduced data sets for each feature can be processed to further reduce their dimensionality and minimise the number of regressors in the post-data processing stage. For this stage, unsupervised machine learning algorithms such as clustering can be applied on each reduced feature data set, to divide it into a categorical variable defining a clustering solution. Potential clustering algorithms include K-means, Agglomerative Hierarchical Clustering (AHC) and k-prototypes. Various building stock EP studies have applied K-means, such as [87, 81, 88, 89]. Agglomerative Hierarchical Clustering (AHC) was applied in [86, 34], while k-prototypes is used to cluster mixed data as conceptualised in [209].

Clustering is subjective and the resulting clustering solution, amongst others, depends on various clustering process factors. These factors include the chosen clustering algorithm, the defined clustering parameters for the chosen algorithm, the number of clusters, and other factors such as the variables included in the clustering analysis and the way the variables are defined (continuous, categorical, ordinal, etc.). Therefore, it is vital to make the clustering method less sensitive to the clustering process used. Objectivity is improved by identifying and investigating multiple clustering solutions via the sequential variation of different cluster process factors to generate multiple, C in number, potential clustering solutions for each feature comprised of the reduced data set. This approach results in a multi-dimensional matrix data set of categorical data having C columns and N (number of building observations) rows.

3.2.2.3 | Stage C : Identification of an optimal clustering solution for each feature

The final clustering solution for each feature is then achieved through the identification of the most recurrent groupings among the multiple generated clustering solutions. The process can be aided using categorical data clustering algorithms that include k-modes conceptualised in [210] or AHC on the resulting MCA principal components explained in [207]. The final clustering solutions for each feature F_1 to F_p are then combined to form data set $\{x_{ci}, \dots, x_{cip}\}_{i=1}^N$.

3.2.2.4 | Stage D : Regression of the clustering solutions with energy consumption data

In this step, regression is performed for data set $\{y_i, x_{ci}, \dots, x_{cip}\}_{i=1}^N$, where $\{y_i\}_{i=1}^N$ is the metered energy consumption data for each building observation, making up the dependent variable vector Y , and $\{x_{ci}, \dots, x_{cip}\}_{i=1}^N$ is the data set of the final clustering solutions that make up the matrix of regressors, X .

3.2.2.5 | Stage E: Model reduction and regressors significance analysis

In this step, model reduction techniques such as stepwise regression, applied in many building stock studies EP studies including [211, 212, 213, 214], are used to find a reduced-order model that best explains the data and retains all significant regressors that explain the dependent variable.

This step is iterative, and if not all regressors that explain the features are retained as significant, the data-processing phase needs to be refined, or a larger data set containing more hotel observations will need to be employed. This process must be repeated until all regressors are statistically retained in the reduced model.

3.2.3 | Data post-processing phase

In this step, the statistically significant regressor data set is further processed using machine learning approaches such as clustering to divide the building stock observations into clusters. Multiple clustering solutions must be identified, compared, and analysed to increase objectivity before deriving the final RB clustering solution XC_{RB} . For each cluster in XC_{RB} , a RB building physics energy model based on an '*archetype*' solution or '*Real (average) RB*' as explained in Chapter 2, Section 2.2.3.1 must be developed to study the building stock.

The clustering solution is then validated using a train-test set approach that includes the use of test sets with the same building observations but with occupancy and energy consumption data generated from a different period or year. This validation assesses the robustness and stability of the final RB clustering solution XC_{RB} . For a building stock with a sufficiently large number of observations, a cross-validation approach, such as k-fold, detailed in [215], can also be applied by splitting the observations into a training and test set to validate the regression model.

3.3 | Hotel building stock case study

The above clustering process is applied to the 5-star hotel building stock on the island of Malta, consisting of ten (10) hotels and representing more than 90 % of the 5-star hotel population in 2017. Improving the EP of hotels is an especially important area of focus for Malta, as tourism on the island contributed to 26.7% of the Gross Domestic Product (GDP) in comparison to the 10.2 % of the world GDP in 2016 and is expected to rise to 34.6 % by 2027 [216]. This increased demand intensifies the need for energy-efficient and sustainable hotel accommodations. Furthermore, such building stocks provide an ideal area of focus to meet the 2050 carbon neutrality targets stipulated in the Green Deal [3]. This is because hotels in Southern Europe and the Mediterranean have been shown in various EU projects² such as in HES [220] and NeZeH [221], to have a high potential for energy savings, with a 63 % in average primary energy savings reported in NeZeH [222, 223].

The 5-star hotel building stock under study can be depicted as an identified building stock cluster derived from the classification stage approach of the RB definition process in Figure 2.4, which must be separately characterised when defining RBs. The requirement to characterise 5-star hotels separately in Malta stems directly from the prescription of the Maltese accommodation legislation [224], which ranks hotels in the different star categories based on their achievement of a minimum number of points for a different pre-defined set of criteria and services. Furthermore, the requirement to consider the star rating as a benchmarking criterion for hotels in Malta has also been statistically established in the BEST project [225] commissioned by the Malta Hotels and Restaurants Association (MHRA). The project applied descriptive statistics to compare between the operational EP of hotels with different star ratings. This hotel classification according to star rating is also consistent with other hotel studies in literature, including Pieri et al. [83] to energy classify hotels in Athens, Bianco et al. [226] to study the EP of the Italian hotel building stock, and Oluseyi et al. [227] to assess hotel energy consumption in Nigeria. Furthermore, once classified according to star rating, no further classification of the hotel building stock according to location and age is required since Malta falls under a single Köppen climate classification [228], and all hotel observations under study were built before the establishment of minimum EP requirements for the envelope and technical building systems [229, 230].

²Various EU projects were implemented during the last twenty years aiming to improve the operational energy performance of the hotel sector. Such projects include XENIOX (2002-2003) [217], HOTRES [218] (2001-2003), RELACS (2010-2013) [219], HES (2008-2011) [220] and NeZEH (2013- 2016) [221].

Tourism accounts for 8 % [231] of total global CO₂ emissions³. The hotel industry is characterised by high energy intensity [199], with significant emissions reaching up to 21 % [233] of the the total CO₂ emissions of the tourism sector. This energy intensity is more than ten times higher per floor area than in residential buildings [234], which is primarily attributed to the presence of specific features that include 24-hour operation and an overall high level of comfort provision, which are not associated with the buildings' typical use [235, 236, 237, 238, 239]. Such non-hosting facilities that include kitchens, laundry, pools, and spas can contribute up to 35 % of the total energy consumption [238].

Given the multitude and potential diversity of such additional services found mainly in 5-star hotels, make this building stock an ideal case study of a '*multi-functional and heterogeneous*' building category to demonstrate the proposed clustering method. In fact, hotels have been described as "*comfort or service-orientated accommodations*" [40] having a high degree of heterogeneity [27] when considering individual characteristics such as business size leading to the conclusion that the "*the idea of a typical hotel, as well as its respective performance remains vague*" [41]. To counteract this heterogeneity, hotel asset rating benchmarking studies have recognised the importance of differentiating between "*hosting and non-hosting functions*" in Tsoutsos et al. [223] or between "*typical and extra energy uses*" in Buso et al. [27], when establishing suitable EP benchmarks for the EPBD. Thus, hotel buildings further justify the methodology in the development of multi-functional RB energy models to statistically account for the diversity in functionality between the individual buildings in a stock.

The heterogeneity of the hotel building stock is reflected not only in the building characteristics but also in the variation in the EP indicators themselves. For example, Lu et al. [240], Oluseyi et al. [227], Wang et al. [239], Pieri et al. [83] and Boemi et al. [241] reviewed average consumption indicators, primarily based on $kWh.m^{-2}.yr^{-1}$, for hotel buildings worldwide and reported a great variation in intensity of energy use not only between countries⁴, but also for regions within the same country and over different time periods [241, 83]. The reason for this variation is that the EP of the hotel varies depending on many factors, which can be grouped in terms of geographical location, type (tower or resort), use, and category [199].

Furthermore, the '*small*' building stock addressed in this thesis provides an ideal case study for the challenges that this method aims to address. The large number

³In Malta, in 2013 the hotel and accommodation sector alone contributed to 10.96 % of the final electricity consumption, while the sector was also the main consumer of liquid and gas fossil fuels for space heating in the non-industrial services sector [232].

⁴In Europe, the normalised average energy consumption of hotels lies between 240 and 300 $kWh.m^{-2}.year^{-1}$ [199]

of factors that potentially affect operational EP, as evidenced by hotel building stock studies employing a top-down approach⁵, makes them susceptible to high-dimensional machine learning challenges detailed in Section 3.1.2.1. The multiple factors considered when studying the EP of hotel building stocks include location/weather [235, 262, 239, 261], size [254, 239, 260], construction year/number of years after the last retrofit [263, 264, 254], types of energy carriers/systems [254, 265], occupancy (occupancy rate, guestroom, guest night and revenue) [40, 262, 264, 265, 260, 239, 266], types of services, amenities and activities made available to guests [263], and the star rating of hotels [264, 265, 254, 255].

3.4 | Application of the developed method to the hotel building stock case study

This section applies the methodology described in Section 3.2 to the 5-star hotel building stock case study to segregate the building stock observations into clusters to define RBs. Figure 3.2 depicts the specific features, variables and data processing steps as applied to the actual hotel building stock when executing the developed approach.

⁵Top-down building stock studies include [242, 243, 244, 235, 87, 245, 246, 247, 248, 240, 249, 250, 227, 251, 252, 253, 254, 255, 256, 257, 258, 259, 260, 261]

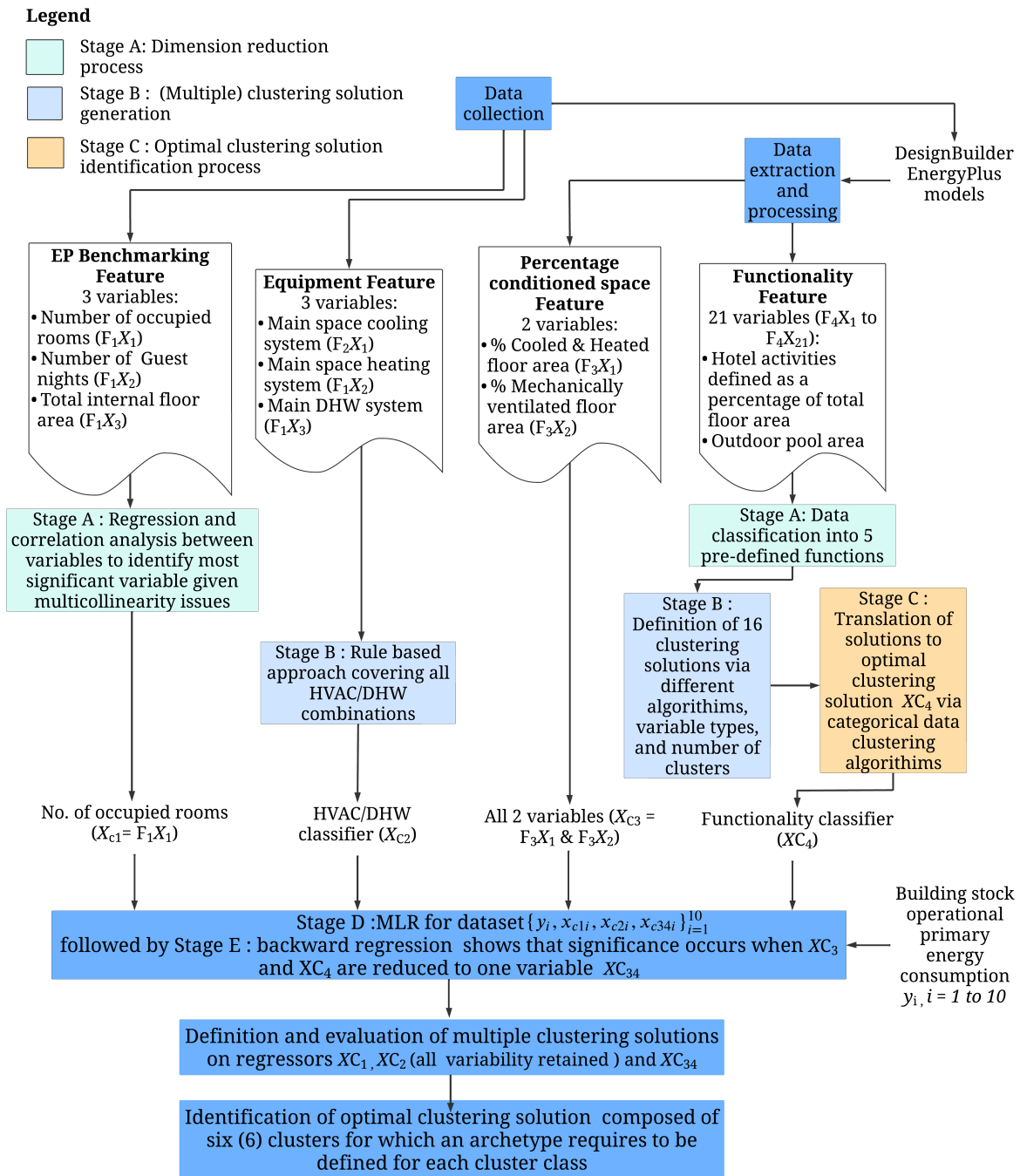


Figure 3.2: Flow chart showing method used to define RBs for the hotel building stock case study

3.4.1 | Data collection and preparation

Data for the case study were collected from individual hotel energy audits, planning application documentation, and actual site visits in collaboration with hotel management and engineers. The following data and documentation were collected for each hotel observation:

- **Building Envelope** comprised the U-values of the building elements, the Solar Heat Gain Coefficient (SHGC) of the glazing and the glazing shading configuration of the guest rooms.
- **Hotel 2D floor plan and elevation layouts for each floor** provided in DXF and other bitmap-type formats. The plans show floor spaces labelled and divided according to the functional activities of the building. For each functional activity zone, the respective space condition classification distinguished between zones that are only cooled heated, zones that are only mechanically ventilated, and zones that are both cooled & heated with mechanical ventilation. This information was gathered through the feedback of the hotel management and the actual site visits.
- **Building Equipment** in terms of the main HVAC system and the Domestic Hot Water (DHW) system required to satisfy the demands of the building's HVAC and DHW. The main parameters describing the EP of the HVAC system, such as the COP for heating and cooling, were also collected from the equipment nameplate or the manufacturer's literature.
- **Building occupancy** with monthly resolution defined based on the number of occupied rooms and the number of guest nights for the years 2017 to 2019. This data was also converted to an annual resolution.
- **Metered energy consumption data** with monthly resolution for site electricity, fuel oil and liquid fuel were also collected for the years 2017 to 2019. The data was converted to operational primary energy consumption and kg of CO₂ emissions both on monthly and annual resolutions using local conversion factors for each fuel to normalise its impact on primary energy and kg of CO₂ emissions equivalent, as required in the EPBD cost-optimal approach [55].⁶

⁶The following conversion factors were used. Site electricity (kWh) to kg of CO₂ emissions equivalent: 0.452, site LPG in litres to kg of CO₂ emissions: 0.215, site liquid fuel oil in litres to kg of CO₂ emissions: 0.252, site electricity in kWh to Primary energy in kWh: 2, site LPG in litres to Primary energy in kWh: 7.39, site liquid fuel oil in litres to Primary energy in kWh: 11.39. These electricity conversion factors data were provided by local policy makers and also reflect the conversion factors applied in the the BEST study [225].

For each separate hotel building, the 2D floor plan and elevation layouts were imported into DesignBuilder [267], a software that provides a Graphical User Interface (GUI) to EnergyPlus [268], offering whole building energy simulation capabilities. These layouts enabled tracing the perimeters of the blocks, the partitions, and the facades to build the geometry of the virtual 3D model of the ten (10) hotel buildings. The DesignBuilder models are depicted in Figure 3.3. The collected technical and operational data parameters served as inputs to each building energy model. Each hotel model was divided into multiple thermal zones, combining spaces having comparable functions, operational schedules, and properties into one zone [269, 270].

Once 3D energy models were developed in DesignBuilder, CSV files containing geometric and non-geometric information of each configured model data were generated by the DesignBuilder software [267] using the inbuilt EnergyPlus IDF ASCII files. A Microsoft Excel workbook was programmed and validated to automatically extract and process the desired geometry, including form and functionality information for each building model. The information generated after this processing exercise for each hotel included the total internal floor area, the space cooled and heated floor area, the mechanically ventilated floor area, and the floor area allocated for each functional activity within the building.

A subset of variables from the above-collected data for each hotel observation were classified according to the following features:

- **Benchmarking EP feature**, which is composed of a data set that quantifies the annual number of occupied rooms, the annual number of guest nights, and the total internal floor area. These are common normalisation variables used in the literature [271, 272, 273] to derive EPIs or benchmark hotel buildings' operational EP.
- **Equipment (or technical building energy services) feature** is made up of three (3) variables explaining building's main space cooling, space heating, and DHW systems.
- **Percentage Conditioned space feature** is made up of variables that give prominence to comfort and indoor air quality (IAQ) when determining EP levels of a building stock in line with the new EPBD [32]. These two variables are the air-conditioned and the mechanically ventilated floor areas each expressed as a percentage of the total internal floor area of the building. This feature is required because the level of space conditioning varies between the hotel observations; for example, not all the hotels have air-conditioned circulation zones.

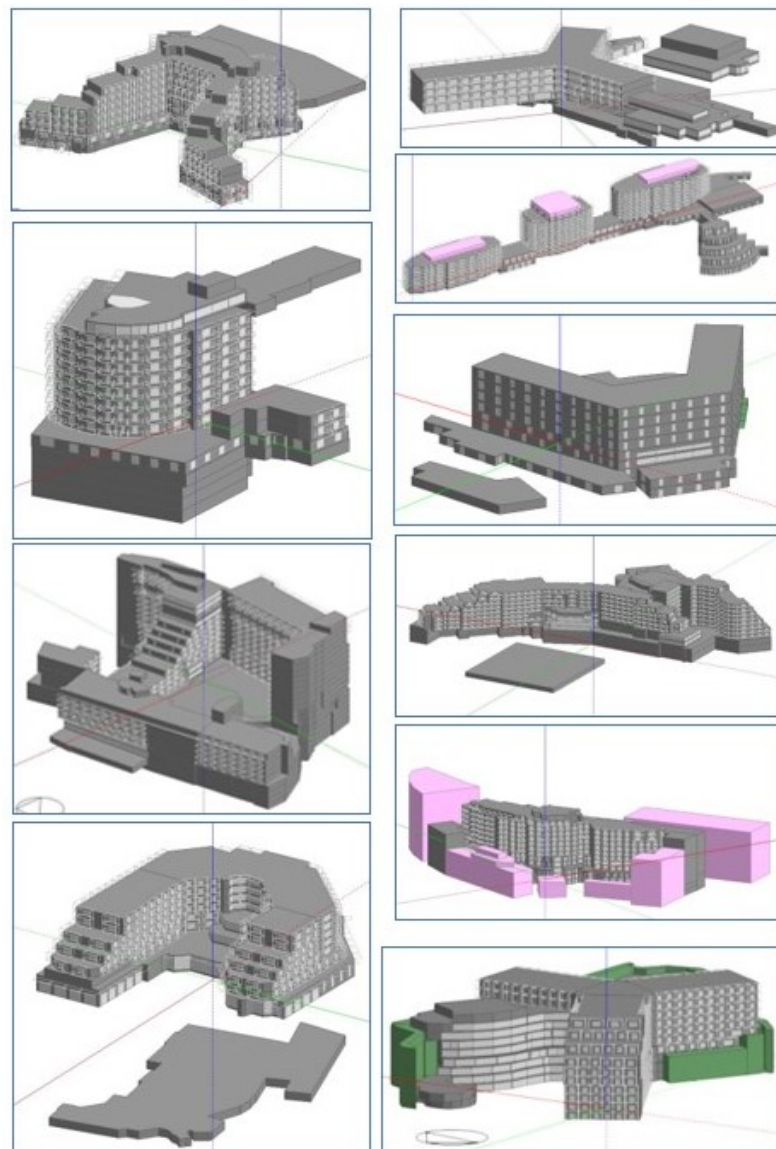


Figure 3.3: Visual depiction of the individual hotel building models making up the building stock under study

- **Functionality feature** comprises twenty-one (21) variables to define and quantify the activities or services performed at each hotel. The explanatory variables for this feature are shown in Figure 3.4.

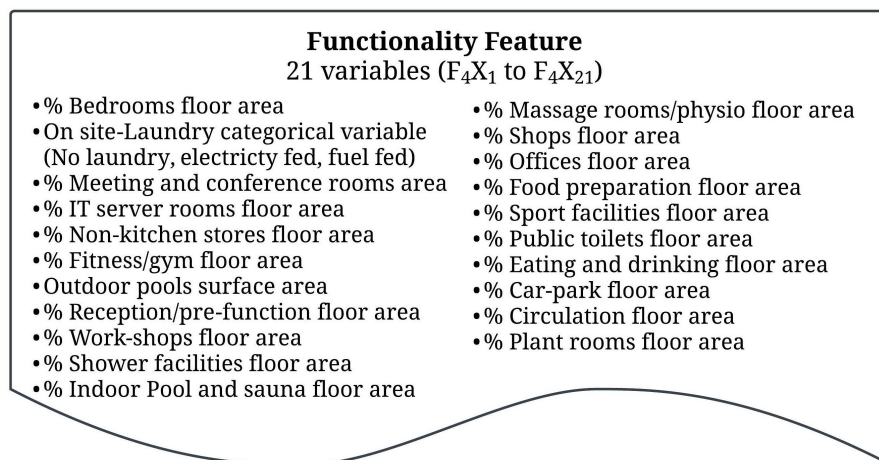


Figure 3.4: The twenty-one (21) explanatory variables considered for the Functionality feature

The building envelope and geometry feature variables to characterise RBs put forward in Torecellini et al. [204] and Corgnati et al. [26] were not included in the analysis to obtain RBs. Malta has a temperate Mediterranean climate described in terms of monthly degree days and solar radiation in Gatt and Yousif [228], and therefore the impact of the building envelope components U-value and form on the energy performance of a building is minimal when compared to other features such as equipment efficiency parameters. This minimal impact of building envelope and form on the total EP of the building is demonstrated specifically for a hotel BEM study in Malta in Gatt and Yousif [274], in the 2018 cost-optimal studies for non-residential building in Malta in Gatt et al. [56] and in various other literature including Caruana and Yousif [275] and Gatt et al. [158]. Furthermore, the hotel roofs for the observations under study were not insulated with U-values ranging between 1.7 and 2 $W.m^{-2}K^{-1}$, while the walls' U-value variation ranged between between 2.1 and 1.5 $W.m^{-2}K^{-1}$. The variability of these component U-values can be easily incorporated within a probabilistic RB model. Concerning fenestration, all hotels have similar overhang shading patterns thanks to the protruded balconies that protect the glazing of guest rooms from direct solar radiation.

It should also be noted that the variables defining the equipment feature were limited to the space heating, space cooling, and DHW systems type. Variability and uncertainty of the parameters that impact EP for these systems can be handled probabilistically within the defined RB themselves, as explained in Section 3.2.1.

Furthermore, the variables that explain the power densities of the lighting and plug loads for each functional activity were not considered in the analysis for the following reasons. All hotel observations have been upgraded to LEDs for lighting with compa-

rable EP in terms of power density ($W.m^{-2}$ of floor area per 100 lux). For plug loads, based on the information collected from hotel energy audits, the two most important variables that impact plug load EP for a hotel have been addressed within the functionality feature variables. These two variables are the food preparation floor area and whether the hotel has a laundry, as further explained in Section 3.4.2.4. Nevertheless, the variation between observations and uncertainties in plug-load power density parameters for specific functions can be probabilistically catered for within the defined RB parameters themselves for the proposed EPBD cost-optimal method.

3.4.2 | Data Processing

The data processing phase is an iterative process consisting of the five sub-stages that were amply described in Section 3.2.2 that aims at reducing the variables, known as the significant regressors, in preparation for further processing in the post-processing stage to cluster the building observation and define RBs.

Sections 3.4.2.1, 3.4.2.2, 3.4.2.3 and 3.4.2.4 describe Stages A to C of the data processing phase detailed in Section 3.2.2 to reduce data for each of the four features separately as graphically depicted for the case study building in Figure 3.2. Section 3.4.2.5 then describes Stage D of the data processing phase, which is the regression analysis of the reduced data with a dependent variable derived directly from individual metered energy consumption data. Finally, Section 3.4.2.6 describes Stage E of the data processing phase, which is the regression model reduction stage identifying statistically significant regressors. The data processing phase needs to be optimised until all the regressors in the reduced order model are both statistically significant and adequately represent all the defined four (4) features required to characterise a RB energy model for this building stock under study.

The results in this section are presented for the annual occupancy and operational metered energy consumption data for the year 2017 for each hotel observation. The method was then validated for its clustering solution stability using both 2018 and 2019 occupancy and operational energy consumption data.

3.4.2.1 | EP Benchmarking Feature data reduction

Only three (3) variables characterise this feature for the case study. Given that these variables are generally used for normalisation to benchmark the EP of hotels, they are expected to explain a major portion of the energy consumption of the buildings. Metered energy consumption was therefore used to perform only stage A of the data reduction stages shown in Figure 3.2, using descriptive statistics and a multivariate analysis

approach. Given the low data dimensionality of this feature, performing data reduction using only stage A of stages A to C shown in Figure 3.2 was sufficient for data reduction.

The multivariate analysis analysed the strength of the relationship between all explanatory variables in this feature and the dependent variables derived from metered energy consumption data. The dependent variables are the operational primary energy consumption in kWh and the annual tonnes of CO₂ emissions equivalent. The strength of the relation between the variables was quantified using Pearson’s r (correlation coefficient) as all variables are continuous. This statistical analysis was performed in Python using the Pandas package [276]. Furthermore, the significance of the relationships was also quantified in terms of p-value using the Pingouin package [277]. Figure 3.5 shows the resulting Pearson correlation heat map for the variables under study.

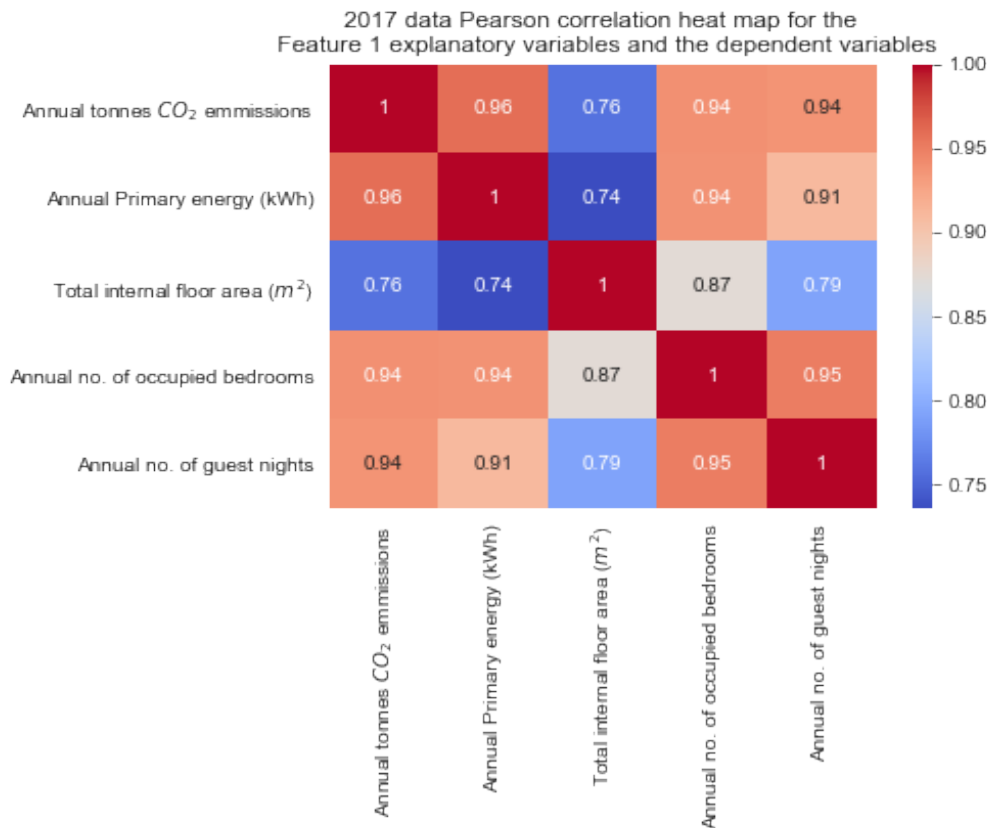


Figure 3.5: 2017 data Pearson correlation heat map depicting the strengths of the relationship between the Benchmarking EP feature explanatory variables and the dependent variables derived from metered energy consumption

One can observe a very strong relationship ($r = 0.96$, $p\text{-value} < 0.001$) between the two dependent variables derived from metered energy consumption data. Given this

strong relationship, the method to develop RBs needs to consider only one dependent variable derived from the metered consumption data for analysis. To be more consistent with the EPBD cost-optimal guidelines [55] and the EPBD cost-optimal studies for Malta [56], the annual primary energy in kWh was chosen as the dependent variable for this case study.

When analysing the strength of the relationship between the explanatory variables, a very strong relationship is obtained between all variables ($r > 0.8$, p -value < 0.01). Thus, to avoid multi-collinearity issues, only one variable should be retained for the data processing regression stage and chosen upon a valid statistical justification. The annual number of occupied bedrooms has the strongest relationship with the annual primary energy consumption ($r = 0.94$, p -value < 0.001) and is, therefore, the regressor chosen for this feature. Furthermore, it explains 88 % of the variability in annual primary energy consumption.

3.4.2.2 | Equipment (or technical building energy services) feature data reduction

This feature considers the HVAC and DHW systems installed for each hotel observation. For space cooling, three (3) different systems are used in the building stock, which are seawater-cooled chillers, air-cooled chillers, and air-cooled VRF systems. Hotels that make use of VRF for space cooling also use the same system for space heating but employ a separate dedicated fuel boiler system for DHW generation. In contrast, hotels that make use of chillers for space cooling make use of fuel boilers or DHW heat pumps for both space heating and DHW. The main HVAC and DHW systems found for each hotel observation are depicted in Table 3.1.

Table 3.1: The main HVAC and DHW systems for each hotel observation

	Main space cooling system	Main space heating system	Main DHW system
Hotel 1	Sea water cooled chiller	Fuel boiler	Fuel boiler
Hotel 2	Sea water cooled chiller	Electric heat pump	Electric heat pump
Hotel 3	VRF	VRF	Fuel boiler
Hotel 4	Sea water cooled chiller	Fuel boiler	Fuel boiler
Hotel 5	Air cooled chiller	Fuel boiler	Fuel boiler
Hotel 6	Air cooled chiller	Fuel boiler	Fuel boiler
Hotel 7	VRF	VRF	Fuel boiler
Hotel 8	Air cooled chiller	Fuel boiler	Fuel boiler
Hotel 9	VRF	VRF	Fuel boiler
Hotel 10	Sea water cooled chiller	Fuel boiler	Fuel boiler

As explained in section 3.4.1, observations with different HVAC and DHW systems cannot be comprehensively modelled within the same RB building physics energy model, given the different components and corresponding parameters that describe each system. Thus, a rule-based approach was used to perform clustering to ensure that the whole variability for the three (3) systems is represented for the categorical HVAC/DHW variable.

Thus, using a rule-based approach for the data reduction process, categorical regressor XC_2 can be defined by dividing the observations into four groups, with the allocated group number established in order of ascending annual primary energy consumption (kWh) corresponding to each observation.

- Group 1: Hotel 5, Hotel 6 and Hotel 8
- Group 2: Hotel 3, Hotel 7 and Hotel 9
- Group 3: Hotel 2
- Group 4: Hotel 1, Hotel 4 and Hotel 10

Therefore, for this feature, data reduction was performed using stage B of the feature reduction stages A to C described in Section 3.2.2, as shown in Figure 3.2.

3.4.2.3 | Conditioned space feature data reduction

The conditioned space feature consists of only two variables, the air-conditioned floor area (column vector F_3X_1) and the mechanically ventilated floor area (column vector F_3X_2) as a percentage of the total internal floor area. These variables are depicted in Figure 3.2. An analysis using the Pearson correlation coefficient between these two variables shows a strong positive relationship ($r= 0.75$, p -value = 0.01). Given the low dimensionality of this feature, both variables are retained as regressors, given that there is no sufficient justification to eliminate one variable over another.

3.4.2.4 | Functionality feature data reduction

The functionality feature is highly dimensional, composed of the twenty-one (21) variables depicted in Figure 3.4. Thus, unlike the other lower-dimensional features, all the feature reduction data processing stages A to C described in section 3.2.2 were employed as depicted in Figure 3.2 and detailed below.

3.4.2.4.1 Stage A: The functionality feature explanatory variables dimension reduction stage

This stage classified the functionality feature's twenty (21) variables into five categories to reduce the data set to five (5) variables. The categories chosen for classification are:

- **Bedroom floor area** expressed as a percentage of total internal floor area. This category is an indicator of whether the building is a (tower) hotel or resort (hotel) [278], as the smaller the ratio of the bedroom floor area to the total floor area, the more area is available for amenities, which makes the location (building) more inclined towards being a resort.
- **Food preparation area** expressed as a percentage of total internal floor area.
- **In-house Laundry** categorical variable taking 3 possible values as to whether the laundry in the hotel is '*liquid or gas fuel operated*', '*electricity operated*' or the hotel has '*no*' laundry.

- **Other Front of House (FOH) areas** expressed as a percentage of the total area of the internal floor. The % other FOH area is the sum of the following functions all expressed as a percentage of total internal floor area :

1. Sport facilities floor area
2. Shops floor area
3. Fitness/gym floor area
4. Shower facilities floor area
5. Eating and drinking floor area
6. Meeting and conference rooms area
7. Indoor Pool and sauna floor area
8. Reception and pre-function floor area
9. Circulation floor area
10. Public toilets floor area
11. Massage rooms/physio floor area

- **Other Back of House (BOH) areas** as a percentage of total internal floor area. The % BOH area is made up of the following functions :

1. Offices floor area
2. Car-park floor area
3. Plant rooms floor area
4. Workshops floor area
5. IT server rooms floor area
6. Non-kitchen stores floor area

- **Outdoor pool surface area** given that pools require pumping and filtration equipment and are therefore energy intensive [279]. Given that outdoor pool energy consumption is not directly considered in the EnergyPlus building energy modelling parameters, data-processing stages considered both options with and without the outdoor pool surface area variable to identify its sensitivity to the outcome.

The functionality data set of the five (5) variables are shown in Table 3.2. This functionality classification was chosen and adapted based on multiple sources, including:

1. ASHRAE [280] and Oluseyi et al. [227] distinguish between three zones in terms of public areas, guest-rooms and back of the house or service areas that are usually diverse in energy trend and intensity.
2. The BEST study [225] for Malta that established statistically using descriptive statistics based on EP data that 'tower' and 'resort' hotels should have a different EP benchmark. This is consistent with [199], who identify this as an important factor impacting EP of individual hotel buildings.
3. Local energy audits that identify food preparation and laundry activities as major energy consumers in a hotel. These findings are consistent with hotel EP studies and benchmarking criteria including [281, 282, 199, 273]. Therefore, these variables are better included directly as classifiers to have a more direct impact on the data processing solutions.

Table 3.2: The functional data set classified according to the five categories for each observation

	Bedroom area (%)	Food preparation area (%)	Laundry type	Outdoor pools area (m ²)	FOH (%)	BOH (%)
Hotel 1	33	3	LFO operated	497	39	24
Hotel 2	27	4	Electricity operated	1399	46	24
Hotel 3	49	3	none	889	32	17
Hotel 4	31	4	none	109	38	27
Hotel 5	33	3	none	561	38	27
Hotel 6	35	4	none	240	43	18
Hotel 7	33	8	none	271	52	9
Hotel 8	32	3	none	110	30	34
Hotel 9	24	5	none	420	57	15
Hotel 10	24	2	none	410	44	31

3.4.2.4.2 Stage B : Multiple clustering solutions identification

The reduced data set consisting of the five explanatory variables shown in Table 3.2 was further processed by first identifying sixteen (16) clustering approaches and generating a unique clustering solution for each approach.

The sixteen (16) approaches were achieved by identifying four (4) clustering characterisation groups in terms of clustering parameters and explanatory variables considered for the analysis and defining four (4) different clustering algorithms to be executed for each characterisation group.

The following four (4) characterisation groups were established:

- **Clustering group 1:** The clustering data set consists of four (4) explanatory variables, given that the pool surface area is excluded. The number of clusters (K) for each algorithm is optimally established to maximise dissimilarity between clusters for AHC algorithms or to minimise the cost function for K-prototypes algorithms.
- **Clustering group 2:** The same clustering data set applied for Clustering group 1 is used. However, the number of clusters considered for each algorithm is increased to K+1, given that the optimal number of clusters was not always easy to identify statistically.
- **Clustering group 3:** The clustering data set consists of all five (5) explanatory variables, and the number of clusters (K) is optimally established using the same approach as explained in Clustering group 1.
- **Clustering group 4:** The same clustering data set applied for Clustering group 3 is used. However, the number of clusters considered for each algorithm is increased to K+1, given that the optimal number of clusters was not always easy to identify statistically.

The following four (4) clustering algorithms were defined:

- **Algorithm a** : FAMD using the Prince package [283] in Python followed by AHC on the resulting principal factors. The adopted linkage criterion used for AHC is Ward's method [284].⁷
- **Algorithm b** : FAMD using the PCAmix algorithm [286] in XLSTAT [287] followed by AHC on the resulting principal factors.
- **Algorithm c** : K-Prototype Huang approach [209] using the k-modes package [288] in Python.
- **Algorithm d** : K-Prototype Cao approach [289] using the k-modes package [288] in Python.

Combining the four characterisation groups with the four algorithms provides the sixteen (16) clustering solutions depicted in Table 3.3. It must be noted that the clustering approaches are labelled according to the cluster characterisation group and the applied algorithm. For example, clustering approach 1A uses the clustering characteristics in group 1 and algorithm A to derive the clustering solution. The cluster group numbers for all clustering solutions are sorted consistently in order of ascending annual primary energy consumption corresponding to each observation.

⁷AHC is chosen over K-means clustering given that the low number of hotel observations makes computational speed not a criterion of choice. Furthermore, compared to K-means, the AHC result is more informative, making the optimal number of clusters generally easier to determine from the dendrogram [285]

Table 3.3: The clustering results obtained for the sixteen clustering approaches

	Clustering approach															
	1a	1b	1c	1d	2a	2b	2c	2d	3a	3b	3c	3d	4a	4b	4c	4d
Hotel 1	3	2	2	2	4	3	3	3	3	2	3	3	4	3	2	2
Hotel 2	2	2	2	2	3	2	3	2	2	1	2	2	3	2	1	1
Hotel 3	1	2	2	1	2	1	2	1	1	2	2	2	2	3	1	1
Hotel 4	1	2	2	1	2	1	3	3	1	2	1	1	2	3	2	2
Hotel 5	1	2	2	1	2	1	3	3	1	2	3	3	2	3	2	2
Hotel 6	1	2	2	1	2	1	2	1	1	2	1	1	2	3	2	2
Hotel 7	1	1	1	1	1	1	1	2	1	1	1	1	1	1	2	2
Hotel 8	1	2	2	1	2	1	3	3	1	2	1	1	2	3	2	2
Hotel 9	1	1	1	1	1	1	1	2	1	1	3	3	1	1	2	2
Hotel 10	1	2	2	1	2	1	3	3	1	2	3	3	2	3	2	2

3.4.2.4.3 Stage C : Identification of optimal clustering solution

From the sixteen (16) potential solutions, the final clustering solution needs to be optimally chosen using an objective approach by identifying the most recurrent groups among the identified solutions. This process can be statistically aided using categorical data clustering algorithms.

For this analysis, multiple categorical data clustering algorithms were applied. The three algorithms considered were the k-modes, using both Cao [289] and Huang [209] approaches, and AHC on MCA principal components algorithms. For each algorithm, different numbers of cluster solutions were determined, aiming to minimise the cost function in the k-modes algorithms and to maximise dissimilarity for the AHC algorithm applied on the resulting MCA principal components. The results of the categorical data clustering algorithms are shown in Table 3.4.

Table 3.4: The results from the multiple categorical data clustering algorithms applied to compare the 16 hotel clustering solutions to identify the most recurrent groups

	Clustering algorithm						MCA + AHC (K=3)	MCA + AHC (K=4)
	k-modes Huang (K=2)	k-modes Huang (K=3)	k-modes Cao (K=2)	k-modes Cao (K=3)	k-modes Cao (K=4)			
Hotel 1	2	3	2	3	4	3	4	
Hotel 2	1	2	2	2	3	2	3	
Hotel 3	1	2	2	3	2	3	2	
Hotel 4	1	3	2	3	2	3	2	
Hotel 5	2	3	2	3	2	3	2	
Hotel 6	1	3	2	3	2	3	2	
Hotel 7	1	1	1	1	1	1	1	
Hotel 8	1	3	2	3	2	3	2	
Hotel 9	2	1	1	1	1	1	1	
Hotel 10	2	3	2	3	2	3	2	

The clustering solution common to both the k-modes Cao and the MCA AHC approach consisting of four (4) clusters is the solution chosen for the functionality feature, given that it is the most recurrent and, therefore, the least subjective solution. It also represents the optimal number of clusters for the AHC on the MCA principal components approach to maximise dissimilarity between the clusters. This clustering solution, defined as categorical variable XC_4 , divides the hotel observations as follows.

- Group 1: Hotel 7 and Hotel 9
- Group 2: Hotel 3, Hotel 4, Hotel 5, Hotel 6, Hotel 8 and Hotel 10
- Group 3: Hotel 2
- Group 4: Hotel 1

From the above-resulting clustering solution for the functionality feature, one can notice that the hotels that have a laundry, that is hotel 1 and hotel 2, have been grouped into separate clusters and segregated from the other hotels that have no laundry. In addition, hotel 2 has a larger outdoor pool and % FOH areas than hotel 1 which explains why the two hotels were clustered separately.

Furthermore, the hotels that have no laundry, that is hotel 3 to hotel 10, were divided into two clusters. Hotel 7 and hotel 9 have a larger % FOH and food preparation areas than the other hotels and were therefore grouped separately.

3.4.2.5 | Stage D : Regression analysis

Following the data reduction process, stage A to stage C in Section 3.2.2, the supervised learning regression analysis, stage D, is carried out as shown in Figure 3.1. This step aims to establish the relationship between the regressor matrix X , composed of the reduced feature variables, and the dependent variable vector denoted by y , the annual primary energy consumption. The data set for the regression composed of matrix X and vector y is shown in Table 3.5. For this purpose, MLR is applied in XLSTAT [287].

Table 3.5: The data set for regression composed of the regressor matrix X and the dependent vector, y

Matrix or row vector notation	XC_1	XC_2	XC_3		XC_4	y
Regressor type	Benchmarking Feature regressor	Equipment Feature regressor	Conditioned Space feature regressor		Functionality feature regressor	Dependent variable
Physical Interpretation	Annual no. of occupied rooms ($F_1 X_1$)	HVAC & DHW system types	% cooled & heated floor area ($F_3 X_1$)	% Mech. vent. floor area ($F_3 X_2$)	Clustering solution from zone functions	Annual Primary energy consumption (kWh)
Hotel 1	111183	4	0.76	0.93	4	23637901
Hotel 2	122154	3	0.83	0.9	3	22499792
Hotel 3	92832	2	0.68	0.81	2	15653405
Hotel 4	75703	4	0.74	0.71	2	11320761
Hotel 5	73369	1	0.48	0.36	2	11149908
Hotel 6	70978	1	0.64	0.26	2	7916273
Hotel 7	39380	2	0.69	0.69	1	6521984
Hotel 8	50096	1	0.47	0.51	2	6003832
Hotel 9	40364	2	0.86	0.91	1	3547070
Hotel 10	114346	4	0.71	0.98	2	15924467

The annual number of occupied rooms, the benchmark feature variable, is a dominant regressor that explains 88 % of the variability in operational EP, as shown in the correlation analysis performed in Section 3.4.2.1. Thus, including this variable and the other four (4) variables of matrix X to define a full linear regression model resulted in an over-fitted solution with a coefficient of determination (R^2) of 1. Therefore, the dimensionality of matrix X needs to be further reduced to define a reduced order model to significantly represent all four (4) feature variables.

3.4.2.6 | Stage E : Regression model reduction

In the reduced regression model solution, the dominant benchmarking feature variable, the annual number of occupied bedrooms, is fully retained, as it explains the major portion of the variability in operational EP. Furthermore, the equipment feature categorical variable also needs to be fully included in the model to ensure that the variability of this feature is fully considered in the data post-processing stage for defining the final RB clustering solution.

Therefore, further data reduction on the matrix X in Table 3.5 was performed on the functionality and space conditioning features variables to identify a single categorical variable that best represents these features. The machine learning solution to identify this variable was again performed by identifying and evaluating multiple clustering so-

lutions for these two variables followed by the choice of the optimal clustering solution using categorical variable clustering algorithms. Following this further data reduction, the regression data set composed of reduced matrix X and vector y is shown in Table 3.6.

Table 3.6: The data set for regression composed of the regressor matrix X and the dependent vector, y

Matrix or row vector notation	XC_1	XC_2	XC_{34}	y
Regressor type	Benchmarking Feature regressor	Equipment Feature regressor	Conditioned Space and functionality feature regressor	Dependent variable
Physical Interpretation	Annual no. of occupied rooms (F_1X_1)	HVAC & DHW system types	Clustering solution from zone functions and space conditioned floor area	Annual Primary energy consumption (kWh)
Hotel 1	111183	4	4	23637901
Hotel 2	122154	3	3	22499792
Hotel 3	92832	2	2	15653405
Hotel 4	75703	4	2	11320761
Hotel 5	73369	1	2	11149908
Hotel 6	70978	1	2	7916273
Hotel 7	39380	2	1	6521984
Hotel 8	50096	1	2	6003832
Hotel 9	40364	2	1	3547070
Hotel 10	114346	4	2	15924467

Multiple Linear Regression (MLR) was then performed using a backward step-wise regression [290]⁸ approach on the data set shown in Table 3.6 using the Python step-wiseSelection package [291]. This regression was carried out to check and ensure the significance of each variable in the reduced regressors matrix in explaining operational primary energy consumption. The three explanatory variables in the matrix X were retained as significant ($p < 0.01$) with an adjusted R^2 of 93.4 %, which means that more than 5 % of the variability in annual primary energy is statistically represented by the equipment, space-conditioned and functionality variables. Thus, all variables in the reduced regressors matrix X can be retained for the post-processing stage.

⁸Backward step-wise regression begins with a full regression model incorporating all explanatory variables and gradually removes variables from the model to find a reduced model that best explains the data.

3.4.3 | Data post-processing stage

In this section, multiple clustering solutions were identified and evaluated on the significant regressor data set depicted in Table 3.6 to establish the final clustering solution of dividing the hotel observations into clusters for which a RB energy model will need to be defined for each cluster.

For this case study, this stage consisted of a two-stage approach as follows:

1. **Data reduction of the Benchmarking feature variable vector XC_1 and the Conditioned space and functionality feature variable vector XC_{34}** to one variable vector denoted by XC_{134} that best represents these variables. Similar to the previous steps involving clustering, the solution to identify this variable was again carried out by investigating multiple clustering approaches, followed by the choice of the optimal clustering solution using categorical variable clustering algorithms.
2. **Identification of the final clustering solution XC_{RB}** for the data set composed of XC_{134} and the equipment feature XC_2 using a rule-based approach to ensure that the variability of XC_2 is fully represented in the final clustering solution to define RBs.

Based on the most-recurrent groupings from the multiple solutions, potential solutions with four (4) and six (6) clusters could be established for XC_{134} , as shown in Table 3.7. However, to minimise the number of clusters that reflect the number of RB energy models, the solution with four (4) clusters was chosen for XC_{134} to reduce the time and computational expense of modelling the building stock. The final clustering solution is justified in Section 3.4.4.

Combining the four cluster solution of XC_{134} with the equipment feature variable XC_2 using a rule-based approach to retain all variability in the equipment feature XC_2 , splits the hotel observations into the six (6) clusters ($K_{RB} = 6$) shown in Figure 3.6. A RB must be defined for each cluster based on an archetype solution. The whole process of deriving this final RB clustering solution for the case study building is graphically shown in Figure 3.2.

Table 3.7: The data set to derive the final clustering solutions showing the four and six cluster options for XC_{134}

Matrix or row vector notation	XC_{134} (4 clusters solution)	XC_{134} (6 clusters solution)	XC_2
Regressor type	Benchmarking, conditioned space and functionality feature regressor		Equipment Feature regressor
Physical Interpretation	Clustering solution from benchmarking feature variables		HVAC & DHW system types
Hotel 1	4	6	4
Hotel 2	4	6	3
Hotel 3	3	4	2
Hotel 4	3	4	4
Hotel 5	2	3	1
Hotel 6	2	3	1
Hotel 7	1	2	2
Hotel 8	2	1	1
Hotel 9	1	2	2
Hotel 10	3	5	4

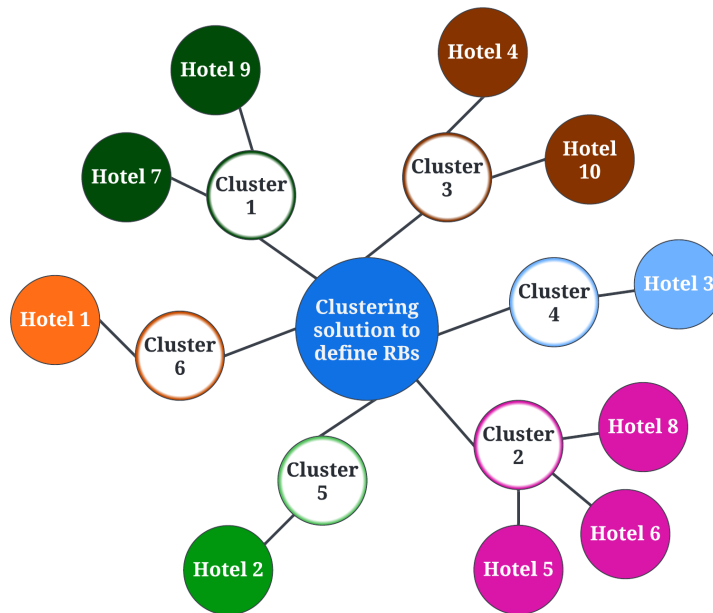


Figure 3.6: Hotel building stock cluster map for which an archetype must be defined for each of the resulting six (6) clusters

The stability of the clustering solution was validated by repeating the method for the same hotel observations but using the annual occupancy and operational energy consumption for the years 2018 and 2019 separately as test data⁹. For both the years 2018 and 2019, the same clustering solution as shown in Figure 3.6 was obtained, confirming the robustness and stability of the approach.

3.4.4 | Discussion on the final RB clustering solution

This section justifies the final RB clustering solution, XC_{RB} , for the case study building stock resulting from the method to develop RBs proposed in this chapter. To facilitate the discussion, Table 3.8 is presented, where the annual primary energy consumption is the dependent variable y , while the annual number of occupied rooms, XC_1 , is the dominant explanatory variable. Variable y was converted to a discrete ordinal variable using the Univariate clustering algorithm proposed by Fisher [292] in XLSTAT [287]. This algorithm generates a solution that has a maximum of three (3) clusters. Furthermore, to enable direct comparison, variable XC_1 has also been converted to a discrete ordinal variable with three (3) cluster classes using the same algorithm¹⁰. In addition, the table shows regressors XC_{134} and XC_2 representing the benchmarking, functionality & space conditioning and equipment features, respectively. The final RB clustering solution, XC_{RB} , is also depicted.

Hotel 1, hotel 2, and hotel 10 belong to the same cluster for variable XC_1 . However, hotel 10 has a lower cluster class for the dependent variable y , which is explained by the different cluster class for XC_{134} given that hotel 1 and hotel 2 both have a laundry on site, in contrast to hotel 10. Furthermore, although hotel 1, hotel 2, and hotel 10 fall within the same cluster class for variables XC_1 , XC_{134} , and y , hotel 1 and hotel 2 do not share the same cluster for XC_2 and therefore these two observations must also be clustered separately. This split ensures that observations having different HVAC and DHW systems fall under different clusters, which is essential to fully characterise and define RBs. This segregation of hotel 1, hotel 2, and hotel 10 into three (3) different cluster classes is missed if the clustering solution of variable XC_1 or the dependent variable y is adapted to define the RBs for the building stock.

⁹The Python Jupyter notebooks to perform the methodology to define RBs for the hotel-building stock case study for the years 2017 to 2019 are found in the GitHub Repository. Refer to GitHub Repository folder 'Ch 3 5 star hotels RB definition methodology'. Refer to Appendix B for a detailed description of all files and folders found in the GitHub Repository.

¹⁰The three (3) cluster solution for variable XC_1 is also the median between a four (4) cluster solution generated using the Fisher [292] Univariate clustering algorithm and a two cluster solution that maximises dissimilarity between clusters in AHC.

Table 3.8: Data set to facilitate the RB buildings stock clustering solution validation

	Annual no. of occ. rooms ordinal variable (K=3)	XC_{134}	XC_2	RB final clustering solution (XC_{RB})	Operational primary energy consumption ordinal variable (K=3)
Hotel 1	3	4	4	6	3
Hotel 2	3	4	3	5	3
Hotel 3	2	3	2	4	2
Hotel 4	2	3	4	3	1
Hotel 5	2	2	1	2	1
Hotel 6	2	2	1	2	1
Hotel 7	1	1	2	1	1
Hotel 8	1	2	1	2	1
Hotel 9	1	1	2	1	1
Hotel 10	3	3	4	3	2

Similarly, suppose that one performs clustering directly on variable XC_1 . In that case, the four hotels made up of hotel 3 to hotel 6 are clustered together, which does not reflect the higher operational energy consumption of hotel 3 reflected by the higher cluster class of variable y . The final clustering solution, XC_{RB} , provides a more comprehensive segregation of these hotels into three (3) separate groups, with hotels 5 and 6 clustered together, and hotels 3 and 4 clustered separately. Hotel 5 and hotel 6 share the same cluster class for XC_{134} and XC_2 and fall within the same cluster class for variable y , which further justifies grouping these two observations together. However, hotel 3 and hotel 4 are not clustered with hotel 5 and hotel 6 because they fall into a different cluster class for XC_{134} due to a higher percentage of the internal floor area that is mechanically ventilated and space heated & cooled. Furthermore, hotel 3 and hotel 4, fall into a different cluster class for the variable XC_2 and therefore need to be clustered separately. The variable XC_2 can therefore explain why hotel 3 and hotel 4 fall into a different cluster class for the dependent variable y .

Hotel 7, hotel 8, and hotel 9 fall into the cluster having the lowest values for y . For these hotels, the classification prediction accuracy between y and XC_1 is perfect. However, while hotel 7 and hotel 9 fall within the same cluster for both XC_{134} and the XC_2 and can be grouped, hotel 8 is best studied separately as it falls into a different cluster for both these variables¹¹. The need to separate these three hotels into two separate

¹¹The different cluster class for hotel 8 for variable XC_{134} compared to hotels 7 and hotel 9 is explained by a different cluster for the functionality variable (XC_4), and a lower mechanically ventilated and space cooled & heated internal floor area described by variables (F_3X_1) and (F_3X_2).

clusters is not evident if one directly considers the clustering classes of variable XC_1 or variable y .

Furthermore, although hotel 4 falls into a lower cluster class than hotel 10 for variable XC_1 , they fall within the same cluster for variables XC_{134} and XC_2 . They can therefore be grouped to minimise the number of RBs and make building stock energy modelling less computationally expensive. The number of occupied bedrooms, XC_1 , can then be statistically defined and input into the RB energy model to best represent the building stock cluster under the study.

The same concept applies in combining hotel 5, hotel 6, and hotel 8, despite hotel 5 and hotel 6 having a higher XC_1 cluster class. It should be noted that these hotels would have been automatically further segregated to reflect this diversity in XC_1 if the six (6) versus four (4) cluster solution was chosen for XC_{134} . However, given only (ten) 10 hotel observations ($N = 10$) in this case study, the number of clusters in the final RB clustering K_{RB} solution will become close to the number of observations N . This large number of clusters will reduce the feasibility of this approach and unjustifiably increase the modelling effort and computational resources to study the building stock using the proposed EPBD cost-optimal method detailed in Chapter 2.

The discussion justifies the method in the need to systematically apply multiple machine learning techniques to high-dimensional explanatory variable data sets from all features to derive significant regressors that define and characterise RBs for a 'small' multi-functional building stock. This approach contrasts clustering based only on easily obtainable benchmarking variables or directly uses the operational metered energy consumption dependent variables, which will not allow RBs to be characterised and comprehensively defined to study the building stock.

3.5 | Conclusion

Defining RBs that are representative of the building stock under study is the first step in the proposed EPBD cost-optimal method described in Chapter 2, Section 2.5 and UBEM. However, there is no standard methodology to define RBs. Therefore, in line with the objectives of this research, an approach was developed to define RB for multi-functional and heterogeneous building stocks '*small*' ($X \gg N$) as the challenges of heterogeneity and data processing to define RBs for such buildings have not been adequately addressed in the literature. The developed approach uses unsupervised and supervised machine learning techniques to systematically combine the data from the building features data with individual metered energy consumption data. These techniques address the high-dimensional data processing challenges of such building stocks, while ensuring that they are fully characterised for bottom-up energy modelling. In addition, a specific '*functionality feature*' is also introduced as a data collection classifier for characterisation, complementary to the four building features of form, envelope, equipment, and operation proposed by Torcellini et al. [204] and Corgnati et al. [26]. This feature ensures that the diversity of the services offered by the individual buildings in a multi-functional building stock is better represented when deriving the final RB clustering solution.

The approach was successfully applied to a '*small*' ($X \gg N$) and heterogeneous 5-star hotel building stock that has a ratio of more than three (3) explanatory variables X for each observation of the building stock N . The approach grouped the ten (10) hotel buildings into six (6) clusters, for which an RB in the form of an archetype must be defined for each cluster. The stability of the resulting clustering solution was validated using test data with occupancy and metered energy consumption for different annual periods. Furthermore, the RB clustering solution provided a more comprehensive approach to defining RBs in contrast to clustering only on easily obtainable benchmarking variables or directly on operational metered energy consumption. This results from the ability of the developed method to uncover building characteristics that need to be considered when developing a building physics RB energy model.

In addition, performing the proposed probabilistic EPBD cost-optimal methodology on six (6) RBs rather than the entire building stock provides a significant reduction in the energy modelling time effort and computational resources to generate multiple simulation runs from computationally expensive multiple zone building physics models required to perform Bayesian calibration with metered energy consumption data for the proposed EPBD cost-optimal method, as explained in Chapter 2. However, the pro-

posed RBs definition approach needs further testing through application to other building stocks to better understand how the resulting cluster-to-observation ratio varies as the number of building observations and the diversity of the building stock change. Such testing is required to better validate the practicality of the proposed approach compared to RB definition approaches explained in Section 3.1.2.1. These RB definition approaches, unlike the proposed approach, generally do not consider functionality as a characterisation feature to develop RBs, use less elaborate data-processing techniques that apply single clustering algorithms/solutions, or do not check the significance of the clustering variables on metered energy consumption data.

In the following chapters, and in order to demonstrate the EPBD cost-optimal method proposed in Chapter 2, an archetype will be developed for a chosen cluster of hotel observations resulting from the final clustering solution XC_{RB} of the hotel building stock case study. The archetype will be defined having parameters for system efficiency and operation defined probabilistically to develop a '*probabilistic RB*' and calibrate it using monthly metered energy consumption data. '*Probabilistic Bayesian calibrated RBs*' will be evaluated in their potential to better handle building stock uncertainty and allow further heterogeneity to be investigated within buildings that fall into the same cluster in the final RB clustering solution XC_{RB} .

Bayesian calibration of a multi-functional Reference Building for the EPBD cost-optimal method - a computationally efficient approach

Chapter Abstract : This chapter demonstrates the first four steps of the proposed EPBD cost-optimal method on a hotel RB identified from Chapter 3. These steps update '*non-calibrated and deterministic RBs*' to '*probabilistic Bayesian calibrated RBs*'. To execute these steps, this research, validated a computationally efficient approach to performing Bayesian calibration of RBs, by replacing full-space, heterogeneous RB EnergyPlus models, termed '*detailed*' models, with reduced-space RB ('*simplified*') EnergyPlus models constructed using the modular and scalable '*reference zone*' approach concept, conceptualised by Gatt et al. [35]. RB EnergyPlus models are required in Bayesian Calibration to run multiple simulation runs for SA and to train the meta-model emulating the EnergyPlus simulator. The '*simplified*' model showed a 4,000 % improvement in computational run-time efficiency over the '*detailed*' model and perfectly replicated its parameter ranking SA results. The '*simplified*' model also successfully reproduced the monthly energy end-use outputs of the '*detailed*' model with a NMBE of 0.38 % and CVRMSE of 3.78 % for simulation runs that trained the GP meta-model. Furthermore, the GP meta-model, trained from the '*simplified*' model, statistically calibrated the meta-model and both the '*simplified*' and '*detailed*' EnergyPlus models with monthly energy consumption, while satisfactorily reducing uncertainty in the calibration parameters. Based on these results, the modular and scalable '*reference zone*' approach provides good potential in bottom-up modelling to replace detailed BEMs for improved computational efficiency, while allowing the variability in the functionality of a building stock to be better represented.

4.1 | Introduction

Reference Buildings (RBs) defined by classifying and characterising the building stock should represent “*the typical and average building stock in a member state*” [9] and therefore provide the basis for MS to study the EP of their building stock using the EPBD [9] cost-optimal approach. Chapter 3 focused on developing a machine learning approach to specifically define RBs for small, multi-functional and heterogeneous building stocks. Once RBs are defined, the cost-optimal approach provides MS with a common tool to establish NZEB benchmarks and devise policies and incentives to facilitate the transition of buildings to NZEB for the EU to facilitate meeting its 2050 carbon neutrality targets.

Despite the positive push enabled by the EPBD cost-optimal method to improve the EP of buildings in the EU, Chapter 2, established limitations in the ability of the current cost-optimal approach to derive realistic benchmarks and effective policies given the resulting policy uncertainties described in Section 2.3.1. It was also discussed that such uncertainties primarily stem from the use of ‘*non-calibrated and deterministic*’ RBs. Therefore, to address these limitations, a new EPBD cost-optimal method was proposed and conceptualised in Figure 2.6, with the objective of establishing a clear framework for integrating state-of-the-art UBEM techniques employing ‘*probabilistic Bayesian calibrated RBs*’ into the current EPBD to construct a novel cost-optimal approach that replaces ‘*non-calibrated and deterministic*’ RBs with ‘*probabilistic Bayesian calibrated RBs*’. To meet the objective of this investigation, the proposed cost-optimal method graphically depicted in Figure 2.6 will test the hypothesis put forward in Chapter 2 of whether state-of-the-art UBEM techniques employing ‘*probabilistic Bayesian calibrated RBs*’ can better address the handling of the uncertainties and diversities of a building stock for a more robust and effective policy making.

4.1.1 | Chapter objective

This chapter aims to demonstrate and validate steps 1 to 4 of the 6 steps of the proposed EPBD cost-optimal method detailed in Chapter 2, Section 2.5, of updating ‘*non-calibrated and deterministic RBs*’ to ‘*probabilistic Bayesian calibrated RBs*’. A cluster of the 5-star hotel building stock in Malta described in Chapter 3, for which an RB energy model must be defined, is used as a case study to demonstrate the steps of the proposed EPBD cost-optimal method.

Furthermore, as detailed in Chapter 2, a limitation of Bayesian calibration is that the iterative calibration process is highly computationally expensive when applied to Building Energy Modelling (BEM), given the need to generate multiple simulation runs

from the RB building physics models. Computationally expensive RB building physics models are synonymous with heterogeneous, multi-functional building stocks that have large floor areas with complex geometries and must be modelled with multiple thermal zones grouped at least according to their operational functions and their air conditioning systems [293, 294]. Given such limitations, the literature has not adequately covered Bayesian calibration for these building stocks. Therefore, this chapter addresses the research objective identified in Chapter 1 for investigating and statistically validating, in terms of simulation output accuracy, innovative techniques to reduce the computational expense of the novel cost-optimal approach and facilitate its implementation. Once calibration is statistically validated, the probabilistic RB energy model with posterior calibration parameter distributions, termed '*probabilistically calibrated RB*', becomes the RB model input for steps 5 and 6 of the proposed EPBD cost-optimal described in Chapter 5, Section 2.5. In these steps, energy efficiency measures are applied to the probabilistic RB model to derive EPIs and to propagate uncertainty and financial risk for each defined NZEB ambition level to establish robust energy renovation policies. The outcomes of Chapters 4 and 5 will allow the hypothesis presented in Chapter 2 and reproduced in this section to be accepted or rejected.

4.2 | Computational expense of Bayesian calibration for the proposed EPBD cost-optimal method

In the proposed EPBD cost-optimal approach shown in Figure 2.6, Step 1 involves the assignment of probabilistic RB energy models, for which the defined deterministic RBs are updated to probabilistic RBs by defining an N-vector uncertain parameter θ as a probability distribution $p(\theta)$.

Step 2 then requires performing a Sensitivity Analysis (SA) to identify the S-vector of significant parameters t , ($t \subset \theta$) from the unknown parameters θ to be employed in the calibration process. For this purpose, both local SA and global SA have been applied in BEM, as discussed in Section 2.5.2. Global SA methods include screening, regression methods, variance-based SA and meta-modelling [142, 295]. Global SA, unlike local SA, provide a better overall picture of the importance of different input parameters and their interactions over the entire design space and are therefore more suitable for assessors to make general conclusions for ranking the importance of different parameters [296, 295]. To perform global SA, screening methods are the most popular as they are the least computationally demanding, making them suitable for building physics energy models that have a large number of uncertain parameters to rank [295]. For this purpose, the

Morris method [137], also known as the elementary effect method [297], is a One-step At a Time (OAT) screening method and is the most popular approach for screening and performing global SA in BEM [136, 295] as it achieves a suitable balance between accuracy and the number of simulation runs [136, 135, 161] and is model independent [298]. Furthermore, Menberg et al. [135] also showed that the Morris method can rank the importance of parameters as well as the more computationally expensive regression and variance-based methods.

For a k dimension vector of uncertain parameters θ , the Morris method divides the input space of dimensions k into a grid of p levels [297], where the k -dimensional, p -level grid is called the experimentation region. The sampling is carried out along a number of r trajectories, where each trajectory consists of a sample of $(k + 1)$ points. For the sample points, the incremental ratios¹ are calculated to output the elementary effect (EE) for each input parameter after each trajectory [135]. This calculation produces two statistical measures per input parameter, the μ^* and σ . The μ^* quantifies the overall influence of the input parameter on the output and is the absolute mean of the elementary effect resulting from each trajectory [300]. This statistical measure is used to classify the parameters according to their importance. The other measure, σ , is the Standard Deviation (SD) of the distribution of the elementary effect resulting from each trajectory and measures non-linearity and parameter interactions. The total number of simulation runs required for the Morris method is $(k + 1)r$ [301, 298], where r is the number of trajectories and is generally taken between 5 and 15 [298]², depending on the number of levels. Wate et al. [301] identify the selection of 4 levels and 10 trajectories as an optimum for a highly dispersed experimentation space.

Once SA is performed, a probabilistic calibration follows in step 3 of the proposed cost-optimal method using Bayesian inference and the generic calibration approach proposed by Kennedy and O'Hagan (KOH) to model the relationship between the measured data, y , and the output of the computer simulations η under known conditions x and uncertain (calibration) parameters t , while accounting for the (structural) inadequacy of the model $\delta(x)$, and observation errors $\varepsilon(x)$ as depicted in Equation 4.1.

$$y(x) = \eta(x, t) + \delta(x) + \varepsilon(x) \tag{4.1}$$

The high computational cost of complex building physics energy models makes it difficult to derive posterior distributions analytically. For this reason, MCMC algo-

¹When only one parameter is changed at a time during an experiment, the incremental ratio compares the size of the parameter's variation to the change in the model output at two different points in the experimentation (input) space. [299].

²Tsvetkova et al. [297] state that r is generally taken between 4 and 10.

rithms are used in Bayesian calibration to sample from posterior distributions³. Bayesian inference using MCMC algorithms is computationally challenging to evaluate likelihoods [295], especially for complex and expensive building physics energy models. Therefore, in BEM and UBEM studies, a meta-model (also called a surrogate model [302, 303, 304]) usually replaces the computationally intensive building physics model to improve the computational speed of the iterative calibration process. Various meta-models have been applied in BEM literature, including MLR in [305, 172, 177], neural networks in [306, 307], GPE in [169, 176, 121, 161, 181, 134, 308, 309, 310], Support Vector Machines in [311], MARS in [312], and Polynomial Regression applied in [128]. Linear regression and GPE are the most popular surrogate models that replace the building physics energy model [295, 127]. Of all meta-models analysed (MLR, NN, SVM, MARS and GPE), Lim and Zhai [154] found GPE to have the best accuracy in both the estimation of the input parameters and the prediction of the energy output when compared to the EnergyPlus model, but has the highest computational cost. In contrast, MLR is the fastest but least accurate, and the accuracy of MLR decreased more than that of the other models as the range of input parameters increased [154].

For replicating complex and non-linear building energy models, the meta-model is usually a Gaussian Process Emulator (GPE) given its flexibility [161, 313, 314]⁴, and its ability to accurately predict out-of-sample (test) data and quantify uncertainty [314]. GP models treat observations as realisations of multivariate Gaussian distributions. The multivariate Gaussian is employed as prior, and this distribution is constrained by existing data leading to a posterior distribution of the possible functions that generated the data [304]. GP models for machine learning are described in detail in [316, 161, 313, 314]. A generally accepted guideline is having at least ten (10) simulation runs per significant parameter [161, 317] for training GP models, where the sample space is generated by performing Latin Hypercube Sampling (LHS) from the probability distributions of the significant parameters.

Thus, performing SA using the Morris method to identify the most significant parameters and fitting a GPE to replace the computationally expensive RB model requires multiple simulation runs from the building physics model itself, and the computational expense of these processes, therefore, depends on the simulation run time of the building physics model. Therefore, this research will aim to provide an additional technique

³Recent research has focused on implementing more efficient sampling algorithms and approximate Bayesian computation methods, as detailed in Section 2.6.3.

⁴Their flexibility comes from their non-parametric Bayesian approach to modelling, allowing them to capture a wide variety of relations between inputs and outputs by using an infinite number of parameters in theory and allowing the data to identify the complexity level through the means of Bayesian inference [315, 313].

to what is found in the UBEM literature detailed in Chapter 2 to improve the computational efficiency of Bayesian calibration for RB energy models. This is done by addressing the research gap identified in Chapter 2 in replacing a computationally expensive building physics model (RB) with a more computationally efficient building physics model that provides a statistically acceptable difference for the simulated fuel consumption (energy end-use) outputs considered for calibration. This simplification of the building physics model will facilitate the implementation of the proposed EPBD cost-optimal method and must be performed on the RB energy model before the SA in step 2 to optimise the computational efficiency of Bayesian calibration.

4.3 | Methodology to improve the computational efficiency of a RB building physics energy model

This research will validate the conceptual reduced-space order modelling approach termed the '*reference zone approach*' proposed by the author of this thesis in Gatt et al. [35]. This approach aims to improve the computational speed of multi-functional RB building physics energy models when performing Bayesian calibration with metered energy consumption data for the proposed EPBD cost-optimal method. The '*reference zone approach*' approach to improve the computational speed from building physics energy models is different from the current approach used in multiple BEM Bayesian calibration studies (studies include [138, 139, 92, 130, 163, 172, 147, 132], refer to Section 2.6.3) that replace full-space (and whole-building), dynamic (white-box) models⁵ with full-space grey-box (simplified/reduced-order) models [171]), most common being the resistance capacitance (RC) models, as these models are more computationally efficient than dynamic (white-box) models.

In the '*reference zone approach*' approach, a whole-building and full-space building physics energy model composed of multiple thermal zones, which can be either a white-box or grey-box model, termed a '*detailed*' model, with the thermal zones defined as a minimum according to the function of the space and the method used to condition the zone, is simplified by splitting the model into a number of simplified geometric representations or building blocks using the following modular approach to modelling. A functional activity, for example, hotel accommodation for which an en suite bedroom is the space used to satisfy this function, is modelled using one or more building blocks termed '*reference zones*'. Each '*reference zone*' is a representative functional unit of a sub-

⁵White-box models include EnergyPlus models [171].

activity. A sub-activity, which is a subset of an activity, is required to be defined for a space that offers the same service (activity) but has a different defining condition impacting EP, such as a different space conditioning system, schedule, or orientation.

Each *'reference zone'*, which in itself is an energy model, is comprehensively characterised in terms of equipment, operation, envelope, and form. In addition, a *'reference zone'* is geometrically constructed and thermally decoupled by carefully considering surface adjacency (boundary) conditions so as to keep the total volume of the space and the heat transfer balance between the interior spaces and the exterior of a sub-activity under study to mimic as closely as possible the actual building conditions when zone multipliers are added to aggregate the EP of the sub-activity. This aggregation is possible given that each defined *'reference zone'* is a functional unit, making it modular and can therefore be scaled up using zone multipliers to model the whole sub-activity space. By considering each activity and related sub-activities in the building, this modular approach can be used to scale up the model from sub-activity functional (*'reference zone'*) units to the entire building. The concept of the *'reference zone'* approach to BEM is visually shown in Figure 4.1, in which the combination of *'reference zones'* coupled with multipliers to model the entire building results in a reduced space model that has the potential to be more computationally efficient than the *'detailed'* model.

It must be noted that the *'reference zone'* approach to BEM has the potential to be applied both using a top-down or bottom-up configuration. In the top-down configuration, a *'detailed'* RB energy model is first developed to represent a group of buildings and then simplified to improve its computational speed and execute the computationally intensive Bayesian calibration process. Similarly, given its modularity and scalability, the approach can also be applied using a bottom-up configuration for building stock modelling. Once the *'reference zone approach'* with defined representative *'reference zones'* is statistically validated for the sample of buildings under study, every building observation in the stock can theoretically be modelled using this approach, which replaces the need to define *'detailed'* building physics models.

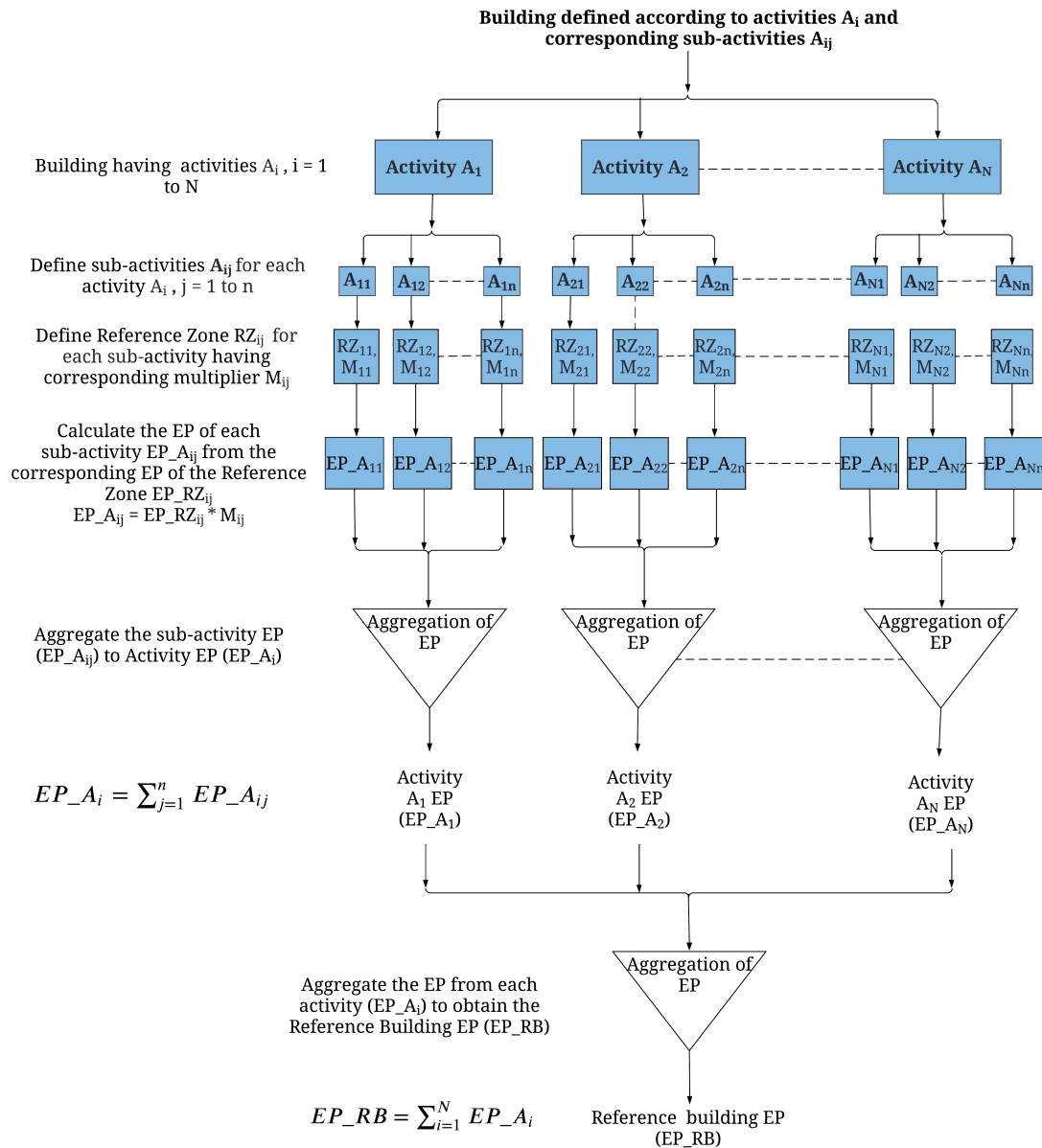


Figure 4.1: Flow chart depicting the 'reference zone' approach that splits the building into 'reference zones' representing building 'sub-activity' functional unit models from which the entire building model can be scaled up using multipliers.

In addition to its potential to improve the computational speed of SA and meta-model development replacing the building physics models⁶ in Bayesian calibration, the '*reference zone*' approach can be applied in applications such as GIS to allow for a simple, modular and flexible aggregation of EP from the '*reference zones*' to individual buildings and even up to the urban level. This ability to allow for a modular and flexible aggregation of EP makes this approach especially suitable for modelling multi-functional heterogeneous buildings stocks, where the defined '*reference zones*' allow for the diversity in the services offered by such buildings to be better represented in BEM in contrast to simpler zoning division techniques discussed in Chapters 2 and 3 that do not fully distinguish between the functions and functional diversity of a space. This is because these simpler zoning division techniques in UBEM generally consider single zone models, one zone per floor models, or multi-zone per floor models [186]. The multi-zone per floor models generally distinguish only between the core zone and four perimeter zones [186], as the core and the different perimeter zones have different external boundary conditions [318].

Another potential application for the '*reference zone*' approach is to provide a better framework for the consideration of probabilistic functional diversity in a RB (archetype) representing a cluster of buildings, when modelled using the '*reference zone*' approach and also to more efficiently analyse the sensitivity of functional diversity on the resulting NZEB EP benchmarks for a given archetype in the EPBD cost-optimal method. This is achievable, for example, by varying multipliers attributed to each sub-activity to propagate functionality diversity. Furthermore, this approach can also allow policy makers to define customisable EP benchmarks, as discussed in Gatt et al. [35]⁷.

Although various potential applications have been identified, this research will focus on validating the '*reference zone*' approach concept on a case study multi-functional RB using the top-down approach to reduce the computational expense of the novel cost-optimal approach and facilitate its implementation. This validation requires statistically quantifying the extent to which the reduced space-order model constructed using the '*reference zone*' approach can replicate the energy end-use simulation outputs under study of the '*detailed*' model.

⁶Computation efficient building physics models may also efficiently allow the propagation of simulation runs directly from the building physics models themselves in the KOH framework without the need to develop meta-models.

⁷A similar but simpler concept to the '*reference zone*' approach to model school buildings in Malta was first applied in Gatt [193]. The modular modelling '*bottom-up*' approach performed in this research allows policy makers to define customisable EP benchmarks within the framework of the EPBD cost-optimal method for school buildings in Malta by considering different classroom orientations and percentage distributions of functional spaces to derive an EP benchmark for a school building.

4.4 | Hotel RB case study

This section demonstrates steps 1 to 4 of the proposed EPBD cost-optimal method detailed in Chapter 2, Section 2.5, by applying these steps on a case study cluster of the 5-star hotel building observations described in Chapter 3, for which a RB energy model must be defined. This section will also apply and validate the '*reference zone*' approach to this case study. For the case study, cluster 4, made up of only hotel 3, was chosen to demonstrate the proposed EPBD cost-optimal method, given that studying only one building facilitates the conceptual understanding and demonstration of the novel cost-optimal approach and the validation of the '*reference zone*' approach to modelling. Furthermore, the reason why cluster 4 was chosen instead of the other clusters that are only made up of one hotel observation, that is, cluster 5 and cluster 6, is because the hotel management was very cooperative in providing information for hotel 2. Also, the hotels in clusters 5 and 6 have more complex HVAC and DHW systems with additional parameters for chilled water pumping requirements and heat exchangers to cool the chiller, which consideration and modelling are beyond the scope of this research work.

DesignBuilder software [267], which provides a graphical interface to EnergyPlus [268], was used to set up EnergyPlus models for this case study. The extracted EnergyPlus idf files were then further customised and processed to create parametric EnergyPlus models required to generate multiple simulation runs at different parameter values from the models by combining the EP-macro auxiliary program [319] and JEPLUS [50]. The multiple simulation runs are required as input both for SA using the Morris method and Bayesian calibration to train a meta-model that will take the place of the building physics model. Both SA and Bayesian calibration were executed in Python [320] using the SALib [321] and Stan [322] packages, respectively, as detailed in the sections that follow. EnergyPlus idf files, the JEPLUS files, and the Python source code for this case study are available on the GitHub repository.

4.4.1 | Hotel 3 description

Hotel 3 under study is a large 5-star beach hotel located in Malta and was built in the mid-2000s. The hotel is a multi-storey building that covers a total interior floor area of more than 40,000 m² and is composed of approximately 300 guest rooms that cover more than 40 % of the total interior floor area, while dining and food preparation together cover approximately 10 % of the total interior floor area. The hotel also has an outside pool area of approximately 900 m². The hotel laundry is contracted to a third party and takes place outside the hotel premises.

The envelope of the hotel building is characterised by non-insulated concrete construction having an average U-Value of $2.1 \text{ W.m}^{-2}.\text{K}^{-1}$ with double-glazed aluminium frame fenestration of average U-value $4 \text{ W.m}^{-2}.\text{K}^{-1}$ and a Solar Heat Gain Coefficient (SHGC) of 0.7.

Regarding the air conditioning systems, more than 65 % of the hotel internal space is air-conditioned, pairing an air-cooled VRF system with a Dedicated Outdoor Air System (DOAS) that has a constant volume flow. The air conditioning system has never undergone major upgrades since the start of hotel operation. Furthermore, hotel circulation areas are naturally ventilated and do not have air heating or cooling systems. For DHW, production is met by using a dedicated LFO boiler system. The hotel produces most of its potable water using a dedicated in house Reverse Osmosis (RO) plant to produce 160 m^3 per day.

Hotel occupancy varies monthly in terms of the percentage number of occupied rooms. The levels of occupancy before COVID-19 ranged from 40 to 60 % between December and February and to 90 % or higher between June and October.

4.4.2 | Hotel 3 case study EnergyPlus (building physics) models

The hotel uses electricity, LFO and LPG as fuels for which consumption data were collected for three years between 2017 and 2019. Electricity is used to supply all end uses, excluding Domestic Hot Water (DHW) which is supplied entirely by the LFO. LPG is used only for a portion of cooking equipment and is excluded from building energy modelling and calibration analysis.

Given that DHW is supplied entirely by LFO, while all other end uses consume electricity and are defined using different and uncorrelated parameters, separate building physics models for DHW and the other end uses supplied by electricity were set up in DesignBuilder [267] using the EnergyPlus simulation tool [268]. Calibration was also performed separately for the two fuels. The advantage of defining two separate models is that the DHW model is characterised by only a small number of parameters and does not require space heat balance calculations, allowing for a more computationally efficient process when multiple simulation runs are generated to calibrate parameters with metered energy consumption data.

4.4.2.1 | Development of a DHW 'Probabilistic' EnergyPlus model for Hotel 3

For DHW, a simplified model was constructed for each year between 2017 and 2019 to consider the difference in the monthly occupancy of rooms and guest nights and the

corresponding energy consumption for each respective year. The simplified EnergyPlus model considers the consumption of LFO that meets the DHW demands of the hotel building as a function of the number of guest nights, the consumption of DHW per guest night, and the efficiency of the boiler system that generates DHW. Therefore, the DHW EnergyPlus model was only characterised in terms of DHW equipment and occupancy schedules, with DHW being the only energy end-use under study. It is to be noted that this hot water consumption includes other uses directly linked to guests such as use of hot water in kitchens and other amenities. Thus, using this simplified approach to modelling, only accommodation which is provided by guest rooms was considered as an activity for DHW modelling in the 'Reference zone' approach framework.

A 'Reference zone' was defined for each sub-activity, where sub-activities distinguish between different DHW schedule occupancy patterns for the guest rooms. Each 'Reference zone' was modelled as a square block having an arbitrary twenty-five (25) m^2 functional unit, characterised in terms of DHW equipment and occupancy, but fictitious in terms of geometry, envelope and form. The number of required sub-activities, each translating to a 'reference zone' was determined using a quasi-stochastic approach to modelling occupancy. Using this approach, monthly occupancy data in terms of the percentage number of occupied rooms was converted to a categorical distribution of schedules to be assigned to each 'reference zone'. This allows hotel schedules to be defined deterministically for each 'reference zone' but at the same time ensures that variation in the monthly occupancy and occupancy density distribution is fully considered in modelling. Each 'reference zone' is then scaled up using block multipliers in proportion to the guest room floor area attributed to each occupancy schedule.

The year 2017 is taken as an example to demonstrate the modelling concept used for the schedules in the DHW EnergyPlus models. Table 4.1 shows the occupancy patterns per month in terms of the % number of occupied rooms, the guest nights per occupied room and the occupational density ratio. The occupational density ratio is defined as the guest nights per occupied room divided by the peak number of guest nights per occupied room for a month in a given year. The occupancy data in Table 4.1 was then translated into twelve (12) categorical and deterministic schedules for the year 2017, as shown in Table 4.4. Twelve 'reference zones', one for each schedule, were therefore defined and attributed multipliers in proportion to the floor area assigned to each schedule shown in Table 4.2; for example, 41 % of the floor area of the guest rooms was occupied for all months and assigned the Schedule A occupancy pattern, while 4 % of the floor area of the guest rooms is never occupied and assigned Schedule L as depicted in Table 4.1.

Table 4.1: 2017 monthly occupancy pattern for hotel 3

Month	% number of occupied guest-rooms	number of guest nights per occupied room	Occupational density ratio
Jan-17	41	2.02	0.72
Feb-17	48	2.29	0.81
Mar-17	66	2.07	0.74
Apr-17	80	2.50	0.89
May-17	86	2.34	0.83
Jun-17	91	2.38	0.85
Jul-17	93	2.73	0.97
Aug-17	95	2.82	1.00
Sep-17	96	2.32	0.82
Oct-17	93	2.41	0.85
Nov-17	79	2.30	0.82
Dec-17	58	2.41	0.86

Table 4.2: Definition of schedules derived from the monthly occupancy patterns in Table 4.1 for the year 2017

Schedule	Guest room occupancy pattern description	% of total guest room floor area
Schedule A	Occupied all year round	41
Schedule B	Schedule A but no occupancy in January	7
Schedule C	Schedule B but no occupancy in February	10
Schedule D	Schedule C but no occupancy in December	8
Schedule E	Schedule D but no occupancy in March	13
Schedule F	Schedule E but no occupancy in November	1
Schedule G	Schedule F but no occupancy in April	6
Schedule H	Schedule G but no occupancy in May	5
Schedule I	Schedule H but no occupancy in June	2
Schedule J	Schedule I but no occupancy in July October	1
Schedule K	Schedule J but no occupancy in September	1
Schedule L	Never occupied	4

Appendix C shows the DHW schedule text file in DesignBuilder for the 'reference zone' characterised by Schedule A. The schedule provides the hourly DHW consumption profile for a typical day per month with hourly input values that range between 0 and 1 defining the DHW operation in terms of a fraction of the peak DHW flow rate. The highest hourly value of the fractional peak flow rate for the typical day of the month is taken to be equal to the occupancy density ratio for the corresponding month shown in Table 4.1 for 2017. The other schedules, namely Schedule B to Schedule L, are the same as Schedule A, but assigned null values for the peak flow fraction for all hours during the unoccupied months.

For the DHW model, the two uncertain parameters that need to be calibrated are the DHW consumption, which is defined in terms of litres of DHW per guest night, and the rated efficiency of the boiler. EnergyPlus, however, does not provide a direct input parameter to define DHW consumption in terms of litres per guest night. Therefore, the

output of the DesignBuilder idf file was configured using the DesignBuilder input parameters of occupancy density ($people.m^{-2}$) and DHW consumption ($litres.m^{-2}.day^{-1}$) to generate a maximum flow rate ($m^3.s^{-1}$) for each 'reference zone' in EnergyPlus that corresponds to a functional unit of one (1) litre of DHW consumption per guest night. A multiplier parameter was then introduced to the maximum flow rate ($m^3.s^{-1}$) in the EnergyPlus idf files using the built-in macro #eval [] in EnergyPlus . This multiplier for BEM calibration directly represents the consumption of DHW in terms of litres per guest night and is used to scale the DHW functional unit consumption to the total consumption. Variation of the multiplier generates multiple simulation runs from the model to allow the DHW per guest night to be calibrated using monthly metered LFO data.

The resulting DHW model idf files for each year for 2017 to 2019 are provided in the GitHub repository folder⁸. To develop a probabilistic model, the priors of the uncertain parameters of the model were assigned a range of values with the upper and lower bound values determined from both the literature (with the literature references depicted in Table 4.3) and local hotel energy audits. The priors are shown in Table 4.3. Once the upper and lower bounds for the calibration parameters were determined, the assignment of flat, non-informative [153, 161] on the bounded priors reflects the given level of knowledge about the parameters. It must be noted that the choice of non-informative priors allows the data contribution in the Bayesian framework to dominate when deriving the resulting posteriors.

Table 4.3: DHW uncertain parameters and corresponding prior distributions

Parameter	Distribution	Lower Value	Upper Value	Source
Boiler heater efficiency	Uniform	0.7	0.98	Energy audits, [323, 324, 325]
DHW consumption (Litres/day/guest night)	Uniform	60	200	Energy audits, [326, 327, 328]

⁸Refer to the DesignBuilder and corresponding EnergyPlus idf files in folder 'Ch 4 DHW BEM model 2017 to 2019'.

4.4.2.2 | Development of a computationally efficient and 'Probabilistic' Energy-Plus model for electricity end-uses for Hotel 3

Four EnergyPlus models were defined with varying levels of detail for modelling electricity consumption, ranging from Model A to Model D. Model A is a full-space model characterised by the actual building geometry, while Model D is the most computationally efficient model. Model D is constructed using the 'reference zone' approach concept described in Section 4.3. The aim of defining multiple models is to compare the simulated output accuracy of each simplified model with Model A, and to ultimately validate Model D for modelling electricity end-uses for Hotel 3. Once validated, defining Model D probabilistically to replace Model A reduces the computational expense of SA and Bayesian calibration for the proposed EPBD cost-optimal method.

All models were characterised with the 2017 weather and occupancy data and were deterministically defined using the main default parameters of the envelope, equipment, comfort and Indoor Air Quality (IAQ) shown in Table 4.5. Furthermore, for all models, it should be noted that the occupancy and plug-load schedules used for food preparation areas and meeting rooms were changed from the DesignBuilder default schedules to match the local occupancy patterns.

The level of detail for all four EnergyPlus models, Model A to Model D for Hotel 3, therefore, only varies in terms of geometric complexity and in the approach to defining the availability schedules for space heating, space cooling and artificial lighting for the guest rooms as described below. DesignBuilder and EnergyPlus files for Model A to Model D are available in the GitHub repository⁹. The models are described below.

- **Model A** : Model A is a detailed full-space model with the thermal zones defined as a minimum according to the function of the space and the method used to air-condition the zone, and characterised by the actual geometry of the building as shown in the rendered format in Figure 4.2. The guest-rooms in the model are defined with hourly resolution schedules for typical days in each month using the quasi-stochastic approach to modelling occupancy, following the same steps as explained for the DHW model in Section 4.4.2.1. Using this approach, the twelve (12) categorical schedules, from schedule A to schedule L, replicated in Table 4.4, were defined to program the availability schedule of use for the space heating and cooling of the guest rooms.

The guest room zones were assigned an appropriate schedule, from Schedules A to L, with the frequency of occurrence of the schedule varying according to the

⁹Refer to folder 'Ch 4 Electricity 2017 BEM models and ref zone validation' .

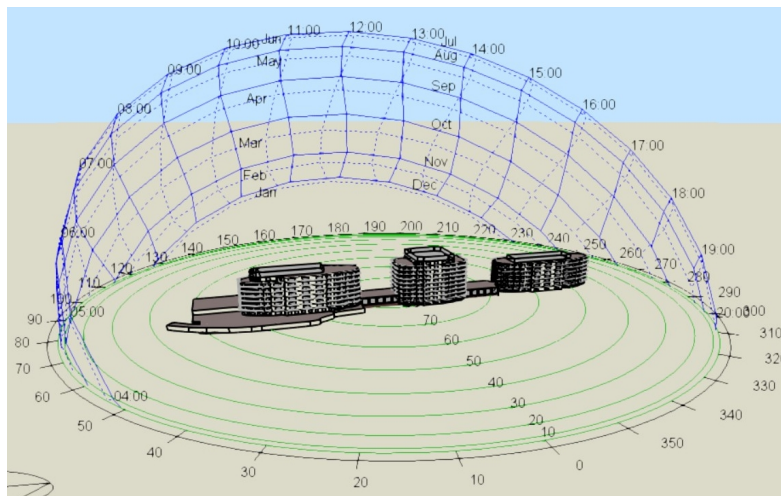


Figure 4.2: Rendered view of Hotel 3 under study

categorical probability distribution shown in Table 4.4. The table also shows the number of guest rooms assigned and defined for each schedule according to the distribution. The purpose of these schedules is different from the DHW model schedules, which defined the DHW operation in terms of the peak flow rate. Here, for each space heating and cooling schedules A to L, the hourly values for typical days in a month are assigned as either being on, with a value of 1, or off, with a value of 0, to program the hours for typical days in a month when space heating and cooling are available for a guest room to meet the defined temperature set points according to the monthly occupancy pattern of the assigned schedule. All schedules have the same hourly values for typical days in a month, but for months in a schedule that have no occupancy, all hourly values for that month are assigned a value of 0. As an example, Schedule B is the same as schedule A, but with all hourly values input as 0 for January, given that January is unoccupied for this schedule.

Furthermore, for this model, the consumption of artificial lighting in the guest room also follows the corresponding assigned schedule for space heating and cooling, but each hourly value for typical days in a month during occupancy is assigned a percentage of the maximum peak power lighting density according to the DesignBuilder default schedules for artificial lighting of ensuite bedrooms. In contrast to space heating and cooling, mechanical ventilation is defined with the same availability schedule for all guest rooms and is activated on a 24/7 basis for all days during the year to mitigate humidity issues that are frequently encountered in Malta due to its coastal climate.

Once Model A was deterministically defined, the model was checked for its calibration with metered monthly energy consumption data for the year 2017. The model is not statistically calibrated for monthly electrical energy consumption, given that the resulting NMBE and CVRMSE calibration statistical indicators are 45 % and 149 % respectively, and fall well outside the 5 % and 15 % ASHRAE [1, 2] thresholds, respectively. Furthermore, the annual electricity consumption discrepancy of Model A with the metered annual electricity consumption is -41.3 %¹⁰. Thus, to increase confidence in the model and execute the next steps of the proposed EPBD cost-optimal approach, the following sections will update the current '*non-calibrated and deterministic*' RB to a '*probabilistically Bayesian calibrated*' RB.

Table 4.4: Guest room occupancy pattern schedules and the number of guest rooms assigned to each schedule for Hotel 3

Schedule	Guest room occupancy pattern description	% of total guest room floor area	Number of guest rooms assigned to Model A
Schedule A	Occupied all year round	41	358
Schedule B	Schedule A but no occupancy in January	7	63
Schedule C	Schedule B but no occupancy in February	10	98
Schedule D	Schedule C but no occupancy in December	8	55
Schedule E	Schedule D but no occupancy in March	13	123
Schedule F	Schedule E but no occupancy in November	1	20
Schedule G	Schedule F but no occupancy in April	6	55
Schedule H	Schedule G but no occupancy in May	5	51
Schedule I	Schedule H but no occupancy in June	2	31
Schedule J	Schedule I but no occupancy in July October	1	14
Schedule K	Schedule J but no occupancy in September	1	33
Schedule L	Never occupied	4	37

¹⁰The calculations are found in the Microsoft Excel file entitled '*2017 Uncalibrated Model A ASHRAE statistics*'. The Excel file is found in the GitHub repository folder '*Ch 4 Electricity 2017 BEM models and ref zone validation*', sub-folder '*Validation*'.

- **Model B:** Model B is similar to Model A in terms of geometric complexity, but an average annual schedule with hourly resolution is defined for space heating and cooling for all guest rooms. This average hourly schedule assumes that the guest rooms are occupied for all months, but the percentage hours of availability of space heating and cooling for typical days in a month is made equal to the percentage number of occupied rooms for the corresponding month. The aim of this model is to validate this simplified approach to modelling occupancy, which defines only one schedule for all guest-rooms.
- **Model C :** Model C is similar to Model B in terms of guest room schedules, but is defined as a reduced space-order model that uses the adiabatic block multiplier concept explained in [329]. In this simplified approach to modelling, the hotel's middle floors, which are characterised by similar zoning, operation, and form (primarily made up of en-suite guest rooms and circulation areas), are combined using block multipliers. A block multiplier is a representative middle floor that replaces all similar floors and outputs energy results that are multiplied by the number of floors that it represents. All other floors below or above it are retained in the model since the upper and lower floors have different surface adjacencies and activities. This model allows one to compare this standard approach to simplify building energy models with the '*reference zone*' approach concept (Model D) in terms of simulation output accuracy and computational speed.

Table 4.5: Main parameter values to characterise the EnergyPlus model for electricity end-uses with respect to envelope, equipment, and operation. Acronyms; BOH : Back-of-house, DB : DesignBuilder, FOH : Front-of-house, RO: Reverse Osmosis, SHGC : Solar heat gain coefficient, U[] : Uniform distribution. Equipment power densities normalised by floor area of the corresponding activity space.

Envelope					
Parameter	Activity space	Units	Known value or uncertainty	Value source	Deterministic model default
Wall U-Value	Whole building	$W.m^{-2}.K^{-1}$	2.1	Observed	2.1
Roof U-value	Whole building	$W.m^{-2}.K^{-1}$	1.7	Observed	1.7
Fenestration U-value	Whole building	$W.m^{-2}.K^{-1}$	4	Observed	4
Glazing SHGC	Whole building	None	0.7	Observed	0.7
Equipment					
Parameter	Activity space	Units	Known value or uncertainty	Value source	Deterministic model default
VRF cooling COP	Whole building	None	U [2, 4.6]	DB database range	3.3 (DB default)
VRF heating COP	Whole building	None	U [2.6, 5.1]	DB database range	3.4 (DB default)
Fan ventilation pressure rise	Whole building	Pa	U [690, 2400]	DB typical values	600 (DB default)
Kitchen equipment power density	Food preparation	$W.m^{-2}$	U [88, 385]	DB default, local energy audits, [330]	130 (author)
Guest room power density	En-suite (guest) rooms	$W.m^{-2}$	U [3.15, 14.6]	DB default, local energy audits, [330]	3.15 (DB default)

Parameter	Activity space	Units	Known value or uncertainty	Value source	Deterministic model default
RO power density	RO plant	$W.m^{-2}$	70	Observed	70
DHW pump power	plant	kW	U [17.2, 25.8]	Site-visit, energy audits	DB auto sized
Operation (comfort and IAQ)					
Parameter	Activity space	Units	Known value or uncertainty	Value source	Deterministic model default
Cooling temperature set-point	En-suite (guest) rooms	°C	U [22,25]	Site-visits, [331], [332], [280]	25.4 (DB default)
Heating temperature set-point	En-suite (guest) rooms	°C	U [20,21]	Site-visits, [331], [332], [280]	21.6 (DB default)
Cooling temperature set-point	Food preparation	°C	U [27,31]	Site-visits, [331, 332], [280], DB default	30.1 (DB default)
Cooling temperature set-point	Eating drinking	°C	25	DB default	25 (DB default)
Heating temperature set-point	Eating drinking	°C	23	DB default	23 (DB default)
BOH ventilation rate	BOH	ACH	U [3,15]	Site-visits, [333], DB default	4.9 (DB default)
FOH ventilation rate	FOH	$m^3.s^{-1}.person^{-1}$	U [0.003,0.014]	DB default, [332], [280]	0.0104 (DB default)

- **Model D** : Model D is also similar to Model B in terms of operation and equipment, but features a reduced space-order model constructed using the proposed '*reference zone*' approach concept detailed in Section 4.3. The use of only one occupancy schedule in Model B versus Model A minimises the required number of sub-activities and the corresponding number of reference zones to model the guest rooms in this model.

The model is defined by the activities, the number of reference zones per activity, and the number of multipliers per reference zone, as shown in Table 4.6. The table also shows the space conditioning attributes for each activity in the model, while Figure 4.3 shows a plan view snapshot of the geometry for Model D.

Each '*reference zone*' is constructed as a rectangular block, and all '*reference zones*' which are space cooled or heated are modelled to represent as accurately as possible perfect average archetype spaces. In addition, each '*reference zone*' is thermally decoupled to carefully maintain as close as possible the space surface adjacency (boundary) conditions¹¹ of Model A for each sub-activity when the multipliers depicted in Table 4.6 are added. This processing aims to enable Model D to replicate as closely as possible the heat-space balance calculations of Model A.

For the '*reference zones*' that are not space cooled or heated, such as the circulation areas, a total floor area approach is used in contrast to an archetype space approach. In this approach, since no heat space balance calculations are required, only the total area and volume of the spaces replicate Model A to correctly quantify the end-uses of plug loads, artificial lighting, and mechanical ventilation. The energy consumption for these end-uses is only a function of the floor area and volume of the non-conditioned space for the defined operational schedules.

¹¹The space surface adjacency (boundary) conditions of Model A were maintained as closely as possible for Model D for all sub-activities in terms of various properties. These properties include the space surface area to volume ratio, the space exposed surface area to the exterior per orientation, the Window to Wall Ratio (WWR) for each orientation, the % unshaded and % shaded glazing per orientation, and the adjacency conditions with other sub-activities.

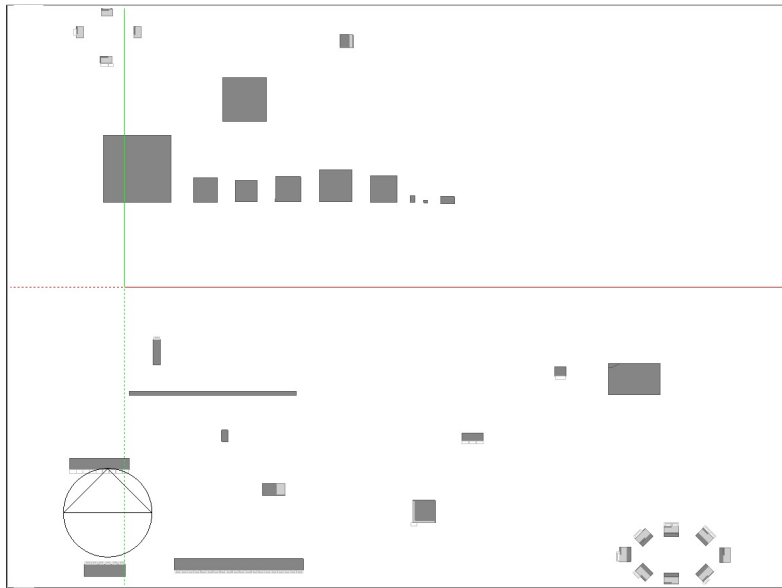


Figure 4.3: Hotel 3 Model D geometry plan view snapshot from DesignBuilder software. Each rectangular block shown in the figure depicts the geometry of a reference zone energy model representing a sub-activity. The sub-activities are defined in Table 4.6

Table 4.6: Definition of hotel 3 according to activities and related sub-activities for the 'reference zone' approach to modelling. Acronyms; C : Cooled, E : Extract, H : Heated, HR : Heat Recovery, MV : Mechanically Ventilated, NV : Naturally Ventilated, S : Supply, WS : Work Shops

Activity (Space)	No. of reference zones	Sub-activity criteria	Multiplier per reference zone	Space conditioning
Accommodation (En-suite rooms)	8	Archetype space per orientation	N (106), NE (8) E (39), SE (8) S (114), SW (8) W (38), NW (7)	C, H, MV (S&E)
Reception	1	Archetype space	8	C, H, MV(S&E) + HR
Circulation	1	Total Floor Area (TFA)		NV
Massage room	1	Total Floor Area (TFA)		C, H, MV(S)
Car-park (E)	1	Total Floor Area (TFA)		MV(S)
Food preparation	1	Archetype space	1	C, H, MV(S&E)
Eating & drinking	1	Archetype space	8	C, H, MV (S)
Meeting rooms	1	Archetype space	2	C, H, MV(S)
Hall	1	Archetype space	1	C, H, MV(S)
Office work (offices)	4	Archetype space per orientation	N (16), E (3) S(3), W(1)	C, H, MV(S)
Swimming (pool/sauna)	1	Archetype space	1	AHU
Fitness (gym)	1	Archetype space	1	C, H, MV(S&E)
Changing rooms				C, H, MV(S&E)
Public toilet	1	Total Floor Area (TFA)		NV
Shop	2	Archetype space per orientation	N (1), S (1)	C, H, MV(S&E)
Server room	1	Archetype space	10	C,H
Linen room (E)	1	Archetype space	1	MV (S)
Stores	2	Space conditioning	WS (TFA) General (TFA)	WS: MV(S&E) General : NV
Plant	3	Equipment & space conditioning	RO plant (TFA) Light plant (TFA) Reservoir (TFA)	RO: MV(S&E) Light: MV(S&E) Reservoir: NV
Work Shops (WS) (E)	1	Total Floor Area (TFA)		MV (S)

One must note that to facilitate the geometric conversion from Model A to Model D, CSV files containing geometric, zone surface adjacency properties, and other non-geometric information of Model A were generated by the DesignBuilder (DB) software from the EnergyPlus IDF ASCII files. A Microsoft Excel workbook was programmed and validated to automatically extract and process the required information to construct the '*reference zones*' for Model D.

This approach is demonstrated for the construction of the '*reference zones*' of the en-suite guest-rooms, using an archetype space per 45° orientation. The Microsoft Excel workbook allowed important information from Model A to be extracted. This information included the total en-suite guest-room floor area per orientation, the average en-suite guest-room floor area, the exposed space wall surface area per orientation, the WWR per exposed wall orientation, the % of glazing that is shaded per exposed wall orientation and the horizontal roof surface area. This information was processed to define an average '*archetype*' guest-room, termed '*reference zone*', to be constructed on DesignBuilder software for every orientation. The '*reference zone*' has an average en-suite guest-room floor area and is characterised by average geometric characteristics that also reflect the average surface adjacency (boundary) conditions for each orientation. Multipliers were then assigned to each '*reference zone*' guest room block accordingly to satisfy the total floor area of the guest rooms per orientation.

The eight (8) '*reference zones*' for the guest-rooms for Hotel 3 are shown in Figure 4.4. The red blocks are '*dummy*' naturally ventilated zones that replicate the heat transfer of the guest rooms with the naturally ventilated circulation spaces. Furthermore, the dark grey top surface represents the proportion of the ceiling, which is modelled as a roof for each orientation, while the light grey ceiling surface for each '*reference zone*' represents an adiabatic ceiling surface. The surfaces with the fenestration are the exposed surfaces. All other surfaces, including the floor and the widths of the blocks, are modelled as adiabatic.

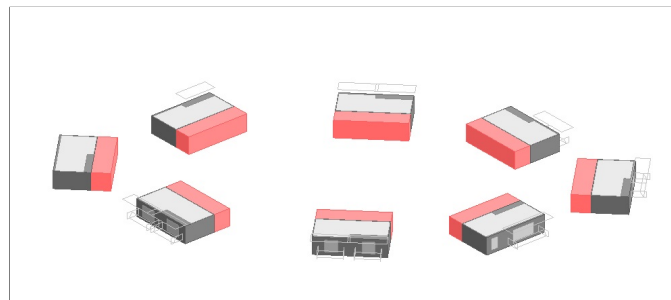


Figure 4.4: 'Reference Zones' geometry for Model D en-suite guest rooms shown on DesignBuilder software where the red zones are naturally ventilated replicating boundary surface conditions to model the heat transfer of the guest-rooms with the naturally ventilated circulation spaces

One must note that there is uncertainty in identifying the impact of the roofs on the actual heat balance of guest rooms, as the roof surfaces in Model A are partially shaded and obstructed. Therefore, three (3) variants, Model D1 to Model D3¹², were considered and analysed to identify which variant can best replace Model A. Model D1 considered 15 % of the guest rooms' ceiling surface area as an external roof, as shown in Figure 4.4. Model D2 assumed the whole ceiling of the guest rooms to be fully adiabatic. Finally, Model D3 was similar to Model D1 but the 15 % exposed roof was reduced by modelling the ceiling surfaces of the 'reference zones' orientated North (N) and East (E) as fully adiabatic.

¹²The DesignBuilder and EnergyPlus files for Models D1 to D3 are found in the GitHub repository folder 'Ch 4 Electricity 2017 BEM models and ref zone validation' sub-folder 'Model D1 D2 D3 plus Passive'. Refer also to Appendix B for a detailed description of all files and folders found in the GitHub Repository.

4.4.2.3 | Statistical validation and computational expense analysis of the simplified electricity end-use models for the default parameters

Table 4.7 provides statistical indicators that compare the monthly EnergyPlus simulated outputs for the end uses of total electricity consumption (kWh), space cooling (kWh), and space heating (kWh) of the simplified models to the monthly EnergyPlus outputs of Model A.

The statistical indicators show that all simplified models are valid and monthly calibrated with Model A for total electrical energy consumption, since the resulting NMBE and CVRMSE calibration statistical indicators fall within the 5 % and 15 % ASHRAE [334] thresholds for CVRMSE and NMBE, respectively. Furthermore, the annual electricity consumption discrepancy with Model A is < 2 % for all simplified models. All simplified models are also statistically calibrated for monthly space cooling with Model A, and the resulting maximum annual space cooling consumption discrepancy is 3.6 % for Model D3¹³. For monthly space heating, Model D2 is also statistically calibrated with Model A with an annual space heating discrepancy of 1.3 %, while Model B and Model D1 also achieve a good agreement for annual space heating with a discrepancy of 4.7 % and 5.3 %, respectively. On the other hand, Models C, D1, and D3 provide inferior results in predicting monthly and annual consumption for space heating.

Table 4.7 also compares the simulation run time for all models when performing a single simulation run. Models D1 to D3 provide a significant reduction in computational time, with a simulation run-time improvement of 4000 % compared to Model A, while Model C provides a substantial simulation run-time improvement of 3000 %. In contrast, Model B does not provide an improvement in simulation run-time over Model A.

Given that all variants of Model D provide the most computationally efficient approach, while Model D2 is also statistically calibrated with Model A for all end-uses considered, Model D2 was chosen to replace Model A for generating multiple simulation runs for SA and Bayesian calibration in a much shorter time span. Therefore, to develop a probabilistic building physics model for the electricity end-uses, Model D2 was defined probabilistically. The priors of the uncertain parameters of Model D2 were assigned a range of values with the upper and lower bound values determined from both the literature (with the references to the literature shown in Table 4.5, column '*Value source*') and the local hotel energy audits. The priors for the uncertain parameters are the distributions shown in Table 4.5, column '*Known value or uncertainty*'. Once the

¹³Space cooling and space heating contribute to 12.7 % and 6.5 % of total electricity consumption respectively for Model A.

upper and lower bounds for the calibration parameters were determined, the assignment of flat, non-informative [153, 161] on the bounded priors reflects the given level of knowledge about the parameters. It must be noted that the choice of non-informative priors allows the data contribution in the Bayesian framework to dominate when deriving the resulting posteriors.

In the sections that follow, Model D2 will also be validated against Model A for its ability to identify the most significant parameters in SA and to accurately predict monthly electricity outputs for LHS simulation runs from the calibration parameters prior distributions. In the following sections, Model D2 and Model D will be used interchangeably.

To provide further confidence in choosing Model D2 over Models D1 and D3 to replace Model A, different combinations of passive measures were applied in Table 4.8 to all variants of Model D with the default parameters defined in Table 4.5. This analysis identifies which simplified model best replaces Model A to predict annual energy savings for space heating and cooling relative to the base scenario¹⁴. Therefore, this analysis indicates the potential of using a simplified model in the proposed cost-optimal analysis to identify improvements in EP when ECMs are applied to the calibrated model for EP benchmarking. Table 4.8 shows that Model D2 provides the closest % energy savings predictions for space cooling and heating to Model A for all combinations of passive measures. The maximum discrepancy is only 4.6 %¹⁵ which occurs when the model is simulated to include all passive measures M1 to M3, which are described in Table 4.8. This result reaffirms the choice of Model D2, given that the model, once calibrated, provides the best potential to also replace Model A in Steps 5 and 6 (refer to Section 2.5) of the proposed EPBD cost-optimal approach.

To develop a probabilistic building physics model for the electricity end-uses, the priors of the uncertain parameters of Model D2 were assigned a range of values with the upper and lower bound values determined from both the literature (with the literature references depicted in Table 4.5) and local hotel energy audits. The priors are shown in Table 4.5. Once the upper and lower bounds for the calibration parameters were determined, the assignment of flat, non-informative [153, 161] on the bounded priors reflects the given level of knowledge about the parameters. It must be noted

¹⁴The DesignBuilder and EnergyPlus files for Models D1 to D3 with and without the passive measures in Table 4.7 are found in the GitHub repository folder '*Ch 4 Electricity 2017 BEM models and ref zone validation*' sub-folder '*Model D1 D2 D3 plus Passive*'. The statistical analysis to derive the results in Table 4.7 is performed in Microsoft Excel file entitled '*Models D1 D2 D3 vs Model A ECMs performance*' under the same sub-folder.

¹⁵The 4.6 % is calculated by subtracting the 19.89 % annual energy savings from Model A with the 15.25 % annual energy savings of Model D2 from column 'M1 to M3'.

that the choice of non-informative priors allows the data contribution in the Bayesian framework to dominate when deriving the resulting posteriors.

Table 4.7: Accuracy and computational efficiency performance of the simplified EnergyPlus models (Model B, Model C, and Model D with variants Model D1, Model D2 and Model D3) in comparison to the full-space detailed EnergyPlus model (Model A)

	Monthly electrical consumption (kWh)		Monthly space cooling (kWh)		Monthly space heating (kWh)		Annual electricity (kWh)	Annual space cooling (kWh)	Annual space heating (kWh)	Model computational efficiency	
	NMBE %	CVRMSE %	NMBE %	CVRMSE %	NMBE %	CVRMSE %	difference %	difference %	difference %	Run time improvement (min)	Run time reduction (%)
EnergyPlus models comparison¹⁶											
Model B vs. Model A	0.36	1.19	-1.37	4.55	5.14	17.04	-0.33	1.26	-4.71	0	0
Model C vs. Model A	0.32	1.06	0.53	1.77	8.5	28.2	-0.29	0.33	-7.79	42	3000
Model D1 vs. Model A	1.06	3.51	-1.15	3.83	-5.77	19.13	-0.97	1.06	5.29	58.5	4000
Model D2 vs. Model A	2.13	7.07	2.54	8.42	1.42	4.73	-1.95	-2.33	-1.31	58.5	4000
Model D3 vs. Model A	0.3	1.01	-3.97	13.17	-10.8	35.82	-0.28	3.64	9.90	58.5	4000

¹⁶For Model B and Model C, the monthly space cooling energy end-use consumption was removed for January, February and December. For Models D1, D2 and D3, the space cooling schedule was not made available for January, February and December in the EnergyPlus models. All models referred to in this table can be found in GitHub repository 'Ch 4 Electricity 2017 BEM models and ref zone validation'. The statistical analysis to derive the results in the table is performed in Microsoft Excel file 'Models B C D vs Model A ASHRAE calibration validation' under sub-folder 'Validation'.

Table 4.8: Comparison of the percentage of annual energy savings from space heating and cooling relative to the base scenario for the different 'Reference Zone' model variants (Models D1 to Model D3) and Model A upon the application of different passive measures. Measure M1 is the application of roof insulation for a final roof U-value of $0.4 \text{ W.m}^{-2}.K^{-1}$. Measure M2 is the application of wall insulation for a final wall U-value of $0.5 \text{ W.m}^{-2}.K^{-1}$. Measure M3 is the application of a 3M PR70 spectrally selective coating on the glazing to achieve a glazing with a U-value of $3 \text{ W.m}^{-2}.K^{-1}$ and SHGC of 0.55. In the 'M1 to M3' scenario, the model is simulated with all passive measures applied.

	Total annual space heating & cooling (kWh) consumption for different passive measures					% Annual space heating & cooling (kWh) energy savings			
	Base scenario	M1	M2	M3	M1 to M3	M1	M2	M3	M1 to M3
Model A	777982	740640	753281	732305	659323	4.80	5.59	5.87	15.25
Model D1	797376	714338	736773	761762	627600	10.41	8.22	4.47	21.29
Model D2	762573	697060	727575	726166	610892	8.59	4.81	4.77	19.89
Model D3	822816	724888	787216	786330	635167	11.90	4.52	4.43	22.80

4.4.3 | Sensitivity Analysis (SA)

The first step in calibrating the RB energy models with metered energy consumption data is to perform SA and rank the parameters according to their impact on the model output. Choosing the correct number of parameters to calibrate, where the number of calibration parameters is denoted by q , is critical to optimise the parameter dimensional space. This optimisation is required because the number of calibration parameters impacts both the required number of simulation runs required to train a meta-model and the computational time required for the Bayesian calibration process.

SA for the case study was performed using the Morris method [137] supported in SALib [321]. The analysis was carried out separately for the DHW (refer to Section 4.4.3.1) and electricity end-uses (refer to Section 4.4.3.2) EnergyPlus models. The source code files for SA are found in the GitHub repository¹⁷. For both cases, SA was carried out with 4 levels and 10 trajectories, as suggested and successfully demonstrated in Wate et al. [301].

4.4.3.1 | DHW model Sensitivity Analysis (SA)

Given that only two uncertain parameters, the DHW consumption per guest night and the boiler water heater efficiency, must be calibrated with the metered LFO energy consumption for the DHW model, SA analysis is not essential. However, for completeness, this section will demonstrate the Morris method applied to the DHW model for the 2017 hotel occupancy schedules.

Figure 4.5 shows the result of the Morris method in terms of the modified mean μ^* and SD σ for each parameter. The ranking of the parameters according to the modified mean μ^* shows that the DHW consumption per guest night has a much greater impact on the annual LFO end-use energy consumption than the boiler water heater efficiency. This ranking was derived when considering the parameter prior distributions depicted in Table 4.3 for the SA. Both parameters for the DHW model will be calibrated with monthly metered LFO consumption in Section 4.4.4.1.

¹⁷Refer to folders 'Ch 4 DHW SA' for the DHW model SA source files and folder 'Ch 4 Electricity SA' for the electricity energy end-uses SA source files.

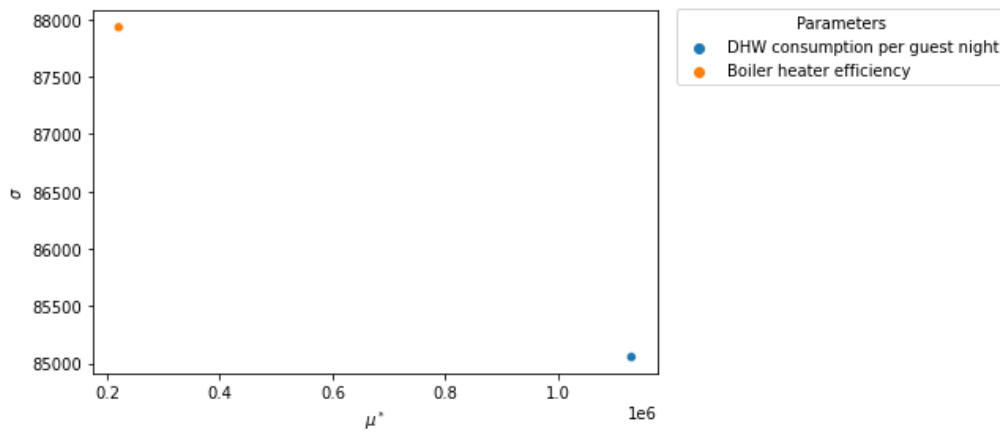


Figure 4.5: Results from the Morris method for the DHW EnergyPlus model to identify which parameters have the largest influence on annual LFO energy consumption

4.4.3.2 | Electricity energy end-uses model SA

For the electricity end uses, SA using the Morris method was performed both for EnergyPlus Model A and EnergyPlus Model D¹⁸ to rank the impact of the 11 uncertain parameters identified in Table 4.5 on the simulated annual electricity energy end-use energy. Performing the Morris method using both models allows one to compare the results of the two models and identify to what extent Model D can replicate the results of Model A and therefore replace Model A for improved computational efficiency when performing SA. Table 4.9 compares the ranking of the eleven (11) uncertain parameters according to the modified mean μ^* for the two models.

Table 4.9: Electricity end uses model parameters ranked according to the modified mean μ^* for both Model A and Model D

Rank	Model A		Model D	
	Parameter	μ^*	Parameter	μ^*
1	Fan ventilation pressure rise	2.42E+06	Fan ventilation pressure rise	2.38E+06
2	Kitchen equipment power density	2.35E+06	Kitchen equipment power density	2.34E+06
3	BOH ventilation rate	1.68E+06	BOH ventilation rate	1.68E+06
4	FOH ventilation rate	9.36E+05	FOH ventilation rate	9.31E+05
5	VRF cooling COP	8.80E+05	VRF cooling COP	8.51E+05
6	Guest rooms equipment power density	7.59E+05	Guest rooms equipment power density	7.64E+05
7	Guest rooms Cooling temp set point	3.68E+05	Guest rooms Cooling temp set point	3.66E+05
8	VRF heating COP	1.53E+05	VRF heating COP	1.46E+05
9	Kitchen cooling set-point temperature	7.38E+04	Kitchen cooling set-point temperature	7.36E+04
10	DHW pump power	3.77E+04	DHW pump power	3.77E+04
11	Guest rooms heating temp set point	2.58E+04	Guest rooms heating temp set point	2.47E+04

¹⁸For both models, the 2017 occupancy schedules were used for SA.

Both models provide the same ranking position result for the parameters under study. This result provides evidence that a reduced space-order building physics model constructed using the 'reference zone' concept has the potential to replace a detailed full space-order model, thus allowing for a more computationally efficient approach to SA in BEM. The suitability of replacing Model A with Model D for SA is further evident given the resulting low discrepancies in the simulated annual electricity energy end-use output values between the two models, with a maximum discrepancy of 2.96 %, a median discrepancy of % 0.30, NMBE of 0.19 % and CVRMSE of 2.06 %¹⁹.

Figure 4.6 shows the result of the Morris method for Model D in terms of the modified mean μ^* and SD σ for each parameter. The seven top-ranking parameters in Table 4.5 will be calibrated for this case study. The choice of seven calibration parameters ($q = 7$) is based on a visual study of Figure 4.6 that shows that the four least significant parameters fall under the same cluster for μ^* and σ , and can therefore be grouped together in terms of having the lowest impact on the model output.

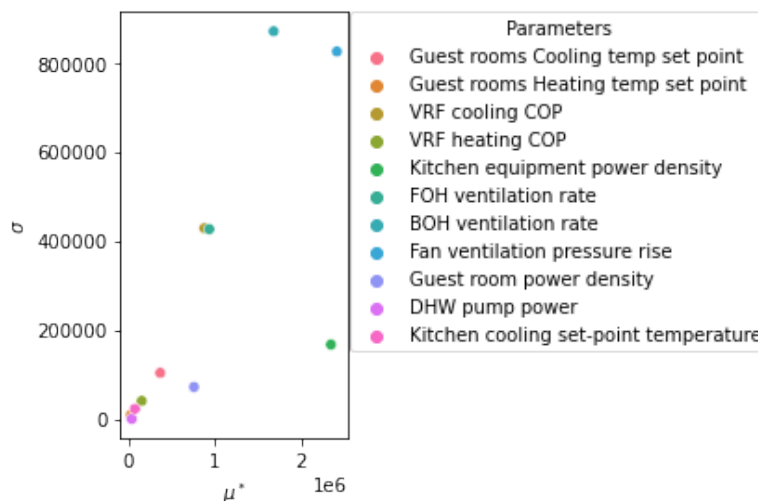


Figure 4.6: Morris method results for the electricity energy end uses Model D to identify which parameters have the biggest impact on total annual electrical energy consumption

¹⁹The Microsoft Excel file 'SA CVRSME and NMBE validation' used to statistically compare the difference in the simulated annual electricity energy end-use output values between Model A and Model D is provided in the GitHub repository folder 'Ch 4 Electricity SA' sub-folder 'SA ASHRAE validation for Model D2 vs Model A'. Refer to Appendix B for a detailed description of all files and folders found in the GitHub Repository.

4.4.4 | Bayesian Calibration

To enable calibration of the q calibration parameters t (t_1 to t_q) using a meta-model that replaces the more computationally intensive building physics model, a field observed input data set matrix D^f is combined with computer simulation data set matrix D^c as prescribed in Higdon et al. [335] and according to the following steps (adapted from [161]):

1. Construct a matrix D^f comprised of the observable output such as the metered fuel consumption data, $y(x^f)$, and the measurable (known) or observable p inputs x^f (x_1^f to x_p^f). Examples of observable or measurable inputs include the outdoor dry-bulb temperature and the monthly number of occupied rooms. For a number n of observed values and only one observable output y , matrix D^f has dimensions $n \times (p+1)$.
2. Generate predicted fuel consumption output data $\eta(x^c, t^c)$ from the building physics model for m observations at the same measurable or observable inputs x^c ($x^c = x^f$). The m simulation points for x^c, t^c for data set [x_1^c to x_p^c and t_1^c to t_q^c] are determined by LHS sampling from the parameter space of the prior distribution calibration parameters t at the observable inputs x^c .
3. Construct matrix D^c composed of the predicted output data $\eta(x^c, t^c)$, and data set [x_1^c to x_p^c and t_1^c to t_q^c] having dimensions $m \times (p + q + 1)$.
4. Combine matrix D^f and matrix D^c in a meta-model in line with Higdon et al. [335] and explore the joint posterior distribution using a full Bayesian statistical inference with MCMC sampling algorithms that include the No-U-Turn sampler (NUTS) [178]²⁰ implemented in Stan [322].
5. Perform Bayesian model diagnostics and calibration validation.

Bayesian calibration was implemented separately for LFO and electricity using monthly resolution data. For calibration, the combined field and the computer-simulated approach to Bayesian statistical inference described above was executed in Stan [322] using the NUTS algorithm. Two source code files were used for Bayesian calibration for each fuel as follows:

²⁰NUTS has been successfully applied in Bayesian calibration of BEM studies, including [176, 161, 121]. NUTS does not require manual tuning and has been shown in [336] to be more effective in terms of convergence given fewer required iterations compared to other commonly used algorithms, such as the Gibbs sampler [337].

1. **Python interface code file** with a .ipynb extension format having D^f and D^c in CSV file format as input. D^f and D^c are processed using the code in Python to set up the data dictionary to input and run into the Stan model. The results from Stan are also extracted using this code to perform Bayesian diagnostics and visualisations of Bayesian inference using the Arviz [151] package in Python and to validate calibration for both in-sample (training) and out-of-sample (test) data.
2. **Stan [322] code** with a .stan extension to construct the meta-model and perform Bayesian calibration.

The code for these files was adapted from Chong et al. [161]. The source code files are found in the GitHub repository²¹.

4.4.4.1 | DHW model Bayesian calibration

For calibrating the DHW model, two-thirds (years 2017 and 2018) of the monthly occupancy and LFO consumption data was employed as the training set for the calibration of the the parameters, while the remaining data (year 2019) was used as the test-set to assess the the model's ability to predict outcomes when given unseen data.

For calibration, the field-observed input data set matrix D^f for the training data set covers 24 months of data and is a 24 by 2 matrix. It is composed of the known input x_1^f , which is the monthly number of guest nights, and the observable output, y , which is the monthly metered consumption of LFO .

Furthermore, the computer simulation data set matrix D^c for the training data set is a 240 by 4 matrix, for which 240 ($m=240$ ²²) LHS simulation runs of the building physics model were performed, 120 simulations each for the year 2017 and 2018. Matrix D^c is composed of $\eta(x^c, t^c)$, the monthly predicted LFO consumption, and data set $[x_1^c, t_1^c, t_2^c]$. For the data-set, x_1^c ($x_1^c = x_1^f$) is the monthly number of guest nights while t_1 and t_2 are the calibration parameters of the simulation model. More specifically, t_1 is the DHW consumption in litres per guest night and t_2 is the boiler heater efficiency.

Given the low dimensionality of the model having only one observable input ($p = 1$) and two calibration parameters ($q = 2$), a Bayesian linear regression model documented in the Stan Guide [338] was used as a meta-model with the likelihood function depicted in Equation 4.2.

²¹Refer to folder 'Ch 4 DHW Bayesian calibration' for the LFO energy end-use (DHW model) calibration source files and folder 'Ch 4 Electricity Bayesian calibration' for the electricity calibration source files. Refer to Appendix B for a detailed description of all files and folders found in the GitHub Repository.

²²The fast simulation time of the DHW EnergyPlus model completing 240 monthly simulations comprised of 20 annual simulations in <620 seconds allowed an abundance of simulations to be executed to train the model.

$$z \sim normal(\alpha + \beta X_t, \sigma) \tag{4.2}$$

In the equation, z is a single vector that has a dimension N ($N = n + m$) combining the n observation output values for $y(x^f, t^f)$ and the m model prediction values for η , where t^f represents the calibration parameter space corresponding to D^f . Furthermore, X_t is an N by $(p + q)$ matrix that combines x^f , t^f , x^c and t^c into a single matrix. The model assumes a normally distributed noise term with scale σ and its intercept and slope parameters are α and β , respectively. Equation 4.2 and the prior parameter distributions derive the posterior distribution of the calibration parameters t^f via Bayesian inference.

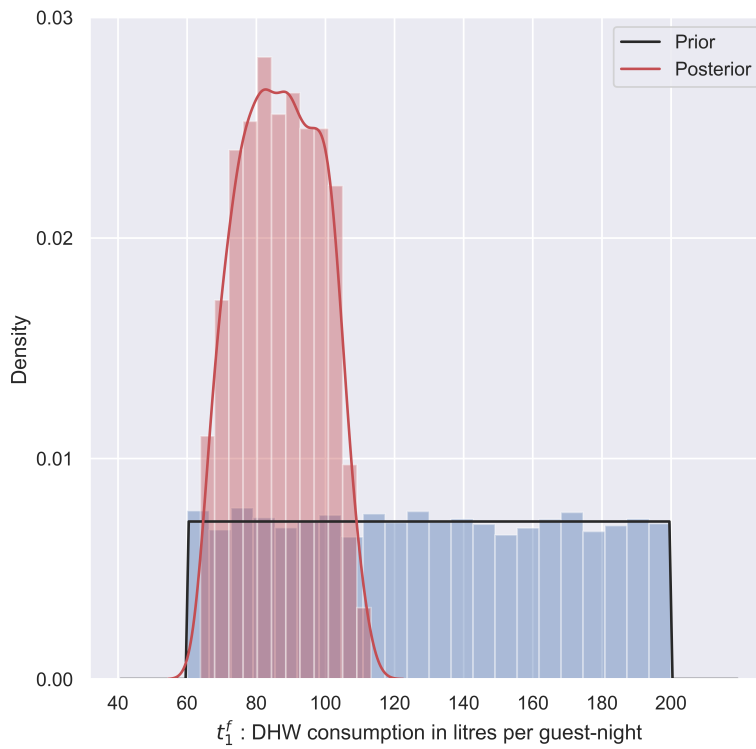
The prior and resulting posterior distribution after Bayesian inference of the calibration parameters t_1^f and t_2^f are visually shown in Figure 4.7, together with a statistical summary of the posterior distributions in Table 4.10. It can be observed that the uncertainty in the value of t_1^f has been significantly reduced following calibration from a prior distribution for DHW ranging from 60 to 200 litres/guest night to a posterior distribution whose 95 % Highest Density Interval (HDI) extends to only between 66 and 106 litres/guest night. In contrast, for parameter t_2^f that has a much lower impact on LFO consumption, the posterior distribution has not narrowed significantly compared to the prior. This means that given the observed data, not much has been learned about the value of t_2^f following calibration.

The overall reduction in the uncertainty of the parameters after calibration is however satisfactory based on the resulting model output before and after calibration, as identified from Figures 4.8 and 4.9. The figures show that both the predicted monthly meta-model (Figure 4.8) and simulated annual EnergyPlus (Figure 4.9²³) LFO consumption distributions generated from the posterior distributions are significantly narrower when compared to EnergyPlus simulation runs propagated from prior distributions.

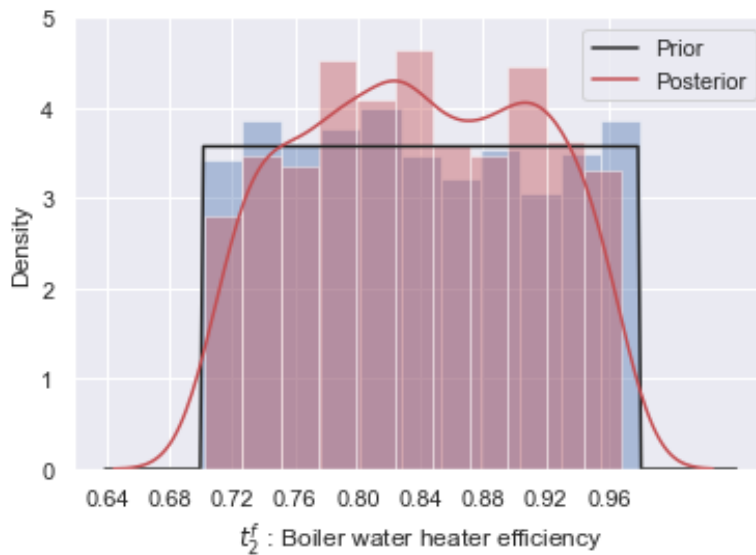
Table 4.10: A statistical summary of the DHW model posterior distribution for each calibration parameter

Symbol	Parameter	Mean	Median	SD	HDI _{5%}	HDI _{95%}
t_1^f	DHW (l/guest night)	87.1	87.1	41.4	66	106
t_2^f	Boiler heater efficiency	0.84	0.84	0.45	0.72	0.96

²³The JEPLUS files required to propagate annual uncertainty in LFO end use from the DHW building physics model and the corresponding simulation results are found in GitHub Repository folder 'Ch 4 Electricity Bayesian calibration' sub-folder 'Physics models Annual uncert propag Prior Post'. Refer to Appendix B for a detailed description of all files and folders found in the GitHub Repository.



(a)



(b)

Figure 4.7: The prior and resulting posterior distributions of the DHW energy model calibration parameters for (a) t_1^f : DHW consumption in litres per guest night and (b) t_2^f : Boiler water heater efficiency

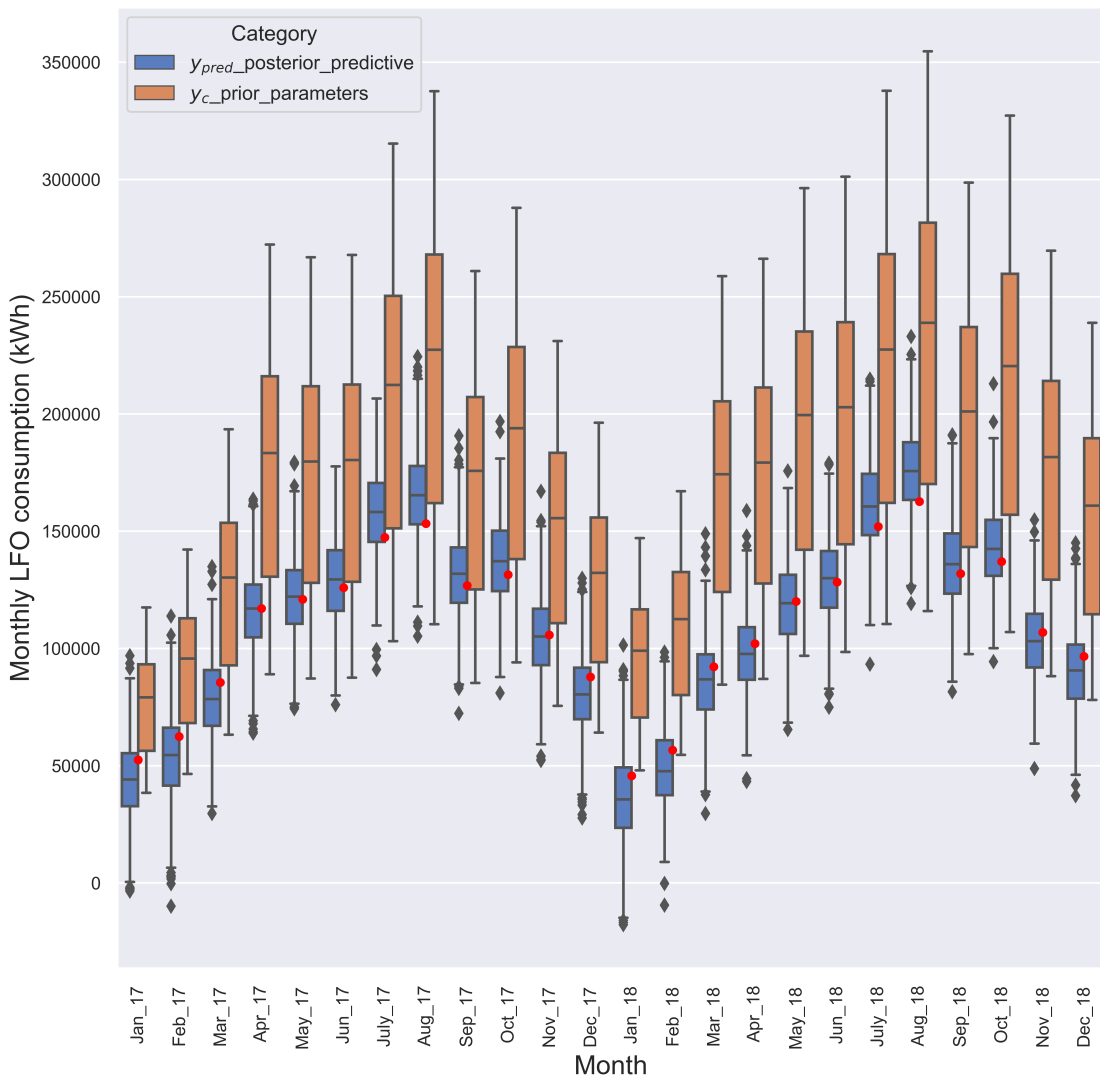


Figure 4.8: Monthly LFO consumption box plot comparing EnergyPlus simulation runs for prior calibration parameters distributions (orange plot) and the posterior predicted consumption from the calibrated meta-model (blue plot). The red dots depict the actual metered monthly LFO consumption

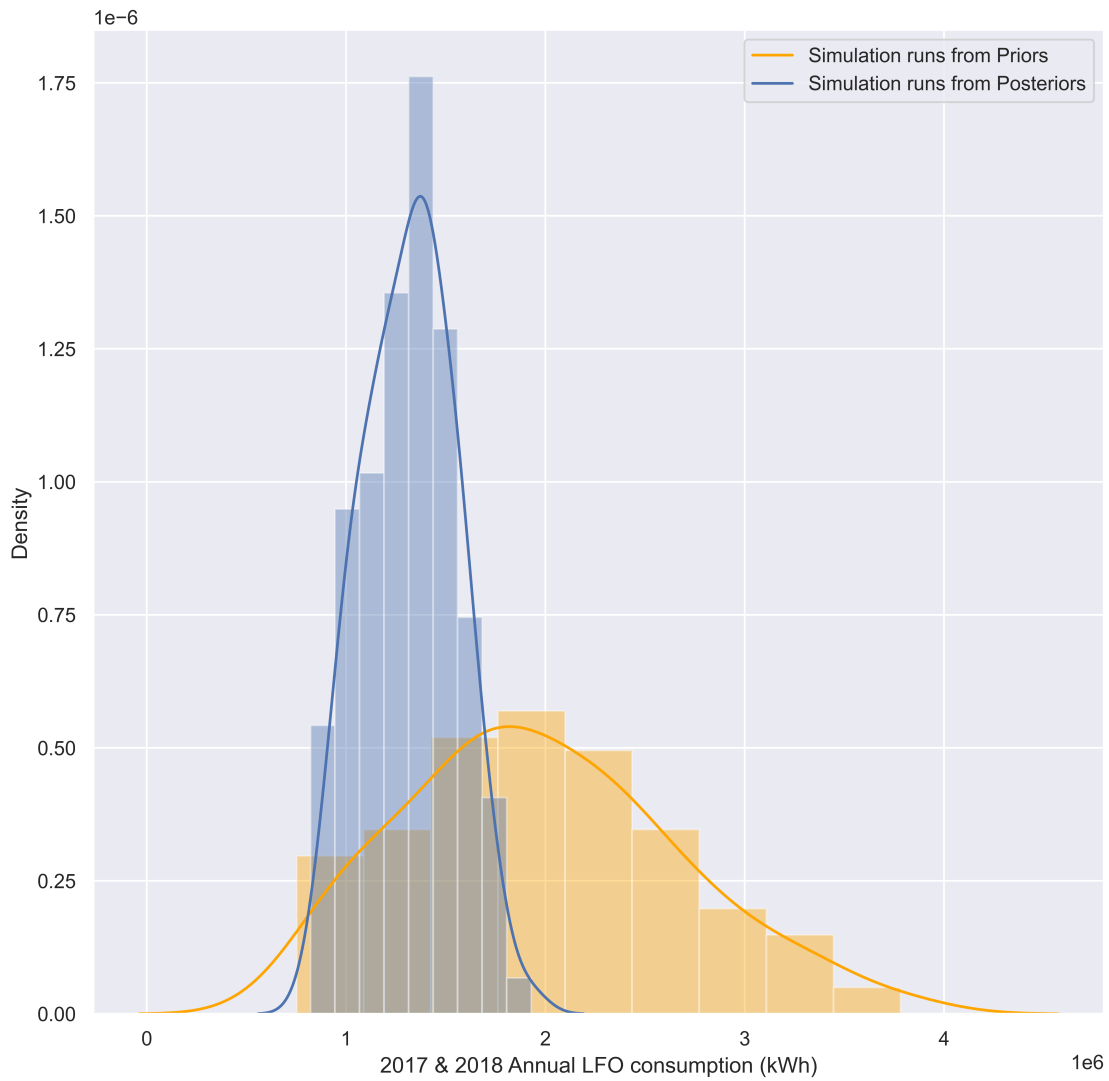


Figure 4.9: Annual LFO consumption distribution generated from EnergyPlus model for simulation runs from prior (orange plot) versus posterior (blue plot) calibration parameter distributions for the years 2017 and 2018.

4.4.4.1.1 DHW Bayesian model diagnostics

The Bayesian model for DHW was checked for adequate convergence using both trace plots (see Figure 4.10) and statistical diagnostic metrics (see Table 4.11). Both the trace plots generated in Arviz and the R-hat statistic²⁴ indicate that the chains have mixed well and that the model has converged given that the trace plots [151] show a good mixture of the chains and the R-hat statistic²⁵ is approximately 1 ± 0.1 [339, 161]. Furthermore, the parallel plot generated from Arviz and shown in Figure 4.11 does not show a divergence for the posterior parameters²⁶.

Table 4.10 also depicts statistical metrics to determine sampling efficiency in terms of Effective Sample Size (ESS) for both the bulk (ESS_{bulk}) and tail (ESS_{tail}) of the distributions, which metrics are defined and explained in Vehtari et al. [339]. The $ESS \geq 100$ [339, 341] for all parameters shows that the model provides reliable estimates for the mean and quartiles of the posterior distributions. Furthermore, the model also has the potential to produce repeatable values in different simulation runs, since the ESS is also ≥ 200 [341].

The Monte Carlo Standard Error (MCSE) of the sample mean, which is another measure of the accuracy of the chains, is also shown in Table 4.10²⁷. The MCSE is smaller than the 5 % threshold [342] for all parameters in the DHW model, therefore, providing additional confidence in the accuracy of the sampling efficiency of the DHW meta-model.

Table 4.11: DHW Bayesian model parameters diagnostic statistical checks

Parameter	R^{hat}	ESS_{bulk}	ESS_{tail}	$MCSE_{mean}$
t_1^f	1.01	497	550	0.004
t_2^f	1.00	469	459	0.0012
α	1.00	695	567	0.001
β_1	1.00	993	558	0.001
β_2	1.00	1234	656	0.001
β_3	1.00	1389	618	0.001
σ	1.01	1145	453	0.000

²⁴R-hat is the ratio of variance between chains and the variance within chains [126], Stan reports "R-hat which is the maximum of rank normalised split-R-hat and rank normalised folded-split-R-hat".

²⁵R-hat is the ratio of variance between chains and the variance within chains [126], Stan reports "R-hat which is the maximum of rank normalised split-R-hat and rank normalised folded-split-R-hat".

²⁶Divergence tests, performed exclusively for the NUTS MCMC algorithm, depict divergences that may indicate that the algorithm has run into regions of high curvature in the posterior that it cannot effectively explore, therefore missing a region of the parameter space and biasing the results [340].

²⁷MCSE is defined as the SD of the chains divided by their ESS and "provides a quantitative suggestion of how big the estimation noise is" [148].

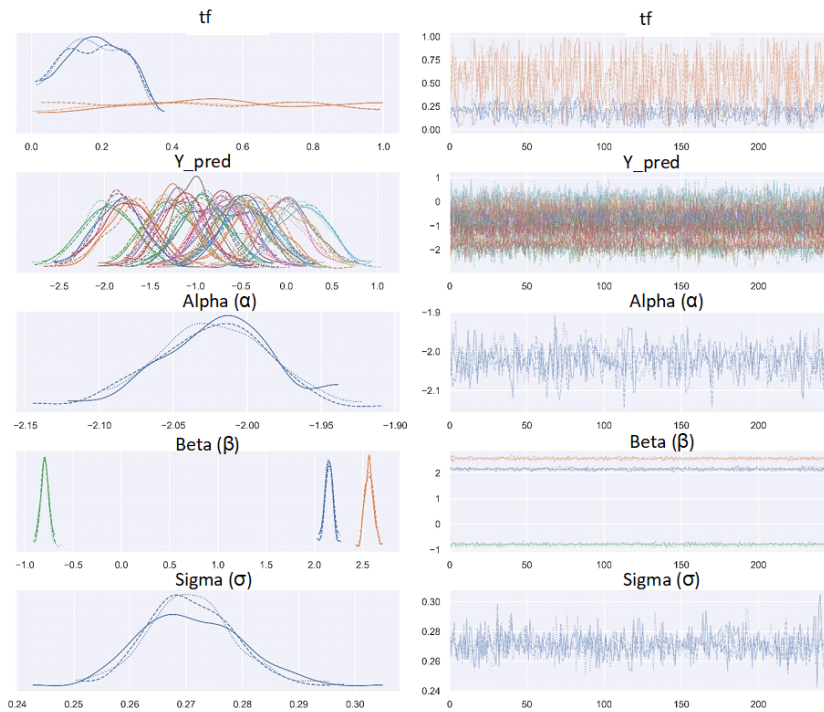


Figure 4.10: DHW model meta-model parameters trace plots to visually monitor convergence. The good mixture of the chains for the model is a good indication that the model has converged.

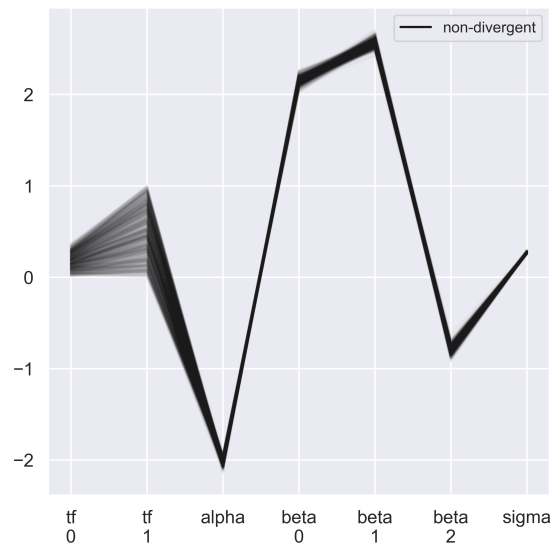


Figure 4.11: DHW model meta-model parameters Parallel Plot showing that the parameter posterior points have no divergences. Note : tf_0 , tf_1 , α , β_0 , β_1 , β_2 , β_3 and σ represent the parameters $t_1^f, t_2^f, \alpha, \beta_1, \beta_2, \beta_3$ and σ shown in Table 4.10 respectively.

4.4.4.1.2 DHW Bayesian model calibration validation

Validation of the calibration exercise must be carried out to ensure that the predicted outputs from the calibrated meta-model match the measured (actual) energy consumption for both the training and test data-sets as closely as possible. Therefore, the corresponding predictive output distribution of the calibrated model, which is a function of the inputs x and the calibrated parameters t , must be inferred for both the training and testing (out-of-sample) data set. Bayesian predictive inference was performed using the same Stan file that was used for calibration in Python.

Figure 4.12 shows the predictive distribution of monthly LFO consumption for the training data set (years 2017 and 2018), where the red dots are the actual monthly LFO consumption measured. The predictive performance of the model is satisfactory since, for all months, the measured energy consumption falls within the interquartile range of the predictive distribution. Furthermore, the Bayesian p-value of the model is 0.5²⁸, and the resulting NMBE and CVRMSE calibration statistical indicators for the training data are - 0.05 % and 0.24 %, respectively, as summarised in Table 4.12²⁹. These values fall within the 5 % and 15 % ASHRAE [1, 2] thresholds for NMBE and CVRMSE, respectively, and therefore the model is considered calibrated.

The calibration was also validated on the DHW building physics EnergyPlus model itself³⁰. As depicted in Table 4.12, when the mean value of the posterior distribution parameters is used as input to the EnergyPlus model that generated the simulated data to train the meta-model, the building physics model is considered calibrated with a NMBE of 0.71 % and CVRMSE of 3.72 %, as shown in Table 4.12. The satisfactory quality of the calibration of the building physics model is also visually evident in Figure 4.12, where the blue dots are the monthly consumption simulated by EnergyPlus for LFO for the years 2017 and 2018.

²⁸According to Gelman [343], the posterior predictive p-value will almost certainly be very close to 0.5 if the model is true or nearly true.

²⁹These statistical calculations consider the mean value of the posterior distribution of the calibration parameters.

³⁰The JEPlus/EnergyPlus models characterised with the mean value of the calibration parameter posterior distributions are found in GitHub Repository folder '*Ch 4 DHW Bayesian calibration*' sub-folder '*Calibration Validation on Physics models*'. Refer to Appendix B for a detailed description of all files and folders found in the GitHub Repository.

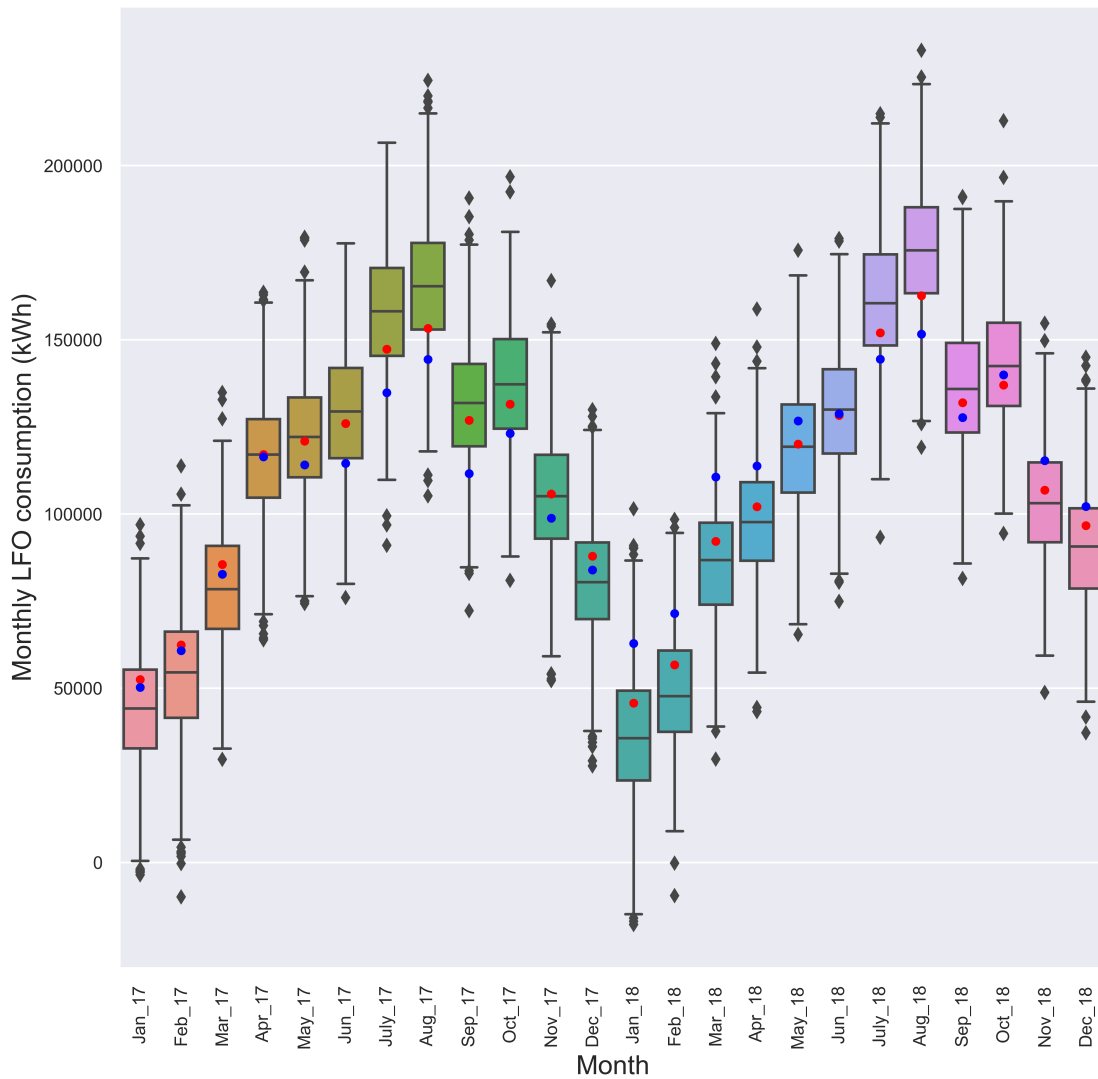


Figure 4.12: Box plot depicting the monthly LFO energy end-use consumption predictive distribution for the training data set (years 2017 and 2018). The red dots depict the actual monthly LFO measured energy consumption, while the blue dots show the simulated LFO consumption considering the mean value of the posterior distribution calibration parameters.

Table 4.12: Calibration validation statistical indicators for the training and testing datasets. Calibration is validated for both the Bayesian meta-model and the corresponding EnergyPlus models considering the mean value of the posterior distribution of the calibration parameters.

	NMBE %	CVRMSE %
Training data meta-model	-0.05	0.24
Test data meta-model	-1.12	3.72
Training data EnergyPlus	0.71	3.43
Test data EnergyPlus	0.56	1.85

The Bayesian calibrated model also showed very good predictive performance for the test data set (year 2019), as shown visually in Figure 4.13 and reflected in the statistical calibration indicators in Table 4.12, where the NMBE is -1.12 %, and the CVRMSE is 3.72 %. Furthermore, when the mean value of the posterior distribution of the calibration parameters is input into the building physics model characterised by occupancy data for the year 2019, the building physics model is considered calibrated with NMBE of 0.56 % and CVRMSE of 1.85 %. The good quality of the calibration is evident in Figure 4.13, where the blue dots once again represent the monthly consumption simulated by EnergyPlus for LFO for 2019.

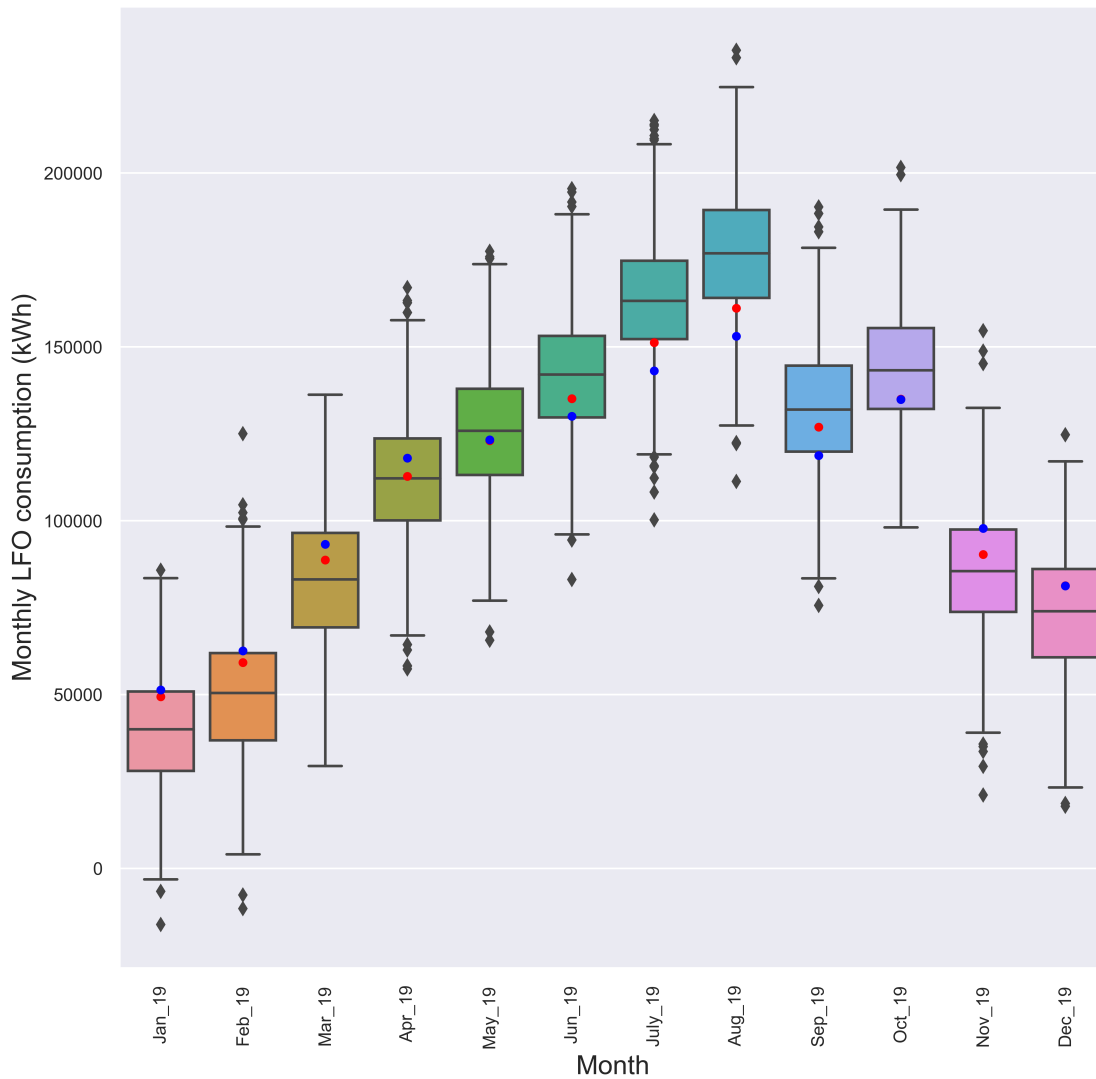


Figure 4.13: Box plot depicting the monthly LFO consumption predictive distribution for the test data set (year 2019). The red dots depict the actual monthly LFO measured energy consumption.

4.4.4.2 | Electricity end-uses model Bayesian calibration

For the electrical energy end-uses model calibration, two-thirds (years 2017 and 2018) of the monthly occupancy, weather parameters, and electricity consumption data (kWh) were used to train the meta-model, while the remaining data (year 2019) were used as a test set to gauge the model's predictive performance when given unseen data.

For calibration, the field-observed input data set matrix D^f for the training data set covers 24 months of data and is a 24×5 matrix. It consists of four ($p = 4$) known inputs x^f , x_1^f to x_4^f , and the observable output, y , which is the monthly metered electrical energy consumption. For the known inputs in matrix D^f , x_1^f is the monthly number of occupied rooms, x_2^f is the monthly average dry bulb temperature ($^{\circ}\text{C}$), x_3^f is the monthly average % relative humidity (% RH), and x_4^f is the monthly direct solar radiation per unit area (kWh.m^{-2}).

Furthermore, the computer simulation data set matrix D^c for the training data set is a 200×12 matrix, for which 200 ($m = 200$) LHS monthly simulation runs of the building physics model, Model D, were performed, 100 simulations each for the year 2017 and 2018. Matrix D^c is composed of $\eta(x^c, t^c)$, which is the predicted monthly electricity consumption, and data set $[x^c, t^c]$. The known inputs x^c (composed of x_1^c to x_4^c) is equal to x^f (composed of x_1^f to x_4^f) while t^c , composed of t_1 to t_7 , are the seven ($q = 7$) calibration parameters of the simulation model. It should be noted that before constructing the computer simulation data set matrix D^c , Model D was validated for its ability to replicate the monthly simulated electricity outputs of Model A for the year 2017 for an LHS sample of the calibration input parameters. For 100 LHS simulation runs, Model D was found to have the ability to satisfactorily replicate the monthly electricity output results of Model A with NMBE of 0.38 %, CVRMSE of 3.78 %, a median discrepancy of 1.35 % and a maximum discrepancy of 3.90 %³¹. Figure 4.14 shows a box plot that compares the monthly electrical simulated output of the two models.

³¹Refer to GitHub Repository folder 'Ch 4 Electricity Bayesian calibration' sub-folder 'Validation of Model D2 for monthly calibration'. Refer also to Appendix B for a detailed description of all files and folders found in the GitHub Repository.

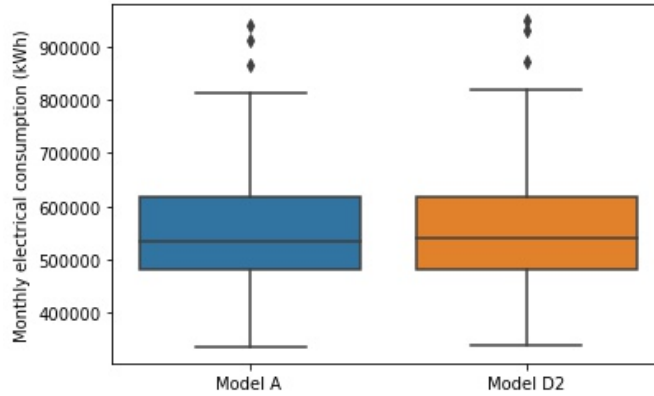


Figure 4.14: Box plot comparing the monthly electricity outputs of Model A with Model D for 100 LHS sample runs from the prior calibration parameters.

GP models combined the field-observed input data set matrix D^f and the computer simulation data set matrix D^c using the KOH framework, for which distinct models were used to emulate the building physics model simulator $\eta(x^c, t^c)$ and the discrepancy term $\delta(x)$ as detailed in Chong et al. [161]. For each GP model, a mean function returning a zero vector and a covariance function is defined, where each covariance function (Σ_η and Σ_δ) includes a precision hyperparameter (λ_η and λ_δ) and correlation hyperparameters (β_1^η to β_{p+q}^η and β_1^δ to β_p^δ). Observation errors are accounted for by a covariance matrix Σ_y having precision hyperparameter λ_ϵ . A likelihood function $L(z | t, \beta^\eta, \beta^\delta, \lambda^\eta, \lambda^\delta, \lambda_\epsilon)$ is then defined. All equations for the GP models and likelihood functions are provided by Chong et al. [161].

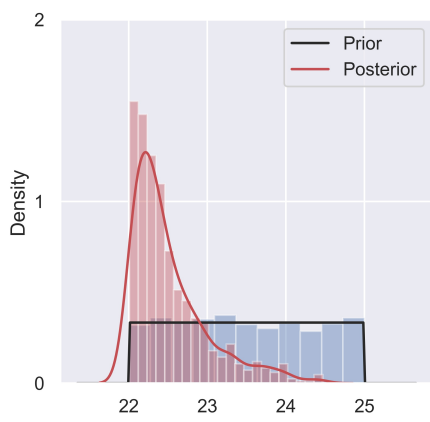
In the likelihood function, z is a single vector that has a dimension N ($N = n + m$) that combines the n observation output values for $y(x^f, t^f)$ and the m model prediction values for η , where t^f represents the calibration parameter space corresponding to D^f . Furthermore, X_t is an N by $(p + q)$ matrix that combines x^f , t^f , x^c , and t^c into one matrix. Using this modelling approach, the joint probability posterior density distribution that results is dependent on the unknown calibration parameters t_1^f to t_7^f , the GP correlation hyperparameters (β_1^η to β_{11}^η and β_1^δ to β_4^δ), and the GP precision hyperparameters ($\lambda_\eta, \lambda_\delta, \lambda_\epsilon$). The same prior distributions for the precision and correlation hyperparameters as defined in Chong et al. [161] were used³².

³²The Python and Stan code, adapted from [161] for electricity end-uses Bayesian calibration, is found in GitHub repository folder entitled 'KOH calibration in PyStan' in folder 'Ch 4 Electricity Bayesian calibration'. The required JEPlus files to execute the LHS simulation runs to train the meta-model are found in GitHub repository folder entitled 'Electricity EnergyPlus JEPLUS files for KOH LHS runs calibration', together with the corresponding simulation run results in GitHub repository folder 'JEPLUS Datacomp simulation outputs'. Both of these files are found in folder 'Ch 4 Electricity Bayesian calibration'. Refer to Appendix B for a detailed description of all files and folders found in the GitHub Repository.

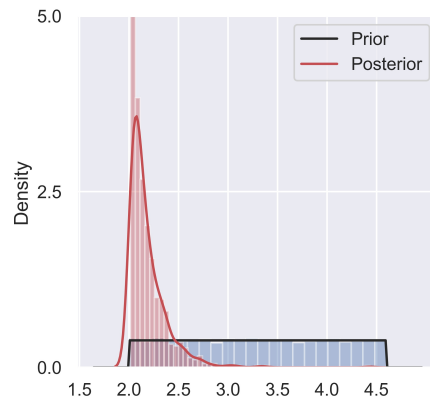
The prior and resulting posterior distribution after Bayesian inference of the calibration parameters t_1^f to t_7^f are visually shown in Figure 4.15, together with a statistical summary of the posterior distributions in Table 4.13. It can be observed that given the available observed data, the uncertainty in the value of t_1^f , t_2^f , t_3^f and t_6^f has been significantly reduced following calibration, while not much has been learned about the value of t_4^f , t_5^f and t_7^f .

However, the overall reduction in the uncertainty of the parameters after calibration is satisfactory based on the resulting model output before and after calibration, as identified from Figure 4.16 and Figure 4.17. The figures show that both the monthly meta-model predicted (Figure 4.16) and annual EnergyPlus simulated (Figure 4.17)³³ electricity consumption distributions generated from the posterior parameter distributions are significantly narrower when compared to EnergyPlus simulation runs propagated from prior parameter distributions.

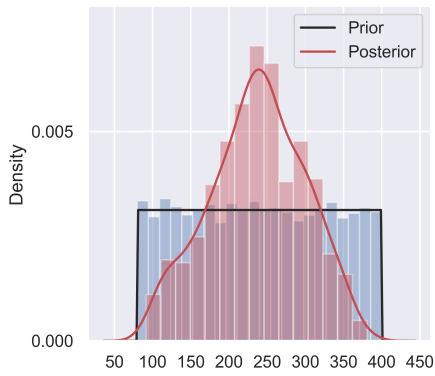
³³The JEPLUS files required to propagate annual uncertainty in electricity energy end use from the building physics model (Model D) and the corresponding simulation results are found in GitHub Repository folder 'Ch 4 Electricity Bayesian calibration' sub-folder 'building physics models Annual uncert propag Prior Post'. Refer to Appendix B for a detailed description of all files and folders found in the GitHub Repository.



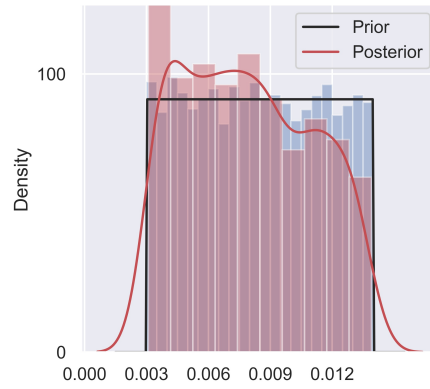
(a) t_1^f



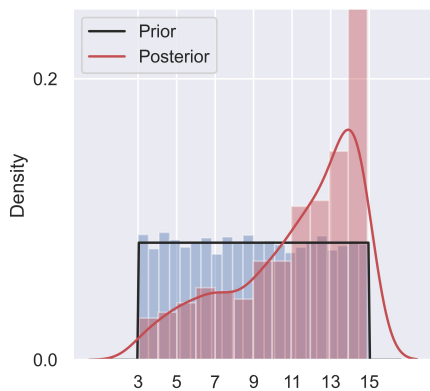
(b) t_2^f



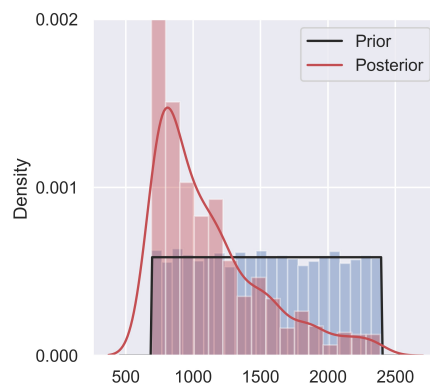
(c) t_3^f



(d) t_4^f



(e) t_5^f



(f) t_6^f

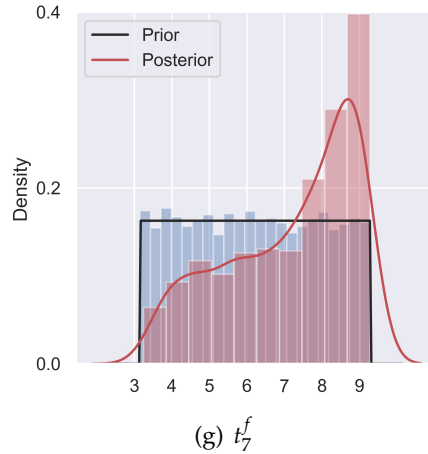


Figure 4.15: The prior and resulting posterior distributions of the electricity end used energy model calibration parameters for (a) t_1^f : Guest rooms cooling temp set-point (deg C), (b) t_2^f : VRF cooling COP, (c) t_3^f : Kitchen equipment power density ($W.m^{-2}$), (d) t_4^f : FOH ventilation rate ($m^3.s^{-1}.person^{-1}$), (e) t_5^f : BOH Zone ACH, (f) t_6^f : Fan ventilation pressure rise (Pa) and (g) t_7^f : Guest rooms equipment power density ($W.m^{-2}$)

Table 4.13: A statistical summary of the electricity end-uses model posterior distribution for each calibration parameter. Posterior statistics for the other meta-model parameters, including the GP hyperparameters, are found in the GitHub repository.

Symbol	Parameter	Prior	Posterior distribution statistics				
		Prior distribution	Mean	Median	SD	HDI _{5%}	HDI _{95%}
t_1^f	Guest rooms cooling temp. Set point (deg C)	U(22,25)	22.5	22.4	0.48	22.01	23.60
t_2^f	VRF cooling COP	U(2,4,6)	2.18	2.12	0.20	2.02	2.55
t_3^f	Kitchen equipment power density ($W.m^{-2}$)	U(88,385)	237	238	62	114	350
t_4^f	FOH ventilation rate ($m^3.s^{-1}.person^{-1}$)	U(0.003,0.014)	0.0079	0.0077	0.0031	0.0032	0.013
t_5^f	BOH Zone ACH	U(3,15)	11.13	12.02	3.23	4.72	14.9
t_6^f	Fan ventilation pressure rise (Pa)	U(600,2400)	1112	990	398	690	1957
t_7^f	Guest rooms equipment power density ($W.m^{-2}$)	U(3.15,9.3)	7.17	7.62	1.7	3.97	9.28

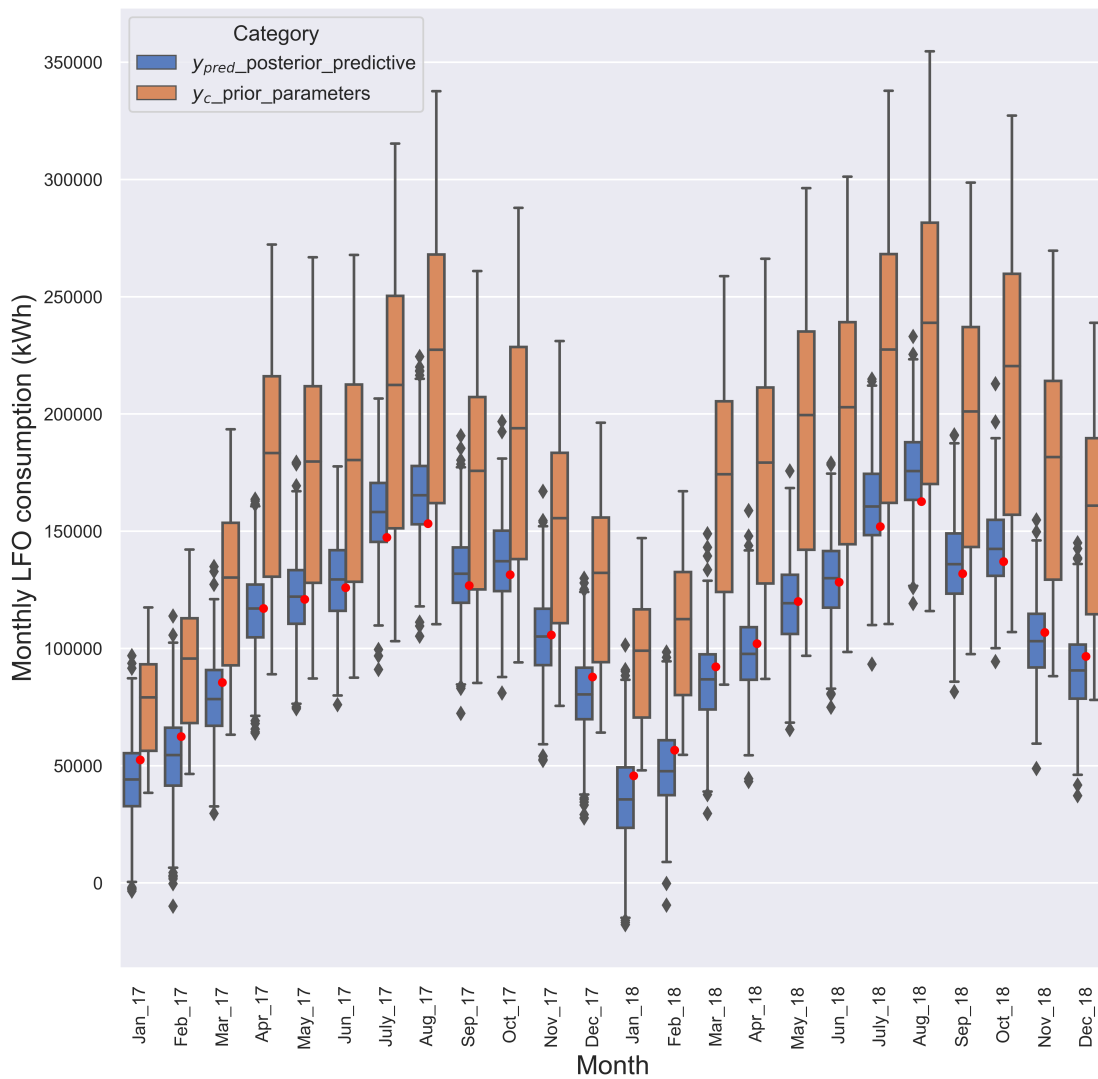


Figure 4.16: Monthly electrical consumption box plot comparing EnergyPlus Model D simulation runs for prior calibration parameters distributions (orange plot) and the posterior predicted consumption from the calibrated meta-model (blue plot). The red dots depict the actual metered monthly electricity consumption.

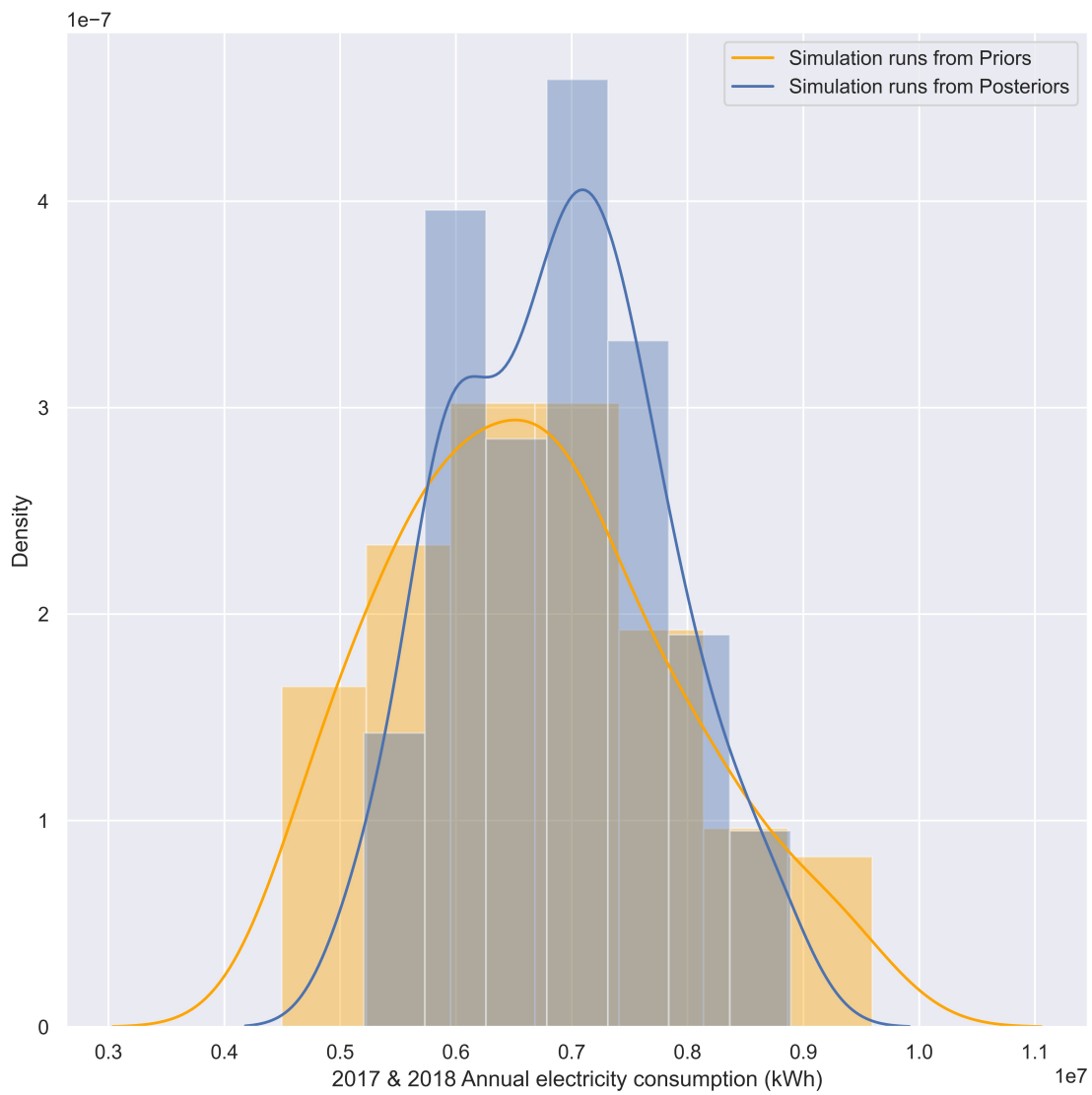


Figure 4.17: Annual electrical consumption distribution generated from EnergyPlus Model D for simulation runs from prior (orange plot) versus posterior (blue plot) calibration parameter distributions for the years 2017 and 2018.

4.4.4.2.1 Electricity end-uses Bayesian model diagnostics

The GP Bayesian model for electricity end-uses was checked for adequate convergence using both trace plots³⁴ and the statistical diagnostic metrics³⁵ provided in Table 4.14. Both the trace plots generated in Arviz [151] and the R-hat statistic generated in Stan indicate that the chains have mixed well and that the model has converged. Furthermore, the parallel plot generated from Arviz and shown in Figure 4.18 does not show a divergence for the posterior parameters.

Table 4.14 also shows that the $ESS \geq 100$ [339, 341] for both the bulk and tail of the distributions, concluding that the model provides reliable estimates for the mean and quartiles of the posterior distributions. Furthermore, the MCSE of the sample mean is less than the 5 % threshold [342] for all parameters in the model, providing additional confidence in the accuracy of the sampling efficiency.

Table 4.14: Electricity energy end uses Bayesian model parameters diagnostic statistical checks for the calibration parameters.

Parameter	R^{hat}	ESS_{bulk}	ESS_{tail}	$MCSE_{mean}$
t_1^f	1.0	678	361	0.006
t_2^f	1.0	811	327	0.003
t_3^f	1.0	361	284	0.011
t_4^f	1.0	498	516	0.012
t_5^f	1.0	404	533	0.014
t_6^f	1.0	402	477	0.012
t_7^f	1.0	753	543	0.010

³⁴Trace plots can be viewed in the GitHub repository, more specifically in the Python Jupyter notebook for the calibration of the electricity end-uses. Refer to the folder '*Ch 4 Electricity Bayesian calibration*' sub-folder '*KOH calibration in PyStan*'. Refer also to Appendix B for a detailed description of all files and folders found in the GitHub Repository.

³⁵Model diagnostic statistics checks for the other meta-model parameters, including the GP hyperparameters, are also found in the Python Jupyter notebook for the calibration of the electricity end-uses. Refer to the folder '*Ch 4 Electricity Bayesian calibration*' sub-folder '*KOH calibration in PyStan*'.

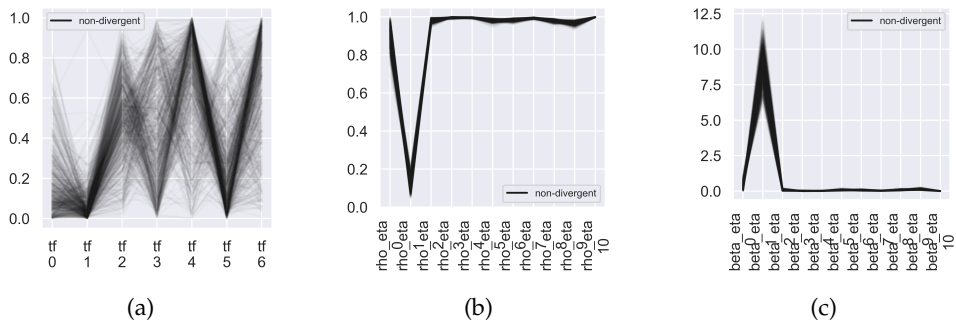


Figure 4.18: Parallel plot showing that the parameter posterior points have no divergences for (a) the calibration parameters t^f . Note: tf_0 to tf_6 correspond to the parameters t_1^f to t_7^f respectively as shown in Table 4.14 (b) the GP correlation hyperparameters β and (c) the GP precision hyperparameters λ .

4.4.4.2.2 Electrical end-uses Bayesian model calibration validation

The predictive output distribution of the calibrated model, which is a function of the inputs x and the calibrated parameters t , was inferred for both the training and testing (out-of-sample) data set using the same Stan file that was used for calibration in Python³⁶.

Figure 4.19 depicts the monthly electricity consumption predictive distribution for the training data (years 2017 and 2018), where the red dots are the actual monthly measured electrical consumption. The predictive performance of the model is satisfactory since, for almost all months, the measured energy consumption is within the predictive distribution’s interquartile range. Furthermore, the Bayesian p-value of the model is 0.45, and the resulting CVRMSE and NMBE calibration statistical indicators for the training data are - 0.05 % and 0.24 %, respectively, as summarised in Table 4.15³⁷. These values fall within the 5 % and 15 % ASHRAE [2] thresholds for NMBE and CVRMSE, respectively, and therefore the model is considered calibrated.

Table 4.15: Calibration validation statistical indicators for the training and testing datasets. Calibration is validated for both the Bayesian electricity end use meta-model and the corresponding EnergyPlus models considering the mean value of the posterior distribution of the calibration parameters. The results are also shown for Model A for the year 2017

	NMBE %	CVRMSE %
Training data meta-model	-0.05	0.24
Test data meta-model	1.53	5.10
2017 EnergyPlus Model A	-0.57	1.90
Training data EnergyPlus Model D	-0.09	4.35
Test data EnergyPlus Model D	0.02	0.06

The calibration was also validated on both EnergyPlus Model D and Model A³⁸. As depicted in Table 4.15, when the mean value of the posterior distribution parameters is used as input to EnergyPlus Model D that generated the simulated data to train the meta-model, the building physics model is considered calibrated with a NMBE of -0.09 % and CVRMSE of 4.35 %, as shown in Table 4.15. The blue dots in Figure 4.19 visualise

³⁶Refer to the Python Jupyter notebook for the calibration of the electricity end-uses found in GitHub Repository folder ‘Ch 4 Electricity Bayesian calibration’ sub-folder ‘KOH calibration in PyStan’. Refer also to Appendix B for a detailed description of all files and folders found in the GitHub Repository.

³⁷These statistical calculations consider the mean value of the posterior distribution of the calibration parameters.

³⁸The JEPlus/EnergyPlus models for both Models A and Model A characterised with the mean value of the calibration parameter posterior distributions are found in GitHub Repository folder ‘Ch 4 Electricity Bayesian calibration’ sub-folder ‘Calibration Validation on Physics models’.

the monthly electricity consumption simulated by EnergyPlus Model D for the years 2017 and 2018, showing that the calibrated model is able to "predict the overall load shape that is reflected in the data" [344]. For the year 2017, the calibration was also validated for Model A with a resulting NMBE of -0.57 % and CVMSE of 1.90 %, as shown in Table 4.15, further confirming that Model D can successfully replace Model A for a computational efficient approach to Bayesian calibration.

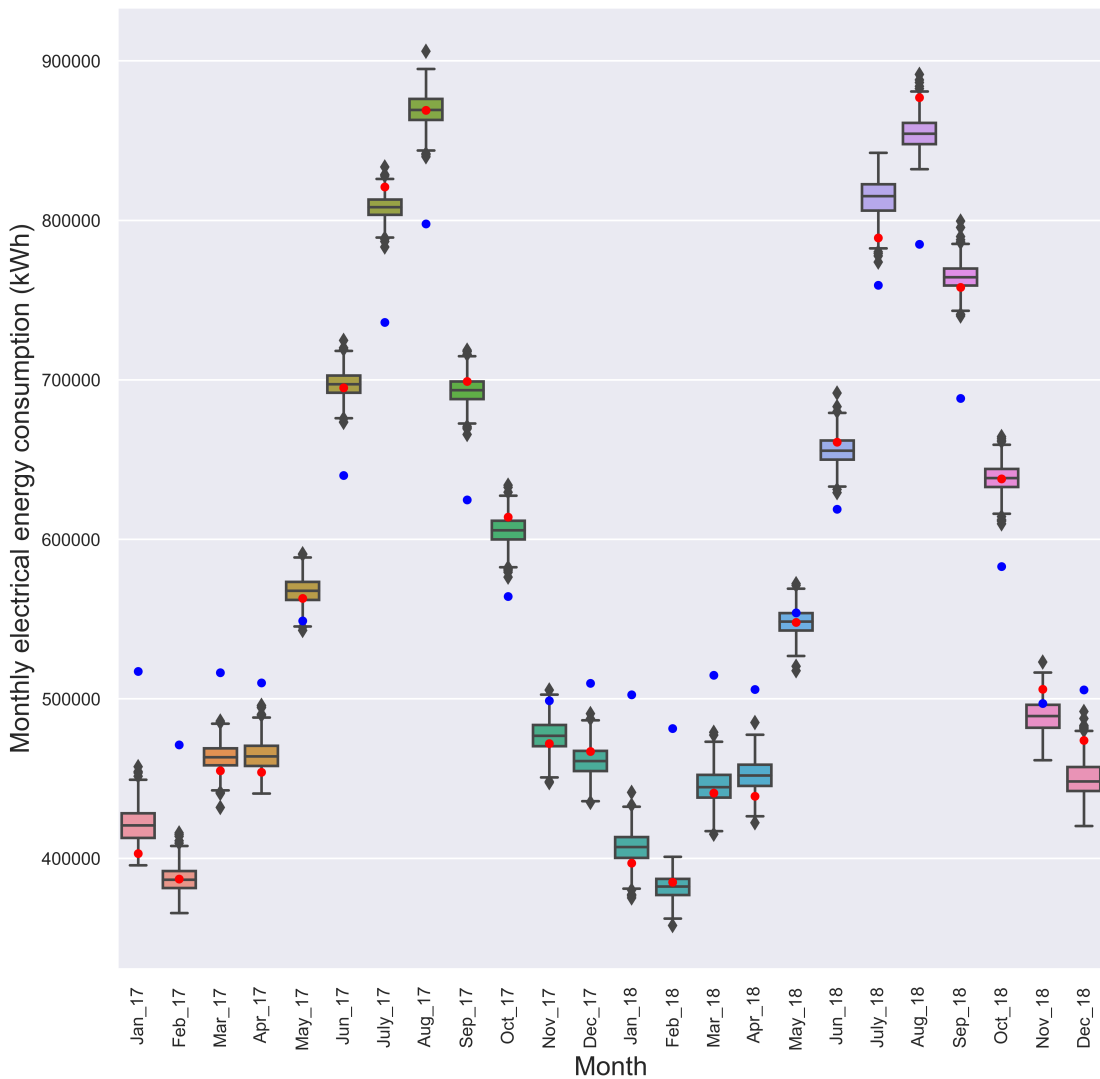


Figure 4.19: Box plot depicting the monthly electricity consumption predictive distribution for the training data set (years 2017 and 2018). The red dots depict the actual monthly measured electrical energy consumption, while the blue dots shows the simulated electrical consumption considering the mean value of the posterior distribution calibration parameters.

The Bayesian calibrated model also showed very good predictive performance for the test data set (year 2019), as shown visually in Figure 4.20 and reflected in the statistical calibration indicators in Table 4.15, where the NMBE is -1.53 %, and the CVRMSE is 5.10 %. Furthermore, when the mean value of the posterior distribution of the calibration parameters are input into the building physics model characterised by occupancy data for the year 2019, the building physics model is considered calibrated with a CVRMSE of 0.56 % and NMBE of 1.85 %. The good quality of the calibration of the building physics model is also reflected in Figure 4.20, where the blue dots represent the monthly electricity consumption simulated by EnergyPlus Model D for the year 2019.

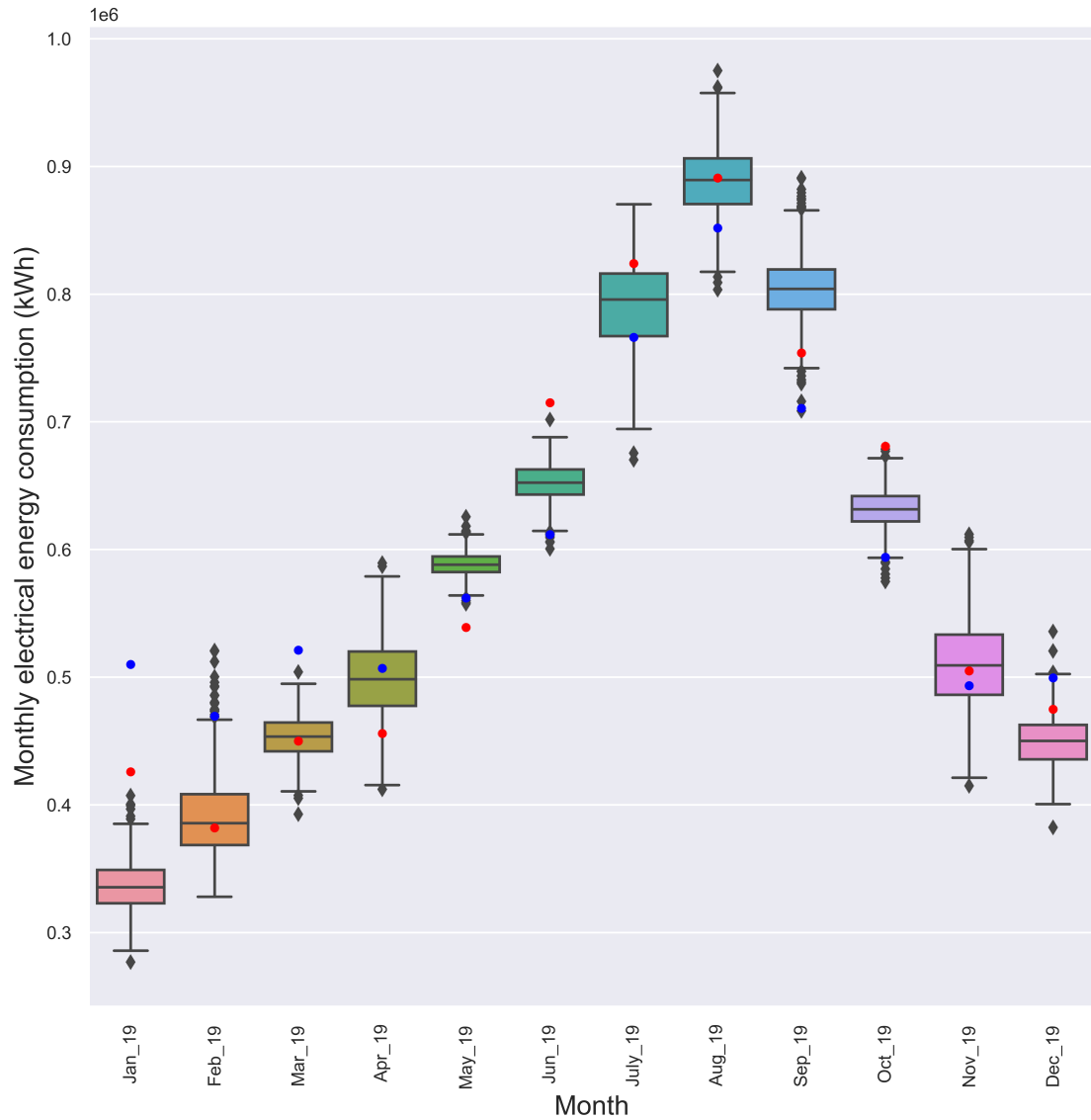


Figure 4.20: Box plot depicting the monthly electricity consumption predictive distribution for the test data set (year 2019). The red dots depict the actual monthly electricity measured energy consumption.

4.5 | Conclusion

This chapter has demonstrated and statistically validated a computationally efficient and innovative approach of updating '*non-calibrated and deterministic RBs*' to '*probabilistic Bayesian calibrated RBs*' to facilitate the implementation of the proposed cost-optimal approach. Improved computational efficiency is achieved by replacing computationally intensive and full-space RB building physics models, termed '*detailed*' models, with reduced-space RB building physics (EnergyPlus) models, referred to as '*simplified*' models that are constructed using the '*reference zone*' approach concept. The '*reference zone*' approach was conceptualised by the author and published in Gatt et al. [35]. Computationally intensive RB models are synonymous with heterogeneous, multi-functional building stocks that are composed of large building blocks with complex geometries and multiple thermal zones. The use of the '*simplified*' models improves the computational efficiency of running multiple simulations from the EnergyPlus RB model for a sample space of uncertain parameters. The EnergyPlus simulation runs are required to perform both SA, to identify the most significant parameters for calibration, and to train the meta-model that emulates the simulator in the iterative BEM Bayesian calibration framework.

The '*reference zone*' approach was successfully demonstrated and validated for a 5-star hotel RB in Malta that falls into cluster 4 in the RB clustering solution of Chapter 3. The validation was performed by comparing the monthly and annual simulation outputs for electricity consumption of the '*simplified*', '*reference zone*' EnergyPlus model to a '*detailed*' EnergyPlus model. The '*simplified*' model showed an improvement of 4000 % in computational run-time efficiency over the '*detailed*' model and perfectly replicated the results of the '*detailed*' model in terms of parameter ranking statistical significance for SA. The '*simplified*' model also satisfactorily reproduced the monthly outputs of the '*detailed*' model for the simulation runs that trained the GP meta-model, emulating the simulator in Bayesian calibration, with a NMBE of 0.38 %, CVRMSE of 3.78 %, and a median discrepancy of 1.35 %. Furthermore, a highly computationally efficient model was also constructed for the monthly consumption of LFO that generates DHW for the hotel, by using a '*reference zone*' concept where no space heat balance calculations are required.

RB Bayesian calibration, performed by applying a GP meta-model that was trained using simulation runs from the '*simplified*' model, also successfully enabled all models under study, that is, the GP meta-model, the '*simplified*' EnergyPlus model, and the '*detailed*' EnergyPlus models to be statistically calibrated with monthly metered energy

consumption data according to the CVRMSE and NMBE ASHRAE [1, 2] thresholds for both the training and test data sets. This calibration was validated for the models simulated with the mean value of the posterior distributions of the calibrated parameters, for which the uncertainty in the calibration parameters was also satisfactorily reduced for the '*flat*' prior calibration parameters distributions used in the study.

Thus, based on the outcome of the 5-star hotel case study, one can conclude that the '*reference zone*' approach provides good potential to achieve a highly computationally efficient and accurate approach to performing Bayesian calibration of multi-functional RBs in UBEM and the proposed cost-optimal approach.

The strength of the '*reference zone*' approach also lies in its scalability and modularity, and therefore its potential to be applied using a bottom-up technique once representative '*reference zones*' for different activities and sub-activities are statistically validated for a sample of the building stock under study. Every building observation in the stock can than theoretically be modelled using this approach, which replaces the need to define '*detailed*' BEMs in GIS. This modelling approach improves computational efficiency and allows the variability in the functionality of a heterogeneous building stock to be fully defined.

The next chapter will demonstrate steps 5 and 6 of the proposed EPBD cost-optimal method, described in Section 2.5, by applying energy efficiency measures to the probabilistic and calibrated RB hotel model with posterior calibration parameter distributions. The potential of replacing the '*detailed*' model with the simplified model constructed using the '*reference zone*' approach for these steps will also be studied to optimise the computational efficiency of the proposed cost-optimal approach.

Developing a probabilistic approach to establish NZEB benchmarks under uncertainty

Chapter Abstract : This chapter establishes a comprehensive framework for developing, applying, and successfully validating the final two steps of the proposed EPBD cost-optimal method, more specifically, of deriving NZEB EP benchmarks from the cost-optimal analysis, for which there are currently no established criteria in the EPBD, followed by a probabilistic risk analysis for the derived benchmarks. To derive NZEB EP benchmarks, an objective approach was developed to defining NZEB EP benchmarks according to four different levels of ambition and was validated using the hotel RB case study calibrated in Chapter 4. For probabilistic risk analysis, uncertainty is propagated from the posterior calibration parameter distributions to visualise and statistically quantify the financial risk the private investor faces to reach each derived benchmark. The results of the RB case study showed that this risk analysis is critical for MS to define more realistic benchmarks and comprehensively quantify financial support requirements. It also contrasts with the current EPBD deterministic financial feasibility analysis, which resulted in being prone to derive unsustainable EP benchmarks and hide financial risk. Furthermore, when repeating the cost-optimal analysis using non-calibrated NCM software, a large EP gap resulted, which makes the analysis highly susceptible to providing misleading policy outcomes. Thus, one can conclude that parameter uncertainty and use of calibrated RBs is critical to devise robust policy measures in the EPBD. Based on the results, other positive aspects of the developed framework include a time-bound tightening approach to higher EP ambitions, improved risk transparency to private investors, and more targeted policies.

5.1 | Introduction and chapter objectives

This chapter will demonstrate and validate the final two steps, more specifically steps 5 and 6 of the proposed EPBD cost-optimal method, as detailed in Chapter 2, Section 2.5. For this purpose, these steps are applied to the '*probabilistic Bayesian calibrated*' hotel RB developed in Chapter 4. Step 5 aims to objectively derive NZEB EP benchmarks through a cost-optimal analysis considering global Life-cycle Costs (LCC) for a RB representing a building stock cluster under study. Step 6 then conducts a probabilistic uncertainty in operational energy savings and the corresponding risk in life cycle financial feasibility for a RB energy model under study to meet the defined NZEB EP benchmarks. This probabilistic risk analysis, which is not performed in the current '*deterministic*' EPBD cost-optimal approach, will be evaluated in its potential to allow EU policy makers to establish more robust energy renovation support policies and facilitate the path for the EU to achieve its carbon neutrality goals for 2050.

As identified in Chapter 2, and as detailed in a state-of-the-art review of different NZEB definitions by Gatt et al. [158] and [29], objectively deriving NZEB EP benchmarks even when considering the current '*deterministic*' EPBD cost-optimal method is not straightforward. The reason being that the term '*Nearly*' in NZEB is not a quantifiable metric and the European Commission (EC) does not provide objective criteria for defining NZEB benchmarks once cost-optimal plots that consider the impact of different Discount Rates (DRs) and Price Development (PD) scenarios are constructed. Therefore, this chapter will also address this methodological research gap by developing an objective and harmonised approach to allow MS to define NZEB EP benchmarks according to different ordinal levels of renovation ambition for a RB under study. For each defined level of NZEB EP ambition, the uncertainty in operational energy savings and the corresponding risk in life cycle financial feasibility for a RB model under study will be propagated and statistically quantified, allowing MS to establish robust energy renovation support policies through a probabilistic approach to risk and uncertainty analysis.

Furthermore, to meet the above objectives, this chapter will also address the research gap identified in chapter 2 by developing a probabilistic approach to risk and uncertainty analysis that considers the joint impact of technical and financial uncertainties on the NZEB EP benchmarks to comply with the EPBD cost-optimal framework described by the EC [345]. More specifically, this framework requires MS to consider both a financial and macroeconomic perspective to LCC and to perform a Sensitivity Analysis (SA) on the impact of different Discount Rates (DRs) and Price Development (PD) scenarios on the resulting EP benchmarks for a RB. In addition, the propagated uncertainty in

EP improvements and LCC risks for a defined NZEB benchmark level generated from the '*Bayesian calibrated RBs*' for the proposed EPBD cost-optimal approach requires to be visualised, statistically quantified and interpreted to allow establishing more robust energy support policies.

The chapter will finally compare, from a statistical and policy perspective, the results and outcomes of the proposed EPBD cost-optimal approach with the current '*deterministic*' approach. To enable this comparison, the current EPBD cost-optimal approach will be applied to the hotel RB case study using SBEM-mt software [346], the National Calculation Methodology (NCM) for Malta. The results of the chapter and the previous chapters will allow the hypothesis presented in Chapter 2 to be accepted or rejected and the research questions put forward in Chapter 1 to be answered.

5.2 | The NZEB EP benchmarking and probabilistic risk analysis framework for the EPBD cost-optimal method

The two-stage framework detailing the approach taken to execute steps 5 and 6 of the proposed EPBD cost-optimal method is visually shown in Figure 5.1 and is described in the sections that follow. Section 5.3 then applies and demonstrates this framework to the '*probabilistic Bayesian calibrated*' hotel RB developed in Chapter 4.

5.2.1 | Step 5: NZEB EP benchmarking approach to different ambition levels

The NZEB EP benchmarking approach in this research applies the mean value of the posterior distributions of the calibration parameters to each RB building physics energy model representing a building stock under study, as shown in Figure 5.1. The calibrated RB model characterised with the mean value of the posterior distributions of the calibration parameters is treated deterministically when deriving EP benchmarks to facilitate the NZEB benchmarking process and make it more objective. The cost-optimal EP and NZEB EP benchmarks are then derived using the EPBD cost-optimal analysis that applies a set of packages of energy efficiency measures (COMs) and calculates the annual primary energy consumption and EN 15459 [54] global LCC for each COM using the current EPBD cost-optimal methodology detailed in Chapter 2, Section 2.2.1. The main inputs to calculate the EP and global LCC required for the EPBD cost-optimal analysis are shown in Figure 5.1.

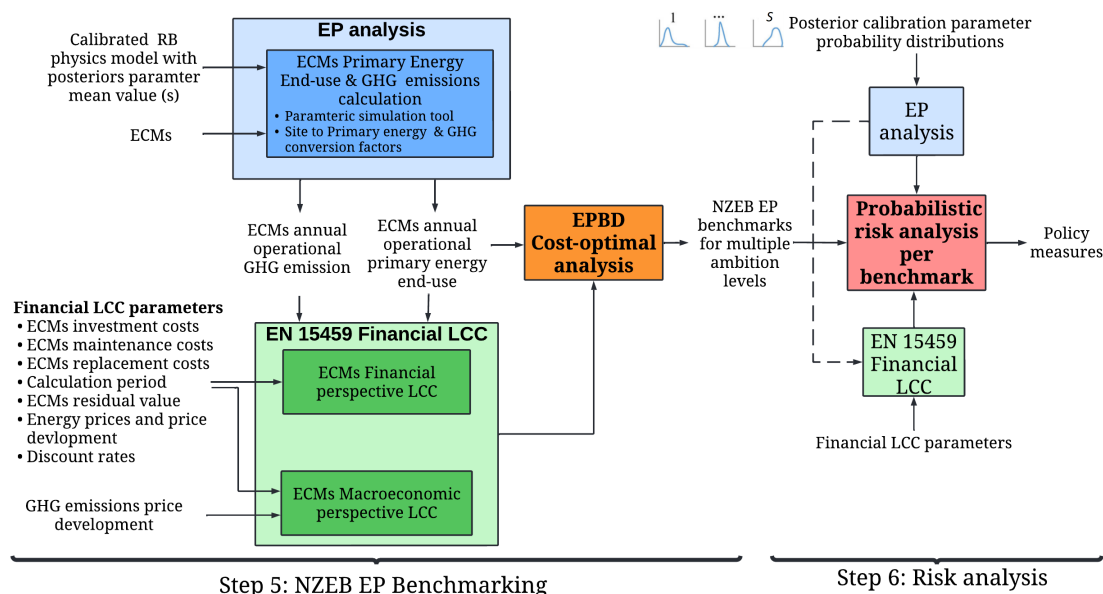


Figure 5.1: Flow chart detailing the approach used in this study to execute steps 5 and 6 of the proposed EPBD cost-optimal approach to establish NZEB benchmarks and perform risk analysis per benchmark to establish robust policies.

The global LCC, $C_g(t)$ for a COM, referred to the starting year t_0 , over the calculation period t , is calculated by summing the different costs incurred, for every energy efficiency measure j constituting the COM and discounting them to the starting year t_0 by means of a discount factor R_d as follows [55]:

$$C_g(t) = CO_{INIT} + \sum_j \left[\sum_{i=1}^t (CO_{a,i}(j) \cdot R_d(i)) + CO_{carbon,i}(j) - VAL_{fin,t}(j) \right] \quad (5.1)$$

where:

- CO_{INIT} is the initial investment costs
- $CO_{a,i}$ is year i annual cost, which is the addition of the running costs and periodic (including annual maintenance costs $CO_{a,maint}$) or replacement costs $CO_{a,RAR}$. This cost is discounted by the discount factor R_d , during every year i
- $CO_{carbon,i}$ is the carbon (GHG emissions) cost for every year i resulting from the operational energy consumption
- $VAL_{fin,t}$ is the residual value discounted to the starting year t_0

R_d (i) for year i is related to the DR, r , as :

$$R_d(p) = \left(\frac{1}{1 + r/100} \right)^p \quad (5.2)$$

where p means the years quantified from the starting period.

Equation 5.1 details the equation for the macroeconomic global LCC calculation that considers each cost without taxes and charges. However, for the financial global LCC calculation, the cost of GHG emissions is not considered and all costs include taxes and charges [55].

The EPBD cost-optimal analysis generates the cost-optimal plots shown in Figure 2.1 as their main output to establish minimum EP requirements for benchmarking. According to the EPBD Commission Regulation [345, 55], the cost-optimal analysis requires to be carried out both from a macroeconomic and financial perspective, and a SA is mandatory to identify the impact of different PD scenarios and DRs on the resulting cost-optimal and NZEB benchmarks. The NZEB benchmarking approach considered in this study directly uses this requirement to objectively define ordinal levels of NZEB EP benchmarks according to different levels of EP ambition levels. More specifically, the approach defines four different levels of NZEB EP ambition levels to complement the current subjective EPBD NZEB definition¹ which are derived by considering the resulting cost-optimal plots for all perspectives and sensitivities as follows:

1. **Low ambition:** The EP corresponding to the financial scenario giving the lowest global LCC when compared to the reference scenario, for the DRs and PD sensitivities considered.
2. **Medium ambition:** The least ambitious EP when choosing between scenario 1 and 2, defined below.
3. **High ambition:** The most ambitious EP when choosing between scenario 1 and 2, defined below.
4. **Highest ambition:** The EP coinciding with the macroeconomic sensitivity scenario giving the best EP in the macroeconomic feasibility region of the cost-optimal plots for the DRs and PD sensitivities considered.

¹According to the 2010 EPBD [9], NZEB is a building that “has a very high energy performance with a low amount of energy required covered to a very significant extent by energy from renewable sources, including energy from renewable sources produced on-site or nearby”.

For the above NZEB EP definitions, Scenario 1 and Scenario 2 are defined as follows:

- **Scenario 1** : The EP arising from the financial perspective that provides the '*best*' EP in the feasibility region of the financial cost-optimal plots for the DRs and PD sensitivities considered. This can be viewed as the theoretically '*best*' EP that private investors are willing to invest without financial incentives.
- **Scenario 2** : The EP corresponding to the macroeconomic scenario giving the lowest global LCC compared to the reference scenario for the DRs and PD sensitivities considered. Private investors are not likely to be willing to invest in this EP level without financial incentives unless this EP also falls within the feasibility region of the financial cost-optimal plots.

The four (4) NZEB EP ambition levels for a RB under study are visually depicted as points A, B, C and D in Figure 5.2. As an example, the ambition levels are demonstrated for a generic cost-optimal analysis that considers four (4) sensitivity combinations for PD and DR for both the financial and macroeconomic perspectives. In the figure, each blue point on the plots represents a COM, and the black dashed lines for each cost-optimal plot show the '*operational*' EP scenario. The '*operational*' EP is shown by the vertical line, and the corresponding global LCC is depicted by the horizontal line. The EP scenario for the calibrated RB prior to the application of energy efficiency measures, termed the '*reference*' scenario, should coincide as closely as possible with the '*operational*' EP scenario for a calibrated model.

Furthermore, the application of a COM that is found below the horizontal black dashed line for each plot in Figure 5.2, provides a lower global LCC than the '*operational*' scenario and its application is therefore feasible for the PD, and DR under consideration. Following this context and the above definitions, point A coincides with the lowest NZEB EP ambition in Figure 5.2. At the same time, Scenario 1 and Scenario 2 are represented by point B and point C, respectively. For the specific context of Figure 5.2, point C coincides with the medium NZEB EP ambition level, while point B coincides with the high EP ambition. Furthermore, the highest NZEB EP ambition level coincides with point D.

From the resulting cost-optimal plots, one can also deterministically quantify the financial risk faced by a private investor to upgrade a RB to each NZEB EP ambition level benchmark. This risk quantification termed the '*deterministic financial risk*' in this thesis, is simply the difference between the global LCC of the reference scenario and the global LCC corresponding to each level of NZEB ambition under study for a considered finan-

cial analysis scenario. This risk can be easily calculated within the current deterministic EPBD cost-optimal analysis framework.

An advantage of defining the above multiple objective NZEB benchmarks according to different ambition levels is determining an objective and time-bound tightening approach [347] to NZEB EP benchmarking. This prepares the market to adapt over time to more stringent EP requirements and allows MS to establish a long-term path for policy makers to continuously improve the EP of their building stock [348]. For a holistic and integrated design approach [349, 350] to NZEB, multiple objective NZEB benchmarks can also be derived for each requirement of the multiple indicator NZEB assessment approach provided in Annex H of ISO 52000-1 [108]. This approach was applied for a case study building by the author of this thesis in Gatt et al. [158].²

²The ISO 52000-1 [108] standard defines four sequential requirements which are to be met for a building to have a qualified NZEB status. The requirements first prioritise the building passive design in terms of *"The building Fabric (Energy needs)"* followed by energy-efficient technical building systems in terms of *"The total primary energy use"* and finally gives weighting renewable energy generation to offset the energy demand and reduce the carbon footprint of the building. Renewable energy generation is reflected in terms of the third requirement *"Non-renewable primary energy use without compensation between energy carriers"* and the final NZEB rating *"Numerical indicator of non-renewable primary energy use with compensation"*.

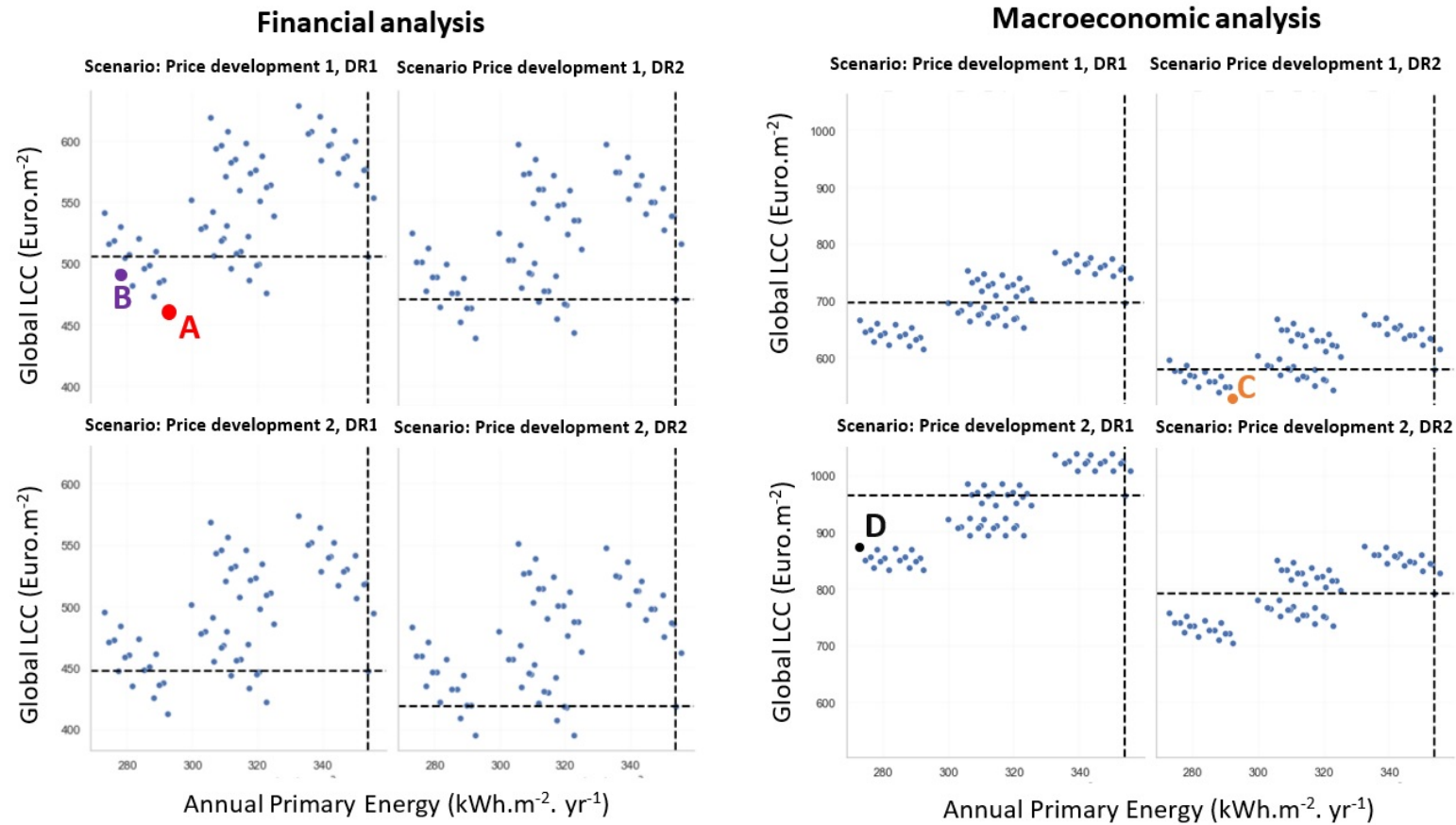


Figure 5.2: The four NZEB EP benchmarks visually depicted using the cost-optimal plots that consider both the financial and Macroeconomic LCC perspectives and different sensitivities for the PD and DRs

5.2.2 | Step 6 : Probabilistic Risk analysis for each defined NZEB benchmark

For the risk analysis, as shown in Figure 5.1, the posterior calibrated parameter probability distributions derived from steps 1 to 4 of the proposed cost-optimal approach are used to define the calibrated RB building physics model. For each defined NZEB EP ambition level found from the above NZEB EP benchmarking approach, uncertainty in operational EP and the corresponding Life-cycle Costs (LCC) is propagated for the RB building physics model implementing the corresponding COM that achieves the desired NZEB EP ambition level under study. To enable this propagation in uncertainty for each NZEB ambition level, a near random sample is generated from the posterior calibrated parameter probability distributions using the LHS sampling method. The RB building physics model characterized with the COM that achieves the NZEB ambition level under study is then run for each sample point to calculate the annual operational EP. The calculated annual operational EP results are fed into the EN 15459 [54] financial LCC tool to calculate the life cycle operational energy cost for the defined energy prices, PD and DR. The resulting operational energy cost is then combined with the other defined financial LCC parameters shown in Figure 5.1 to calculate the other EN 15459 [54] LCC that makes up the total global LCC for each sample point. The main output from the uncertainty propagation for each NZEB ambition level is a data set consisting of the annual operational EP and the corresponding total global LCC for each sample point.

For a comprehensive risk analysis in line with the EPBD commission regulation [55], the above uncertainty propagation for a defined NZEB ambition level must calculate the EN 15459 [54] financial LCC³ considering different sensitivities for different PD scenarios and DRs. For quantifying risk, the uncertainty in operational EP and global LCC for each defined NZEB ambition level and each sensitivity must then be compared against the '*Reference*' or '*as is*' scenario of not implementing energy efficiency measures. The latter is performed by propagating uncertainty for the calibrated RB building physics model without energy efficiency measures for a LHS sample space of the posterior calibrated parameter probability distributions.

In this framework, joint plots [351]⁴ are proposed to visualise the EP and financial risk for achieving a NZEB ambition level. These plots facilitate the combination of bi-

³A risk analysis that considers the macroeconomic perspective to LCC is not considered mandatory for this step, given that the main objective is to establish policies that objectively and more realistically quantify financial support measures that reduce risk to the private investor to reduce the technical and financial uncertainty barriers. These are the main barriers to energy renovation [42, 43, 44] and EP contracting [45], to facilitate the transition of the building stock to the established EP benchmarks.

⁴Joint plots are also called joint grids [352], or marginal plots [353].

variate scatter plots with marginal uni-variate probability distributions. The scatter plots analyse the correlation between the global LCC and the annual primary energy for the uncertainty propagation. In addition, the marginal probability density plots on the top and right margin of the scatter plot show the distribution of annual primary energy and global LCC along both axes. Figure 5.3 shows the proposed joint plot construction that can be implemented for this stage of the cost-optimal method for a NZEB ambition level that has four (4) PD and DRs combination scenarios. Figure 5.3 uses different colours to distinguish between the uncertainty propagation from the *'reference'* scenario and NZEB ambition level under consideration for both the annual primary energy and global LCC. For this framework, the joint-plots shown in Figure 5.3 need to be constructed for all NZEB ambition levels defined in Section 5.2.1.

From the joint plots shown in Figure 5.3, policy makers can perform various data analysis techniques to identify policy options to facilitate the transition of building stocks to a defined NZEB EP ambition level. For a given PD and DR scenario, financial risk is eliminated for the private investor in theory when the global LCC probability density plots for the *'reference'* scenario and the NZEB ambition level under study do not intersect each other. An objective and statistical approach to policy making to calculate the worst-case or *'robust'* [354] financial risk is therefore to establish a % Highest Density Interval (HDI), typically 89 % or 95 % HDI [355], to identify the points that cover most of the distribution for the global LCC for both the ambition level under consideration and the *'reference'* scenario density plots. The robust financial risk is the quantification of the global LCC that causes the HDI credible interval of the density plots to intersect with each other.

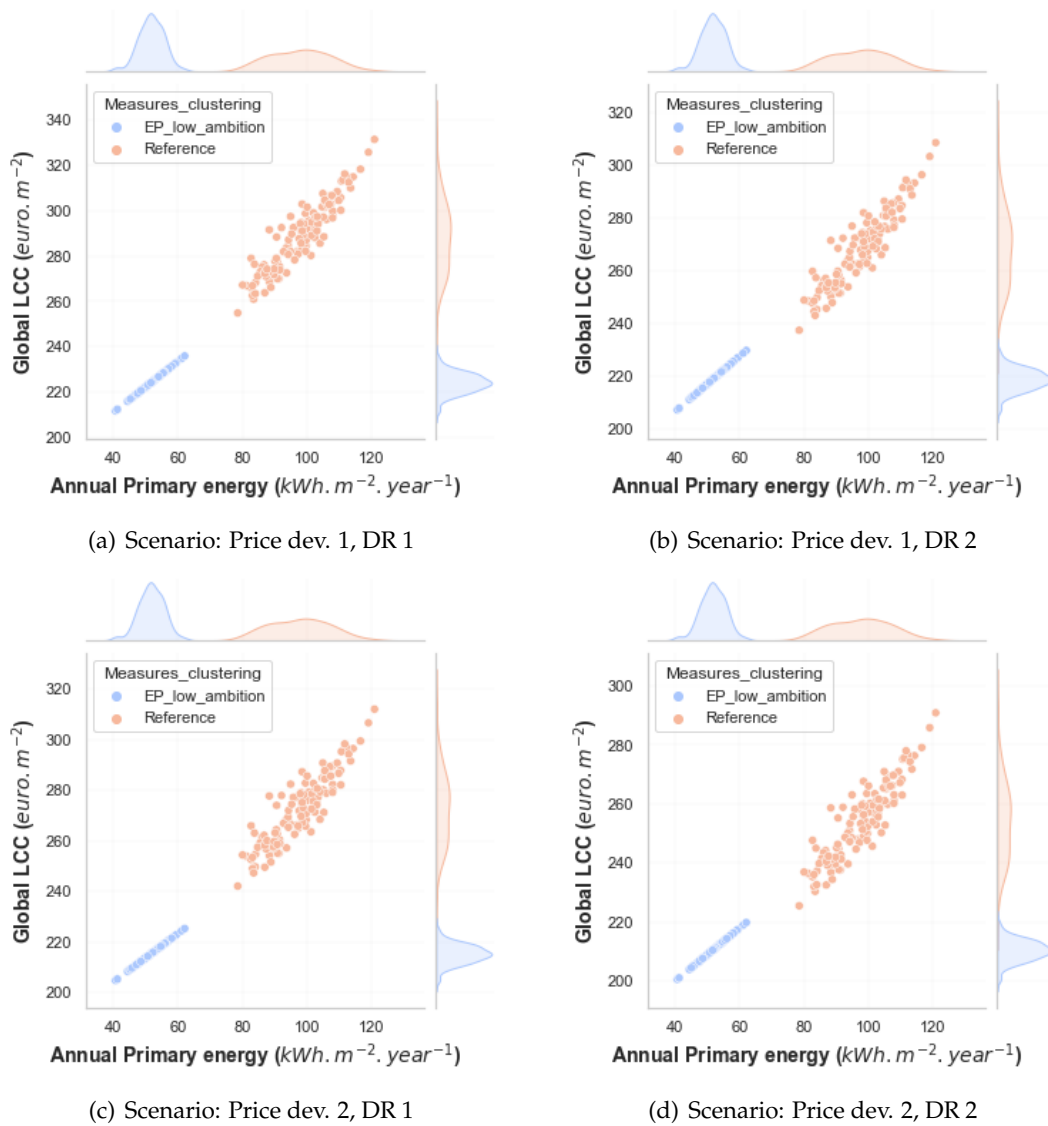


Figure 5.3: Joint plots combining scatter plots with probability distributions to analyse operational EP and financial global LCC uncertainty of a package of measures corresponding to a NZEB benchmark versus the 'reference' scenario

To better visualise and provide a mathematical context to robust financial risk, Figure 5.4 shows a typical joint plot for a defined ambition level for a specific DR and Price Development (PD) combination scenario. The marginal distribution plot for the financial global LCC is magnified, and the density plot for both the 'reference' and NZEB ambition level scenarios are described in terms of the upper and lower bounds of a % HDI credible interval that covers most of the distribution. From Figure 5.4, the robust global LCC financial risk that causes the intersection between the two credible intervals is calculated as shown in Equation 5.3.

$$Robust\ LCC\ financial\ risk\ (euro.m^{-2}) = Amb_HDI_upper - Ref_HDI_lower \quad (5.3)$$

where Amb_HDI_upper is the upper bound of the HDI credible interval ambition level distribution under study, and Ref_HDI_lower is the lower bound of the 'reference' scenario distribution credible interval. This calculation can be performed for each DR and PD under consideration to identify the impact of varying these financial parameters on the robust global LCC financial risk for each defined NZEB ambition level in Section 5.2.1 to ensure well informed policy decision making under uncertainty.

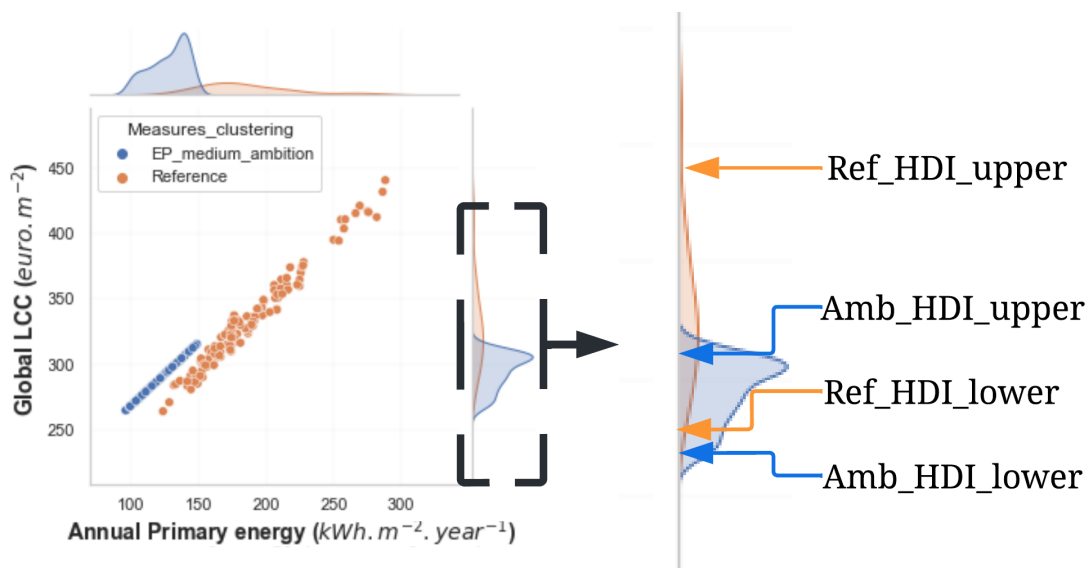


Figure 5.4: Joint plot visualising the uncertainty propagation for a defined NZEB ambition level versus the 'reference' scenario visualising the parameters to calculate the robust global LCC financial risk at a given DR and PD scenario for well informed policy making to facilitate the transition of a building to NZEB.

5.3 | Application of the framework to the hotel RB case study

This section applies the NZEB EP benchmarking and probabilistic risk analysis framework described in Section 5.2 to the '*probabilistic Bayesian calibrated*' hotel RB case study energy model developed in Chapter 4. The '*probabilistic Bayesian calibrated*' hotel RB energy model is composed of the electricity end-uses calibrated RB building physics model coupled with the calibrated RB DHW building physics model described in Section 4.4.2.1. The electricity end-uses calibrated RB building physics model was characterised in Section 4.4.2.2 both as a detailed full-space model (Model A) and a computationally efficient model constructed using the '*reference zone*' approach concept (Model D). Therefore, this section will first assess the suitability of replacing Model A with Model D to improve BEM computational efficiency in the context of this proposed framework. If Model D is deemed suitable to replace Model A, it will be the electricity end-uses model applied to derive NZEB benchmarks and perform risk analysis. It should be noted that the ECMs chosen for application to the case study are only intended to demonstrate the framework and not to provide a comprehensive list of energy efficiency measure options that can be applied to hotels in Malta to improve their operational EP.

5.3.1 | Evaluating computationally efficient RB building physics models for application to the framework

Similarly to the iterative Bayesian calibration process performed in Chapter 4, the framework described in Section 5.2 that executes step 5 and step 6 of the proposed EPBD cost-optimal approach requires multiple simulation runs from the RB Physics model(s) itself to derive EP benchmarks and to analyse risk and therefore its computational efficiency depends on the computational expense of the applied building physics model(s). Thus, similar to the Bayesian calibration process performed in Chapter 4, the framework can also be made more computationally efficient for the hotel case study by replacing Model A with Model D for electricity end-uses, given that Model D showed a 4000 % run-time efficiency improvement over Model A.

However, before replacing Model A with Model D, one must specifically assess for this framework how well Model D can replicate the results of Model A in predicting the annual energy savings for space heating plus cooling and total energy end use relative to the '*reference*' scenario when the different packages of passive measures considered

for the cost-optimal analysis are applied⁵. It must be highlighted that the adequacy of replacing Model A with Model D for Bayesian calibration was analysed differently in Chapter 4. The analysis in Chapter 4 for Bayesian calibration made use of '*probabilistic Bayesian calibrated*' RB building physics models for the '*reference*' scenario without considering the impact of energy efficiency measures.

It must be noted that a preliminary evaluation that considers the impact of passive ECMs was already carried out in Section 4.4.2.2 for the non-calibrated RB building physics models characterised with the default parameters shown in Table 4.5. The results successfully showed that Model D could correctly predict annual energy savings for space heating and cooling compared to Model A, with a maximum discrepancy of only 4.6 % in energy savings potential when all passive measures under study were applied to the EnergyPlus models. However, to further increase confidence in the suitability of applying Model D to replace Model A for this framework, this evaluation must be repeated using the calibrated RB building physics models defined with the mean value of the posterior parameter distributions. This reflects the way the RB model must be characterised for NZEB EP benchmarking as described in Section 5.2.1.

To demonstrate this framework for the hotel case study, the same passive measures M1 to M3 described in Table 4.8, referred to as MP1 to MP3 in this section, are considered for this case study. Table 5.1 below describes the passive measures.

Table 5.1: Passive measures considered for the hotel case study

Measure	Initial parameter values	Measures description	Final parameter values
MP1	Wall U-value = $2.1 \text{ W.m}^{-2}.\text{K}^{-1}$	Application of 5 cm XPS on external walls	Wall U-value = $0.5 \text{ W.m}^{-2}.\text{K}^{-1}$
MP2	Roof U-value = $1.7 \text{ W.m}^{-2}.\text{K}^{-1}$	Application of 8 cm EPS on roof	Roof U-value = $0.4 \text{ W.m}^{-2}.\text{K}^{-1}$
MP3	Glazing U-value = $3.1 \text{ W.m}^{-2}.\text{K}^{-1}$, SHGC = 0.7, Light transmission = 0.8	Application of 3M corporation PR70 film on fenestration glazing	Glazing U-value = $3 \text{ W.m}^{-2}.\text{K}^{-1}$, SHGC = 0.4, Light transmission = 0.5

⁵In the context of deriving benchmarks and propagating uncertainty, the building energy systems (active) measures for space heating, cooling and ventilation are assumed to provide the same seasonal and annual energy efficiency performance parameters for both Model A and Model D. That is the performance of the space heating, cooling and ventilation equipment is independent of the partial load (hourly) performance. This assumption is in line with the monthly EP calculation energy use approach described in ISO 52016-1 [356].

For both Model A and Model D EnergyPlus models, defined with mean posterior calibration parameter distributions shown in Table 4.13, a full parameterisation simulation exercise considering all possible passive COMs was carried out in JEPlus [50] and both the annual energy end-uses for space heating and cooling and the annual electricity consumption were analysed as shown in Table 5.2. The JEPlus, EnergyPlus models and the spreadsheet calculation required to derive Table 5.2 are found in the GitHub repository⁶. From Table 5.2, one can see that the maximum difference in the energy savings potential for Model D compared to Model A for annual space heating plus cooling and total electrical energy end uses outputs is only 4.3 % and 1.25 %, respectively. This difference occurs when the package of passive measures comprised of MP1 and MP2 is applied to the models. The results in Table 5.2 for the case study also clearly show that both Model A and Model D predict a minimal EP improvement potential when passive measures are applied given Malta's temperate climate⁷.

Table 5.2: Comparison of improvements between Model A and Model D for all cases of passive combination of measures for the simulated hotel case study with the mean value of the posterior distribution of the calibrated parameters. The ECMs applied for each case are marked with an X.

Measures applied			Annual space heating & cooling energy end uses (kWh)			Total annual electricity energy end uses (kWh)		
			% EP improvement from Reference scenario		Delta	% EP improvement from Reference scenario		Delta
MP1	MP2	MP3	Model A	Model D		Model A	Model D	
			0.00	0.00	0.00	0.00	0.00	0.00
	x		2.45	3.22	-0.77	0.71	0.96	-0.25
		x	3.23	2.73	0.50	0.84	0.75	0.08
	x	x	6.09	6.22	-0.13	1.64	1.78	-0.13
x			3.59	6.38	-2.79	0.93	1.70	-0.77
x	x		6.14	10.48	-4.34	1.67	2.92	-1.25
x		x	7.39	9.58	-2.19	1.91	2.58	-0.67
x	x	x	10.51	14.03	-3.52	2.78	3.88	-1.10

⁶Refer to GitHub Repository folder 'Ch 5 Model D justification'. Refer also to Appendix B for a detailed description of all files and folders found in the GitHub Repository.

⁷Chapter 3, Section 3.4.1 explains the impact of Malta's temperate climate on the potential of different ECMs.

Therefore, based on the results in Table 5.2, Model D was deemed suitable to replace Model A to achieve a computationally efficient approach to executing this framework. Furthermore, the choice to replace Model A with Model D for this framework is further corroborated by the spreadsheet calculation results provided in the GitHub Repository⁸. As shown in these results, for all parameterisation cases, the maximum discrepancy in the annual total space heating plus cooling and the annual total electricity use output from the models is only 4.3 % and 3.7 %, respectively. Furthermore, Model D can replicate the parameterisation results for both the annual total space heating plus cooling and annual total electricity energy use with a CVRMSE < 8 % and NMBE < 3.4 %. These statistics, which fall within the ASHRAE [152] thresholds, demonstrate the ability of Model D to predict the overall load shape in the output data with minimal bias error when compared to Model A.

⁸Refer to GitHub Repository folder '*Ch 5 Model D justification*'. Refer also to Appendix B for a detailed description of all files and folders found in the GitHub Repository.

5.3.2 | Step 5 : NZEB EP Benchmarking applied to the RB case study

This section applies the proposed EPBD NZEB EP benchmarking approach described in Section 5.2.1 to the hotel case study. For this case study, both Model D and the DHW building physics model are treated deterministically by applying the mean value of the calibration parameters posterior distributions summarised in Table 4.10 and Table 4.14 for DHW and electricity end-uses, respectively.

5.3.2.1 | Description of the ECMs under consideration

The passive and building energy systems (active) ECMs for the EPBD cost-optimal method used to derive NZEB EP benchmarks are shown in Table 5.1 and Table 5.3, respectively. In total, three passive ECMs were considered, MP1 to MP3. MP1 is the application of external wall insulation, MP2 is the addition of roof insulation, and MP3 is the application of a spectrally selective film to the glazing fenestration. As shown in Table 5.1, the application of insulation reduces the U-value or thermal transmittance of the components of the building envelope under study, while the spectrally selective film is applied to reduce the heat gain from solar radiation. For each ECM, MP1 to MP3, two discrete options or parameter values were investigated. The two options constitute the initial parameter values that are known (deterministic) for the building envelope as shown in Table 4.5 and that characterise the 'reference' RB scenario, and the final parameter values after the application of ECMs.

Similarly, three building energy systems (active) ECMs, MA1 to MA3, were considered for NZEB EP benchmarking, as shown in Table 5.3. MA1 upgrades the existing VRF system to improve its rated COP in both heating and cooling, MA2 replaces the DHW boiler with a DHW heat pump, and MA3 improves Specific Fan Power (SFP) of the mechanical ventilation system. Furthermore, ECMs MA1 to MA3 each investigate two discrete options for NZEB EP. More specifically, the mean value of the calibration parameter posterior distributions describe the initial, 'reference' RB scenario parameters, while the final parameter values follow the application of ECMs. It should be noted that for the VRF rated heating COP, the default parameter shown in Table 5.1 was taken as the initial parameter value. Unlike the VRF rated cooling COP, the VRF rated heating COP was not calibrated, as it was not found to be one of the most significant parameters that impacts annual electricity consumption after the SA exercise in Section 4.4.3.2.

Table 5.3: Building energy systems (active) measures considered for the hotel case study

Measure	Initial parameter values for NZEB EP Benchmarking	Initial parameter values for Risk analysis	Measures description	Final parameter values
MA1	VRF rated cooling COP = 2.18 , VRF rated heating COP = 3.4	VRF rated cooling COP posterior distribn, VRF rated heating COP = 3.4	Upgrade/RAR air-cooled VRF system	VRF rated cooling COP = 4.2, VRF rated heating COP = 4.31
MA2	DHW boiler heater efficiency = 0.84	DHW boiler heater efficiency posterior distribn	RAR fuel boiler with DHW heat-pump	DHW heat pump rated COP = 4
MA3	Mech vent system fan pressure rise = 1112 Pa	Mech vent system fan pressure rise posterior distribn	Upgrade/RAR mechanical vent system	Mech vent system fan pressure rise = 945 Pa

5.3.2.2 | The EN 15459 global LCC financial parameters

For the case study, the values of the global LCC financial parameters for each ECM and the corresponding 'reference' scenario of not implementing ECM are shown in Table 5.4 and Table 5.5 for the passive and building energy systems (active) ECMs, respectively. The DRs considered for the financial calculation are DR 1 of 3.2 %, to reflect the average landing rate in October 2021 in Malta [357], and DR 2 of 4 %, which reflects the financial DR recommended by EC [358] to be used as a reference for the long-term real opportunity cost of capital for the programming period 2014-2020 [359]. Furthermore, the values of the global LCC macroeconomic parameters for the ECMs are the same as for the financial calculations, but the 18 % Value Added Tax (VAT) is deducted from the costs. The DR chosen for macroeconomic calculation are DR 1 of 3 % according to the EC guidelines [55] and DR 2 of 5 % according to the 2018 cost-optimal studies for Malta [56]. The calculation period for both financial and macroeconomic calculations is taken to be 20 years, as required by the EC guidelines [55] for commercial buildings. The period starting from the year 2022 to the year 2042 was considered for the case study.

Table 5.4: Financial global LCC parameters for the passive ECMs considered for the hotel case study

Passive ECM	CO_{INIT} (euro.m ⁻²) ^b	$CO_{a,maint}$ (% of CO_{INIT})	Life time (Years)	$CO_{a,RAR}$ (euro)	Year of RAR	VAL_{fin}^c (euro.m ⁻²)
Reference scenario ^a	0	0	0	0	0	0
MP1	45	0	30	0	0	15
MP2	70	0	30	0	0	23
MP3	106	10	30	0	0	35

^a Scenario when no ECMs are applied.

^b Area in m² refers to surface area of building element on which the passive ECM is applied. For the case study, wall area for MP1 is 19,796 m², roof area for MP2 is 19,825 m², glazing area for MP3 is 4,476 m².

^c Non-discounted VAL_{fin} values shown.

Table 5.5: Financial global LCC parameters for the building energy systems (active) ECMs considered for the hotel case study

Active measure	CO_{INIT} (euro.m ⁻²)	CO_{INIT} (euro)	$CO_{a,maint}$ (% of CO_{INIT})	$CO_{a,maint}$ (euro)	Lifetime (years)	$CO_{a,RAR}^d$ (euro)	Year of RAR	VAL_{fin}^e (euro)
MA1	136	4,130,025	2	82,061	15	4,130,025	15	2,735,350
Reference_MA1 ^a				205,151				
MA2		649,000	2	12,980	15	649,000	15	432,667
Reference_MA2 ^b				25,960	20	519,200	10	259,600
MA3	94	3,338,429	4	135,377	15	3,338,429	15	2,256,286
Reference_MA3 ^c				169,221				

^a Reference_MA1 refers to the reference scenario of operating using the current VRF system throughout the calculation period. The cost of operating with this scenario is fully reflected in the $CO_{a,maint}$, that considers the replacement of the system to be spread over 20 years.

^b Reference_MA2 refers to the reference scenario of operating using the current DHW boiler system that has a 10 year remaining lifetime. The DHW boiler system is replaced after 10 years with a similar DHW boiler system having a 20 years lifespan.

^c Reference_MA3 refers to the reference scenario of operating using the current mechanical ventilation system throughout the calculation period. The cost of operating with this scenario is fully reflected in the $CO_{a,maint}$, that considers the replacement of the system to be spread over 20 years.

^d No learning rate assumed.

^e Non-discounted VAL_{fin} values shown.

For the development of the price for the fuel and carbon emissions costs, two scenarios are considered, Price Development (PD) 1 and PD 2. PD 1 considers the future price escalation trend to follow the same % annual average EU linear PD rate of the past years. In contrast, PD 2 considers future price escalations based on EU outlook studies or machine learning regression prediction trends based on a time series of previous observations.

More specifically, for PD 1, the following fuel prices were considered for the global LCC calculation period:

- An increase in the electricity price of 2.5 % per year reflects the development of the EU annual average electricity price between 2008 and the first half of 2021 according to the Eurostat electricity price statistics [360].
- An increase in the LFO price of 5 % per year to reflect the development of the EU annual average LFO price between 1998 and 2018 according to the European Environmental Agency [361].
- An increase in the price of carbon emissions by 27 % per year to reflect the development of the price of carbon emissions allowances between 2005 and the end of 2021 documented on the Trading Economics website [362] for the EU Emissions Trading System (ETS).

As for PD 2, the following fuel prices were considered for the global LCC calculation period:

- Development of electricity prices according to the Policy Oriented Tool for Energy and Climate Change Impact Assessment (POTEnCIA) central scenario EU energy outlook for 2050 [363]. This scenario depicts stable electricity prices up to 2040⁹.
- Development of LFO prices according to the POTEnCIA central scenario EU energy outlook for 2050 [363]. This scenario depicts an increase in LFO electricity prices of approximately 4 % per annum up to 2040¹⁰.
- Carbon emissions price forecast using a statistical regression trend developed from a time series of monthly carbon emission price observations between 2007 and 2021 that was collected from the investing.com website [364] for EU ETS. The trend of exponential regression analysis that provides a R^2 of 0.85 is shown in Figure 5.5. The carbon prices for the months considered in the calculation period, that is between the period year 2022 to 2042, were forecast using this regression model.

⁹The electricity generation cost trend up to 2050 is in depicted in Figure 107 of [363] and the actual price development ratios applied for the case study are shown in Python notebook '*cost-optimal Python note book*' found in GitHub Repository folder '*Ch 5 Cost-optimal Python note book*'. Refer also to Appendix B for a detailed description of all files and folders found in the GitHub Repository.

¹⁰The LFO cost trend up to 2050 is in depicted in Figure 9 of [363] and the actual price development ratios applied for the case study are shown in Python notebook '*cost-optimal Python note book*' found in GitHub Repository folder '*Ch 5 Cost-optimal Python note book*'. Refer also to Appendix B for a detailed description of all files and folders found in the GitHub Repository.

The prices were then converted to annual resolution data using pivot tables in Microsoft Excel¹¹.

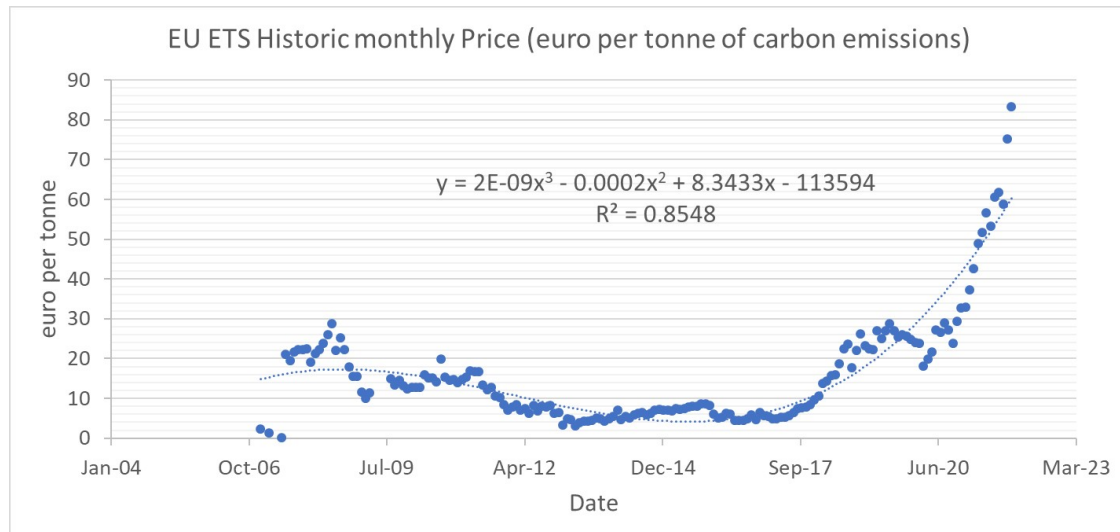


Figure 5.5: Time-series of carbon emission monthly price observations between 2007 and 2021 collected from the investing.com website [364] for the EU ETS. The exponential regression analysis exponential trend provides a R^2 of 0.85.

Thus, NZEB EP benchmarking for the case study was performed for the following four financial perspective sensitivity scenarios:

1. Scenario A_f : PD 1, DR 1 (3.2 %)
2. Scenario B_f : PD 1, DR 2 (4 %)
3. Scenario C_f : PD 2, DR 1 (3.2 %)
4. Scenario D_f : PD 2, DR 2 (4 %)

and for the following four macroeconomic perspective sensitivity scenarios:

1. Scenario A_m : PD 1, DR 1 (3 %)
2. Scenario B_m : PD 1, DR 2 (5 %)
3. Scenario C_m : PD 2, DR 1 (3 %)
4. Scenario D_m : PD 2, DR 2 (5 %)

¹¹The source code data to develop the regression analysis in Figure 5.5 is provided in the Microsoft Excel file 'Carbon Emissions Price regression analysis' found in GitHub repository folder 'Ch 5 GHG Price development regression'. Refer to Appendix B for a detailed description of all files and folders found in the GitHub Repository.

5.3.2.3 | EP analysis and EN 15459 global LCC calculations for different COMs

The six ECMs shown in Table 5.1 and Table 5.3, each defined with two discrete options of 64 (2^6) cases (COMs), define a complete parametric EnergyPlus simulation exercise for the hotel RB case study. This parametric simulation EP analysis exercise to calculate the annual site energy consumption for each COM was carried out in JEPlus [50] using both Model D and the DHW building physics model. The JEPlus models to generate simulation runs for each year from 2017 to 2019, and the corresponding energy end-use simulation results are found in the GitHub Repository¹². The EP output for each COM was then fed into an EN 15459 [54] global LCC tool programmed in Python Notebook '*cost-optimal Python note book*' found in the GitHub Repository¹³. The notebook is programmed from the first principles using Equation 5.1 and characterised by the financial parameters described in Section 5.3.2.2 above. The '*cost-optimal python note book*' also converts the site energy consumption for each COM to both primary energy and operational carbon emissions using the local conversion factors of Malta for each fuel, as specified in Chapter 3, Section 3.4.1.

The '*cost-optimal Python note book*' was also programmed to perform the global LCC analysis for each sensitivity scenario, Scenario A_f to Scenario D_f and Scenario A_m to Scenario D_m, described in Section 5.3.2.2 above, and programmed to automatically generate cost-optimal plots and combine the cost-optimal plots for all global LCC sensitivity scenarios using the visualisation layout shown in Figure 5.2. The program also automatically derives using logical operators, the four levels of NZEB EP benchmarks detailed in Section 5.2.1 and their corresponding COM. The cost-optimal analysis for the case study was carried out separately for three consecutive years, 2017 to 2019, using the corresponding '*cost-optimal Python note book*', the appropriate weather file and the actual monthly occupancy patterns for that year. Testing for more than one year was carried out to demonstrate the robustness of the approach.

Furthermore, the results were also compared to the outcome of the current EPBD cost-optimal approach of Section 5.4 using SBEM-mt [346], the NCM software for Malta. The analysis was performed with Model D characterised with the occupancy of 2018 and the 2010 weather file as input. The latter analysis is described with the notation '*year 2018-10*'. The year 2018 was chosen because it provides the median hotel annual

¹²Refer to GitHub Repository folder '*Ch 5 Model D JEPlus Parametric simul electric*' to find the JEPlus parametric models and corresponding annual electricity end-use energy consumption results from Model D. Furthermore, the GitHub Repository folder '*Ch 5 JEPlus Parametric simulations DHW*' provides the JEPlus parametric models for the DHW building physics model and the corresponding annual DHW (LFO) end-use consumption simulation results. Refer also to Appendix B for a detailed description of all files and folders found in the GitHub Repository.

¹³Refer to GitHub Repository folder '*Ch 5 Cost-optimal Python note book*'.

occupancy between 2017 and 2019, while the SBEM-mt [346] software uses the weather file for the year 2010 for the EP calculations.

The annual operational primary energy consumption for the '*year 2018-10*' could not be derived from metered site energy consumption for the hotel case study but was theoretically calculated using the Degree days modelling method detailed in [1]. Using this modelling method, the monthly hotel site electrical energy consumption data for the years 2017 to 2019, the dependent variable, was plotted against the monthly total degree days. The sum of the heating and cooling degree days is the total degree days. The total degree days were calculated using hourly outside dry-bulb temperatures for a defined range of base temperatures for both cooling and heating, as detailed in [1]. A Python program termed '*Degree days notebook*', provided in the GitHub repository¹⁴, was then programmed to test all combinations of cooling and heating base temperatures. This analysis was done to determine the combination of base temperatures that achieves the optimal coefficient of determination (R^2) between monthly site electrical consumption and monthly total degree days. The optimal R^2 of 0.96 was achieved when a base temperature of 12 °C was applied for both cooling and heating. The regression plot that achieves the optimal R^2 is depicted in Figure 5.6. The total monthly and annual degree days were determined from the regression equation shown in Figure 5.6 by inputting the identified optimal base temperatures and the hourly dry-bulb outside temperatures for the year 2010¹⁵. These results were used to model the monthly and annual electric consumption for the year 2010. The consumption of LFO to generate DHW was the same as in 2018, given that the same occupancy patterns characterised the DHW EnergyPlus model.

¹⁴Refer to GitHub Repository folder '*Ch 5 Degree days notebook*'

¹⁵Microsoft Excel file '*Heating cooling DD calculator 2010 2016 2017 2018 2019*' found in GitHub Repository folder '*Ch 5 Degree days notebook*' sub-folder '*Excel DD calculator*' contains hourly dry-bulb temperature data for the year 2010 and years 2016 to 2020. This data allows degree days to be calculated on a monthly resolution for these years for a given set of base temperatures. Refer also to Appendix B for a detailed description of all files and folders found in the GitHub Repository.

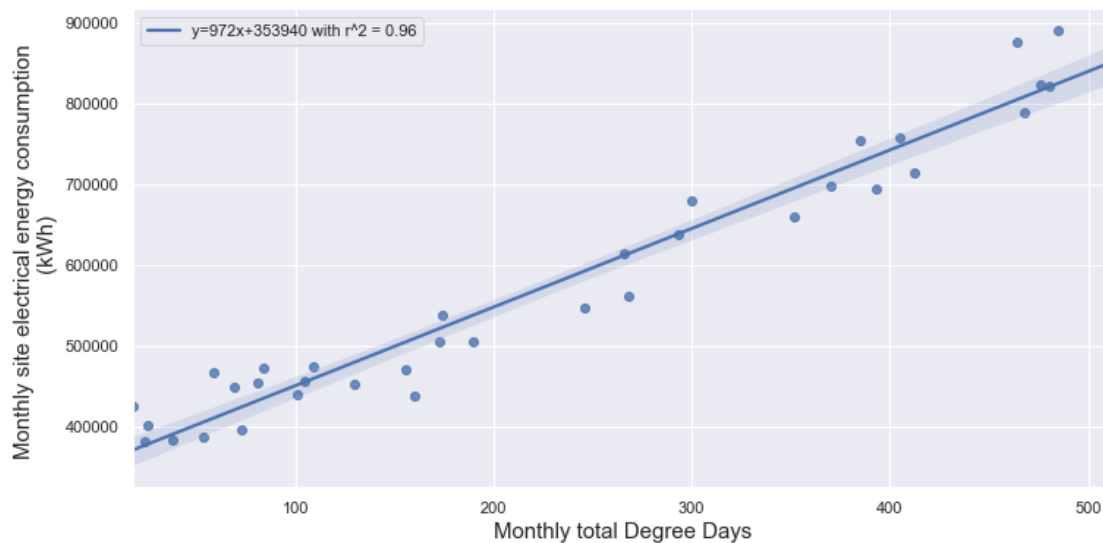


Figure 5.6: Regression plot analysing monthly site electrical consumption for the hotel case study using Degree Days modelling. The plot is shown for the cooling and heating base temperature of 12 °C that achieve the optimal R^2 of 0.96.

Table 5.6 shows the results for the four different NZEB ambition benchmark levels for each year considered. It can be seen that the ECMs, marked with an X in the table, which makes up the COM required to achieve the four NZEB benchmark ambition levels, are the same for all years. The EP benchmark values for each respective ambition level defined in $kWh.m^{-2}.year^{-1}$ are also stable, and their sensitivity to weather and occupancy patterns for the years under consideration is minimal. The NZEB EP benchmark values obtained for each respective ambition level for the years considered can also be visualised in Figure 5.7.

Furthermore, as also shown in Table 5.6, the potential percentage of energy savings calculated from the reference scenario is also stable throughout the years and varies between 17.45 and 19.36 % for the low-ambition benchmark and between 22.90 and 24.72 % for the highest ambition benchmark. The resulting potential energy savings from the different COMs achieving each benchmark are consistent with other studies detailed in Chapter 3, Section 3.4.1. More specifically, given Malta’s temperate climate, the potential for EP improvements by upgrading the building from medium to higher NZEB EP benchmarks through more stringent passive ECMs are minimal compared to the EP improvements that can be achieved by upgrading building energy (active) systems.

Table 5.6: Derived NZEB EP benchmarks are corresponding ECMs for the hotel case study for all years 2017 to 2019 under consideration

Year	NZEB EP benchmark level	Primary EP benchmark ($kWh.m^2.year^{-1}$)	% EP improvement	Passive ECMs			Active ECMs		
				MP1	MP2	MP3	MA1	MA2	MA3
2017	Reference	354							
	Operational	355							
	Low	292	17.45				x	x	
	Medium	282	20.46				x	x	x
	High	274	22.50				x	x	x
	Highest	273	22.90	x	x	x	x	x	x
2018	Reference	357							
	Operational	355							
	Low	289	19.04				x	x	
	Medium	278	22.04				x	x	x
	High	272	23.79				x	x	x
	Highest	270	24.27	x	x	x	x	x	x
2018_10	Reference	348							
	Operational	349							
	Low	284	18.39				x	x	
	Medium	273	21.55				x	x	x
	High	268	22.99				x	x	x
	Highest	266	23.56	x	x	x	x	x	x
2019	Reference	365							
	Operational	362							
	Low	294	19.36				x	x	
	Medium	284	22.29				x	x	x
	High	277	24.19				x	x	x
	Highest	275	24.72	x	x	x	x	x	x

Table 5.6 also shows that the annual primary EP gap between the annual simulated EP for the EnergyPlus model without ECMs, termed the '*reference scenario*', and the annual operational primary EP is negligible for all considered years. This clearly highlights the importance of calibrating the RB energy model for the cost-optimal analysis, to obtain realistic EP benchmarks and the corresponding quantification of primary energy savings when upgrading buildings to the defined NZEB EP benchmark levels.

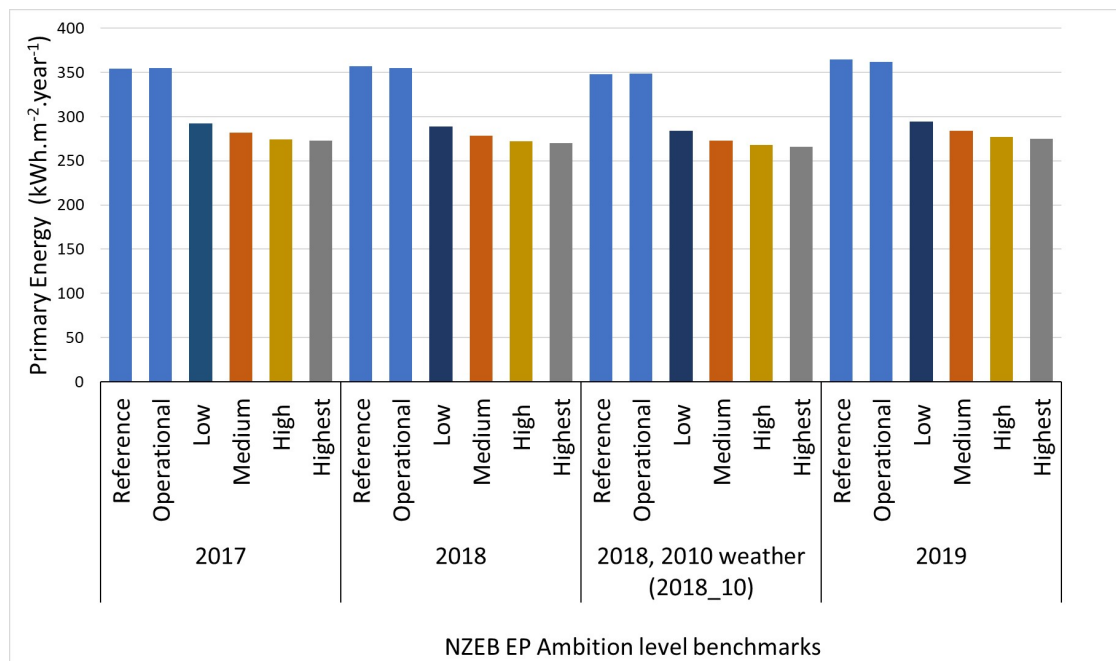


Figure 5.7: The NZEB primary EP benchmark results for each considered year 2017 to 2019

The resulting cost-optimal plots to allow a better visualisation of the derived NZEB benchmarks in Table 5.6, are shown in Figure 5.8 for the year 2018_10. Using the same notation as in Section 5.2.1, point A coincides with COM giving the lowest NZEB EP ambition level, point B and point C are the COMs giving the high and medium NZEB EP ambition levels, respectively, while point D is the COM providing the highest NZEB EP ambition level. The resulting cost-optimal plots for the other considered years provide a similar outcome and can be found in the GitHub repository¹⁶.

¹⁶Refer to GitHub Repository folder 'Ch 5 Cost-optimal python note book', which provides the cost-optimal and NZEB benchmarking results for each year under study in a separate Python Notebook entitled 'Hotel_3_cost_opt_analysis'. Refer also to Appendix B for a detailed description of all files and folders found in the GitHub Repository.

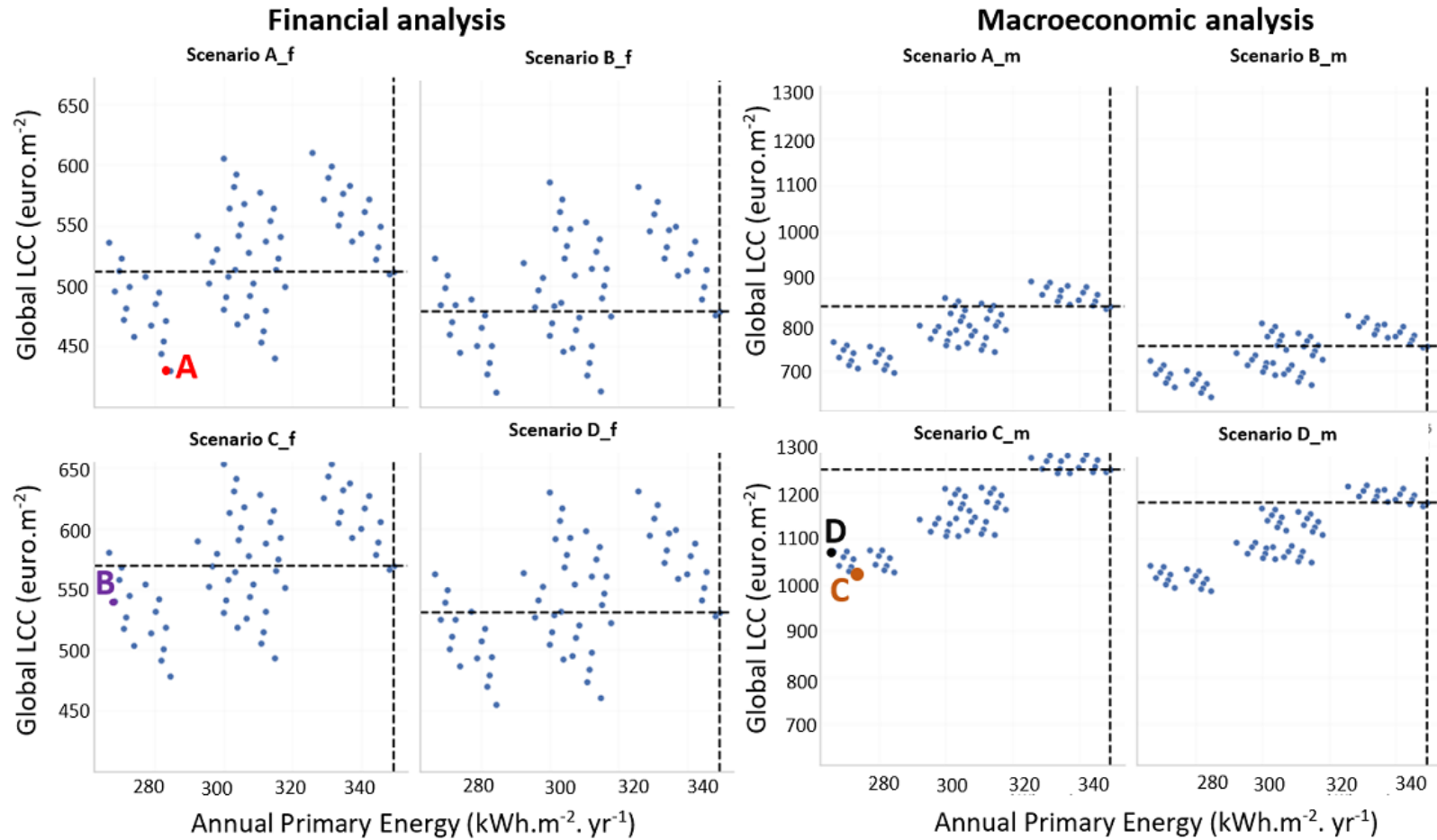


Figure 5.8: The four NZEB EP benchmarks derived for the case study for the year 2018-10. Point A, Point B, Point C, and Point D coincide with the COM giving low, high, medium and highest NZEB EP benchmarks respectively as described in Table 5.6

5.3.3 | Step 6 : Risk analysis for each defined NZEB benchmark applied to the RB case study

This section applies the proposed EPBD probabilistic risk analysis described in Section 5.2.1 to the hotel RB case study for each of the four NZEB EP ambition levels derived in the previous section considering all the years 2017 to 2019 under study. The risk analysis joint plots in the format shown in Figure 5.3 were constructed using the '*cost-optimal python note book*'. For this analysis, both Model D and the DHW building physics model were treated probabilistically with the calibration parameters defined according to the posterior distributions of the calibration parameters summarised in Table 4.10 and Table 4.14 for DHW and electricity end-uses, respectively.

The main inputs to the '*cost-optimal python note book*', set up with the financial parameters defined in Section 5.3.2.2, are the uncertainty in operational EP propagated from the posterior calibrated parameter probability distributions for each of the derived NZEB EP ambition levels under study and for the '*Reference*' scenario. The derived NZEB EP ambition levels under study are shown in Table 5.6. The uncertainty propagation exercise was carried out using the LHS sampling method in JEPPlus [50] for Model D and the DHW building physics model separately for sample points taken from posterior calibrated parameter probability distributions¹⁷.

The joint plots that visualise the EP and financial risk to upgrade to each defined NZEB ambition level when compared with the '*reference*' scenario for the low, medium, high and highest ambition levels are shown in Figure 5.9, Figure 5.10, Figure 5.11 and Figure 5.12, respectively for the year 2018_10. The joint plots for the years 2017, 2018 and 2019 provide a similar outcome. These plots are found in the GitHub repository¹⁸. Four joint plots are constructed for each ambition level, that is, one plot for each financial perspective scenario considered, Scenario A_f to Scenario D_f. The x-axis for each joint plot shows the operational primary energy use per m^2 of floor area. It must be noted that the operational primary energy on each plot only considers the energy end-uses impacted by the COM that is implemented to achieve the required NZEB ambition level¹⁹. In addition, the y-axis for each joint plot depicts the global LCC corresponding

¹⁷The JEPPlus/EnergyPlus files to execute the risk analysis simulation runs and corresponding results for each year under consideration, and each NZEB EP ambition level including the reference scenario are found in GitHub repository folder '*Ch 5 Model D JEPPlus risk propag*' for Model D and folder '*Ch 5 JEPPlus DHW risk propag*' for the DHW EnergyPlus model. Refer also to Appendix B for a detailed description of all files and folders found in the GitHub Repository.

¹⁸Refer to GitHub Repository folder '*Ch 5 Cost-optimal python note book*', which provides the risk analysis results for every year under study in a separate Python notebook entitled '*Hotel_3_cost_opt_analysis*'.

¹⁹As an example, the x-axis for the joint plots for the NZEB low ambition level depicts the annual operational primary energy per m^2 of floor area for DHW, space heating and cooling given that measures

to the energy end uses under study. The 'cost-optimal python note book' was also programmed to calculate the global LCC robust financial risk according to Equation 5.3 for each ambition level and corresponding joint plots.

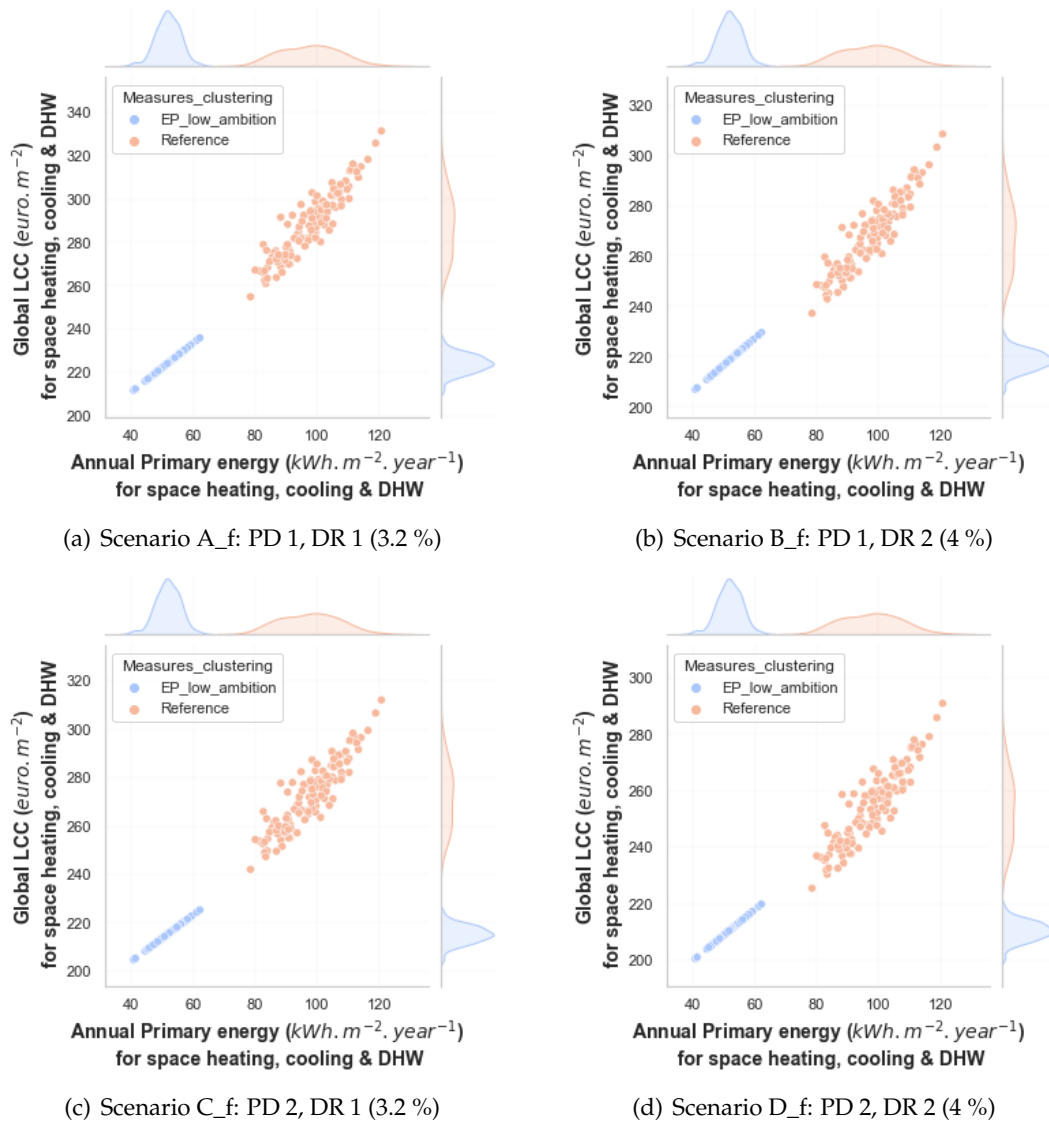


Figure 5.9: Joint plots combining scatter plots for with probability distributions to analyse operational EP and financial global LCC uncertainty of the COM corresponding to the low ambition NZEB EP benchmark versus the 'reference' scenario

MA1 and MA2 improve the EP for these energy end-uses. For the other ambition levels, the x-axis for the joint plots also includes the operational primary energy end-use per m^2 for mechanical ventilation. The reason is that, unlike the lower ambition level, the other (higher) ambition levels also implement measure MA3 that improves the EP for mechanical ventilation

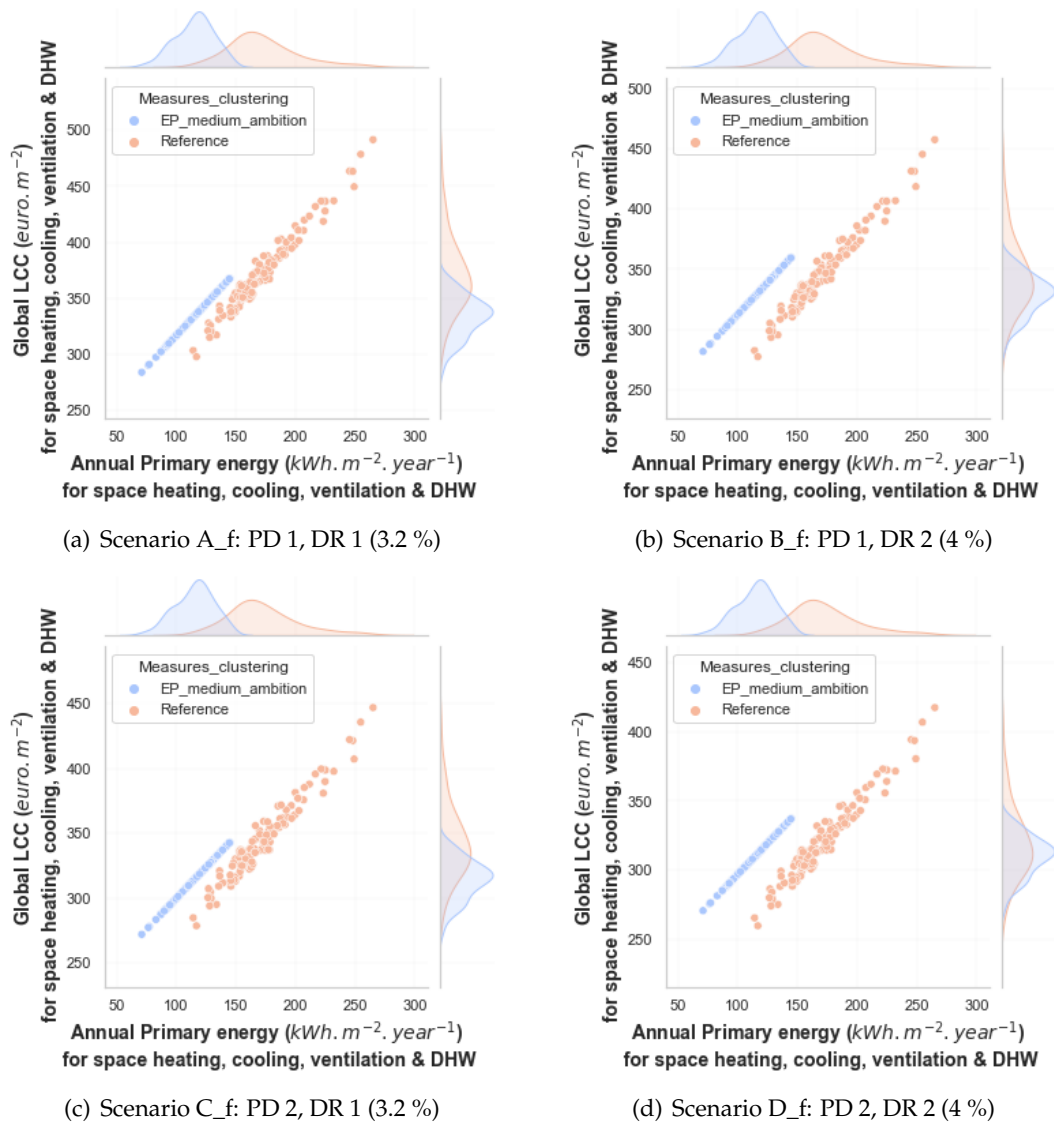


Figure 5.10: Joint plots combining scatter plots for with probability distributions to analyse operational EP and financial global LCC uncertainty of the COM corresponding to the medium ambition NZEB EP benchmark versus the 'reference' scenario

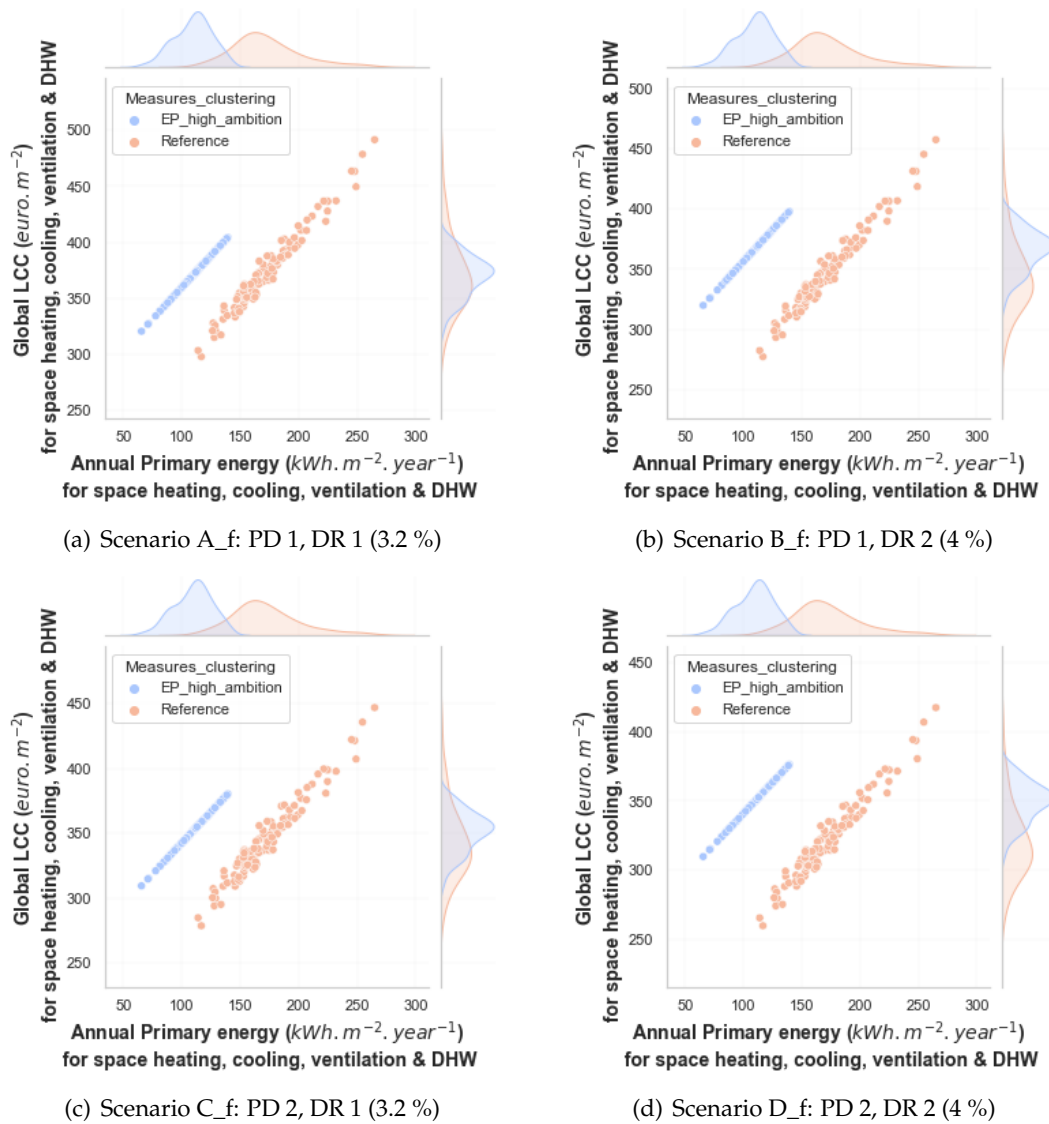
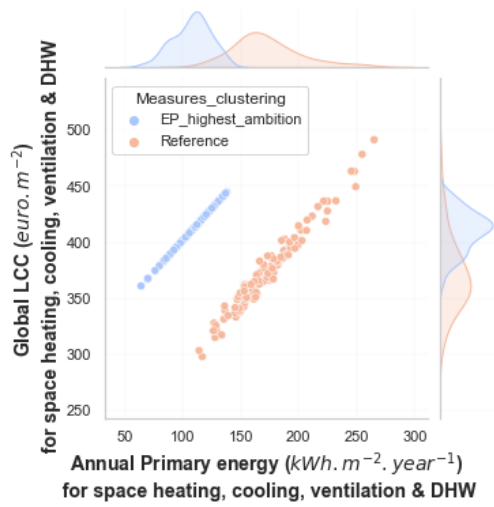
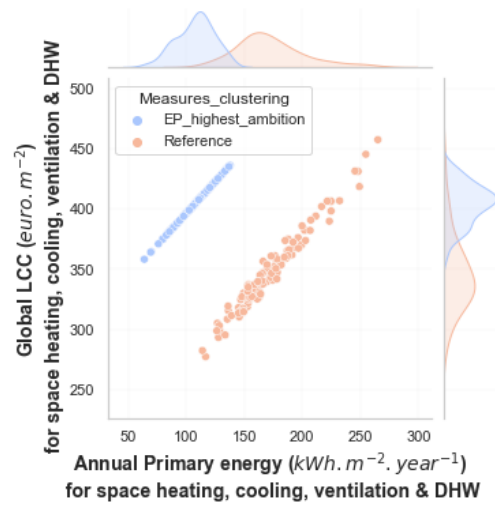


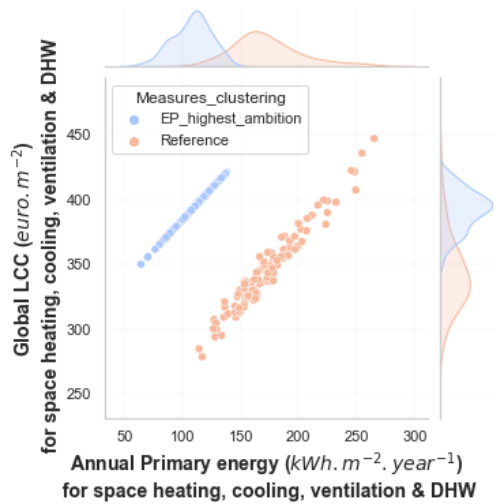
Figure 5.11: Joint plots combining scatter plots for with probability distributions to analyse operational EP and financial global LCC uncertainty of the COM corresponding to the high ambition NZEB EP benchmark versus the 'reference' scenario



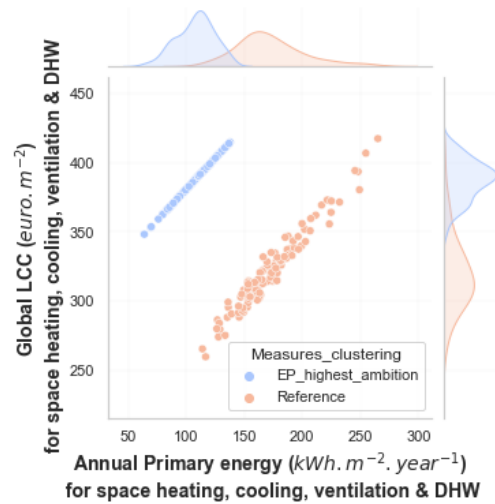
(a) Scenario A_f: PD 1, DR 1 (3.2 %)



(b) Scenario B_f: PD 1, DR 2 (4 %)



(c) Scenario C_f: PD 2, DR 1 (3.2 %)



(d) Scenario D_f: PD 2, DR 2 (4 %)

Figure 5.12: Joint plots combining scatter plots for with probability distributions to analyse operational EP and financial global LCC uncertainty of the COM corresponding to the highest ambition NZEB EP benchmark versus the 'reference' scenario

5.3.4 | A critical comparison between outcome of the deterministic and robust financial risk results

Table 5.7 compares the results of the deterministic and robust global LCC financial risks for each NZEB EP ambition level for all years 2017 to 2019. The financial risk results are also presented visually for the year 2018_10 in Figure 5.13 for each financial perspective scenario. It should be noted that negative financial global LCC risk values shown in Table 5.7 and Figure 5.13 translate into financial feasibility ($NPV > 0$) that will add value to the private investor. Furthermore, from Table 5.7 and Figure 5.13, one can conclude that the financial global LCC risk is not very sensitive to the financial perspective scenarios considered for this RB case study.

Table 5.7: Comparison of the resulting deterministic versus robust global LCC financial risk calculation for each NZEB EP ambition level and financial perspective scenario for the years 2017 to 2019

NZEB EP ambition benchmark level	Financial Perspective Scenario	2017 Global LCC financial risk (euro.m ⁻²)		2018 Global LCC financial risk (euro.m ⁻²)		2018_10 Global LCC financial risk (euro.m ⁻²)		2019 Global LCC financial risk (euro.m ⁻²)	
		Deterministic	Robust (Equation 5.3)	Deterministic	Robust (Equation 5.3)	Deterministic	Robust (Equation 5.3)	Deterministic	Robust (Equation 5.3)
Low	A_f	-87	-19	-94	-35	-89	-30	-91	-33
	B_f	-78	-7	-83	-22	-79	-18	-80	-21
	C_f	-71	-16	-78	-31	-73	-26	-75	-29
	D_f	-62	-5	-68	-19	-64	-14	-65	-17
Medium	A_f	-61	80	-68	67	-63	69	-65	66
	B_f	-50	92	-56	80	-51	82	-52	79
	C_f	-40	74	-46	62	-41	64	-43	62
	D_f	-29	86	-35	75	-30	77	-32	75
High	A_f	-27	115	-33	101	-27	105	-30	98
	B_f	-14	129	-19	116	-14	120	-16	113
	C_f	-4	110	-9	97	-3	101	-7	95
	D_f	8	124	3	112	8	116	6	111
Highest	A_f	14	155	8	141	14	145	10	138
	B_f	27	167	21	154	27	158	24	151
	C_f	35	150	29	138	35	141	31	136
	D_f	47	162	42	151	47	154	44	149

Both the deterministic and robust risk values are negative for all the financial perspective scenarios for the low NZEB EP ambition level. Therefore, upgrading the building to the low NZEB EP ambition level is robust to financial risk and financially feasible to the private investor without the need for financial support. The risk analysis joint plots in Figure 5.9 reflect these results and show that the global LCC distribution plots for the 'reference' and low ambition scenario do not intersect for all considered financial perspective scenarios. It should be noted, however, that the deterministic risk values provide financial feasibility outcomes that are more optimistic than the robust risk values for the low ambition level for all years and financial perspective scenarios, as depicted in Table 5.7.

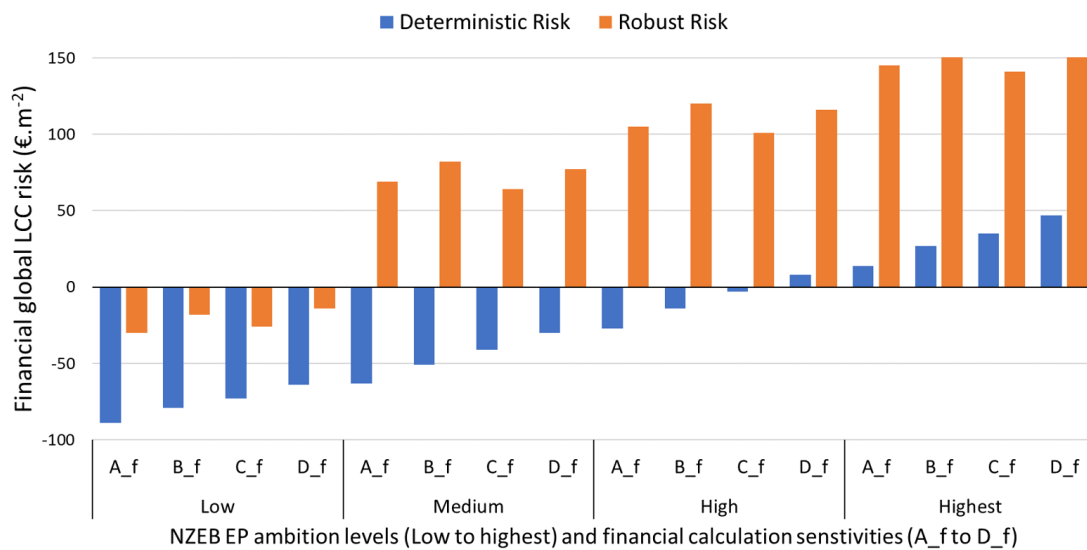


Figure 5.13: Comparison of the resulting deterministic versus robust global LCC financial risk calculation for each NZEB EP ambition level and financial perspective scenario for the year 2018_10

When performing energy retrofitting to the medium ambition level, the results of deterministic financial risk also show financial feasibility regardless of the financial perspective scenario. However, in contrast to the low ambition level, the robust financial risk values and the corresponding intersecting distributions in the joint plot (refer to Figure 5.10) show that upgrading to the medium ambition level does not provide a robust risk-free implementation for the private investor. A similar trend in the deterministic and probabilistic risk analysis outcomes is also observed for the high ambition level. However, for the high ambition level, the financial risk values are higher, and the financial feasibility is low to negligible even for the more optimistic deterministic analysis.

Furthermore, as expected, the highest ambition level shows the financial feasibility outcome that performs worst because, regardless of the risk analysis performed, deterministic or probabilistic, implementing ECMs to achieve this NZEB EP benchmark is not financially feasible for the private investor and is only feasible from a macroeconomic perspective when considering the cost of operational carbon emissions. Therefore, while the current EPBD cost-optimal regulations [345, 55] give the option to establish benchmarks from either the financial or macroeconomic perspective, the financial feasibility results of this study indicate that the establishment of benchmarks derived from the macroeconomic calculations should be considered with caution, as upgrading to such

benchmarks can pose a high financial risk to the private investor, which is only fully exposed when calculating the robust financial risk from the probabilistic risk analysis.

It should be noted that although the case study is a RB derived from a single typical building, the financial risk results can also be interpreted from the perspective of a RB representing a cluster of buildings in UBEM. As shown from the deterministic risk results for the medium and, to a lesser extent, the high ambition levels, if one considers a cluster where each building observation is characterised only by the mean parameter values for the envelope and equipment in the analysis, the risk results could be overoptimistic and misleading for a random building observation within the building stock cluster under study, given that the robust financial risk defined by Equation 5.3 is ignored.

The case study results above therefore indicate that a deterministic risk assessment is prone to provide an over-optimistic financial feasibility outcome. Thus, performing only a deterministic risk assessment without a probabilistic risk analysis can make mandating minimum EP requirements to higher ambition levels, such as the medium or high versus low NZEB EP benchmark for the RB case study, a natural choice for the entire building stock to maximise reductions in GHG emissions. However, as shown from the probabilistic risk analysis, mandating to these higher ambition benchmarks without providing financial support can negatively impact individual buildings with unsustainable EP and unrealistic benchmarks that are counterproductive in the long term [168]. This outcome may decrease investors' faith in the policy-making procedure as well as the overall desired outcomes of the energy renovation of the building stock under consideration. Moreover, this would go against the general spirit of the EPBD that energy efficiency measures need to be financially feasible.

The case study results also demonstrate the economic law of diminishing marginal utility for the energy renovation of the building stock, as highlighted by the EC [365]. The low level of EP ambition in the RB case study addresses the low-hanging fruit, which is shown in Table 5.6 to provide more than 70 % of the EP improvements achievable by the highest NZEB EP benchmark and is economically feasible for all financial risk scenarios. Making such results transparent to investors and ESCOs for different building stocks provides them with a better assurance of the financial and energy savings benefits of performing energy renovation, thus addressing the uncertainty barrier and triggering energy renovation. Although this does not undermine the importance of focusing on deep energy renovation, as highlighted in the EU energy renovation wave [4], renovation as a minimum to ambition levels that address low-hanging fruit is critical for MS to meet the carbon neutrality goals for 2050, as this renovation provides the highest potential for EP improvements in building stock.

For mandating higher EP ambition levels to trigger deeper energy renovation, a probabilistic risk analysis also provides the appropriate framework to objectively quantify the necessary financial support measures to trigger energy renovation. This quantification is critical, as the lack of appropriate financial incentives for commercial buildings was found by the EC to be a relevant barrier to energy renovation [4]. More specifically, within this framework, a customised financial incentive value can be attributed to a building based on the recommendation of a certified EPC assessor or an approved energy auditor and with a maximum incentive threshold equal to the robust risk value for a given ambition level. The total financial incentive can still be budgeted by MS using the deterministic risk calculated for each level of ambition and identifying the number of buildings to be targeted. This financial support can then be coupled with a time-bound tightening approach to higher EP ambition levels, as discussed in Section 5.2.1, with the financial support progressively reduced within this long-term framework. Such long-term EP targets and a progressive reduction in financial incentives trigger an improvement in the learning rate [366] to achieve a self-sustainable framework for investors that continuously improves the EP of building stocks for a sustainable renovation path with minimal financial incentives.

Finally, the above probabilistic risk analysis framework allows policy makers to quantify the impact of wide calibration parameter posterior distributions in the decision-making process of defining NZEB EP benchmarks and when quantifying financial incentive requirements. The narrowing of the posterior calibrated parameter distributions results in less uncertainty in the probabilistic risk analysis step that consequently allows the definition of NZEB EP more targeted benchmarks and financial incentives for effective and more ambitious policy making. The need for narrower posterior calibration parameter distributions will automatically trigger policy makers to gather more data and define more informative priors in the Bayesian calibration process. Alternatively, a more refined RB clustering approach can be established to better handle the diversity of heterogeneous building stocks. The Bayesian calibration approach coupled with a probabilistic risk analysis framework in the proposed EPBD cost-optimal method therefore has the advantage of allowing for a continuous and progressive learning process in policy making as discussed in Section 2.6.1.

5.4 | Comparison of results with the 'deterministic' asset rating NCM methodology for the RB case study

For the RB case study, this chapter will compare the NZEB EP benchmarks and financial risk results for the year 2018_10 from the previous section (which were derived using the proposed cost-optimal approach detailed in Section 2.5), with the results obtained using the current and 'deterministic' EPBD cost-optimal approach. The current cost-optimal approach is described in Section 2.2.1. The SBEM-MT software [346] is used as a building energy modelling tool to perform the 'deterministic' cost-optimal approach for this study, as it is the asset rating NCM for Malta. SBEM-MT was also used to carry out the 2018 cost-optimal studies for non-residential buildings [56]. Unlike EnergyPlus, a fully dynamic simulation tool, SBEM-MT uses the ISO 13790 [173] monthly quasi-steady state calculation method, as explained by the author in Gatt [228], to evaluate annual energy use for space heating and cooling.

The geometry and envelope construction of Model D was first replicated in the SBEM-MT software to enable the above-mentioned comparison between the two approaches. Given that NCM for Malta is based on an asset rating approach, SBEM-MT operates under standard conditions, and all occupancy and equipment schedules, including comfort and IAQ parameter set points, are fixed and could not be changed. Furthermore, the software does not allow the modeller to customise the equipment plug-load parameters.

To provide a comprehensive comparative analysis of the results achieved from the proposed EPBD cost-optimal approach with the current approach, a SA on the impact of the SBEM-MT input parameter values on the NZEB EP benchmarking outcome was carried out by defining two RB SBEM-MT models having the HVAC and DHW equipment parameters characterised as follows:

1. **Asset SBEM-MT (mean_calib_par) model** : This model is characterised with the VRF space cooling and heating COP, the DHW boiler efficiency, and the fan ventilation pressure rise having the mean value of the calibration parameters posterior distributions summarised in Table 4.10 and Table 4.14 for DHW and electricity end-uses, respectively. This SBEM-MT model allows direct comparison with the calibrated RB EnergyPlus (composed of Model D and the DHW building physics models) model used to derive the NZEB EP benchmarks in Section 5.3.2.

2. **Asset SBEM-MT (datasheet_par) model** : This model is characterised as the above '*Asset SBEM-MT (mean_calib_par) model*' but with a space heating and cooling COP of 3.8 and 4.42, respectively. These reflect the seasonal COP values found in the manufacturer's data sheet for this case study and, in the absence of a calibration exercise with metered EP data, are generally deemed to be the most appropriate values to characterise the energy models.

For both of these models²⁰, the NZEB EP benchmarking process, as detailed in Section 5.2.1, was performed in Python using the '*SBEM cost-optimal python note book*' found in the GitHub repository²¹. The same ECMs and EN 15459 [54] global LCC parameters were applied, as defined in Section 5.3.2.1 and Section 5.3.2.2 respectively, for the RB case study. It should be noted that the only difference in the input parameters of the benchmarking process was specifically for the '*Asset SBEM-MT (datasheet_par)*' model. In this model, active measure MA1 described in Table 5.3 was characterised by the initial COP parameter values of 3.8 and 4.42 for space heating and cooling, respectively, as discussed above, and by the final parameters having COP values of 4.2 and 6.8 for space heating and cooling, respectively. These final parameter values reflect the high efficiency seasonal values for space heating and cooling used in the cost-optimal studies for Malta [56]²² and assure consistency with the technical documentation approach used to characterise the '*Asset SBEM-MT (datasheet_par)*' model.

As shown in Table 5.8, the primary energy consumption of the calibrated model for the reference scenario matches the annual operational primary energy consumption with a discrepancy or energy performance gap of only 0.3 %, while the SBEM models overestimate the energy consumption with an EP gap greater than 35 %, specifically 37.5 % and 49.3 % for the '*Asset SBEM-MT (datasheet_par)*' and '*Asset SBEM-MT (mean_calib_par)*' models respectively.

²⁰SBEM-MT energy models for the RB case study that calculate the energy demand (i.e. the models are defined with a COP of 1 for space heating and cooling) are available in the GitHub Repository folder '*Ch 5 SBEM analysis*' sub-folder '*SBEM models COPs of 1*' for all the considered passive combination of measures. The full parametric EP analysis involving the 64 COMs was enabled by using the results from this energy demand analysis and converting the energy demand to end-use energy consumption by varying the COP of the space cooling and space heating systems for each COM under consideration using Microsoft Excel file '*ASSET_Cost_opt_sheets_for_Python_input*' found in sub-folder '*SBEM COMS EP analysis*'. Refer to Appendix B for a detailed description of all files and folders found in the GitHub Repository.

²¹Refer to GitHub repository folder '*Ch 5 SBEM analysis*' sub-section '*Python cost-opt analysis*'.

²²The high efficiency seasonal values used in the cost-optimal studies for Malta were chosen instead of the minimum compliance efficiency requirements found in European Ecodesign regulation [367]. The reason being that the initial parameter COP values of 3.8 and 4.42 for space heating and cooling in the Asset SBEM-MT (datasheet_par) model are already almost in compliance with the seasonal efficiency COP and Energy Efficiency Ratio (EER) requirements of 3.8 and 4.6 for space heating and cooling in the European Ecodesign regulation [367].

Table 5.8: Comparison of the primary energy consumption for the 'reference scenario' and the resulting % EP gap for the RB energy models under study

RB model	Reference scenario primary energy consumption ($kWh.m^2.yr^{-1}$)	% energy performance gap
Calibrated EnergyPlus model	348	-0.29
Asset SBEM-MT (mean_calib_par)	521	49.28
Asset SBEM-MT (datasheet_par)	480	37.54

This EP gap resulting from the asset rating EPC software is consistent with the local and foreign studies reviewed in Chapter 2. Thus, a detailed investigation of why the EP gap occurs for Malta, specifically concerning the SBEM-MT software, is beyond the scope of this thesis, and this analysis is detailed in Vassallo [24]. However, similar to the result of this case study, Vassallo [24] also reported large EP gaps of up to 60 %. Furthermore, an evaluation of the accuracy of the resulting energy end-uses of SBEM-MT compared to EnergyPlus for individual buildings has already been carried out in Bartolo [368] and Mallia [369] for non-residential buildings and is also not within the scope of this thesis. However, the results of these two studies indicate that the SBEM-MT software is prone to overestimate the annual energy consumption for space heating and cooling compared to EnergyPlus.

To allow a better evaluation of the EP benchmarking results, the analysis required for the case study is simply a comparison of the resulting annual site energy end-use consumption for the reference scenario. The results of this analysis are shown in Figure 5.14 for the three RB models. From Figure 5.14, it can be seen that the largest discrepancy is for DHW, which is more than 400 % higher for SBEM-mt models. The reason is that SBEM-mt mostly follows the United Kingdom (UK) NCM schedules found in the DesignBuilder software that consider a 100 % hotel occupancy for all months and a 60 % higher DHW consumption per guest night compared to the calibrated EnergyPlus model. Furthermore, SBEM-mt clearly underestimates the auxiliary energy required to drive the mechanical ventilation fans compared to the calibrated model and does not account for the LPG consumption for the cooking equipment. In addition, the energy consumption of the artificial lighting end-use is higher for SBEM-MT models, despite not accounting for exterior lighting.

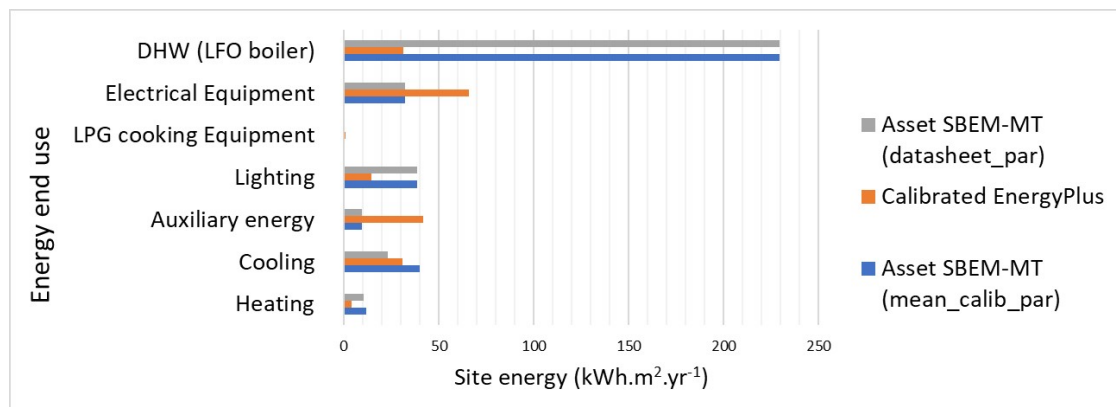


Figure 5.14: 'Reference scenario' site energy end-use consumption breakdown comparison between the RB energy models under study

On the other hand, the electrical equipment consumption is higher for the calibrated EnergyPlus model since the RO system was included and modelled as an electrical plug load and the food preparation areas were characterised with a higher calibrated plug load power density than the UK NCM values reflecting the findings of local hotel energy audits.

These differences in energy end-uses between the SBEM-MT and the EnergyPlus calibrated model result in a significant discrepancy in the EP benchmarks and the corresponding ECMs for each NZEB EP ambition level, as shown in Table 5.9 and Figure 5.15. The corresponding cost-optimal plots that derive these benchmarks for both SBEM-mt models are shown in the '*SBEM cost-optimal python note book*' found in the GitHub repository.

Table 5.9: Comparison of the resulting NZEB EP benchmarks and corresponding COMs for the RB energy models under study

RB energy model	NZEB EP benchmark level	Primary EP benchmark ($kWh.m^2.yr^{-1}$)	% EP improvement from reference scenario	Passive ECMs			Active ECMs		
				MP1	MP2	MP3	MA1	MA2	MA3
Calibrated EnergyPlus (Model D & DHW model)	Reference	348							
	Low	284	18.4				x	x	
	Medium	273	21.6				x	x	x
	High	268	23	x	x		x	x	x
	Highest	266	23.6	x	x	x	x	x	x
Asset SBEM-MT (mean_calib_par)	Reference	521							
	Low	228	56.3				x	x	
	Medium	215	58.7	x			x	x	
	High	204	60.9	x	x	x	x	x	x
	Highest	204	60.9	x	x	x	x	x	x
Asset SBEM-MT (datasheet_par)	Reference	480							
	Low	237	50.6					x	
	Medium	210	56.3	x			x	x	
	High	201	58.1	x	x	x	x	x	x
	Highest	201	58.1	x	x	x	x	x	x

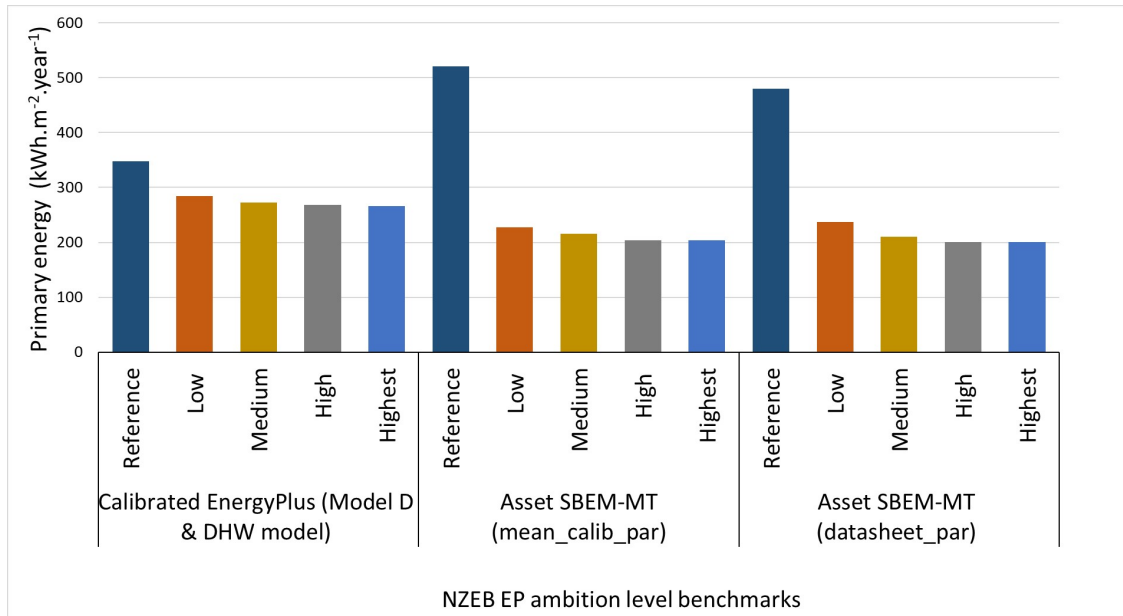


Figure 5.15: Comparison of NZEB EP benchmarks obtained for the different RB energy models under study

Given the above difference in the energy consumption end-uses, most notably the overestimation for the DHW energy end-use consumption predicted by the SBEM-MT models, both SBEM-MT models provide a much more optimistic scenario in the potential EP improvements that are achievable for each NZEB EP benchmark. More specifically, the maximum potential in EP improvements is 60.9 % for the SBEM-MT models versus 23.6 % for the calibrated EnergyPlus model. Furthermore, the resulting COMs corresponding to each ambition NZEB EP benchmark are different between the EnergyPlus and SBEM-MT models. For the SBEM-MT models, ECM MA3 only appears first at the high EP ambition level instead of the medium EP ambition level as for the calibrated EnergyPlus model, mainly due to the underestimated annual auxiliary energy consumption in SBEM-MT. Similarly, passive ECM MP3 appears both at the high and highest EP ambition levels versus only at the highest EP ambition level for the calibrated EnergyPlus model.

It should be noted that although the resulting NZEB EP benchmarks defined in $kWh.m^{-2}.yr^{-1}$ are fairly consistent between the two SBEM-MT models, some discrepancies can be observed from Table 5.9 in the resulting COMs corresponding to each ambition NZEB EP. More specifically, active ECM MA1 does not appear for the '*Asset SBEM-MT (datasheet_par)*' model at the lower ambition benchmark level as opposed to the other models, because, as shown in Figure 5.14, its lower annual energy end-use consumption for space cooling results in a reduced potential for energy savings when implementing ECM MA1.

The deterministic global LCC financial risk results were also calculated, as discussed in Section 5.2.1, for the SBEM-MT models directly from the resulting cost-optimal plots using the '*SBEM cost-optimal python note book*'. These results are compared directly to the deterministic and robust global LCC financial risk result obtained for the calibrated EnergyPlus RB model discussed in the previous section, as shown in Figure 5.16. It is evident that both SBEM-MT models portray a very optimistic scenario for financial risk in contrast to the calibrated EnergyPlus model. From the analysis, it is shown that for the SBEM-MT models, even upgrading the RB to the highest ambition EP level is still financially feasible to the private investor, irrespective of the financial sensitivity scenario under consideration.

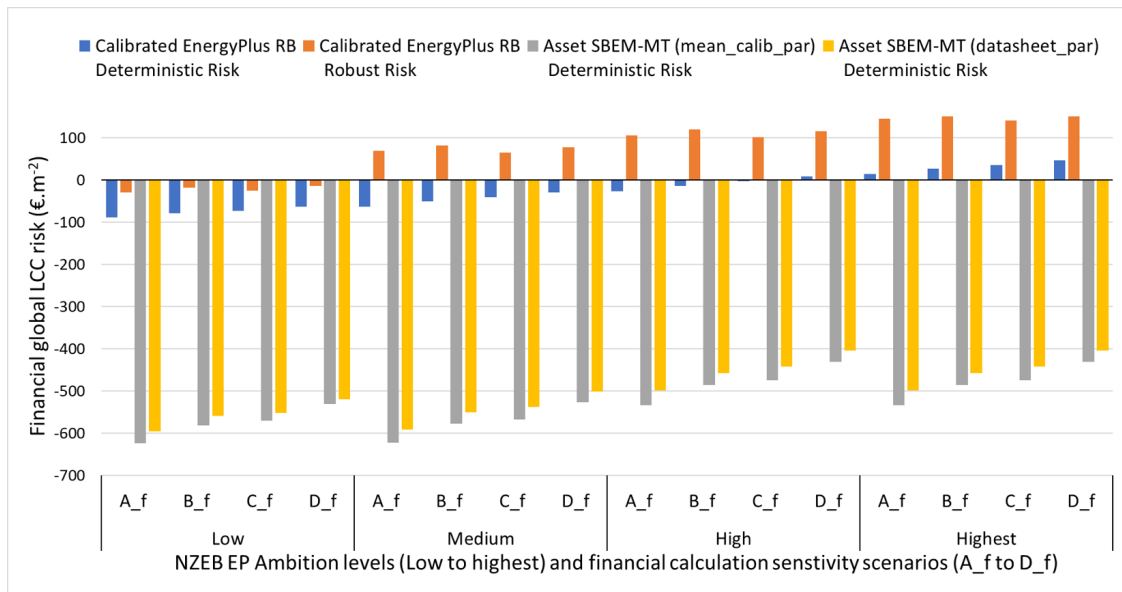


Figure 5.16: Comparison of the resulting financial global LCC risk for the different RB energy models under study for each NZEB EP ambition level and financial perspective scenario. For the calibrated RB EnergyPlus model, both robust and deterministic risk are evaluated, while only deterministic is considered for the Asset SBEM-MT models.

Clearly, the over-optimistic results for financial feasibility of SBEM-MT are not credible. For example, one can observe from Figure 5.16 that both SBEM-MT models show that upgrading to the highest EP ambition level is up to four times more financially feasible than when upgrading the calibrated Energy Plus RB model to the low ambition level using the more optimistic deterministic financial risk scenario. Such a discrepancy cannot be underestimated and therefore it is not wise to commit to maximum renovation measures based on the SBEM-MT results, when the calibrated Energy Plus RB model results demonstrate a significant financial risk.

Therefore, using uncalibrated RB models with ECMs tend to produce optimistic EP and carbon emission savings, as well as unrealistic financial feasibility, which on the long-run could result in loss of investment and reduced confidence in the energy models. Consequently, a change in direction will need to be implemented by using calibrated models that take into consideration not only calibration with actual energy consumption for the reference building for each category under consideration, but also the range of probabilistic risk encountered in energy savings and costings.

5.5 | Conclusion

This chapter established a comprehensive framework to develop, apply, and successfully validate the final two steps of the proposed EPBD cost-optimal method detailed in Chapter 2, Section 2.5, namely to derive NZEB EP benchmarks from the global LCC cost-optimal analysis in step 5, followed by a probabilistic risk analysis for the derived NZEB EP benchmarks in the final step, step 6.

Step 5 has developed and validated an innovative and objective approach to defining NZEB EP benchmarks according to four different ordinal levels of EP ambition. To date, there are no established and objective criteria in the EPBD to facilitate a step-change pathway towards the decarbonisation of buildings. Moreover, this approach provides a harmonised approach to define NZEB benchmarks and can be easily implemented by MS, given that the same mandatory global LCC calculations are used in the current EPBD cost-optimal method.

For step 6, a probabilistic risk analysis approach has been developed and validated using posterior calibrated parameter distributions. The outcome has been demonstrated to more realistically quantify financial risk for each identified NZEB EP ambition level benchmark, thus enabling private investors as well as policy makers to take informed decisions on the pathway towards decarbonisation.

The approach has been demonstrated to significantly bring a step-change in the current deterministic financial feasibility analysis of the EPBD cost-optimal method by adding transparency to any potential financial risks associated with the implementation of ECMs for different energy efficiency ambition levels leading progressively to full decarbonisation of buildings.

The proposed method has credibly demonstrated the need for calibrating NCM software(s) with operational EP data and using probabilistic approaches to integrate risks in the decision-making process for EPBD cost-optimal analysis and subsequent policy making including financial support decisions. Only then will the prevailing reported EP gap be minimised, and financial risks associated with acting on misleading optimistic EP results be avoided.

All in all, the proposed approach contributes towards fulfilling some of the most pressing requirements of the EPBD, including transparency in cost-optimal calculations through the inclusion of risk and uncertainty analysis, harmonisation of '*cross-national*' benchmarks among MS through objective and calibrated reference buildings and the establishment of more targeted EP benchmarks and policies through a continuous building stock learning process for policy makers.

Conclusions

This chapter concludes the thesis by synthesising the key findings in relation to the research aim, objectives, and questions and by discussing the value and contribution of these findings to the fields of energy policy and building stock energy modelling. The chapter also reviews the limitations of the study and proposes opportunities for future research.

6.1 | Achieved Aim, Objectives and Key Research Findings

This research aimed to propose and validate an innovative approach to the EPBD cost-optimal method to allow policy makers to optimally handle the diversity and uncertainties of the building stock when deriving EP benchmarks for heterogeneous multi-functional building stocks under different defined ambition levels of EP.

After reviewing the methodological similarities and the resulting limitations of conventional UBEM studies and the current EPBD cost-optimal method, several limitations were identified, which were demonstrated to ignore uncertainties and diversities of the parameters in RB energy modelling that impact the EP of the building stock. These limitations make the current EPBD cost-optimal method prone to optimistic savings and unrealistically attractive economic benefits that cannot be achieved when buildings adopt them. Consequently, the goal of significantly reducing carbon dioxide emissions from renovated buildings by 2030 and full decarbonisation by 2050 may not be met.

Following a deep analysis of the state-of-the-art UBEM literature to handle these limitations, a clear and innovative EPBD cost-optimal approach has been proposed, as shown in Chapter 2, Section 2.5, Figure 2.6, to integrate state-of-the-art UBEM tech-

niques employing '*probabilistic Bayesian calibrated RBs*' into the current EPBD. This framework was hypothesised to better address the diversity and uncertainties of the buildings' different parameters compared to the current EPBD cost-optimal approach, ultimately leading to the establishment of more robust policy measures and strategies that trigger energy renovation and facilitate the transition of buildings to NZEB.

Every step of the proposed approach, shown in Figure 2.6, which can be applied to any building stock irrespective of its size and diversity, was further developed and successfully applied and validated for a small, multi-functional and heterogeneous building stock case study, which was the 5-star hotel building stock in Malta.

Consequently, the research objectives were successfully met for the development of the proposed EPBD cost-optimal approach, to enable its application to multi-functional, heterogeneous building stocks, as follows:

- The development and application of a machine learning approach to define RBs for '*small*' ($X \gg N$)¹ multi-functional, heterogeneous building stocks and the employment of the novel cost-optimal approach to a defined RB.
- The investigation and statistical validation of innovative techniques to reduce the computational expense of the novel cost-optimal approach without loss in accuracy.
- The development of a harmonised and ordinal scale approach to define the NZEB EP ambition levels and the identification of an approach to propagate the EP and financial uncertainty for each defined ambition level for a RB under study ultimately leading to robust results that assure solid basis for energy renovation support policies.
- A comparison of the novel cost-optimal approach with the current deterministic approach and the establishment of the strengths and limitations of each approach.

As a prelude to the final conclusions of the thesis, this section will first synthesize the research findings that address the above objectives.

¹For the scope of this research, a '*small*' building stock is one where the number of explanatory variables '*X*' impacting energy performance is greater than the number of building observations '*N*' in a population.

- An approach to define RBs for '*small*' ($X \gg N$), multi-functional and heterogeneous building stocks has not been adequately addressed in the literature. The current and generic approach to define RBs, detailed in Section 2.2.3.1, if not further developed, is more applicable to the larger and less diverse building stocks, such as residential and office buildings. This research grouped the challenges posed by '*small*', multi-functional and heterogeneous building stocks into two categories. These are building energy modelling challenges to collect information and represent the various activities and functionalities for these building stocks, as well as the high-dimensional data processing challenges inherent with these specific building stocks due to their diverse activities and the limited number of building observations.

- The objective and innovative approach developed in Chapter 3 successfully addresses the above research gaps by applying multiple methodological and machine learning concepts to objectively tackle the above challenges and provide a comprehensive approach to define RBs specifically for these building stocks. The approach was tested successfully on the five-star hotel building stock case study, whereby through appropriate statistical approaches, the buildings were comprehensively clustered to define and fully characterise RBs, while taking into account the diversity of their services (functionality) offered by these buildings in the final clustering solution. The approach was further validated for the case study to be more comprehensive to defining RBs when compared to simplified clustering approaches that perform clustering only on easily obtainable bench-marking variables or directly on operational metered energy consumption. This is because the strength of this approach lies in its ability to uncover building characteristics and functionalities to successfully characterise a heterogeneous physics building RB energy model.

The key innovations are summarised below:

1. The application of multiple supervised and non-supervised machine-learning techniques to successfully and systematically reduce and combine building feature data with individual metered energy consumption to address the high-dimensional data processing challenges posed by such buildings stocks. The use of individual metered energy consumption data overcomes a limitation of national typology methodologies employed, for example, by Mata et al. [202] and the TABULA project [75, 203] that characterise RBs using only

- building feature data without considering the relative importance of different building characteristics on metered energy consumption.
2. The use of additional features to characterise RBs that complement the four features presented by Torcellini et al. [204] and Corgnati et al. [26], which includes a specific '*functionality feature*' to ensure that the diversity of the services offered by the individual buildings in a stock is better represented by the final RB clustering solution.
 3. The investigation of multiple clustering solutions for each feature, to make RB clustering solution less sensitive to the chosen clustering approach.
- The proposed EPBD cost-optimal approach which applies '*probabilistic Bayesian calibrated RBs*' is significantly more computationally intensive than the current EPBD cost-optimal approach due to the additional requirements to perform multiple simulation runs from the building physics model. Simulation runs are required for SA to identify the calibration parameters for Bayesian calibration and to train the meta-model for Bayesian calibration, as discussed in Section 4.2. Once the model is calibrated, further simulation runs are required to perform the probabilistic risk analysis developed in Section 5.2.2.
 - Once RBs are defined, this thesis's developed '*reference zone*' approach is a computationally efficient and innovative approach for performing Bayesian calibration of RB energy models by replacing computationally intensive and full-space multi-functional RB EnergyPlus (Physics) models with reduced-space RB EnergyPlus models to improve simulation run-time. The approach constructs an EnergyPlus model from a defined number of '*reference zones*' using multipliers. '*Reference zones*' are simple EnergyPlus geometric representations or building blocks, each modelling a functional unit of a sub-activity in the building. The reduced-space model improved the simulation run-time computation efficiency by 4,000 % over the full-space model for the RB case study. Furthermore, the '*reference zone*' approach for the RB case study also produced statistically accurate monthly outputs to successfully calibrate RB models in compliance with the CVRMSE and NMBE thresholds provided in ASHRAE [1, 2] and to reduce the uncertainty of the defined prior parameters satisfactorily.
 - The thesis has highlighted the challenges for objectively deriving NZEB EP benchmarks even when considering the current '*deterministic*' EPBD cost-optimal method, mainly because the term '*Nearly*' in NZEB is not a quantifiable metric, and the European Commission (EC) does not provide objective criteria for defining NZEB

EP benchmarks. This challenge was successfully addressed by developing an objective approach that defines NZEB EP benchmarks for the EPBD cost-optimal method according to four distinct and ordinal levels of EP ambition, that directly employ the same mandatory global LCC calculations used in the current EPBD cost-optimal method. The approach was successfully programmed in Python, applied to a calibrated hotel RB case study, and validated to provide well-distinct EP benchmarks, whereby the low level of EP ambition tackles the low-hanging fruit.

■ In a nutshell, the proposed EPBD cost-optimal approach developed in this research has successfully achieved the following advances:

1. The use of '*probabilistic Bayesian calibrated RBs*' in the proposed approach versus '*deterministic RBs*' employed in the current cost-optimal approach allows policy makers to express their initial beliefs of the building parameters diversities and uncertainties in the RB energy model. This is done by defining uncertain parameters as '*prior*' probability distributions and to update them to narrower '*posterior*' distributions via a Bayesian approach using metered EP data.
2. The probabilistic risk analysis enabled by propagating uncertainties from the resulting calibration parameter '*posterior*' distributions allows policy makers to visualise and statistically quantify the financial risk faced by the private investor when upgrading each defined NZEB EP ambition level.
3. The probabilistic risk analysis is critical as findings from the hotel RB case study revealed that the application of the current deterministic financial feasibility analysis in the EPBD cost-optimal approach can provide over-optimistic outcomes even for the higher more costly NZEB EP ambition levels. Such outcomes make the current deterministic approach highly prone to hiding financial risks for the private investor in the cost-optimal analysis, which can lead to the establishment of unsustainable and counterproductive NZEB EP benchmarks and erroneously nullify the need for any financial support requirements to trigger more aggressive energy renovation.
4. The developed equations as derived from the developed probabilistic risk analysis provides an objective approach to allow policy makers to calculate the maximum global LCC financial support that should be considered for a '*random*' individual building within a cluster of buildings, represented by the RB under study, to upgrade it to a defined NZEB EP ambition level.

5. The Bayesian calibrated approach successfully allows RB energy models to be defined with a minimal EP gap. This was successfully demonstrated when the EP gap resulted to be less than 1 % for the hotel RB case study, as compared to more than 30 % when the asset rating NCM methodology software SBEM was used. Clearly, the uncalibrated NCM software could not deliver realistic EP benchmarks. Therefore, the calibrated methodology approach provide an objective guidance to policy makers, increases confidence in expected energy efficiency financial benefits and accelerates the building renovation wave.
6. Aggregating the entire building stock EP probabilistically from the calibrated RBs allows better validation of the choice of RBs representing the building stock under study. This is done by statistically comparing the resulting aggregated EP distribution from the RBs models with the metered energy consumption distribution of individual buildings in the buiding stock under study.

Consequently, the hypothesis developed in this work can be accepted and it can be concluded that an EPBD cost-optimal framework that employs this innovative approach of '*Bayesian calibrated RBs*' better handles the uncertainties and diversities of the building stock and will potentially lead to the establishment of more robust policy measures and strategies that accelerate energy renovation and facilitate the transition of buildings to NZEB.

6.2 | Research value and contribution

This section describes the value of the conducted research and its contribution to the fields of EU energy policy and building stock energy modelling.

6.2.1 | Research value and contribution to EU energy policy

The value of research and its contribution to the field of EU energy policy can be summarised as follows.

- This research has EU-wide significance by objectively demonstrating the main limitations of the current EPBD cost-optimal methodology and proposing an innovative EPBD cost-optimal approach that facilitates the definition of more robust policy measures and strategies to accelerate energy renovation and the transition

of building stocks to NZEB to meet the 2050 carbon neutrality [3] and Renovation Wave [4] goals.

- The research has potential to contribute to the establishment of a '*stronger long-term renovation strategy*', which is one of the main goals of the 2018 EPBD and the EU Green deal [3]. This strategy is better achieved for the proposed cost-optimal method EPBD as follows:

1. Handling uncertainties and building stock diversities when deriving NZEB measures and benchmarks to achieve more realistic EP benchmarks and EP improvements for a building stock under study, as well as a more accurate quantification of the financial support policies required for energy renovation.
2. Providing a transparent approach to more accurately quantify the financial risk of renovation investment for private investors and ESCOs when upgrading to the most beneficial NZEB EP level. This transparency triggers energy renovation by directly addressing financial uncertainty, one of the main barriers to energy renovation [42, 43, 44].
3. Increasing options for achieving high energy efficiency by objectively defining multiple NZEB EP benchmarks according to different EP ambition levels for the building stock under study instead of a single NZEB benchmark. This also facilitates a progressive approach [347] to NZEB EP benchmarking that prepares the market to adapt with time to more stringent EP requirements to achieve the long-term decarbonisation objectives [348]. The developed NZEB EP benchmarking approach can easily be incorporated into Building Renovation passports to allow a road map for staged renovation by progressively allowing buildings to update to each NZEB ambition level. Staged renovation within the framework of Building Renovation passports is promoted in the proposed EPBD [370] as one of the solutions to address the high upfront costs of renovation.
4. The financial support quantified from the developed probabilistic risk analysis can also be coupled with this time-bound tightening approach to higher EP ambition levels, with progressively diminishing fiscal support within this long-term framework, thus making better use of available funds in a sustainable manner. Such long-term EP targets and a progressive reduction in financial incentives trigger an improvement in the learning rate and energy

efficiency of different technologies to achieve a self-sustainable framework for investors.

5. The NZEB EP benchmarking approach proposed in this study can also allow the EC to more objectively define the concept of '*deep renovation*', which is being strongly advocated in the EU energy renovation wave [4] but has not yet been appropriately defined [370]. This objectivity is achievable by coupling the achievement of '*deep renovation*' with the high or highest NZEB EP benchmarking levels.
 6. The probabilistic Bayesian calibration and risk analysis approach facilitate more focused EP benchmarks and policies by establishing a continuous learning process of building stocks with diminishing uncertainties and more refined RBs to limit variability in EUI and financial risk workings.
- The proposed EPBD cost-optimal approach, in conjunction with the new EPB standards, provides a better framework for establishing and defining cross-national comparable EP benchmarks between MS as follows:
 1. The calibration process defines EP benchmarks that more closely reflect the operational EP of the buildings.
 2. The NZEB EP benchmarking approach developed in this study provides a standardised approach to define NZEB benchmarks directly from the resulting cost-optimal plots.

6.2.2 | Research value and contribution to the field of building stock energy modelling

The value of the research and its contribution to the field of building stock energy modelling can be summarised as follows:

- The machine-learning and innovative method to define RB energy models for multi-functional and heterogeneous '*small*' building stocks provides researchers with a tangible methodology to increase knowledge on the EP of these building stocks, which have so far received far less attention than residential buildings and other less diverse building stocks.
- The developed '*reference zone*' building energy modelling concept provides an effective solution to significantly reduce the computational time required for processing iterative Bayesian calibration of multi-functional and heterogeneous RBs,

and facilitates the incorporation of Bayesian calibration into building energy modelling in practical terms.

- The scalability and modularity of 'reference zone' approach to define RB models has the potential to allow the building stock to be more efficiently modelled using a bottom-up technique without the need to define full-space RB energy models (in GIS). This is possible once representative 'reference zones' for different activities and sub-activities are statistically validated for a sample of the building stock under study. Each individual building in the stock can then theoretically be custom-modelled using a reduced-space-order building physics model to improve computational efficiency while allowing the definition of variable functionalities that are synonymous with heterogeneous building stocks.

6.3 | Research Limitations

The findings of this study should be seen in light of the following limitations.

- The methodology to define RBs for 'small' ($X \gg N$), multi-functional, and heterogeneous building stocks was applied and validated using only a single building stock case study. This limitation resulted from the fact that no EN standard defines the requirements of a building renovation passport. Thus, there are currently no requirements for such heterogeneous buildings to keep and update building envelope and energy systems data, energy consumption, and other relevant parameters required for this research. As a result, a laborious exercise had to be carried out to comprehensively collect the required data, which is time-consuming. This exercise involved multiple site visits to validate plans and measure different dimensions, long meetings with the management of each building to understand the processes used and their inter-connectivity, reviewing, and validating existing energy audits or performing actual energy audits, as well as collecting electricity, fuel and water consumption data manually for three years.
- The proposed EPBD cost-optimal approach was applied using only one RB case study representing one building observation. This limitation resulted from time constraints and the lack of computational resources required to set-up and perform multiple simulation runs from the EnergyPlus/JEPlus models and develop the required Python programs for Bayesian calibration and the EPBD cost-optimal analysis, including for the probabilistic risk analysis.

- Based on the available knowledge of the RB case study and the available resolution of operational energy consumption data, Bayesian calibration was only performed with calibration parameters defined using flat priors and calibration metered energy consumption of the whole building.
- The '*reference zone*' approach was applied and validated for only one multi-functional building observation operating under one climate and only for monthly resolution energy end-use fuel data. This limitation resulted from time constraints and lack of computational resources required to conceptualise and formalise the '*reference zone*' approach concept, by constructing and running a detailed full-space building energy model and comparing its outcomes to the simplified '*reference zone*' model.

6.4 | Recommendations for Future Research

Based on the research findings and limitations of this thesis, the fields of building stock modelling and EU energy policy would benefit from the following additional research to further analyse and substantiate the proposed EPBD approach and the corresponding methodologies, including concepts developed in this research.

- Applying and testing the methodology to define RBs for '*small*' ($X \gg N$), multi-functional, and heterogeneous building stocks to other building stocks with a larger population, to better understand how the resulting cluster-to-observation ratio varies as the observations and building stock diversity change.
- Applying the proposed EPBD cost-optimal method to all other derived hotel RBs in Chapter 3 to further analyse the impact of multiple observations on the resulting benchmarks and financial risk analysis. The analysis can compare the outcomes of representing the multiple building observation in each derived cluster as follows²:
 1. Using the median typical '*real*' building as a RB in each derived cluster and defining the building envelope and equipment parameters probabilistically
 2. Constructing a fictitious '*archetype*' RB which represents the average or median characteristics in terms of functionality and geometry of the building

²For configurations 1 to 3 below, Bayesian calibration can be carried out using only metered energy consumption data of the building representing each cluster or alternatively by calibrating the chosen building per cluster multiple times using individual metered data of the other building observations falling under the same cluster. The posterior calibrated parameter distributions for each calibration exercise per cluster can then be merged. The resulting EUI distributions for each calibration approach can also be compared using statistical tests as performed in [74, 128].

- stock cluster and defining the building envelope and equipment parameters probabilistically.
3. Using the the typical '*real*' RB or fictitious '*archetype*' RB described in No. 2 above but constructed using the '*reference zone*' approach rather than a full-space energy model to improve computational speed.
 4. Defining the building envelope and equipment parameters probabilistically and constructing full-space energy models for each building, potentially testing different zoning configurations, to calibrate each building individually.
 5. Defining the building envelope and equipment parameters probabilistically and using energy models constructed based on the '*reference zone*' approach for each building to calibrate each building individually.
- Performing the proposed approach on all the derived RBs that represent a whole building stock under study allows one to understand whether any refinements to the RB clustering solution and the '*prior*' calibration parameter definitions need to be devised to derive narrow posterior calibration parameter distributions leading to more specific NZEB EP benchmarks and financial support requirements.
 - Applying and testing the '*reference zone*' approach concept to include other configurations for different building types, climates, and finer resolution data to identify whether the '*reference zone*' approach has the same potential in replicating the data from full-space models under these different scenarios. Potentially, one can also establish specific guidelines for constructing representative '*reference zones*' in terms of the number of optimal sub-activities and boundary conditions for these different scenarios.
 - Analysing the potential of applying the '*reference zone*' approach concept to define RB models in GIS using a bottom-up approach for improved computational efficiency and to allow the diverse functionalities of individual buildings in a heterogeneous building stock to be better represented. The results of the '*reference zone*' approach can then be compared with the simpler zoning division techniques in UBEM that generally consider single zone models, one zone per floor models, or multi-zone per floor models [186].
 - Performing a SA on the choice of priors, the amount of parameters to be calibrated, and the meta-model choice (potentially also propagating simulation runs from the building physics '*reference zone*' model itself without developing a meta-model in the KOH framework), when calibrating a RB model to study their impact on the

resulting NZEB EP benchmarks and probabilistic risk analysis for the proposed EPBD cost-optimal method. This SA also allows parameter identifiability issues in the Bayesian calibration process to be identified.

- Incorporating higher resolution energy consumption data and potentially sub-metering data to identify the potential to further fine-tune the calibration process and understand the impact of these data on the resulting NZEB EP benchmarks and probabilistic financial risk analysis.
- Identifying and analysing an approach to optimally handle uncertainties and the diversity of other global LCC financial parameters, such as the capital costs of ECMs, in addition to performing only SA on the PD and DR as required by current EPBD.
- Identifying the potential of applying multi-objective genetic algorithms in the proposed cost-optimal analysis to find non-dominated solutions (Pareto front) for the RB model to converge faster to the NZEB EP ambition levels rather than performing a full parameterisation exercise simulating all potential COMs.
- Analysing through multiple calibrated RB case studies how the proposed cost-optimal approach can perform refinements to derived NZEB EP benchmarks and financial risk calculations to ensure compliance with the EN 16798-1 [332] comfort and IAQ set-points requirements.
- Investigating how the proposed cost-optimal approach can facilitate the smartness indicator compliance introduced in Section 2.6.2.3. A potential approach is to mandate minimum EP requirements of the buildings using an operational versus or in combination with an asset-rating approach, given the lower EP gap resulting from the calibrated models. Minimum EP requirements can be derived using the proposed approach using comfort set-points that encourage energy-efficient occupant behaviour and the implementation of smart building energy management systems.

6.5 | Final Remark

This research has provided tangible findings and insight for future upgrading of the EPBD cost-optimal approach. This will significantly address the limitations of the current approach and establish robust policy measures required for the EU to successfully meet its 2050 carbon-neutrality goals. Furthermore, it is only by devising such robust

policy measures that energy renovation can be triggered and sustained, while providing for new job opportunities and investments, thus contributing to the much needed stimulus in the economy and the sustainable regeneration of society following the recent pandemic and political shocks across Europe.

Publications by the author

Peer-reviewed publications directly related to this research

- Gatt, D., Yousif, C., Cellura, M., Camilleri, L., & Guarino, F. (2020). "Assessment of building energy modelling studies to meet the requirements of the new Energy Performance of Buildings Directive". *Renewable and Sustainable Energy Reviews*, 127, 109886. <https://doi.org/10.1016/J.RSER.2020.109886>
- Gatt, D., Yousif, C., Cellura, M., & Camilleri, L. (2018). "An innovative approach to manage uncertainties and stock diversity in the EPBD cost-optimal methodology". *European Journal of Technique*, 8(1), 35–49. <http://dergipark.gov.tr/ejt/issue/39607/467910>

Peer-reviewed publications, book chapters, and conference proceedings related to the fields of building energy modelling, the EPBD cost-optimal method, and NZEB buildings

- Granados-López, D., Gatt, D., Yousif, C., Díez Mediavilla, & M., Alonso-Tristán, C. (2023), "Exploitation of indoor illumination for typical flat dwellings in the Mediterranean area", *Energy Reports*, 9, pp.1473-1489. <https://doi.org/10.1016/j.egy.2022.12.085> [371]
- Gatt, D., Caruana, C., & Yousif, C. (2020). "Building Energy Renovation and Smart Integration of Renewables in a Social Housing Block Toward Nearly-Zero Energy Status". *Frontiers in Energy Research*. <https://doi.org/10.3389/fenrg.2020.560892>
- Gatt, D., & Yousif, C. (2020). "Policy measures addressing nearly zero-energy buildings in the small island state of Malta". In L. Briguglio, J. Byron, S. Moncada, W.

- Veenendaal (Eds.), *Handbook of Governance in Small States* (1st ed.). Routledge. <https://doi.org/10.4324/9780429061356-9>
- Vella, R. C., Martinez, F. J. R., Yousif, C., & Gatt, D. (2020). "A study of thermal comfort in naturally ventilated churches in a Mediterranean climate". *Energy and Buildings*. <https://doi.org/10.1016/j.enbuild.2020.109843>
 - Rey Hernandez, J. M., Yousif, C., Gatt, D., Velasco Gomez, E., San Jose, J., & Rey Martinez, F. J. (2018). "Modelling the long-term effect of climate change on a zero energy and carbon dioxide building through energy efficiency and renewables". *Energy and Buildings*, 172. <https://www.sciencedirect.com/science/article/pii/S0378778817335764>
 - Gatt, D., Yousif, C., Barbara, C., Caruana, T. F., & Degiorgio, M. (2019). "EPBD cost-optimal analysis for non-residential buildings in Malta". SBE19 Malta International Conference, Qawra. <https://www.um.edu.mt/library/oar/handle/123456789/55782>
 - Cutajar, A., Gatt, D., Yousif, C., & Camilleri, L. (2019). "Feasibility study of a heat recovery system in an office building in Malta". SBE19 Malta International Conference, Qawra. <https://www.um.edu.mt/library/oar/handle/123456789/55783>
 - Barbara, F. N., Gatt, D., & Yousif, C. (2019). "Prioritising energy efficiency measures in Maltese restaurants". SBE19 Malta International Conference, Qawra. <https://www.um.edu.mt/library/oar/handle/123456789/55785>
 - Gatt, D., & Yousif, C. (2018). "Interreg Europe ZERO CO2 Project - action plan for Malta to promote near zero CO2 emission buildings". The ESSE '18 Conference, St. Paul's Bay. 8-16. <https://www.um.edu.mt/library/oar/handle/123456789/30539>
 - Gatt, D., & Yousif, C. (2016). "Renovating primary school buildings in Malta to achieve cost-optimal energy performance and comfort levels". 2016 International Sustainable Built Environment Conference (SBE2016) Europe and the Mediterranean Towards a Sustainable Built Environment, Valletta. 453-461. <https://www.um.edu.mt/library/oar/handle/123456789/6611>
 - Gatt, D., & Yousif, C. (2016). "Intelligent Retrofitting of a Primary School Building in Malta," in *Engineering Today* August 2016 Issue 54, Chamber of Engineers, Malta, pp. 18–27. <https://www.um.edu.mt/library/oar/handle/123456789/26131>
 - Gatt, D., & Yousif, C., "Zero CO2 Building - How low can we go: A Case Study of a Small Hotel in Gozo - Malta," in *ISE Conference 2016*, 2016, pp. 30–37. <https://www.um.edu.mt/library/oar/handle/123456789/23300>

GitHub Repository Folders and Files

Introduction

All the building energy model files, JEPlus files, Microsoft Excel files, and Python source code used for this research are found in the following repository link: https://drive.google.com/drive/folders/1S2Y2-TIHlwabHn1zLHHUa8n06GByf_Nd?usp=sharing

This section provide a detailed description of all folders and files in this link, making reference to the Chapter, Section, and Footnote where each folder, file, and source code are used to implement this research.

Chapter 3 Folders and Files

This section provides a detailed description of all folders and files referred to in Chapter 3.

Table B.1: Description of GitHub repository folders and sub-folders for Chapter 3

Section	Footnote	Folder name	Sub-folders	Description
3.4.3	9	Ch 3 5 star hotels RB definition methodology	1. Clustering 2017 Primary energy 2. Clustering 2018 Primary energy 3. Clustering 2019 Primary energy	The sub-folders contains the Python Jupyter notebooks and corresponding characterisation and energy performance data to execute the methodology to define RBs for the hotel-building stock case-study for the years 2017 to 2019 occupancy schedules.

Chapter 4 Folders and Files

This section provides a detailed description of all folders and files referred to in Chapter 4.

Table B.2: Description of GitHub repository folders and sub-folders for Chapter 4

Section	Footnote	Folder name	Sub-folders	Description
4.4.2.1	8	Ch 4 DHW BEM model 2017 to 2019	Not applicable	The folder contains the hotel RB case-study DHW building energy model as DesignBuilder and EnergyPlus idf files for all years i.e. 2017 to 2019 occupancy schedules.
4.4.2.2	9	Ch 4 Electricity 2017 BEM models and ref zone validation	1. Model A 2. Model B 3. Model C 4. Model D (2)	The folders contains the DesignBuilder and corresponding EnergyPlus files for the hotel RB case-study electricity energy end-uses models, Model A and Model D.
4.4.2.2	10	Ch 4 Electricity 2017 BEM models and ref zone validation	Validation	The folder contains Microsoft Excel file '2017 Uncalibrated Model A ASHRAE statistics' that provides NMBE and CVRMSE calibration statistical indicators for Model A.
4.4.2.2	14	Ch 4 Electricity 2017 BEM models and ref zone validation	Model D1 D2 D3 plus Passive	The folder contains DesignBuilder and EnergyPlus files for Models D1 to Model D3 with and without the passive measures in Table 4.8 . The folder also contains the Microsoft Excel file entitled 'Models D1 D2 D3 vs Model A ECMs performance' to perform the statistical analysis in Table 4.8.
4.4.2.2	16	Ch 4 Electricity 2017 BEM models and ref zone validation	Validation	The folder contains Microsoft Excel file 'Models B C D vs Model A ASHRAE calibration validation' to perform the statistical analysis in in Table 4.7.
4.4.3	17	Ch 4 DHW SA	1.SA DHW JEPLUS files and models 2.SA DHW JEPLUS simulation results 3.SA DHW Morris SA Python implementation	The folders contains the JEPlus files to execute the DHW model EnergyPlus simulation runs for the Morris Method and the corresponding results. The Python Jupyter notebook via the SOBOL package constructs the Morris grid of required simulation runs executed in the JEPlus files and calculates the Morris method statistical parameters shown in Figure 4.5.
4.4.3	17	Ch 4 Electricity SA	1. SA Ref Zone Model D2 2. SA Full model Model A	The folders contains the JEPlus files to execute Model A and Model D EnergyPlus simulation runs from the uncertain paramters for the Morris Method and the corresponding results. The Python Jupyter notebooks for Model A and Model D via the SOBOL package constructs the Morris grid of required simulation runs executed in the JEPlus files and calculates the Morris method statistical parameters shown in Table 4.9 and Figure 4.6.
4.4.3.2	19	Ch 4 Electricity SA	SA ASHRAE validation for Model D2 vs Model A	The folder contains Microsoft Excel file 'SA CVRSME and NMBE validation' used to statistically compare the difference in the simulated annual electricity energy end-use output values between Model A and Model D.
4.4.4	21	Ch 4 DHW Bayesian calibration	1. DHW EnergyPlus & JEPLUS files for LHS runs calibration 2. JEPLUS Datacomp simulation outputs 3. Calibration in PyStan	The folders contain the JEPlus files to execute the DHW model simulation runs from the calibration paramters required to train the meta-model. The monthly energy end use output results from JEPlus are an input to the Python Jupyter notebook 'Bayesian calibration model DHW_linear_2017_2018_test.ipynb' found in these folders . The Python Jupyter notebook and the corresponding Stan code, called directly from the notebook, perform, diagnose and validate Bayesian calibration.
4.4.4.4.4.4.2	21,32,34,35,36	Ch 4 Electricity Bayesian calibration	1. Electricity EnergyPlus & JEPLUS files for KOH LHS runs calibration 2. JEPLUS Datacomp simulation outputs 3. KOH calibration in PyStan	The folders contain the JEPlus files to execute Model D simulation runs from the calibration parameters required to train the meta-model. The monthly energy end use output results from JEPlus are an input to the Python Jupyter notebook 'Model D2_ Bayesian calibration.ipynb' found in these folders. The Python Jupyter notebook and the corresponding Stan code, called directly from the Python notebook, perform, diagnose and validate Bayesian calibration.

Table B.3: Description of GitHub repository folders and sub-folders for Chapter 4...ctd

Section	Footnote	Folder name	Sub-folders	Description
4.4.4.1	23	Ch 4 DHW Bayesian calibration	<ol style="list-style-type: none"> 1. Physics models Annual uncert propag Prior Post 2. Calibration in PyStan 	The folders contain the JEPlus files to execute the annual simulation runs for the DHW model from both the Prior and Posterior distributions. The results of these simulation runs is fed into the Python Jupyter Notebook 'Bayesian calibration model 'DHW_linear_2017_2018_test.ipynb' to generate Figure 4.9
4.4.4.1.2	30	Ch 4 DHW Bayesian calibration	<ol style="list-style-type: none"> 1. Calibration Validation on Physics models 2. Calibration in PyStan 	The folders contain the JEPlus/EnergyPlus models characterised with the mean value of the calibration parameter posterior distributions . The monthly simulation energy end-use results are fed into the Python Jupyter notebook Bayesian calibration model 'DHW_linear_2017_2018_test.ipynb' to calculate the statistics in Table tab:DHW_CVRMSE_NMBE for the EnergyPlus models.
4.4.4.2	31	Ch 4 Electricity Bayesian calibration	<ol style="list-style-type: none"> 1. Validation of Model D2 for monthly calibration /2017 Model A LHS 2. Validation of Model D2 for monthly calibration /2017 Model D LHS 3. Validation of Model D2 for monthly calibration /Model D vs Model A ASHRAE validation 	The folders contains JEPlus files for both Model A and Model D to execute 100 LHS sample runs from the prior calibration parameters. The validation folder contains a Microsoft Excel file 'Model D CVRSME and NMBE calib month validation' to statistically compare using ASHRAE validation criteria the monthly electricity outputs from the two models. The validation folder also contains a Python notebook 'Box_plot_modelD_cal_valid.ipynb' to generate the box plot in Figure 4.14.
4.4.4.2	33	Ch 4 Electricity Bayesian calibration	<ol style="list-style-type: none"> 1. Physics models Annual uncert propag Prior Post 2. KOH calibration in PyStan 	The folders contain the JEPlus files to execute the annual simulation runs for Model D from both the Prior and Posterior distributions. The results of these simulation runs are fed into the Python Jupyter notebook 'Model D2_ Bayesian calibration.ipynb' to generate Figure 4.17.
4.4.4.1.2	30	Ch 4 Electricity Bayesian calibration	<ol style="list-style-type: none"> 1. Calibration Validation on Physics models 2. KOH calibration in PyStan 	The folders contain the JEPlus/EnergyPlus models characterised with the mean value of the calibration parameter posterior distributions for both Model A and Model D . The monthly simulation energy end-use results are fed into the Python Jupyter Notebook ' Model D2_ Bayesian calibration. .ipynb' to calculate the statistics in Table 4.15 for the EnergyPlus models.

Chapter 5 Folders and Files

This section provides a detailed description of all folders and files referred to in Chapter 5.

Table B.4: Description of GitHub repository folders and sub-folders for Chapter 5

Section	Footnote	Folder name	Sub-folders	Description
5.3.1	6, 8	Ch 5 Model D justification	<ol style="list-style-type: none"> 1. 2017 Model A EPlus files and results 2. 2017 Model D EPlus files and results 3. Model D validation 	<p>The folders contain JEPlus and corresponding EnergyPlus models for Model A and Model D. The corresponding energy end-use simulation results from the parametric simulation runs for all package of passive measures combinations in Table 5.1 are also provided.</p> <p>The statistical calculations to derive Table 5.2 are also found in Microsoft Excel file '2017 Model D vs Model A validation calculations'.</p>
5.3.2.2	11	Ch 5 GHG Price development regression	Not applicable	<p>The data and modelling to develop the GHG carbon emission regression price trend analysis in Figure 5.5 is provided in Microsoft Excel file 'Carbon Emissions Price regression analysis'.</p>
5.3.2.3	12	Ch 5 Model D JEPlus Parametric simul electric	<ol style="list-style-type: none"> 1. 2017 Model & results 2. 2018 Model & results 3. 2018_10 Model & results 4. 2019 Model & results 	<p>The folders contains the JEPlus parametric models and corresponding parametric simulation results from Model D for annual electricity end-use consumption. Results are provided for each year 2017 to 2019 weather and occupancy schedules. The results together with the parametric simulation results from the DHW model (refer to folder 'Ch 5 JEPlus Parametric simulations DHW') are combined in Microsoft Excel file 'Cost_opt_study_simulations_mean_post_values' in folder 'Ch 5 Cost-optimal Python note book' for each year separately. These simulation results are an input to the Python Jupyter notebook 'Hotel_3_cost_opt_analysis' in folder 'Ch 5 Cost-optimal Python note book' set-up for each year under study. These results are used by the notebook to execute step 5 of the proposed cost-optimal approach to derive NZEB EP benchmarks for each year under study separately.</p>
5.3.2.3	12	Ch 5 JEPlus Parametric simulations DHW	<ol style="list-style-type: none"> 1. 2017 Model & results 2. 2018 Model & results 3. 2018_10 Model & results 4. 2019 Model & results 	<p>The folders contains the JEPlus parametric models and corresponding parametric simulation results from the DHW energyPlus model for annual LFO end use consumption. Results are provided for each year 2017 to 2019 occupancy schedules. The results together with the parametric simulation results from Model D (refer to folder 'Ch 5 JEPlus Parametric simulations elec') are combined in Microsoft Excel file 'Cost_opt_study_simulations_mean_post_values' in folder 'Ch 5 Cost-optimal Python note book' for each year separately. These simulation results are an input to the Python Jupyter notebook 'Hotel_3_cost_opt_analysis' in folder 'Ch 5 Cost-optimal Python note book' set-up for each year under study. This results are used by the notebook to execute step 5 of the proposed cost-optimal approach to derive NZEB EP benchmarks for each year under study separately.</p>

Table B.5: Description of GitHub repository folders and sub-folders for Chapter 5...ctd

Section	Footnote	Folder name	Sub-folders	Description
5.3.2.3	14, 15	Ch 5 Degree days notebook	<ol style="list-style-type: none"> 1. Python DD analysis 2. Excel DD calculator 	<p>The folders contain Python notebook 'Degree_day_analysis.ipynb' that uses outside hourly dry-bulb temperature data for the years 2017 to 2019 obtained from the Malta International Airport and the monthly metered electrical energy consumption data of the hotel RB case-study. The notebook automatically determines the optimal base temperatures using the Degree Day analysis approach described in ASHRAE [372]. The folders also contain a Microsoft Excel file 'Heating cooling DD calculator 2010 2016 2017 2018 2019' containing hourly dry-bulb temperature data for the year 2010 and years 2016 to 2020, that allows degree days to be calculated on a monthly resolution for these years for given base temperatures.</p>
5.3.3	17	Ch 5 Model D JEPlus risk propag	<ol style="list-style-type: none"> 1. 2017 JEPlus models & results 2. 2018 JEPlus models & results 3. 2018_10 JEPlus models & results 4. 2019 JEPlus models & results 	<p>The folders contain the JEPlus/EnergyPlus files to execute the risk analysis simulation runs from Model D and corresponding results for each year and NZEB EP ambition level including the reference scenario under consideration. The simulation results in spreadsheet format are combined with the simulation results for the DHW model from folder 'Ch 5 JEPlus DHW risk propag' for each year and ambition level separately and are an input to the Python Jupyter notebook 'Hotel_3_cost_opt_analysis' found in folder 'Ch 5 Cost-optimal Python note book'. A different notebook is used for each year under study. These results are used by the notebook to execute step 6 of the proposed cost-optimal approach and to construct the required joint plot visualisations shown in Figure 5.3.</p>
5.3.3	17	Ch 5 JEPlus DHW risk propag	<ol style="list-style-type: none"> 1. 2017 JEPlus models & results 2. 2018 JEPlus models & results 3. 2018_10 JEPlus models & results 4. 2019 JEPlus models & results 	<p>The folders contain the JEPlus/EnergyPlus files to execute the risk analysis simulation runs from the DHW model and corresponding results for each year and NZEB EP ambition level including the reference scenario under consideration. The simulation results in spreadsheet format are combined with the simulation results for Model D from folder 'Ch 5 JEPlus Model D risk propag' for each year and ambition level separately and are an input to the Python Jupyter Notebook 'Hotel_3_cost_opt_analysis' found in folder 'Ch 5 Cost-optimal Python note book'. A different notebook is used for each year under study. These results are used by the notebook to execute step 6 of the proposed cost-optimal approach and to construct the required joint plot visualisations shown in Figure 5.3.</p>
5.3.2.3, 5.3.3	13,16,18,9,10	Ch 5 Cost-optimal Python note book	<ol style="list-style-type: none"> 1. 2017 models & results 2. 2018 models & results 3. 2018_10 models & results 4. 2019 models & results 	<p>Each subfolder, one for each year under study, contains a Python Jupyter notebook entitled 'Hotel_3_cost_opt_analysis'. The notebook first defines the global LCC parameters for all ECMs, shown in Section 5.3.2.2 for the RB case-study. It then uses these financial parameters values and the combined simulation results of Model D and the DHW model to calculate the EN 15459 [54] global LCC for each COM, to generate the cost-optimal plots using the visualisations shown in Figure 5.2 and to automatically define the four NZEB EP ambition levels defined in Section 5.2.1. The Python notebook also uses the combined risk propagation results of Model D and the DHW model to perform the risk analysis for each defined NZEB EP ambition level and to derive the joint plot visualisations shown in Figure 5.3. The same Python notebook also calculates the robust and deterministic financial risk for each ambition level as defined in Equation 5.3 and Section 5.2.1 respectively.</p>

Table B.6: Description of GitHub repository folders and sub-folders for Chapter 5...ctd

Section	Footnote	Folder name	Sub-folders	Description
5.4	20	Ch 5 SBEM analysis	<ol style="list-style-type: none"> 1. SBEM models COPs of 1 2. SBEM COMS EP analysis 	<p>The folders provide SBEM-MT energy models for the RB case study that calculate the energy demand (i.e. the models are defined with a seasonal COP of 1 for space heating and cooling) for all considered passive combination of measures. Using the results from this energy demand analysis, the full parametric EP analysis involving 64 COMs for each of the two RB SBEM-MT model configurations defined in Section 5.4 was carried out. This was possible by converting the energy demand to energy end-use energy consumption by varying the COP of the space cooling and space heating systems for each COM under consideration using Microsoft Excel file 'ASSET_Cost_opt_sheets_for_Python_input' found in sub-folder 'SBEM COMS EP analysis'. These parametric results are an input to the Python Jupyter Notebook 'Hotel_3_cost_opt_analysis' found in folder 'Ch 5 Cost-optimal Python note book'. A separate notebook was set-up for each RB SBEM-MT model configuration. These results are used by the notebook to execute step 5 of the proposed cost-optimal approach to derive NZEB EP benchmarks and to calculate the deterministic financial risk for each resulting NZEB EP ambition level.</p>
5.4	21	Ch 5 SBEM analysis	<ol style="list-style-type: none"> 1. Python cost-opt analysis/2018_10 Manuf_Data_sheet_values 2. Python cost-opt analysis/2018_10 Post_calibrated_values 	<p>Each subfolder, one for each SBEM RB model under study configuration, as defined in Section 5.4, contains a Python Jupyter notebook. The notebook first defines the global LCC parameters for all ECMs, shown in Section 5.3.2.2 for the RB case-study. It then uses these financial parameter values and the parametric results from Microsoft Excel file 'ASSET_Cost_opt_sheets_for_Python_input', found in sub-folder 'SBEM COMS EP analysis', to calculate the EN 15459 [54] global LCC for each COM, generate the cost-optimal plots using the visualisations shown in Figure 5.2, and to automatically define the four NZEB EP ambition levels defined in Section 5.2.1. The notebook also calculates the deterministic risk for each NZEB ambition level as defined in Section 5.2.1.</p>

2017 DHW Schedule A

Schedule:Compact,
Hotel_EnsuiteBed_Occ,
Fraction,
Through: 31 Jan,
For: Weekdays SummerDesignDay,
Until: 08:00, 0.72,
Until: 09:00, 0.18,
Until: 21:00, 0,
Until: 22:00, 0.18,
Until: 23:00, 0.54,
Until: 24:00, 0.72,
For: Weekends,
Until: 08:00, 0.72,
Until: 09:00, 0.18,
Until: 21:00, 0,
Until: 22:00, 0.18,
Until: 23:00, 0.54,
Until: 24:00, 0.72,
For: Holidays,
Until: 08:00, 0.72,
Until: 09:00, 0.18,
Until: 21:00, 0,
Until: 22:00, 0.18,
Until: 23:00, 0.54,
Until: 24:00, 0.72,

For: WinterDesignDay AllOtherDays,
Until: 24:00, 0,
Through: 28 Feb,
For: Weekdays SummerDesignDay,
Until: 08:00, 0.81,
Until: 09:00, 0.20,
Until: 21:00, 0,
Until: 22:00, 0.20,
Until: 23:00, 0.61,
Until: 24:00, 0.81,
For: Weekends,
Until: 08:00, 0.81,
Until: 09:00, 0.20,
Until: 21:00, 0,
Until: 22:00, 0.20,
Until: 23:00, 0.61,
Until: 24:00, 0.81,
For: Holidays,
Until: 08:00, 0.81,
Until: 09:00, 0.20,
Until: 21:00, 0,
Until: 22:00, 0.20,
Until: 23:00, 0.61,
Until: 24:00, 0.81,
For: WinterDesignDay AllOtherDays,
Until: 24:00, 0,
Through: 31 Mar,
For: Weekdays SummerDesignDay,
Until: 08:00, 0.74,
Until: 09:00, 0.185,
Until: 21:00, 0,
Until: 22:00, 0.185,
Until: 23:00, 0.555,
Until: 24:00, 0.74,
For: Weekends,
Until: 08:00, 0.74,
Until: 09:00, 0.185,

Until: 21:00, 0,
Until: 22:00, 0.185,
Until: 23:00, 0.555,
Until: 24:00, 0.74,
For: Holidays,
Until: 08:00, 0.74,
Until: 09:00, 0.185,
Until: 21:00, 0,
Until: 22:00, 0.185,
Until: 23:00, 0.555,
Until: 24:00, 0.74,
For: WinterDesignDay AllOtherDays,
Until: 24:00, 0,
Through: 30 Apr,
For: Weekdays SummerDesignDay,
Until: 08:00, 0.89,
Until: 09:00, 0.2225,
Until: 21:00, 0,
Until: 22:00, 0.2225,
Until: 23:00, 0.6675,
Until: 24:00, 0.89,
For: Weekends,
Until: 08:00, 0.89,
Until: 09:00, 0.2225,
Until: 21:00, 0,
Until: 22:00, 0.2225,
Until: 23:00, 0.6675,
Until: 24:00, 0.89,
For: Holidays,
Until: 08:00, 0.89,
Until: 09:00, 0.2225,
Until: 21:00, 0,
Until: 22:00, 0.2225,
Until: 23:00, 0.6675,
Until: 24:00, 0.89,
For: WinterDesignDay AllOtherDays,
Until: 24:00, 0,

Through: 31 May,
For: Weekdays SummerDesignDay,
Until: 08:00, 0.83,
Until: 09:00, 0.21,
Until: 21:00, 0,
Until: 22:00, 0.21,
Until: 23:00, 0.6225,
Until: 24:00, 0.83,
For: Weekends,
Until: 08:00, 0.83,
Until: 09:00, 0.21,
Until: 21:00, 0,
Until: 22:00, 0.21,
Until: 23:00, 0.6225,
Until: 24:00, 0.72,
For: Holidays,
Until: 08:00, 0.72,
Until: 09:00, 0.21,
Until: 21:00, 0,
Until: 22:00, 0.21,
Until: 23:00, 0.6225,
Until: 24:00, 0.83,
For: WinterDesignDay AllOtherDays,
Until: 24:00, 0,
Through: 30 Jun,
For: Weekdays SummerDesignDay,
Until: 08:00, 0.85,
Until: 09:00, 0.2125,
Until: 21:00, 0,
Until: 22:00, 0.2125,
Until: 23:00, 0.6375,
Until: 24:00, 0.85,
For: Weekends,
Until: 08:00, 0.85,
Until: 09:00, 0.2125,
Until: 21:00, 0,
Until: 22:00, 0.2125,

Until: 23:00, 0.6375,
Until: 24:00, 0.85,
For: Holidays,
Until: 08:00, 0.85,
Until: 09:00, 0.2125,
Until: 21:00, 0,
Until: 22:00, 0.2125,
Until: 23:00, 0.6375,
Until: 24:00, 0.85,
For: WinterDesignDay AllOtherDays,
Until: 24:00, 0,
Through: 31 Jul,
For: Weekdays SummerDesignDay,
Until: 08:00, 0.97,
Until: 09:00, 0.2425,
Until: 21:00, 0,
Until: 22:00, 0.2425,
Until: 23:00, 0.7275,
Until: 24:00, 0.97,
For: Weekends,
Until: 08:00, 0.97,
Until: 09:00, 0.2425,
Until: 21:00, 0,
Until: 22:00, 0.2425,
Until: 23:00, 0.7275,
Until: 24:00, 0.97,
For: Holidays,
Until: 08:00, 0.97,
Until: 09:00, 0.2425,
Until: 21:00, 0,
Until: 22:00, 0.2425,
Until: 23:00, 0.7275,
Until: 24:00, 0.97,
For: WinterDesignDay AllOtherDays,
Until: 24:00, 0,
Through: 31 Aug,
For: Weekdays SummerDesignDay,

Until: 08:00, 1,
Until: 09:00, 0.25,
Until: 21:00, 0,
Until: 22:00, 0.25,
Until: 23:00, 0.75,
Until: 24:00, 1,
For: Weekends,
Until: 08:00, 1,
Until: 09:00, 0.25,
Until: 21:00, 0,
Until: 22:00, 0.25,
Until: 23:00, 0.75,
Until: 24:00, 1,
For: Holidays,
Until: 08:00, 1,
Until: 09:00, 0.25,
Until: 21:00, 0,
Until: 22:00, 0.25,
Until: 23:00, 0.75,
Until: 24:00, 1,
For: WinterDesignDay AllOtherDays,
Until: 24:00, 0,
Through: 30 Sep,
For: Weekdays SummerDesignDay,
Until: 08:00, 0.82,
Until: 09:00, 0.205,
Until: 21:00, 0,
Until: 22:00, 0.205,
Until: 23:00, 0.615,
Until: 24:00, 0.82,
For: Weekends,
Until: 08:00, 0.82,
Until: 09:00, 0.205,
Until: 21:00, 0,
Until: 22:00, 0.205,
Until: 23:00, 0.615,
Until: 24:00, 0.82,

For: Holidays,
Until: 08:00, 0.82,
Until: 09:00, 0.205,
Until: 21:00, 0,
Until: 22:00, 0.205,
Until: 23:00, 0.615,
Until: 24:00, 0.82,
For: WinterDesignDay AllOtherDays,
Until: 24:00, 0,
Through: 31 Oct,
For: Weekdays SummerDesignDay,
Until: 08:00, 0.85,
Until: 09:00, 0.2125,
Until: 21:00, 0,
Until: 22:00, 0.2125,
Until: 23:00, 0.6375,
Until: 24:00, 0.85,
For: Weekends,
Until: 08:00, 0.85,
Until: 09:00, 0.2125,
Until: 21:00, 0,
Until: 22:00, 0.2125,
Until: 23:00, 0.6375,
Until: 24:00, 0.85,
For: Holidays,
Until: 08:00, 0.85,
Until: 09:00, 0.2125,
Until: 21:00, 0,
Until: 22:00, 0.2125,
Until: 23:00, 0.6375,
Until: 24:00, 0.85,
For: WinterDesignDay AllOtherDays,
Until: 24:00, 0,
Through: 30 Nov,
For: Weekdays SummerDesignDay,
Until: 08:00, 0.82,
Until: 09:00, 0.205,

Until: 21:00, 0,
Until: 22:00, 0.205,
Until: 23:00, 0.615,
Until: 24:00, 0.82,
For: Weekends,
Until: 08:00, 0.82,
Until: 09:00, 0.205,
Until: 21:00, 0,
Until: 22:00, 0.205,
Until: 23:00, 0.615,
Until: 24:00, 0.82,
For: Holidays,
Until: 08:00, 0.82,
Until: 09:00, 0.205,
Until: 21:00, 0,
Until: 22:00, 0.205,
Until: 23:00, 0.615,
Until: 24:00, 0.82,
For: WinterDesignDay AllOtherDays,
Until: 24:00, 0,
Through: 31 Dec,
For: Weekdays SummerDesignDay,
Until: 08:00, 0.86,
Until: 09:00, 0.215,
Until: 21:00, 0,
Until: 22:00, 0.215,
Until: 23:00, 0.645,
Until: 24:00, 0.86,
For: Weekends,
Until: 08:00, 0.86,
Until: 09:00, 0.215,
Until: 21:00, 0,
Until: 22:00, 0.215,
Until: 23:00, 0.645,
Until: 24:00, 0.86,
For: Holidays,
Until: 08:00, 0.86,

Until: 09:00, 0.215,
Until: 21:00, 0,
Until: 22:00, 0.215,
Until: 23:00, 0.645,
Until: 24:00, 0.86,
For: WinterDesignDay AllOtherDays,
Until: 24:00, 0;

References

- [1] ASHRAE, “Chapter 19: Energy estimating and modeling methods,” in *2021 ASHRAE Handbook Fundamentals (SI)*, H. E. Kennedy, Ed. ASHRAE, 2021, ch. 19.
- [2] ANSI/ASHRAE, “ASHRAE Guideline 14-2014 Measurement of Energy and Demand Savings,” *Ashrae*, p. 140, 2014.
- [3] European Commission, “Communication from the commission to the european parliament, the european council, the council, the european economic and social committee and the committee of the regions - the european green deal,” pp. 2019–2022, 2019. [Online]. Available: https://ec.europa.eu/info/sites/info/files/european-green-deal-communication-annex-roadmap_en.pdf
- [4] EU Commission, “A renovation wave for europe - greening our buildings, creating jobs, improving lives,” 11 2020. [Online]. Available: <https://eur-lex.europa.eu/legal-content/EN/TXT/?uri=CELEX%3A52020DC0662>
- [5] I. Jankovic, A. Mayer, D. Staniaszek, and X. F. Álvarez, “Ready for carbon neutral by 2050? assessing ambition levels in new building standards across the eu.” [Online]. Available: <https://www.bpie.eu/publication/ready-for-carbon-neutral-by-2050-assessing-ambition-levels-in-new-building-standards-across-the-eu/>
- [6] Y. Xing, N. Hewitt, and P. Griffiths, “Zero carbon buildings refurbishment—A Hierarchical pathway,” *Renewable and Sustainable Energy Reviews*, vol. 15, no. 6, p. 3229–3236, 2011.
- [7] A. V. Lițiu and J. Hogeling, “The evolution of building energy performance assessment and certification schemes in europe,” *REHVA Journal*, pp. 82–86, 2 2021.
- [8] European Commission, “COM(2021) 802 DIRECTIVE OF THE EUROPEAN PARLIAMENT AND OF THE COUNCIL on the energy performance of buildings (recast) ‘Fit for 55’: delivering the EU’s 2030 Climate Target on the way to climate neutrality,” Tech. Rep., dec 2021. [Online]. Available: <https://eur-lex.europa.eu/legal-content/EN/TXT/PDF/?uri=CELEX:52021DC0550&from=EN>

- [9] EU Commission, "Directive 2010/31/EU of the European Parliament and of the Council of 19 May 2010 on the energy performance of buildings (recast)," *Official Journal of the European Union*, pp. 13–33, 2010. [Online]. Available: <https://eur-lex.europa.eu/legal-content/EN/TXT/PDF/?uri=CELEX:32010L0031&from=EN>
- [10] T. Hong, J. Langevin, and K. Sun, "Building simulation : Ten challenges," *Building Simulation*, vol. 11, no. 5, pp. 871–898, 2018.
- [11] K. Gram-Hanssen and S. Georg, "Energy performance gaps: promises, people, practices," *Building Research and Information*, vol. 46, pp. 1–9, 1 2018.
- [12] V. Corrado and H. E. Mechri, "Uncertainty and sensitivity analysis for building energy rating," *Journal of Building Physics*, vol. 33, no. 2, pp. 125–156, 2009.
- [13] L. Tronchin and K. Fabbri, "A Round Robin Test for buildings energy performance in Italy," *Energy and Buildings*, vol. 42, no. 10, pp. 1862–1877, 2010.
- [14] E. Cayre, B. Allibe, M. Laurent, and D. Osso, "There are people in the house ! how the results of purely technical analysis of residential energy consumption are misleading for energy policies," *European Council for an Energy Efficient Economy (ECEEE) Summer School*, 2011.
- [15] S. Petersen and C. A. Hviid, "THE EEPD: Comparison of Calculated and Actual Energy Use in a Danish Office Building," *Building Simulation and Optimization Conference*, no. September 2012, pp. 43–48, 2012.
- [16] R. Galvin and M. Sunikka-Blank, "The prebound effect: Discrepancies between measured and calculated consumption," *Green Energy and Technology*, vol. 148, 2013.
- [17] E. Burman, D. Mumovic, and J. Kimpian, "Towards measurement and verification of energy performance under the framework of the European directive for energy performance of buildings," *Energy*, vol. 77, pp. 153–163, 2014. [Online]. Available: <http://dx.doi.org/10.1016/j.energy.2014.05.102>
- [18] Gram-Hanssen and Hansen, "The difference between measured and calculated energy consumption for heating of detached houses (in danish)," 2016.
- [19] K. Gram-Hanssen, S. Georg, E. Christiansen, and P. K. Heiselberg, "How building regulations ignore the use of buildings , what that means for energy consumption and what to do about it," 2017.
- [20] L. Thaler and D. Kellenberger, "Addressing performance gaps: User behavior and sufficiency in the planning and operation phase of a 2000-watt site," vol. 122, 2017.
- [21] F. Flourentzos, Y. I. Antonov, and S. Pantet, "Understand, simulate, anticipate and correct performance gap in nzeb refurbishment of residential buildings," vol. 1343, 2019.

- [22] S. Cozza, J. Chambers, C. Deb, J.-L. Scartezzini, A. Schlüter, and M. K. Patel, "Do energy performance certificates allow reliable predictions of actual energy consumption and savings? learning from the swiss national database," *Energy and Buildings*, vol. 224, p. 110235, 2020. [Online]. Available: <https://www.sciencedirect.com/science/article/pii/S0378778820303315>
- [23] S. Cozza, J. Chambers, and M. K. Patel, "Measuring the thermal energy performance gap of labelled residential buildings in switzerland," *Energy Policy*, vol. 137, p. 111085, 2020. [Online]. Available: <https://www.sciencedirect.com/science/article/pii/S030142151930672X>
- [24] P. Vassallo, "Analysing the "performance gap" between energy performance certificates and actual energy consumption of non-residential buildings in malta," 2020.
- [25] G. Chiesa, "D1.2 - operational dynamic epc specifications," 9 2020. [Online]. Available: <https://edyce.eu/>
- [26] S. P. Corgnati, E. Fabrizio, M. Filippi, and V. Monetti, "Reference buildings for cost optimal analysis: Method of definition and application," *Applied Energy*, vol. 102, pp. 983–993, 2 2013. [Online]. Available: <http://linkinghub.elsevier.com/retrieve/pii/S0306261912004394>
- [27] T. Buso and S. P. Corgnati, "A customized modelling approach for multi-functional buildings – Application to an Italian Reference Hotel," *Applied Energy*, vol. 190, pp. 1302–1315, 2017. [Online]. Available: <http://dx.doi.org/10.1016/j.apenergy.2017.01.042>
- [28] D. D'Agostino, "Assessment of the progress towards the establishment of definitions of Nearly Zero Energy Buildings (nZEBs) in European Member States," *Journal of Building Engineering*, vol. 1, pp. 20–32, 2015. [Online]. Available: <http://dx.doi.org/10.1016/j.jobe.2015.01.002>
- [29] D. D'Agostino and L. Mazzarella, "What is a nearly zero energy building? overview, implementation and comparison of definitions," *Journal of Building Engineering*, vol. 21, pp. 200–212, 2019.
- [30] D. D'Agostino, S. T. Tzeiranaki, P. Zangheri, and P. Bertoldi, "Assessing nearly zero energy buildings (nzebs) development in europe," *Energy Strategy Reviews*, vol. 36, p. 100680, 7 2021.
- [31] "Epb center | epb standards." [Online]. Available: <https://epb.center/>
- [32] EU, "Directive (EU) 2018/844 of the European Parliament and of the Council of 30 May 2018 amending Directive 2010/31/EU on the energy performance of buildings and Directive 2012/27/EU on energy efficiency," *Official Journal of the European Union*, pp. 75–91, 2018.
- [33] J. Kurnitski, T. Buso, S. P. Corgnati, A. Derjanecz, and A. Litiu, "nZEB definitions in Europe," *The REHVA European HVAC Journal*, vol. 51, no. 2, pp. 6–9, 2014.
- [34] A. Schaefer and E. Ghisi, "Method for Obtaining Reference Buildings," *Energy and Buildings*, vol. 128, pp. 660–672, 2016. [Online]. Available: <http://dx.doi.org/10.1016/j.enbuild.2016.07.001>

- [35] D. Gatt, C. Yousif, M. Cellura, and L. Camilleri, "An innovative approach to manage uncertainties and stock diversity in the EPBD cost-optimal methodology," *European Journal of Technique*, vol. 8, no. 1, pp. 35–49, 6 2018. [Online]. Available: <http://dergipark.gov.tr/ejt/issue/39607/467910>
- [36] D. Gatt, C. Yousif, M. Cellura, L. Camilleri, and F. Guarino, "Assessment of building energy modelling studies to meet the requirements of the new Energy Performance of Buildings Directive," *Renewable and Sustainable Energy Reviews*, vol. 127, no. May, p. 109886, 2020. [Online]. Available: <https://doi.org/10.1016/j.rser.2020.109886>
- [37] R. Choudhary, "Energy analysis of the non-domestic building stock of Greater London," *Building and Environment*, vol. 51, pp. 243–254, 2012.
- [38] G. Kazas, E. Fabrizio, and M. Perino, "Energy demand profile generation with detailed time resolution at an urban district scale: A reference building approach and case study," *Applied Energy*, vol. 193, pp. 243–262, 2017. [Online]. Available: <http://dx.doi.org/10.1016/j.apenergy.2017.01.095>
- [39] G. V. Fracastoro and M. Serraino, "A methodology for assessing the energy performance of large scale building stocks and possible applications," *Energy and Buildings*, vol. 43, no. 4, pp. 844–852, 2011. [Online]. Available: <http://dx.doi.org/10.1016/j.enbuild.2010.12.004>
- [40] S. Becken, C. Frampton, and D. Simmons, "Energy consumption patterns in the accommodation sector - The New Zealand case," *Ecological Economics*, vol. 39, no. 3, pp. 371–386, 2001.
- [41] S. N. Boemi, T. Slini, A. M. Papadopoulos, and Y. Mihalakakou, "A statistical approach to the prediction of the energy performance of hotel stock," *International Journal of Ventilation*, vol. 10, no. 2, pp. 163–172, 2011.
- [42] Z. Ma, P. Cooper, D. Daly, and L. Ledo, "Existing building retrofits: Methodology and state-of-the-art," *Energy and Buildings*, vol. 55, pp. 889–902, 12 2012. [Online]. Available: <http://linkinghub.elsevier.com/retrieve/pii/S0378778812004227>
- [43] C. C. Menassa and W. Ortiz-Vega, "Uncertainty in the Refurbishment Investment," in *Nearly Zero Energy Building Refurbishment: A Multidisciplinary Approach*. Springer-Verlag London, 2013, pp. 143–175.
- [44] J. Palm and K. Reindl, "Understanding barriers to energy-efficiency renovations of multifamily dwellings," *Energy Efficiency*, vol. 11, pp. 53–65, 2018. [Online]. Available: <https://doi.org/10.1007/s12053-017-9549-9>
- [45] E. Naber, R. Volk, and F. Schultmann, "From the Building Level Energy Performance Assessment to the National Level: How are Uncertainties Handled in Building Stock Models," *Procedia Engineering*, vol. 180, pp. 1443–1452, 2017. [Online]. Available: <http://dx.doi.org/10.1016/j.proeng.2017.04.307>

- [46] S. Hansen and J. Brown, *Investment Grade Energy Audit:: Making Smart Energy Choices*, 1st ed. River Publishers, 2004. [Online]. Available: <https://doi.org/10.1201/9781003151012>
- [47] D. C. Matisoff, D. S. Noonan, and M. E. Flowers, "Policy monitor-green buildings: Economics and policies," *Review of Environmental Economics and Policy*, vol. 10, 2016.
- [48] E. S. Chan, F. Okumus, and W. Chan, "The Applications of Environmental Technologies in Hotels," *Journal of Hospitality Marketing and Management*, vol. 26, no. 1, pp. 23–47, 2017. [Online]. Available: <http://dx.doi.org/10.1080/19368623.2016.1176975><https://doi.org/10.1080/19368623.2016.1176975>
- [49] R. Yadav, A. K. Dokania, and G. S. Pathak, "The influence of green marketing functions in building corporate image: Evidences from hospitality industry in a developing nation," *International Journal of Contemporary Hospitality Management*, vol. 28, 2016.
- [50] Y. Zhang and I. Korolija, "Performing complex parametric simulations with jEPlus," *SET2010-9th International Conference on Sustainable Energy Technologies*, 2010.
- [51] M. Kavgic, A. Mavrogianni, D. Mumovic, A. Summerfield, Z. Stevanovic, and M. Djurovic-Petrovic, "A review of bottom-up building stock models for energy consumption in the residential sector," *Building and Environment*, vol. 45, no. 7, pp. 1683–1697, 2010. [Online]. Available: <http://dx.doi.org/10.1016/j.buildenv.2010.01.021>
- [52] M. Brøgger and K. B. Wittchen, "Estimating the energy-saving potential in national building stocks - A methodology review," *Renewable and Sustainable Energy Reviews*, vol. 82, no. July 2017, pp. 1489–1496, 2017. [Online]. Available: <https://doi.org/10.1016/j.rser.2017.05.239>
- [53] L. G. Swan and V. I. Ugursal, "Modeling of end-use energy consumption in the residential sector: A review of modeling techniques," *Renewable and Sustainable Energy Reviews*, vol. 13, no. 8, pp. 1819–1835, 2009.
- [54] CEN, "EN 15459-1:2017 Energy performance of buildings - Economic evaluation procedure for energy systems in buildings- Part 1: Calculation procedures, Module M1-14," 2017.
- [55] European Commission, "Guidelines accompanying Commission Delegated Regulation (EU) No 244/2012 of 16 January 2012 supplementing Directive 2010/31/EU of the European Parliament and of the Council on the energy performance of buildings by establishing a comparative methodology f," European Commission, Tech. Rep., 2012. [Online]. Available: <https://eur-lex.europa.eu/legal-content/EN/ALL/?uri=CELEX{%}3A52012XC0419{%}2802{%}29>
- [56] D. Gatt, C. Yousif, C. Barbara, F. Caruana, and M. Degiorgio, "Epbid cost-optimal analysis for non-residential buildings in malta." SBE19, 12 2019.
- [57] M. Akbari, P. Asadi, M. K. B. Givi, and G. Khodabandehlouie, "Artificial neural network and optimization," *Advances in Friction-Stir Welding and Processing*, pp. 543–599, 1 2014.

- [58] R. Mohanty, S. Suman, and S. K. Das, "Modeling the axial capacity of bored piles using multi-objective feature selection, functional network and multivariate adaptive regression spline," 2017.
- [59] S. Attia, H. Mohamed, S. Carlucci, P. Lorenzo, S. Bucking, and A. Hasan, "Building performance optimization of net zero-energy buildings," in *Modeling, design, and optimization of net zero-energy buildings*, 1st ed., A. Athienitis and W. O'Brien, Eds. Ernst & Sohn - A Wiley Brand, 2015, ch. 5, pp. 175–206.
- [60] M. Brøgger, P. Bacher, and K. B. Wittchen, "A hybrid modelling method for improving estimates of the average energy-saving potential of a building stock," *Energy and Buildings*, vol. 199, pp. 287–296, 2019.
- [61] L. M. Hall and A. R. Buckley, "A review of energy systems models in the UK: Prevalent usage and categorisation," *Applied Energy*, vol. 169, pp. 607–628, 2016. [Online]. Available: <http://dx.doi.org/10.1016/j.apenergy.2016.02.044>
- [62] IEA Annex 31, "Methods for Evaluating the Environmental Performance of Building Stocks," *Buildings*, p. 30, 2004. [Online]. Available: <http://www.iisbe.org/annex31/index.html>
- [63] W. Li, Y. Zhou, K. Cetin, J. Eom, Y. Wang, G. Chen, and X. Zhang, "Modeling urban building energy use: A review of modeling approaches and procedures," *Energy*, vol. 141, pp. 2445–2457, 2017. [Online]. Available: <http://linkinghub.elsevier.com/retrieve/pii/S0360544217319291>
- [64] G. M. Mauro, M. Hamdy, G. P. Vanoli, N. Bianco, and J. L. M. Hensen, "A new methodology for investigating the cost-optimality of energy retrofitting a building category," *Energy and Buildings*, vol. 107, pp. 456–478, 2015. [Online]. Available: <http://dx.doi.org/10.1016/j.enbuild.2015.08.044>
- [65] H. Lim and Z. J. Zhai, "Review on stochastic modeling methods for building stock energy prediction," *Building Simulation*, vol. 10, no. 5, pp. 607–624, 2017.
- [66] C. F. Reinhart and C. Cerezo Davila, "Urban building energy modeling - A review of a nascent field," *Building and Environment*, vol. 97, pp. 196–202, 2016. [Online]. Available: <http://dx.doi.org/10.1016/j.buildenv.2015.12.001>
- [67] T. Alves, L. Machado, R. G. de Souza, and P. de Wilde, "A methodology for estimating office building energy use baselines by means of land use legislation and reference buildings," *Energy and Buildings*, vol. 143, pp. 100–113, 2017. [Online]. Available: <http://dx.doi.org/10.1016/j.enbuild.2017.03.017>
- [68] Nic Rivers and Mark Jaccard, "Combining Top-Down and Bottom-Up Approaches To Energy-Economy Modeling Using Discrete Choice Methods," *The Energy Journal*, vol. 26, no. 1, pp. 83–106, 2005. [Online]. Available: <http://www.jstor.org/stable/41323052>
- [69] W. Tian and R. Choudhary, "A probabilistic energy model for non-domestic building sectors applied to analysis of school buildings in greater London," *Energy and Buildings*, vol. 54, pp. 1–11, 2012. [Online]. Available: <http://dx.doi.org/10.1016/j.enbuild.2012.06.031>

- [70] Mata, G. Medina Benejam, A. Sasic Kalagasidis, and F. Johnsson, "Modelling opportunities and costs associated with energy conservation in the Spanish building stock," *Energy and Buildings*, vol. 88, pp. 347–360, 2015. [Online]. Available: <http://dx.doi.org/10.1016/j.enbuild.2014.12.010>
- [71] P. Tuominen, R. Holopainen, L. Eskola, J. Jokisalo, and M. Airaksinen, "Calculation method and tool for assessing energy consumption in the building stock," *Building and Environment*, vol. 75, pp. 153–160, 2014. [Online]. Available: <http://dx.doi.org/10.1016/j.buildenv.2014.02.001>
- [72] C. Cerezo, J. Sokol, C. Reinhart, and A. Al-mumin, "Three methods for characterizing building archetypes in urban energy simulation. A case study in Kuwait City," in *Proceedings 14th International IBPSA Building Simulation Conference*, India, 2015.
- [73] F. Johari, G. Peronato, P. Sadeghian, X. Zhao, and J. Widén, "Urban building energy modeling: State of the art and future prospects," *Renewable and Sustainable Energy Reviews*, vol. 128, no. September 2019, 2020.
- [74] C. Cerezo, J. Sokol, S. AlKhaled, C. Reinhart, A. Al-Mumin, and A. Hajiah, "Comparison of four building archetype characterization methods in urban building energy modeling (UBEM): A residential case study in Kuwait City," *Energy and Buildings*, vol. 154, pp. 321–334, 2017. [Online]. Available: <https://doi.org/10.1016/j.enbuild.2017.08.029>
- [75] I. Ballarini, S. P. Corgnati, and V. Corrado, "Use of reference buildings to assess the energy saving potentials of the residential building stock: The experience of TABULA project," *Energy Policy*, vol. 68, pp. 273–284, 5 2014. [Online]. Available: <http://linkinghub.elsevier.com/retrieve/pii/S0301421514000329>
- [76] M. Aksoezen, M. Daniel, U. Hassler, and N. Kohler, "Building age as an indicator for energy consumption," *Energy and Buildings*, vol. 87, pp. 74–86, 2015. [Online]. Available: <http://dx.doi.org/10.1016/j.enbuild.2014.10.074>
- [77] A. A. Famuyibo, A. Duffy, and P. Strachan, "Developing archetypes for domestic dwellings - An Irish case study," *Energy and Buildings*, vol. 50, pp. 150–157, 2012. [Online]. Available: <http://dx.doi.org/10.1016/j.enbuild.2012.03.033>
- [78] O. Pasichnyi, J. Wallin, and O. Kordas, "Data-driven building archetypes for urban building energy modelling," *Energy*, vol. 181, pp. 360–377, 2019.
- [79] A. Brandão de Vasconcelos, M. D. Pinheiro, A. Manso, and A. Cabaço, "A Portuguese approach to define reference buildings for cost-optimal methodologies," *Applied Energy*, vol. 140, no. January 2012, pp. 316–328, 2015.
- [80] M. Bhatnagar, J. Mathur, and V. Garg, "Development of reference building models for India," *Journal of Building Engineering*, vol. 21, no. November 2018, pp. 267–277, 2019. [Online]. Available: <https://doi.org/10.1016/j.job.2018.10.027>

- [81] M. Heidarinejad, M. Dahlhausen, S. McMahon, C. Pyke, and J. Srebric, "Cluster analysis of simulated energy use for LEED certified U.S. office buildings," *Energy and Buildings*, vol. 85, pp. 86–97, 2014. [Online]. Available: <http://dx.doi.org/10.1016/j.enbuild.2014.09.017>
- [82] K. N. Streicher, P. Padey, D. Parra, M. C. Bürer, and M. K. Patel, "Assessment of the current thermal performance level of the Swiss residential building stock: Statistical analysis of energy performance certificates," *Energy and Buildings*, vol. 178, pp. 360–378, 2018. [Online]. Available: <https://doi.org/10.1016/j.enbuild.2018.08.032>
- [83] S. P. Pieri, I. Tzouvadakis, and M. Santamouris, "Identifying energy consumption patterns in the Attica hotel sector using cluster analysis techniques with the aim of reducing hotels' CO2 footprint," *Energy and Buildings*, vol. 94, pp. 252–262, 2015. [Online]. Available: <http://dx.doi.org/10.1016/j.enbuild.2015.02.017>
- [84] N. Ghiassi and A. Mahdavi, "Reductive bottom-up urban energy computing supported by multivariate cluster analysis," *Energy & Buildings*, vol. 144, pp. 372–386, 2017. [Online]. Available: <http://dx.doi.org/10.1016/j.enbuild.2017.03.004>
- [85] G. Tardioli, R. Kerrigan, M. Oates, J. O. Donnell, and D. P. Finn, "Identification of representative buildings and building groups in urban datasets using a novel pre-processing, classification, clustering and predictive modelling approach," *Building and Environment*, vol. 140, no. May, pp. 90–106, 2018. [Online]. Available: <https://doi.org/10.1016/j.buildenv.2018.05.035>
- [86] I. Ballarini, S. P. Corgnati, V. Corrado, and N. Talà, "Improving energy modeling of large building stock through the development of archetype buildings," *Building Simulation*, pp. 2874–2881, 2011.
- [87] I. Farrou, M. Kolokotroni, and M. Santamouris, "A method for energy classification of hotels: A case-study of Greece," *Energy and Buildings*, vol. 55, pp. 553–562, 2012. [Online]. Available: <http://dx.doi.org/10.1016/j.enbuild.2012.08.010>
- [88] G. Yang, Z. Li, and G. Augenbroe, "Development of prototypical buildings for urban scale building energy modeling: A reduced order energy model approach," *Science and Technology for the Built Environment*, vol. 24, no. 1, pp. 33–42, 2017. [Online]. Available: <https://doi.org/10.1080/23744731.2017.1328943>
- [89] P. Borges, O. Travesset-Baro, and A. Pages-Ramon, "Hybrid approach to representative building archetypes development for urban models – a case study in andorra," *Building and Environment*, vol. 215, p. 108958, 5 2022. [Online]. Available: <https://linkinghub.elsevier.com/retrieve/pii/S0360132322002001>
- [90] U. Ali, M. Haris, F. Alshehri, E. Mangina, and J. O'Donnell, "Comparative Analysis of Machine Learning Algorithms for Building Archetypes Development," in *1. Ali U, Haris M, Alshehri F, Mangina E, O'Donnell J. Comparative Analysis of Machine Learning Algorithms for Building Archetypes Development. In 2018.* Chicago: ASHRAE and IBPSA-USA, 2018.

- [91] N. Gaitani, C. Lehmann, M. Santamouris, G. Mihalakakou, and P. Patargias, "Using principal component and cluster analysis in the heating evaluation of the school building sector," *Applied Energy*, vol. 87, no. 6, pp. 2079–2086, 2010.
- [92] A. T. Booth, R. Choudhary, and D. J. Spiegelhalter, "Handling uncertainty in housing stock models," *Building and Environment*, vol. 48, no. 1, pp. 35–47, 2012. [Online]. Available: <http://dx.doi.org/10.1016/j.buildenv.2011.08.016>
- [93] H. X. Zhao and F. Magoulès, "A review on the prediction of building energy consumption," *Renewable and Sustainable Energy Reviews*, vol. 16, no. 6, pp. 3586–3592, 2012. [Online]. Available: <http://dx.doi.org/10.1016/j.rser.2012.02.049>
- [94] A. Fouquier, S. Robert, F. Suard, L. Stéphan, and A. Jay, "State of the art in building modelling and energy performances prediction: A review," *Renewable and Sustainable Energy Reviews*, vol. 23, pp. 272–288, 2013.
- [95] R. Kumar, R. K. Aggarwal, and J. D. Sharma, "Energy analysis of a building using artificial neural network: A review," *Energy and Buildings*, vol. 65, pp. 352–358, 2013. [Online]. Available: <http://dx.doi.org/10.1016/j.enbuild.2013.06.007>
- [96] X. Li and J. Wen, "Review of building energy modeling for control and operation," *Renewable and Sustainable Energy Reviews*, vol. 37, pp. 517–537, 2014. [Online]. Available: <http://dx.doi.org/10.1016/j.rser.2014.05.056>
- [97] N. Fumo, "A review on the basics of building energy estimation," *Renewable and Sustainable Energy Reviews*, vol. 31, pp. 53–60, 2014. [Online]. Available: <http://dx.doi.org/10.1016/j.rser.2013.11.040>
- [98] A. S. Ahmad, M. Y. Hassan, M. P. Abdullah, H. A. Rahman, F. Hussin, H. Abdullah, and R. Saidur, "A review on applications of ANN and SVM for building electrical energy consumption forecasting," *Renewable and Sustainable Energy Reviews*, vol. 33, pp. 102–109, 2014. [Online]. Available: <http://dx.doi.org/10.1016/j.rser.2014.01.069>
- [99] CIBSE, *AM 11 Building performance modelling*, 2nd ed., H. Awbi, Ed. London: The Chartered Institution of Building Services Engineers (CIBSE), 2015.
- [100] E. H. Borgstein, R. Lamberts, and J. L. Hensen, "Evaluating energy performance in non-domestic buildings: A review," *Energy and Buildings*, vol. 128, pp. 734–755, 2016. [Online]. Available: <http://dx.doi.org/10.1016/j.enbuild.2016.07.018>
- [101] M. L. Chalal, M. Benachir, M. White, and R. Shrahily, "Energy planning and forecasting approaches for supporting physical improvement strategies in the building sector: A review," *Renewable and Sustainable Energy Reviews*, vol. 64, pp. 761–776, 2016. [Online]. Available: <http://dx.doi.org/10.1016/j.rser.2016.06.040>

- [102] V. S. K. V. Harish and A. Kumar, "A review on modeling and simulation of building energy systems," *Renewable and Sustainable Energy Reviews*, vol. 56, pp. 1272–1292, 2016. [Online]. Available: <http://dx.doi.org/10.1016/j.rser.2015.12.040>
- [103] Z. Wang and R. S. Srinivasan, "A review of artificial intelligence based building energy use prediction: Contrasting the capabilities of single and ensemble prediction models," *Renewable and Sustainable Energy Reviews*, vol. 75, no. September 2015, pp. 796–808, 2017. [Online]. Available: <http://dx.doi.org/10.1016/j.rser.2016.10.079>
- [104] Y. Wei, X. Zhang, Y. Shi, L. Xia, S. Pan, J. Wu, and M. Han, "A review of data-driven approaches for prediction and classification of building energy consumption," *Renewable and Sustainable Energy Reviews*, vol. 82, no. May 2017, pp. 1027–1047, 2018. [Online]. Available: <http://dx.doi.org/10.1016/j.rser.2017.09.108>
- [105] K. Amasyali and N. M. El-Gohary, "A review of data-driven building energy consumption prediction studies," *Renewable and Sustainable Energy Reviews*, vol. 81, no. April 2017, pp. 1192–1205, 2018. [Online]. Available: <http://dx.doi.org/10.1016/j.rser.2017.04.095>
- [106] C. Deb and A. Schlueter, "Review of data-driven energy modelling techniques for building retrofit," *Renewable and Sustainable Energy Reviews*, vol. 144, p. 110990, 7 2021.
- [107] X. Yang, S. Liu, Y. Zou, W. Ji, Q. Zhang, A. Ahmed, X. Han, Y. Shen, and S. Zhang, "Energy-saving potential prediction models for large-scale building: A state-of-the-art review," *Renewable and Sustainable Energy Reviews*, vol. 156, p. 111992, 3 2022.
- [108] ISO, "ISO 52000-1:2017 Energy performance of buildings — Overarching EPB assessment — Part 1: General framework and procedures," Switzerland, 2017.
- [109] W. Kim, J. Choi, and H. Cho, "Performance analysis of hybrid solar-geothermal CO₂ heat pump system for residential heating," *Renewable Energy*, vol. 50, pp. 596–604, 2013. [Online]. Available: <http://dx.doi.org/10.1016/j.renene.2012.07.020>
- [110] Y. J. Kim, S. H. Yoon, and C. S. Park, "Stochastic comparison between simplified energy calculation and dynamic simulation," *Energy and Buildings*, vol. 64, pp. 332–342, 2013. [Online]. Available: <http://dx.doi.org/10.1016/j.enbuild.2013.05.026>
- [111] D. B. Crawley, J. W. Hand, M. Kummert, and B. T. Griffith, "Contrasting the capabilities of building energy performance simulation programs," *Building and Environment*, vol. 43, no. 4, pp. 661–673, 4 2008. [Online]. Available: <http://linkinghub.elsevier.com/retrieve/pii/S0360132306003234>
- [112] D. van Dijk, "Epb standards: Why choose hourly calculation procedures?" *The REHVA European HVAC Journal*, vol. 55, pp. 6–12, 2018. [Online]. Available: https://www.rehva.eu/fileadmin/REHVA_Journal/REHVA_Journal_2018/RJ1/RJ.06-12/06-12_RJ1801.pdf

- [113] M. H. Kristensen, R. E. Hedegaard, and S. Petersen, "Hierarchical calibration of archetypes for urban building energy modeling," *Energy and Buildings*, 2018.
- [114] M. Österbring, Mata, L. Thuvander, M. Mangold, F. Johnsson, and H. Wallbaum, "A differentiated description of building-stocks for a georeferenced urban bottom-up building-stock model," *Energy and Buildings*, vol. 120, pp. 78–84, 2016. [Online]. Available: <http://dx.doi.org/10.1016/j.enbuild.2016.03.060>
- [115] Q. Li, S. J. Quan, G. Augenbroe, P. Pei, J. Yang, and J. Brown, "Building Energy Modelling At Urban Scale: Integration of Reduced Order Energy Model With Geographical Information," *Ibpsa*, no. Bepc 2012, p. 190, 2015.
- [116] D. Robinson, F. Haldi, J. H. Kämpf, P. Leroux, D. Perez, a. Rasheed, and U. Wilke, "CITYSIM: Comprehensive Micro-Simulation Of Resource Flows For Sustainable Urban Planning," *International IBPSA Conference*, pp. 1083–1090, 2009.
- [117] T. Hong, Y. Chen, S. H. Lee, and M. A. Piette, "CityBES : A Web-based Platform to Support City-Scale Building Energy Efficiency," in *Urban Computing*, 2016.
- [118] T. Hong, Y. Chen, X. Luo, N. Luo, and S. H. Lee, "Ten questions on urban building energy modeling," *Building and Environment*, vol. 168, no. October 2019, p. 106508, 2020. [Online]. Available: <https://doi.org/10.1016/j.buildenv.2019.106508>
- [119] W. Tian, Y. Heo, P. de Wilde, Z. Li, D. Yan, C. S. Park, X. Feng, and G. Augenbroe, "A review of uncertainty analysis in building energy assessment," *Renewable and Sustainable Energy Reviews*, vol. 93, no. May, pp. 285–301, 2018. [Online]. Available: <https://doi.org/10.1016/j.rser.2018.05.029>
- [120] E. Prataiviera, J. Vivian, G. Lombardo, and A. Zarrella, "Evaluation of the impact of input uncertainty on urban building energy simulations using uncertainty and sensitivity analysis," *Applied Energy*, vol. 311, p. 118691, 4 2022.
- [121] K. Menberg, Y. Heo, and R. Choudhary, "Influence of error terms in Bayesian calibration of energy system models," *Journal of Building Performance Simulation*, vol. 1493, no. May, 2018.
- [122] F. Scarpa, L. A. Tagliafico, and V. Bianco, "Financial and energy performance analysis of efficiency measures in residential buildings. a probabilistic approach," *Energy*, vol. 236, 12 2021.
- [123] S. Copiello, L. Gabrielli, and P. Bonifaci, "Evaluation of energy retrofit in buildings under conditions of uncertainty: The prominence of the discount rate," *Energy*, vol. 137, pp. 104–117, 10 2017.
- [124] E. D. Giuseppe, A. Massi, and M. D'Orazio, "Impacts of Uncertainties in Life Cycle Cost Analysis of Buildings Energy Efficiency Measures: Application to a Case Study," *Energy Procedia*, vol. 111, no. September 2016, pp. 442–451, 2017. [Online]. Available: <http://dx.doi.org/10.1016/j.egypro.2017.03.206>

- [125] E. Togashi, "Risk analysis of energy efficiency investments in buildings using the monte carlo method," *Journal of building performance simulation*, vol. 12, pp. 504–522, 2019.
- [126] A. Gelman, C. John B., S. Hal S., D. David B., V. Aki, and R. Donald B., *Bayesian data analysis*, 3rd ed. CRC press Taylor & Francis group, 2014.
- [127] D. Hou, I. G. Hassan, and L. Wang, "Review on building energy model calibration by bayesian inference," *Renewable and Sustainable Energy Reviews*, vol. 143, p. 110930, 6 2021.
- [128] J. Sokol, C. Cerezo Davila, and C. F. Reinhart, "Validation of a Bayesian-based method for defining residential archetypes in urban building energy models," *Energy and Buildings*, vol. 134, pp. 11–24, 2017. [Online]. Available: <http://dx.doi.org/10.1016/j.enbuild.2016.10.050>
- [129] Y. Yamaguchi, R. Choudhary, A. Booth, Y. Suzuki, and Y. Shimoda, "Urban-scale energy modelling of food supermarket considering uncertainty," *The proceedings of BS*, 2013.
- [130] A. T. Booth, R. Choudhary, and D. J. Spiegelhalter, "A hierarchical bayesian framework for calibrating micro-level models with macro-level data," *Journal of Building Performance Simulation*, vol. 6, no. 4, pp. 293–318, 2013.
- [131] A. T. Booth and R. Choudhary, "Decision making under uncertainty in the retrofit analysis of the UK housing stock: Implications for the Green Deal," *Energy and Buildings*, vol. 64, pp. 292–308, 2013. [Online]. Available: <http://dx.doi.org/10.1016/j.enbuild.2013.05.014>
- [132] R. E. Hedegaard, M. H. Kristensen, T. H. Pedersen, A. Brun, and S. Petersen, "Bottom-up modelling methodology for urban-scale analysis of residential space heating demand response," *Applied Energy*, vol. 242, no. November 2018, pp. 181–204, 2019. [Online]. Available: <https://doi.org/10.1016/j.apenergy.2019.03.063>
- [133] M. P. Prieto, P. M. Álvarez de Urbarri, and G. Tardioli, "Applying modeling and optimization tools to existing city quarters," in *Urban Energy Systems for Low-Carbon Cities*, 2019.
- [134] A. Chong, W. Xu, S. Chao, and N. T. Ngo, "Continuous-time Bayesian calibration of energy models using BIM and energy data," *Energy and Buildings*, 2019.
- [135] K. Menberg, Y. Heo, and R. Choudhary, "Sensitivity analysis methods for building energy models: Comparing computational costs and extractable information," *Energy and Buildings*, vol. 133, pp. 433–445, 2016. [Online]. Available: <http://dx.doi.org/10.1016/j.enbuild.2016.10.005>
- [136] W. Tian, "A review of sensitivity analysis methods in building energy analysis," *Renewable and Sustainable Energy Reviews*, vol. 20, pp. 411–419, 2013. [Online]. Available: <https://www.sciencedirect.com/science/article/pii/S1364032112007101>

- [137] M. D. Morris, "Factorial sampling plans for preliminary computational experiments," *Technometrics*, vol. 33, no. 2, pp. 161–174, 1991.
- [138] Y. Heo, "Bayesian Calibration of Building Energy Models for Energy Retrofit Decision-Making under Uncertainty," Ph.D. dissertation, Georgia Institute of Technology, 2011.
- [139] Y. Heo, R. Choudhary, and G. A. Augenbroe, "Calibration of building energy models for retrofit analysis under uncertainty," *Energy and Buildings*, vol. 47, pp. 550–560, 2012.
- [140] Y. Heo, D. J. Graziano, L. Guzowski, and R. T. Muehleisen, "Evaluation of calibration efficacy under different levels of uncertainty," *Journal of Building Performance Simulation*, vol. 8, no. 3, pp. 135–144, 2015.
- [141] Y. Heo, G. Augenbroe, D. Graziano, R. T. Muehleisen, and L. Guzowski, "Scalable methodology for large scale building energy improvement: Relevance of calibration in model-based retrofit analysis," *Building and Environment*, vol. 87, pp. 342–350, 2015. [Online]. Available: <http://dx.doi.org/10.1016/j.buildenv.2014.12.016>
- [142] S. Yang, W. Tian, E. Cubi, Q. Meng, Y. Liu, and L. Wei, "Comparison of Sensitivity Analysis Methods in Building Energy Assessment," *Procedia Engineering*, vol. 146, pp. 174–181, 2016. [Online]. Available: <http://dx.doi.org/10.1016/j.proeng.2016.06.369>
- [143] W. Tian, R. Choudhary, G. Augenbroe, and S. H. Lee, "Importance analysis and meta-model construction with correlated variables in evaluation of thermal performance of campus buildings," *Building and Environment*, vol. 92, pp. 61–74, 2015. [Online]. Available: <http://dx.doi.org/10.1016/j.buildenv.2015.04.021>
- [144] S. Lee, P. Karava, A. Tzempelikos, and I. Bilonis, "Inference of thermal preference profiles for personalized thermal environments with actual building occupants," *Building and Environment*, vol. 148, 2019.
- [145] H. Carstens, X. Xia, and S. Yadavalli, "Bayesian energy measurement and verification analysis," *Energies*, vol. 11, no. 2, pp. 1–20, 2018.
- [146] M. C. Kennedy and A. O'Hagan, "Bayesian calibration of computer models," *Journal of the Royal Statistical Society: Series B (Statistical Methodology)*, vol. 63, no. 3, pp. 425–464, 2001. [Online]. Available: <http://doi.wiley.com/10.1111/1467-9868.00294>
- [147] M. H. Kristensen, R. Choudhary, and S. Petersen, "Bayesian calibration of building energy models: Comparison of predictive accuracy using metered utility data of different temporal resolution," *Energy Procedia*, vol. 122, pp. 277–282, 2017. [Online]. Available: <https://doi.org/10.1016/j.egypro.2017.07.322>
- [148] J. K. Kruschke, *Doing Bayesian data analysis: A tutorial with R, JAGS, and Stan*, 2nd ed. Elsevier, 2014.

- [149] J. Gabry, “shinystan: interactive visual and numerical diagnostics and posterior analysis for Bayesian models.” 2017. [Online]. Available: [//mc-stan.org/shinystan/](https://mc-stan.org/shinystan/)
- [150] J. Gabry and T. Mahr, “bayesplot plotting bayesian models,” 2018. [Online]. Available: <https://mc-stan.org/bayesplot/>
- [151] R. Kumar, C. Carroll, A. Hartikainen, and O. Martin, “Arviz a unified library for exploratory analysis of bayesian models in python,” *Journal of Open Source Software*, vol. 4, p. 1143, 1 2019.
- [152] ANSI/ASHRAE, “ASHRAE Guideline 14-2014 Measurement of Energy and Demand Savings,” *Ashrae*, p. 140, 2014.
- [153] B. Lambert, *A student’s guide to Bayesian Calibration*, 1st ed., J. Seaman, Ed. London: SAGE Publications Ltd, 2018.
- [154] H. Lim and Z. J. Zhai, “Comprehensive evaluation of the influence of meta-models on Bayesian calibration,” *Energy and Buildings*, vol. 155, pp. 66–75, 2017. [Online]. Available: <http://dx.doi.org/10.1016/j.enbuild.2017.09.009>
- [155] Y. Kang and M. Krarti, “Bayesian-Emulator based parameter identification for calibrating energy models for existing buildings,” *Building Simulation*, vol. 9, no. 4, pp. 411–428, 2016.
- [156] Q. Li, L. Gu, G. Augenbroe, C. F. J. Wu, and J. Brown, “a Generic Approach To Calibrate Building Energy Models Under Uncertainty Using Bayesian Inference,” in *14th Conference of International Building Performance Simulation Association*, no. 2012, India, 2015, pp. 2913–2922.
- [157] Y. Heo, G. Augenbroe, and R. Choudhary, “Quantitative risk management for energy retrofit projects,” *Journal of Building Performance Simulation*, vol. 6, no. 4, pp. 257–268, 2013.
- [158] D. Gatt, C. Caruana, and C. Yousif, “Building Energy Renovation and Smart Integration of Renewables in a Social Housing Block Toward Nearly-Zero Energy Status,” *Frontiers in Energy Research*, vol. 8, 2020.
- [159] European Commission, “COMMISSION RECOMMENDATION (EU) 2016/1318 of 29 July 2016 on guidelines for the promotion of nearly zero-energy buildings and best practices to ensure that, by 2020, all new buildings are nearly zero-energy buildings,” Tech. Rep., 2016. [Online]. Available: <https://eur-lex.europa.eu/legal-content/EN/TXT/PDF/?uri=CELEX:32016H1318&from=RO>
- [160] S. Nagpal, J. Hanson, and C. Reinhart, “A framework for using calibrated campus-wide building energy models for continuous planning and greenhouse gas emissions reduction tracking,” *Applied Energy*, vol. 241, no. February, pp. 82–97, 2019. [Online]. Available: <https://doi.org/10.1016/j.apenergy.2019.03.010>

- [161] A. Chong and K. Menberg, "Guidelines for the Bayesian calibration of building energy models," *Energy & Buildings*, vol. 174, pp. 527–547, 2018. [Online]. Available: <https://doi.org/10.1016/j.enbuild.2018.06.028>
- [162] Kim Y.J., K. K.C., P. C.S., and K. I.H., "Deterministic vs. Stochastic Calibration of Energy Simulation Model for an Existing Building," in *IBPSA Asia Conference 2014*, 2014, pp. 586–593.
- [163] G. S. Pavlak, A. R. Florita, G. P. Henze, and B. Rajagopalan, "Comparison of traditional and bayesian calibration techniques for gray-box modeling," *Journal of Architectural Engineering*, vol. 20, no. 2, 2014.
- [164] S. Rouchier, M. Rabouille, and P. Oberlé, "Calibration of simplified building energy models for parameter estimation and forecasting: Stochastic versus deterministic modelling," *Building and Environment*, vol. 134, no. February, pp. 181–190, 2018. [Online]. Available: <https://doi.org/10.1016/j.buildenv.2018.02.043>
- [165] Q. Deng, X. Jiang, L. Zhang, and Q. Cui, "Making optimal investment decisions for energy service companies under uncertainty: A case study," *Energy*, vol. 88, 2015.
- [166] P. Lee, P. T. Lam, and W. L. Lee, "Performance risks of lighting retrofit in energy performance contracting projects," *Energy for Sustainable Development*, vol. 45, 2018.
- [167] P. Langlois and S. J. Hansen, *World ESCO Outlook*. River Publishers, 2020. [Online]. Available: https://books.google.com.mt/books?id=4kMPEAAAQBAJ&source=gbs_book_other_versions_r&redir_esc=y
- [168] R. Galvin, "Why German homeowners are reluctant to retrofit," *Building Research and Information*, vol. 42, no. 4, pp. 398–408, 2014.
- [169] M. Riddle and R. T. Muehleisen, "A Guide to Bayesian Calibration of Building Energy Models," in *2014 ASHRAE/IBPSA-USA Building Simulation Conference*, 2014.
- [170] R. T. Muehleisen and J. Bergerson, "Bayesian Calibration - What , Why And How," in *International High Performance Buildings Conference*. Lemont: Purdue University, 2016. [Online]. Available: <http://docs.lib.purdue.edu/ihpbc/167>
- [171] Y. Li, Z. O'Neill, L. Zhang, J. Chen, P. Im, and J. DeGraw, "Grey-box modeling and application for building energy simulations-a critical review," *Renewable and Sustainable Energy Reviews*, vol. 146, p. 111174, 2021.
- [172] F. Zhao, S. H. Lee, and G. Augenbroe, "Reconstructing building stock to replicate energy consumption data," *Energy and Buildings*, vol. 117, pp. 301–312, 2016. [Online]. Available: <http://dx.doi.org/10.1016/j.enbuild.2015.10.001>

- [173] ISO, "ISO 13790: Energy performance of buildings—Calculation of energy use for space heating and cooling (EN ISO 13790: 2008)," *European Committee for Standardization (CEN), Brussels*, 2008.
- [174] Q. Li, G. Augenbroe, and J. Brown, "Assessment of linear emulators in lightweight Bayesian calibration of dynamic building energy models for parameter estimation and performance prediction," *Energy and Buildings*, vol. 124, pp. 194–202, 2016.
- [175] W. Tian, S. Yang, Z. Li, S. Wei, W. Pan, and Y. Liu, "Identifying informative energy data in Bayesian calibration of building energy models," *Energy and Buildings*, vol. 119, pp. 363–376, 2016. [Online]. Available: <http://dx.doi.org/10.1016/j.enbuild.2016.03.042>
- [176] A. Chong, K. P. Lam, M. Pozzi, and J. Yang, "Bayesian calibration of building energy models with large datasets," *Energy and Buildings*, vol. 154, pp. 343–355, 2017. [Online]. Available: <https://doi.org/10.1016/j.enbuild.2017.08.069>
- [177] H. Lim and Z. J. Zhai, "Influences of energy data on Bayesian calibration of building energy model," *Applied Energy*, vol. 231, no. September, pp. 686–698, 2018. [Online]. Available: <https://doi.org/10.1016/j.apenergy.2018.09.156>
- [178] M. D. Hoffman and A. Gelman, "The No-U-Turn Sampler: Adaptively Setting Path Lengths in Hamiltonian Monte Carlo," *Journal of Machine Learning Research*, vol. 15, pp. 1593–1623, 2014. [Online]. Available: <http://arxiv.org/abs/1111.4246>
- [179] L. Raillon and C. Ghiaus, "An efficient Bayesian experimental calibration of dynamic thermal models," *Energy*, vol. 152, pp. 818–833, 2018. [Online]. Available: <https://doi.org/10.1016/j.energy.2018.03.168>
- [180] Stan development team, "Stan version 2.19.3," 2020. [Online]. Available: <http://mc-stan.org/>
- [181] J. Yuan, V. Nian, B. Su, and Q. Meng, "A simultaneous calibration and parameter ranking method for building energy models," *Applied Energy*, vol. 206, no. May, pp. 657–666, 2017. [Online]. Available: <https://doi.org/10.1016/j.apenergy.2017.08.220>
- [182] C. Zhu, W. Tian, B. Yin, Z. Li, and J. Shi, "Uncertainty calibration of building energy models by combining approximate bayesian computation and machine learning algorithms," *Applied energy*, vol. 268, p. 115025, 2020.
- [183] F. Monari, "An approach for identifying sources of inadequacy and upgrades in models with high-dimensional outputs and boundary conditions," no. March, 2018. [Online]. Available: <https://www.researchgate.net/publication/325049095%0AAn>
- [184] D. H. Yi, D. W. Kim, and C. S. Park, "Parameter identifiability in Bayesian inference for building energy models," *Energy and Buildings*, 2019. [Online]. Available: <https://linkinghub.elsevier.com/retrieve/pii/S0378778819301574>

- [185] D. Yu, "A two-step approach to forecasting city-wide building energy demand," *Energy and Buildings*, vol. 160, pp. 1–9, 2018. [Online]. Available: <http://dx.doi.org/10.1016/j.enbuild.2017.11.063>
- [186] F. Johari, G. Peronato, P. Sadeghian, X. Zhao, and J. Widén, "Urban building energy modeling: State of the art and future prospects," *Renewable and Sustainable Energy Reviews*, vol. 128, p. 109902, 2020.
- [187] P. Raftery, M. Keane, and A. Costa, "Calibrating whole building energy models: Detailed case study using hourly measured data," *Energy and Buildings*, vol. 43, no. 12, pp. 3666–3679, 2011. [Online]. Available: <http://dx.doi.org/10.1016/j.enbuild.2011.09.039>
- [188] ASHRAE, "Ansi/ashrae/ies standard 90.1–2013. energy standard for buildings except low-rise residential buildings," 2013.
- [189] H. Yi, "User-driven automation for optimal thermal-zone layout during space programming phases," *Architectural Science Review*, vol. 59, 2016.
- [190] T. Dogan, C. Reinhart, and P. Michalatos, "Autozoner: an algorithm for automatic thermal zoning of buildings with unknown interior space definitions," *Journal of Building Performance Simulation*, vol. 9, no. 2, pp. 176–189, 2016. [Online]. Available: <https://doi.org/10.1080/19401493.2015.1006527>
- [191] P. Nageler, G. Zahrer, R. Heimrath, T. Mach, F. Mauthner, I. Leusbrock, H. Schranzhofer, and C. Hochenauer, "Novel validated method for gis based automated dynamic urban building energy simulations," *Energy*, vol. 139, 2017.
- [192] Y. Chen and T. Hong, "Impacts of building geometry modeling methods on the simulation results of urban building energy models," *Applied Energy*, vol. 215, no. January, pp. 717–735, 2018. [Online]. Available: <https://doi.org/10.1016/j.apenergy.2018.02.073>
- [193] D. Gatt and C. Yousif, "Renovating primary school buildings in Malta to achieve cost-optimal energy performance and comfort levels ISBN 978-99957-0-935-8," in *Proceedings of the 2016 International Sustainable Built Environment Conference (SBE2016) Europe and the Mediterranean Towards a Sustainable Built Environment, 16-18 March*, R. Paul Borg, Ed. Valletta, Malta: Sustainable Built Environment Malta, 2016, pp. 453–460. [Online]. Available: <https://www.um.edu.mt/library/oar/handle/123456789/26272>
- [194] U. Ali, M. Haris, F. Alshehri, E. Mangina, and J. O'Donnell, "Comparative analysis of machine learning algorithms for building archetypes development." ASHRAE and IBPSA-USA, 2018.
- [195] J. Reyna, E. Wilson, A. Satre-meloy, A. Egerter, C. Bianchi, M. Praprost, A. Speake, L. Liu, A. Parker, R. Horsey, S. Rothgeb, L. Berkeley, J. Reyna, E. Wilson, A. Satre-meloy, A. Egerter, C. Bianchi, M. Praprost, A. Speake, L. Liu, A. Parker, R. Horsey, and S. Rothgeb, "U.s. building stock characterization study: A national typology for decarbonizing u.s. buildings. part 1: Residential buildings," 2021. [Online]. Available: www.nrel.gov/docs/fy22osti/81186.pdf

- [196] T. Buso, C. Becchio, and S. P. Corgnati, "NZEB, cost- and comfort-optimal retrofit solutions for an Italian Reference Hotel," *Energy Procedia*, vol. 140, pp. 217–230, 2017. [Online]. Available: <https://doi.org/10.1016/j.egypro.2017.11.137>
- [197] M. Economidou, "Europe's buildings under the microscope a country-by-country review of the energy performance of buildings," Buildings Performance Institute Europe (BPIE), Brussels, Belgium, Tech. Rep., 2011. [Online]. Available: http://www.bpie.eu/documents/BPIE/LR_CbC_study.pdf
- [198] D. D'Agostino, B. Cuniberti, and P. Bertoldi, "Data on european non-residential buildings," *Data in Brief*, vol. 14, 2017.
- [199] F. O. Cunha and A. C. Oliveira, "Benchmarking for realistic nzeb hotel buildings," *Journal of Building Engineering*, vol. 30, p. 101298, 7 2020.
- [200] R. Bointner and A. Toleikyte, "Deliverable 2.1 shopping mall features in eu-28 + norway," pp. 1–31, 2014. [Online]. Available: <papers2://publication/uuid/68B4ECB6-9F24-4B54-8D56-72B80658CE6B>
- [201] M. Ferrando, F. Causone, T. Hong, and Y. Chen, "Urban Building Energy Modeling (UBEM) Tools: A State-of-the-Art Review of bottom-up physics-based approaches," *Sustainable Cities and Society*, vol. 62, no. July, p. 102408, 2020. [Online]. Available: <https://doi.org/10.1016/j.scs.2020.102408>
- [202] Mata, A. Sasic Kalagasidis, and F. Johnsson, "Building-stock aggregation through archetype buildings: France, Germany, Spain and the UK," *Building and Environment*, vol. 81, pp. 270–282, 2014. [Online]. Available: <http://dx.doi.org/10.1016/j.buildenv.2014.06.013>
- [203] T. Loga, B. Stein, and N. Diefenbach, "TABULA building typologies in 20 European countries—Making energy-related features of residential building stocks comparable," *Energy and Buildings*, vol. 132, pp. 4–12, 2016. [Online]. Available: <http://dx.doi.org/10.1016/j.enbuild.2016.06.094>
- [204] P. Torcellini, M. Deru, B. Griffith, and K. Benne, "DOE Commercial Building Benchmark Models Preprint," *ACEEE Summer Study on Energy Efficiency in Buildings*, no. Eia 2005, p. 12, 2008. [Online]. Available: <http://www.nrel.gov/docs/fy08osti/43291.pdf>
- [205] C. E. Kontokosta, "A market-specific methodology for a commercial building energy performance index," *Journal of Real Estate Finance and Economics*, vol. 51, 2015.
- [206] R. Todeschini, V. Consonni, A. Mauri, and M. Pavan, "Detecting "bad" regression models: Multicriteria fitness functions in regression analysis," *Analytica Chimica Acta*, vol. 515, 2004.
- [207] A. Kassambara, *Practical Guide To Principal Component Methods in R: PCA, M (CA), FAMD, MFA, HCPC, factoextra.*, 2017, vol. 2.

- [208] M. Greenacre and J. Blasius, Eds., *Multiple Correspondence Analysis and Related Methods*, 1st ed. Chapman and Hall/CRC, 2006.
- [209] Z. Huang, "Extensions to the k-means algorithm for clustering large data sets with categorical values," *Data Mining and Knowledge Discovery*, vol. 2, 1998.
- [210] A. Chaturvedi, K. Foods, P. E. Green, and J. D. Carroll, "K-modes clustering," *Journal of Classification*, vol. 18, 2001.
- [211] A. Aranda, G. Ferreira, M. D. Mainar-Toledo, S. Scarpellini, and E. Llera Sastresa, "Multiple regression models to predict the annual energy consumption in the Spanish banking sector," *Energy and Buildings*, vol. 49, pp. 380–387, 2012. [Online]. Available: <http://dx.doi.org/10.1016/j.enbuild.2012.02.040>
- [212] A. Kavousian, R. Rajagopal, and M. Fischer, "Determinants of residential electricity consumption: Using smart meter data to examine the effect of climate, building characteristics, appliance stock, and occupants' behavior," *Energy*, vol. 55, 2013.
- [213] S. S. Amiri, M. Mottahedi, and S. Asadi, "Using multiple regression analysis to develop energy consumption indicators for commercial buildings in the U.S." *Energy and Buildings*, vol. 109, pp. 209–216, 2015. [Online]. Available: <http://dx.doi.org/10.1016/j.enbuild.2015.09.073>
- [214] M. Mangold, M. Österbring, and H. Wallbaum, "Handling data uncertainties when using swedish energy performance certificate data to describe energy usage in the building stock," *Energy and Buildings*, vol. 102, 2015.
- [215] P. Refaeilzadeh, L. Tang, and H. Liu, "Cross-validation," pp. 1–7, 2016. [Online]. Available: https://doi.org/10.1007/978-1-4899-7993-3_565-2
- [216] World Travel & Tourism Council (WTTC), "Travel & Tourism economic impact 2017 Malta," WORLD TRAVEL & TOURISM COUNCIL (WTTC), United Kingdom, Tech. Rep., 2017. [Online]. Available: <https://www.wttc.org/-/media/files/reports/economic-impact-research/countries-2017/malta2017.pdf>
- [217] E. Dascalaki and C. A. Balaras, "XENIOS - A methodology for assessing refurbishment scenarios and the potential of application of RES and RUE in hotels," *Energy and Buildings*, vol. 36, no. 11, pp. 1091–1105, 2004.
- [218] M. Karagiorgas, T. Tsoutsos, V. Drosou, S. Pouffary, T. Pagano, G. L. Lara, and J. M. Melim Mendes, "HOTRES: Renewable energies in the hotels. An extensive technical tool for the hotel industry," *Renewable and Sustainable Energy Reviews*, vol. 10, no. 3, pp. 198–224, 2006.
- [219] RELACS Project Team, "RELACS – Sustainable Energy for competitive tourist accommodation, RELACS publications," 2013. [Online]. Available: <https://ec.europa.eu/energy/intelligent/>

- projects/sites/iee-projects/files/projects/documents/relacs_final_report_en.pdf
- [220] Hotel Energy Solutions, “HES E-Toolkit User Manual, Energy efficiency and Renewable Energy Applications in the Hotel Sector,” Hotel Energy Solutions project publications, Tech. Rep., 2011.
- [221] T. Tsoutsos, S. Tournaki, C. A. d. Santos, and R. Vercellotti, “Nearly Zero Energy Buildings Application in Mediterranean Hotels,” *Energy Procedia*, vol. 42, pp. 230–238, 2013. [Online]. Available: <http://www.sciencedirect.com/science/article/pii/S1876610213017256>
- [222] S. Tournaki, M. Frangou, T. Tsoutsos, and R. Morell, “Nearly Zero Energy Hotels—From European Policy to Real Life Examples: the neZEH Pilot Hotels,” *Nezeh.Eu*, 2014. [Online]. Available: http://www.nezeh.eu/assets/media/PDF/neZEH_EinB2014_Proceedings63.pdf
- [223] T. Tsoutsos, S. Tournaki, M. Frangou, and M. Tsitoura, “Creating paradigms for nearly zero energy hotels in South Europe,” *AIMS Energy*, vol. 6, no. October 2017, pp. 1–18, 2018.
- [224] “Tourism accommodation establishments regulations,” 2012. [Online]. Available: <https://legislation.mt/eli/sl/409.4/eng/pdf>
- [225] “Malta Hotels and Restaurants Association (MHRA).” [Online]. Available: <http://mhra.org.mt/>
- [226] V. Bianco, D. Righi, F. Scarpa, and L. A. Tagliafico, “Modeling energy consumption and efficiency measures in the Italian hotel sector,” *Energy and Buildings*, vol. 149, pp. 329–338, 2017. [Online]. Available: <http://dx.doi.org/10.1016/j.enbuild.2017.05.077>
- [227] P. O. Oluseyi, O. M. Babatunde, and O. A. Babatunde, “Assessment of energy consumption and carbon footprint from the hotel sector within Lagos, Nigeria,” *Energy and Buildings*, vol. 118, pp. 106–113, 2016. [Online]. Available: <http://dx.doi.org/10.1016/j.enbuild.2016.02.046>
- [228] D. Gatt and C. Yousif, “Policy measures addressing nearly zero-energy buildings in the small island state of Malta,” in *Handbook of Governance in Small States*, 1st ed., L. Briguglio, J. Byron, S. Moncada, and W. Veenendaal, Eds. Routledge, 2020, ch. 9.
- [229] Building Regulation Office (BRO), “Technical Document F Part 1: Minimum Energy Performance Requirements for Buildings in Malta,” Building Regulation Office (BRO), Malta, Tech. Rep., 2015. [Online]. Available: <https://epc.gov.mt/legislation>
- [230] BRO, “Technical Guide F Part 2 : Minimum Energy Performance Requirements for Buildings Services in Malta,” Building Regulation Office (BRO), Malta, Tech. Rep., 2015. [Online]. Available: <https://epc.gov.mt/legislation>
- [231] M. Lenzen, Y.-Y. Sun, F. Faturay, Y.-P. Ting, A. Geschke, and A. Malik, “The carbon footprint of global tourism,” *Nature Climate Change*, vol. 8, pp. 522–528, 2018. [Online]. Available: <https://doi.org/10.1038/s41558-018-0141-x>

- [232] E. Borg, "Analysis for a Cost-Effective and Efficient Heating & Cooling," Malta, 2015. [Online]. Available: <https://ec.europa.eu/energy/sites/ener/files/documents/HCComprehensiveAssessment-Art141and143.pdf>
- [233] United Nations Environment Programme and World Tourism Organization (UNWTO), *Tourism in the Green Economy – Background Report*. Madrid: United Nations Environment Programme and World Tourism Organization (UNWTO), 2012. [Online]. Available: <https://www.e-unwto.org/doi/book/10.18111/9789284414529>
- [234] A. Pinto, M. Bernardino, A. S. Santos, and F. E. Santo, "Climate change impact assessment in hotels: methodology and adaptation strategies for high quality hotels," *WIT Transactions on The Built Environment*, vol. 161, no. Arc, pp. 33–44, 2016. [Online]. Available: <http://library.witpress.com/viewpaper.asp?pcode=ARC16-004-1>
- [235] S. M. Deng and J. Burnett, "Study of energy performance of hotel buildings in hong kong," *Energy and Buildings*, vol. 31, pp. 7–12, 2000.
- [236] C. W. Hsu, T. C. Kuo, G. S. Shyu, and P. S. Chen, "Low carbon supplier selection in the hotel industry," *Sustainability*, vol. 6, no. 5, pp. 2658–2684, 2014.
- [237] F. Tang, "Research of low-carbon transition path of star hotels-A case study of Guilin," *2015 International Seminar on Social Science and Humanistic Education (Sshe 2015)*, vol. 24, pp. 1–7, 2016.
- [238] S. Tournaki, M. Frangou, T. Tsoutsos, R. Morell, I. Guerrero, Z. Urosevic, and A. Derjanecz, "Towards Nearly Zero Energy Hotels Technical Analysis and Recommendations," in *5th International Conference on Renewable Energy Sources and Energy Efficiency*, Nicosia, Cyprus, 2016, pp. 323–331. [Online]. Available: http://www.nezeh.eu/assets/media/PDF/RES&EE_2016_CY_conference_paper487.pdf
- [239] J. C. Wang, "A study on the energy performance of hotel buildings in Taiwan," *Energy and Buildings*, vol. 49, pp. 268–275, 2012. [Online]. Available: <http://dx.doi.org/10.1016/j.enbuild.2012.02.016>
- [240] S. Lu, S. Wei, K. Zhang, X. Kong, and W. Wu, "Investigation and analysis on the energy consumption of starred hotel buildings in Hainan Province, the tropical region of China," *Energy Conversion and Management*, vol. 75, pp. 570–580, 2013. [Online]. Available: <http://dx.doi.org/10.1016/j.enconman.2013.07.008>
- [241] S. N. Boemi and O. Irulegi, "The hotel industry: Current situation and its steps beyond sustainability," in *Energy Performance of Buildings: Energy Efficiency and Built Environment in Temperate Climates*, S.-N. Boemi, O. Irulegi, and M. Santamouris, Eds., 2015, ch. 12, pp. 235–250.
- [242] F. AlFaris, B. Abu-Hijleh, and A. Abdul-Ameer, "Using integrated control methodology to optimize energy performance for the guest rooms in UAE hospitality sector," *Applied Thermal Engineering*,

- vol. 100, pp. 1085–1094, 2016. [Online]. Available: <http://dx.doi.org/10.1016/j.applthermaleng.2016.01.154>
- [243] Y. Ali, M. Mustafa, S. Al-Mashaqbah, K. Mashal, and M. Mohsen, "Potential of energy savings in the hotel sector in Jordan," *Energy Conversion and Management*, vol. 49, no. 11, pp. 3391–3397, 2008.
- [244] V. Cingoski and B. Petrevska, "Making hotels more energy efficient: The managerial perception," *Economic Research-Ekonomska Istrazivanja*, vol. 31, no. 1, pp. 87–101, 2018. [Online]. Available: <http://doi.org/10.1080/1331677X.2017.1421994>
- [245] L. O. Idahosa, N. N. Marwa, and J. O. Akotey, "Energy (electricity) consumption in South African hotels: A panel data analysis," *Energy and Buildings*, vol. 156, pp. 207–217, 2017. [Online]. Available: <http://dx.doi.org/10.1016/j.enbuild.2017.09.051>
- [246] M. E. Kahn and P. P. Liu, "Utilizing "Big Data" to Improve the Hotel Sector's Energy Efficiency: Lessons from Recent Economics Research," *Cornell Hospitality Quarterly*, vol. 57, no. 2, pp. 202–210, 2016.
- [247] M. Karagiorgas, T. Tsoutsos, and A. Moiá-Pol, "A simulation of the energy consumption monitoring in Mediterranean hotels. Application in Greece," *Energy and Buildings*, vol. 39, no. 4, pp. 416–426, 2007.
- [248] J. H. Lai, "Energy use and maintenance costs of upmarket hotels," *International Journal of Hospitality Management*, vol. 56, pp. 33–43, 2016. [Online]. Available: <http://dx.doi.org/10.1016/j.ijhm.2016.04.011>
- [249] A. Mardani, E. K. Zavadskas, D. Streimikiene, A. Jusoh, K. M. Nor, and M. Khoshnoudi, "Using fuzzy multiple criteria decision making approaches for evaluating energy saving technologies and solutions in five star hotels: A new hierarchical framework," *Energy*, vol. 117, pp. 131–148, 2016. [Online]. Available: <http://dx.doi.org/10.1016/j.energy.2016.10.076>
- [250] D. S. Nheta and N. Tondani, "Measures and practices implemented by hotels to minimise the causes and effects of global warming : the case of Vhembe District," vol. 5, no. 3, pp. 1–19, 2016.
- [251] S. Önüt and S. Soner, "Energy efficiency assessment for the Antalya Region hotels in Turkey," *Energy and Buildings*, vol. 38, no. 8, pp. 964–971, 2006.
- [252] M. d. P. Pablo-Romero, R. Pozo-Barajas, and J. Sánchez-Rivas, "Relationships between tourism and hospitality sector electricity consumption in Spanish Provinces (1999-2013)," *Sustainability (Switzerland)*, vol. 9, no. 4, 2017.
- [253] K. Poldrugovac, M. Tekavcic, and S. Jankovic, "Efficiency in the hotel industry : an empirical examination of the most influential factors," *Economic Research-Ekonomska Istrazivanja*, vol. 29, no. 1, pp. 1–15, 2016. [Online]. Available: <http://dx.doi.org/10.1080/1331677X.2016.1177464>

- [254] R. Priyadarsini, W. Xuchao, and L. S. Eang, "A study on energy performance of hotel buildings in Singapore," *Energy and Buildings*, vol. 41, no. 12, pp. 1319–1324, 2009.
- [255] B. Rosselló-Batlé, A. Moià, A. Cladera, and V. Martínez, "Energy use, CO2 emissions and waste throughout the life cycle of a sample of hotels in the Balearic Islands," *Energy and Buildings*, vol. 42, no. 4, pp. 547–558, 2010.
- [256] M. Tang, X. Fu, H. Cao, Y. Shen, H. Deng, and G. Wu, "Energy Performance of Hotel Buildings in Lijiang, China," *Sustainability*, vol. 8, no. 8, p. 780, 2016. [Online]. Available: <http://www.mdpi.com/2071-1050/8/8/780>
- [257] K. T. Tsai, T. P. Lin, R. L. Hwang, and Y. J. Huang, "Carbon dioxide emissions generated by energy consumption of hotels and homestay facilities in Taiwan," *Tourism Management*, vol. 42, pp. 13–21, 2014. [Online]. Available: <http://dx.doi.org/10.1016/j.tourman.2013.08.017>
- [258] X. Wang, N. Q. Wu, Y. Qiao, and Q. B. Song, "Assessment of energy-saving practices of the hospitality industry in Macau," *Sustainability (Switzerland)*, vol. 10, no. 1, pp. 1–14, 2018.
- [259] Y. Xin, S. Lu, N. Zhu, and W. Wu, "Energy consumption quota of four and five star luxury hotel buildings in Hainan province, China," *Energy and Buildings*, vol. 45, pp. 250–256, 2012. [Online]. Available: <http://dx.doi.org/10.1016/j.enbuild.2011.11.014>
- [260] W. Xuchao, R. Priyadarsini, and L. Siew Eang, "Benchmarking energy use and greenhouse gas emissions in Singapore's hotel industry," *Energy Policy*, vol. 38, no. 8, pp. 4520–4527, 2010. [Online]. Available: <http://dx.doi.org/10.1016/j.enpol.2010.04.006>
- [261] Z. Yao, Z. Zhuang, and W. Gu, "Study on Energy Use Characteristics of Hotel Buildings in Shanghai," *Procedia Engineering*, vol. 121, pp. 1977–1982, 2015.
- [262] S. Deng, "Energy and water uses and their performance explanatory indicators in hotels in Hong Kong," *Energy and Buildings*, vol. 35, no. 8, pp. 775–784, 2003.
- [263] P. Bohdanowicz and I. Martinac, "Determinants and benchmarking of resource consumption in hotels-Case study of Hilton International and Scandic in Europe," *Energy and Buildings*, vol. 39, no. 1, pp. 82–95, 2007.
- [264] S. M. Deng and J. Burnett, "Study of energy performance of hotel buildings in Hong Kong," *Energy and Buildings*, vol. 31, no. 1, pp. 7–12, 2000.
- [265] D. N. Trung and S. Kumar, "Resource use and waste management in Vietnam hotel industry," *Journal of Cleaner Production*, vol. 12, no. 2, pp. 109–116, 2005.

- [266] Y. Zhao, Y. Lu, C. Yan, and S. Wang, "MPC-based optimal scheduling of grid-connected low energy buildings with thermal energy storages," *Energy and Buildings*, vol. 86, pp. 415–426, 2015. [Online]. Available: <http://dx.doi.org/10.1016/j.enbuild.2014.10.019>
- [267] V. Garg, J. Mathur, S. Tetali, and A. Bhatia, *Building energy simulation: A workbook using designbuilder™*, 2017.
- [268] D. B. Crawley, L. K. Lawrie, F. C. Winkelmann, W. F. Buhl, Y. J. Huang, C. O. Pedersen, R. K. Strand, R. J. Liesen, D. E. Fisher, M. J. Witte, and J. Glazer, "EnergyPlus: Creating a new-generation building energy simulation program," *Energy and Buildings*, vol. 33, no. 4, pp. 319–331, 2001. [Online]. Available: <https://www.sciencedirect.com/science/article/abs/pii/S037877880001146>
- [269] W. O'Brien, A. Athienitis, and T. Kesik, "Thermal zoning and interzonal airflow in the design and simulation of solar houses: A sensitivity analysis," *Journal of Building Performance Simulation*, vol. 4, 2011.
- [270] Q. Li, R. Choudhary, Y. Heo, and G. Augenbroe, "Effective and scalable modelling of existing non-domestic buildings with radiator system under uncertainty," 2020.
- [271] S. C. M. Hui and K. F. Wong, "Benchmarking the energy performance of hotel buildings in Hong Kong," *Liaoning (Dalian) – Hong Kong Joint Symposium*, no. September, pp. 56–69, 2010.
- [272] G. Dall'O', *Green Energy Audit of Buildings, A guide for a sustainable energy audit of buildings*, 1st ed. London: Springer London, 2013. [Online]. Available: <https://link.springer.com/book/10.1007/978-1-4471-5064-0>
- [273] E. Ricaurte and R. Jagarajan, "Hotel sustainability benchmarking index 2021: Carbon, energy, and water," 9 2021. [Online]. Available: <https://ecommons.cornell.edu/handle/1813/109990>
- [274] D. Gatt and C. Yousif, "ZeroCO2 Building - How low can we go: A Case Study of a Small Hotel in Gozo - Malta," in *Proceedings of the Sustainable Energy 2016: The ISE Annual Conference ISBN No. 978-99957-853-1-4*. Valletta, Malta: Institute for Sustainable Energy, University of Malta, 2016, pp. 30–37. [Online]. Available: <https://www.um.edu.mt/library/oar/handle/123456789/23284>
- [275] T. Caruana and C. Yousif, "The Effect of Different Glazing Apertures on the Thermal Performance of Maltese Buildings," in *Proceedings of the 2016 International Sustainable Built Environment Conference (SBE2016) Europe and the Mediterranean Towards a Sustainable Built Environment, 16-18 March 2016*, C. S. S. Ruben Paul Borg, Paul Gauci, Ed. Valletta, Malta: SBE, 2016, pp. 435–442. [Online]. Available: <https://www.um.edu.mt/library/oar/handle/123456789/26268>
- [276] NumFOCUS, "pandas - python data analysis library," 2 2022. [Online]. Available: <https://pandas.pydata.org/>

- [277] R. Vallat, “pingouin · pypi statistical package for python,” 2022. [Online]. Available: <https://pypi.org/project/pingouin/>
- [278] MHRA and Energy 7, “Benchmarking Energy Sustainability Targets (BEST),” 2017. [Online]. Available: <http://mbb.org.mt/wp-content/uploads/2017/07/BEST-MHRA.pdf>
- [279] A. Mousia and A. Dimoudi, “Energy performance of open air swimming pools in greece,” *Energy and Buildings*, vol. 90, pp. 166–172, 3 2015.
- [280] ASHRAE, *2019 ASHRAE Handbook - Heating Ventilation and Air Conditioning Applications*. ASHRAE, 2019.
- [281] Hotel Energy Solutions, “Analysis on the energy use of European hotels: online survey and desk research,” Hotel Energy Solutions project publications, Tech. Rep., 2011.
- [282] D. M. Said, K. Youssef, and H. Waheed, “Energy efficiency opportunities in hotels,” *Renewable Energy and Sustainable Development (RES D)*, vol. 3, 2017. [Online]. Available: <http://dx.doi.org/10.21622/RES D.2017.03.1.099>
- [283] M. Halford, “prince · pypi statistical factor analysis in python,” 2020. [Online]. Available: <https://pypi.org/project/prince/>
- [284] J. H. Ward, “Hierarchical grouping to optimize an objective function,” *Journal of the American Statistical Association*, vol. 58, 1963.
- [285] M. Kaushik and M. Mathur, “Comparative study of k-means and hierarchical clustering techniques,” *International Journal of Software Hardware Research in Engineering (IJSHRE)*, vol. 2, 2014.
- [286] M. Chavent, V. Kuentz-Simonet, A. Labenne, and J. Saracco, “Multivariate analysis of mixed type data: The pcamixdata r package,” 2014.
- [287] Addinsoft, “XLSTAT.” [Online]. Available: <https://www.xlstat.com/en/>
- [288] J. de Vos Nelis, “kmodes · pypi python implementations of the k-modes and k-prototypes clustering algorithms for clustering categorical data.” 2022. [Online]. Available: <https://pypi.org/project/kmodes/>
- [289] F. Cao, J. Liang, and L. Bai, “A new initialization method for categorical data clustering,” *Expert Systems with Applications*, vol. 36, 2009.
- [290] P. Bruce, A. Bruce, and P. Gedeck, *Practical statistics for data scientists: 50+ essential concepts using R and Python*. O’Reilly Media, 2020.

- [291] S. Talha Hascelik, "python_stepwiseSelection," 2019. [Online]. Available: [https://github.com/talhahascalik/python\({}\)stepwiseSelection](https://github.com/talhahascalik/python({})stepwiseSelection)
- [292] W. D. Fisher, "On grouping for maximum homogeneity," *Journal of the American Statistical Association*, vol. 53, pp. 789–798, 1958. [Online]. Available: <https://www.tandfonline.com/doi/abs/10.1080/01621459.1958.10501479>
- [293] T. Hong, F. Buhl, P. Haves, S. Selkowitz, and M. Wetter, "Comparing computer run time of building simulation programs," *Building Simulation*, vol. 1, no. 3, pp. 210–213, 8 2008. [Online]. Available: <http://link.springer.com/10.1007/s12273-008-8123-y>
- [294] A. Tindale, "Working with large models and speeding up simulations - designbuilder," 3 2020. [Online]. Available: <https://support.designbuilder.co.uk/index.php?/Default/Knowledgebase/Article/View/26/7/working-with-large-models-and-speeding-up-simulations>
- [295] A. Chong, Y. Gu, and H. Jia, "Calibrating building energy simulation models: A review of the basics to guide future work," *Energy and Buildings*, vol. 253, p. 111533, 2021.
- [296] P. Westermann and R. Evins, "Surrogate modelling for sustainable building design—a review," *Energy and Buildings*, vol. 198, pp. 170–186, 2019.
- [297] O. Tsvetkova and T. B. Ouarda, "A review of sensitivity analysis practices in wind resource assessment," *Energy Conversion and Management*, vol. 238, p. 114112, 6 2021.
- [298] A.-T. Nguyen and S. Reiter, "A performance comparison of sensitivity analysis methods for building energy models," *Building Simulation*, vol. 8, no. 6, pp. 651–664, 2015. [Online]. Available: <http://link.springer.com/10.1007/s12273-015-0245-4>
- [299] F. D. Sepulveda, L. A. Cisternas, and E. D. Gálvez, "Global sensitivity analysis of a mineral processing flowsheet," *Computer Aided Chemical Engineering*, vol. 32, pp. 913–918, 1 2013.
- [300] F. Campolongo, J. Cariboni, and A. Saltelli, "An effective screening design for sensitivity analysis of large models," *Environmental Modelling Software*, vol. 22, pp. 1509–1518, 10 2007.
- [301] P. Wate and V. Coors, "3D data models for urban energy simulation," *Energy Procedia*, vol. 78, no. 0, pp. 3372–3377, 2015. [Online]. Available: <http://dx.doi.org/10.1016/j.egypro.2015.11.753>
- [302] Y. J. Kim, "Comparative study of surrogate models for uncertainty quantification of building energy model: Gaussian Process Emulator vs. Polynomial Chaos Expansion," *Energy and Buildings*, vol. 133, pp. 46–58, 2016. [Online]. Available: <http://dx.doi.org/10.1016/j.enbuild.2016.09.032>
- [303] A. N. Aijazi and L. R. Glicksman, "Comparison of regression techniques for surrogate models of building energy performance," *ASHRAE and IBPSA-USA SimBuild 2016 - Building Performance*

- Modeling Conference*, pp. 327–334, 2016. [Online]. Available: <https://www.ashrae.org/FileLibrary/docLib/Events/Simbuild2016/Papers/C043.pdf>
- [304] P. Westermann and R. Evins, “Surrogate modelling for sustainable building design – a review,” *Energy and Buildings*, vol. 198, pp. 170–186, 9 2019.
- [305] Q. Li, L. Gu, G. Augenbroe, C. F. Jeff Wu, and J. Brown, “Calibration of dynamic building energy models with multiple responses using Bayesian inference and linear regression models,” *Energy Procedia*, vol. 78, pp. 979–984, 2015.
- [306] S. L. Wong, K. K. Wan, and T. N. Lam, “Artificial neural networks for energy analysis of office buildings with daylighting,” *Applied Energy*, vol. 87, no. 2, pp. 551–557, 2010.
- [307] S. Singaravel, J. Suykens, and P. Geyer, “Deep-learning neural-network architectures and methods: Using component-based models in building-design energy prediction,” *Advanced Engineering Informatics*, vol. 38, pp. 81–90, 2018.
- [308] S. Chen, D. Friedrich, Z. Yu, and J. Yu, “District heating network demand prediction using a physics-based energy model with a bayesian approach for parameter calibration,” *Energies*, vol. 12, no. 18, p. 3408, 2019.
- [309] Y. J. Kim and C. S. Park, “Stepwise deterministic and stochastic calibration of an energy simulation model for an existing building,” *Energy and Buildings*, vol. 133, pp. 455–468, 2016. [Online]. Available: <http://dx.doi.org/10.1016/j.enbuild.2016.10.009>
- [310] M. Manfren, N. Aste, and R. Moshksar, “Calibration and uncertainty analysis for computer models - A meta-model based approach for integrated building energy simulation,” *Applied Energy*, vol. 103, pp. 627–641, 2013. [Online]. Available: <http://dx.doi.org/10.1016/j.apenergy.2012.10.031>
- [311] B. Eisenhower, Z. O’Neill, S. Narayanan, V. A. Fonoberov, and I. Mezić, “A methodology for meta-model based optimization in building energy models,” *Energy and Buildings*, vol. 47, pp. 292–301, 2012.
- [312] W. Tian, J. Song, Z. Li, and P. de Wilde, “Bootstrap techniques for sensitivity analysis and model selection in building thermal performance analysis,” *Applied Energy*, vol. 135, pp. 320–328, 2014.
- [313] E. Schulz, M. Speekenbrink, and A. Krause, “A tutorial on Gaussian process regression: Modelling, exploring, and exploiting functions,” *Journal of Mathematical Psychology*, vol. 85, pp. 1–16, 2018. [Online]. Available: <https://doi.org/10.1016/j.jmp.2018.03.001>
- [314] S. Myren and E. Lawrence, “A comparison of gaussian processes and neural networks for computer model emulation and calibration,” *Statistical Analysis and Data Mining*, vol. 14, 2021.

- [315] C. K. I. Williams, "Prediction with gaussian processes: From linear regression to linear prediction and beyond," 1998.
- [316] C. E. Rasmussen and C. K. I. Williams, *Gaussian Processes for Machine Learning*. The MIT Press, 12 2005.
- [317] J. L. Loepky, J. Sacks, and W. J. Welch, "Choosing the sample size of a computer experiment: A practical guide," *Technometrics*, 2009.
- [318] L. Brackney, A. Parker, D. Macumber, and K. Benne, *Building energy modeling with OpenStudio*. Springer, 2018.
- [319] US Department of Energy, "Running the ep-macro program: Auxiliary programs — energyplus 8.2," 2021. [Online]. Available: <https://bigladdersoftware.com/epx/docs/8-2/auxiliary-programs/running-the-ep-macro-program.html>
- [320] Python software foundation, "Welcome to python.org," 2022. [Online]. Available: <https://www.python.org/>
- [321] J. Herman and W. Usher, "Salib: An open-source python library for sensitivity analysis," *The Journal of Open Source Software*, vol. 2, 2017.
- [322] B. Carpenter, A. Gelman, M. D. Hoffman, D. Lee, B. Goodrich, M. Betancourt, M. A. Brubaker, J. Guo, P. Li, and A. Riddell, "Stan: A probabilistic programming language," *Journal of Statistical Software*, vol. 76, 2017.
- [323] J. Curtis and A. Pentecost, "Household fuel expenditure and residential building energy efficiency ratings in Ireland," *Energy Policy*, vol. 76, pp. 57–65, 2015. [Online]. Available: <https://www.sciencedirect.com/science/article/abs/pii/S0301421514005540>
- [324] ASHRAE, *ASHRAE Handbook 2016 - HVAC Systems and Equipment : SI Edition*, 2016.
- [325] D. Oughton and A. Wilson, *Faber & Kell's Heating & Air-Conditioning of Buildings*, 11th ed., AECOM, Ed. Routledge, 2015. [Online]. Available: <https://www.routledge.com/Faber--Kells-Heating-and-Air-Conditioning-of-Buildings/Oughton-Oughton-Hodkinson-Hodkinson-Brailsford/p/book/9780415522656>
- [326] BSI, "BS ISO 13612: Heating and cooling systems in buildings - Method for calculation of the system performance and system design for heat pump systems," 2014.
- [327] CEN/CENELEC, "EN 12831-1 Energy performance of buildings - Method for calculation of the design heat load - Part 1: Space heating load, Module M3-3," 2017.

- [328] CIBSE, *Guide G: Public health and plumbing engineering*. London: CIBSE, 2014. [Online]. Available: <https://www.cibse.org/knowledge-research/knowledge-portal/guide-g-public-health-and-plumbing-engineering-2014>
- [329] DesignBuilder, “DesignBuilder Help - Zone Multiplier.” [Online]. Available: <https://designbuilder.co.uk/helpv7.0/{#}ZoneMultiplier.htm?Highlight=zonemultiplier>
- [330] U.S. Department of Energy, “Commercial Reference Buildings | Department of Energy.” [Online]. Available: <https://www.energy.gov/eere/buildings/commercial-reference-buildings>
- [331] CIBSE, *CIBSE Guide A: Environmental Design*, 8th ed., K. J. Butcher and B. Craig, Eds. London: The Chartered Institution of Building Services Engineers (CIBSE), 2015.
- [332] CEN, “EN 16798-1 Energy performance of buildings - Ventilation for buildings - Part 1: Indoor environmental input parameters for design and assessment of energy performance of buildings addressing indoor air quality, thermal environment, lighting and acoustics-,” Brussels, Belgium, 2019.
- [333] Engineering Toolbox, “Air Change Rates in typical Rooms and Buildings.” [Online]. Available: https://www.engineeringtoolbox.com/air-change-rate-room-d_{_}867.html
- [334] ASHRAE, *ASHRAE Handbook Fundamentals 2021, SI Edition*, H. E. Kennedy, Ed. Atlanta: ASHRAE, 2021.
- [335] D. Higdon, M. Kennedy, J. C. Cavendish, J. A. Cafeo, and R. D. Ryne, “Combining Field Data and Computer Simulations for Calibration and Prediction,” *SIAM Journal on Scientific Computing*, 2004.
- [336] A. Chong and K. Poh Lam, “A Comparison of MCMC Algorithms for the Bayesian Calibration of Building Energy Models,” *15th IBPSA Conference*, pp. 494–503, 2017.
- [337] S. Geman and D. Geman, “Stochastic relaxation, gibbs distributions, and the bayesian restoration of images,” *IEEE Transactions on Pattern Analysis and Machine Intelligence*, vol. PAMI-6, 1984.
- [338] Stan Development team, “Stan User’s Guide version 2.29,” 2019. [Online]. Available: https://mc-stan.org/docs/2_{_}29/stan-users-guide/index.html
- [339] A. Vehtari, A. Gelman, D. Simpson, B. Carpenter, and P.-C. Bürkner, “Rank-normalization, folding, and localization: An improved r for assessing convergence of mcmc (with discussion),” *Bayesian Analysis*, vol. 16, p. 667 – 718, 2021. [Online]. Available: <https://doi.org/10.1214/20-BA1221>
- [340] O. Martin, *Bayesian Analysis with Python: Introduction to statistical modeling and probabilistic programming using PyMC3 and ArviZ*. Packt Publishing Ltd, 2018.

- [341] —, *Bayesian analysis with Python : Unleash the power and flexibility of the Bayesian framework*, 1st ed. Packt Publishing, 2016. [Online]. Available: <https://books.google.com.mt/books/about/Bayesian{ }Analysis{ }with{ }Python.html?id=HhMBvgAACAAJ{&}redir{ }esc=y>
- [342] M. Clark, “Bayesian basics,” 2022. [Online]. Available: <https://m-clark.github.io/bayesian-basics/>
- [343] A. Gelman, “Two simple examples for understanding posterior p-values whose distributions are far from uniform,” *Electronic Journal of Statistics*, vol. 7, 2013.
- [344] J. Granderson, S. Touzani, C. Custodio, M. Sohn, and S. Fernandes, “Assessment of automated measurement and verification (mv) methods,” 7 2015. [Online]. Available: <https://www.osti.gov/servlets/purl/1236174>
- [345] European Commission, “Commission delegated regulation (EU) No 244/2012 of 16 January 2012 supplementing Directive 2010/31/EU of the European Parliament and of the Council on the energy performance of buildings by establishing a comparative methodology framework for calculating,” European Commission, Tech. Rep., 2012. [Online]. Available: <https://eur-lex.europa.eu/legal-content/EN/TXT/?uri=CELEX{%}3A32012R0244>
- [346] Ministry for Resources and Rural Affairs, “SBEMmt: Simplified Building Energy Model for Malta,” Malta, 2012.
- [347] L. Sunderland and M. Santini, “Filling the policy gap: Minimum energy performance standards for european buildings - regulatory assistance project,” 6 2020. [Online]. Available: <https://www.raponline.org/knowledge-center/filling-the-policy-gap-minimum-energy-performance-standards-for-european-buildings/>
- [348] Department for Business, Energy Industrial Strategy, “Non-domestic private rented sector minimum energy efficiency standards: Epc b implementation,” 2021. [Online]. Available: <https://www.gov.uk/government/consultations/non-domestic-private-rented-sector-minimum-energy-efficiency-standards-epc-b-implementation>
- [349] The MaTrID project, “INTEGRATED DESIGN Market transformation towards nearly zero energy buildings through widespread use of integrated energy design.” [Online]. Available: <http://www.integrateddesign.eu/about/index.php>
- [350] A. Athienitis and W. O’Brien, Eds., *Modeling, design, and optimization of net-zero energy buildings*, 1st ed. Ernst & Sohn - A Wiley Brand, 2015. [Online]. Available: <https://onlinelibrary.wiley.com/doi/book/10.1002/9783433604625>
- [351] M. Waskom, “seaborn.jointplot — seaborn 0.11.2 documentation.” [Online]. Available: <https://seaborn.pydata.org/generated/seaborn.jointplot.html>

- [352] M.Waskom, "seaborn.jointgrid — seaborn 0.11.2 documentation." [Online]. Available: <https://seaborn.pydata.org/generated/seaborn.JointGrid.html>
- [353] Y. Holtz, "Marginal distribution with ggplot2 and ggextra – the r graph gallery," 2018. [Online]. Available: <https://r-graph-gallery.com/277-marginal-histogram-for-ggplot2.html>
- [354] A. Fertis, M. Baes, and H. J. Lüthi, "Robust risk management," *European Journal of Operational Research*, vol. 222, 2012.
- [355] D. Makowski, M. Ben-Shachar, and D. Lüdecke, "bayestestr: Describing effects and their uncertainty, existence and significance within the bayesian framework," *Journal of Open Source Software*, vol. 4, 2019.
- [356] ISO, "ISO 52016-1 Energy performance of buildings — Energy needs for heating and cooling, internal temperatures and sensible and latent heat loads — Part 1: Calculation procedures," vol. 2017, 2017.
- [357] "Malta bank lending rate, 1999 – 2022 | ceic data," 2021. [Online]. Available: <https://www.ceicdata.com/en/indicator/malta/bank-lending-rate>
- [358] European Commission, "Regulation (eu) no 1303/2013 of the european parliament and of the council of 17 december 2013 laying down common provisions on the european regional development fund, the european social fund, the cohesion fund, the european agricultural fund for rural development and the european maritime and fisheries fund and laying down general provisions on the european regional development fund, the european social fund, the cohesion fund and the european maritime and fisheries fund and repealing council regulation (ec) no 1083/2006," 3 2014. [Online]. Available: <https://eur-lex.europa.eu/legal-content/EN/TXT/?uri=CELEX%3A32014R0480>
- [359] D. Sartori, G. Catalano, M. Genco, C. Pancotti, E. Sirtori, S. Vignetti, and C. D. Bo, "Guide to cost-benefit analysis of investment projects for cohesion policy 2014-2020 - regional policy - european commission," 12 2014. [Online]. Available: https://ec.europa.eu/regional_policy/en/information/publications/guides/2014/guide-to-cost-benefit-analysis-of-investment-projects-for-cohesion-policy-2014-2020
- [360] Eurostat, "Electricity price statistics - statistics explained," 4 2022. [Online]. Available: https://ec.europa.eu/eurostat/statistics-explained/index.php?title=Electricity_price_statistics#Electricity_prices_for_non-household_consumers
- [361] European Environment Agency, "Transport fuel prices and taxes in europe — european environment agency," 2021. [Online]. Available: <https://www.eea.europa.eu/data-and-maps/indicators/fuel-prices-and-taxes/assessment-4>
- [362] "Eu carbon permits - 2022 data - 2005-2021 historical - 2023 forecast - price - quote," 2022. [Online]. Available: <https://tradingeconomics.com/commodity/carbon>

- [363] L. Mantzos, T. Wiesenthal, F. Neuwahl, and M. Rózsai, "The potential. central scenario. an eu energy outlook to 2050," 2019. [Online]. Available: <https://publications.jrc.ec.europa.eu/repository/handle/JRC118353#:~:text=This%20report%20describes%20the%20evolution,beyond%20the%20end%20of%202017>.
- [364] "Carbon emissions futures price - investing.com," 2022. [Online]. Available: <https://www.investing.com/commodities/carbon-emissions>
- [365] European Commission and Directorate-General for Energy, *Comprehensive study of building energy renovation activities and the uptake of nearly zero-energy buildings in the EU : final report*. Publications Office, 2019. [Online]. Available: <https://data.europa.eu/doi/10.2833/14675>
- [366] J. Lilliestam, M. Melliger, L. Ollier, T. S. Schmidt, and B. Steffen, "Understanding and accounting for the effect of exchange rate fluctuations on global learning rates," *Nature Energy*, vol. 5, 2020.
- [367] European Commission, "Commission Regulation (EU) 2016/2281 of 30 November 2016 implementing Directive 2009/125/EC of the European Parliament and of the Council establishing a framework for the setting of ecodesign requirements for energy-related products, with regard to ecodes," *Official Journal of the European Union*, vol. L, no. 346, pp. 1–50, 2016.
- [368] M. Bartolo, "Pushing the limits of applying energy efficiency measures to Maltese non-residential buildings," 2017. [Online]. Available: <https://www.um.edu.mt/library/oar//handle/123456789/27383>
- [369] M. Mallia and O. Prizeman, "Energy performance certification: Is the software currently used in malta suitable for the energy assessment of its historic buildings?" in *The 3rd International Conference on Energy Efficiency in Historic Buildings (EEHB2018), Visby, Sweden, September 26th to 27th, 2018*. Uppsala University, 2018, pp. 264–273.
- [370] EU Commission, "Proposal for a directive of the european parliament and of the council on the energy performance of buildings (recast) com/2021/802 final," 12 2021. [Online]. Available: <https://eur-lex.europa.eu/legal-content/EN/TXT/?uri=celex%3A52021PC0802>
- [371] D. Granados-López, D. Gatt, C. Yousif, M. Díez-Mediavilla, and C. Alonso-Tristán, "Exploitation of indoor illumination for typical flat dwellings in the mediterranean area," *Energy Reports*, vol. 9, pp. 1473–1489, 2023.
- [372] ASHRAE, "Energy estimating and modelling methods," in *ASHRAE Handbook-Fundamentals*, 2021, ch. 19.

Index

- Archetypes, 17
- Bayesian calibration
 - Computational expense, 91
 - Computationally efficiency improvement, 42
 - Computer model calibration, 123–124
 - Concept, 32–33
 - Diagnostic and posterior analysis, 123
 - Diagnostics and posterior analysis, 33–35, 129, 142
 - Hotel RB case study, 123–146
 - Kennedy and O’Hagan (KOH) framework, 32, 92
 - Limitations, 42–46
 - Positive attributes, 38–42
 - Stan probabilistic programming language, 98, 123, 124, 129, 131, 142, 144
 - Validation, 35, 131–134, 144–146
 - versus *frequentist*’ approaches, 38
- Building stock energy modelling, 202
 - Approaches, 13–15
 - Bottom-up approach, 13
 - Top-down approach, 13
- Clustering, 18, 60
 - Hierarchical Clustering (AHC), 59, 76
 - K-means, 59, 76
 - k-modes, 59
 - k-prototypes, 59, 76
- Coefficient of the Variation of the Root Mean Square Error (CVRMSE), 35, 114, 131, 144, 166
- Conclusion, 195–207
 - Achieved aim and objectives, 195
 - Findings, 195
 - Future research recommendations, 204
 - Research contribution, 200
 - Research limitations, 203
 - Research value, 200
- Data dimension reduction
 - Factor Analysis of Mixed Data (FAMD), 58
 - Multiple Correspondence Analysis (MCA), 58
 - Principal Component Analysis (PCA), 58
 - Stepwise Regression, 60, 81

- Defining RBs approach
 - Data Collection and Classification phase, 54
 - Data post-processing phase, 60
 - Data processing phase, 57
 - Data processing phase - Feature explanatory variables dimension reduction, 58
 - Data processing phase - Feature optimal clustering solution, 59
 - Data processing phase - Model reduction, 60
 - Data processing phase - Multiple clustering solutions, 59
 - Data processing phase - Regression, 60
- Degree Days modelling, 173
- DesignBuilder software, 98, 99, 103
- Deterministic financial risk, 156
- Diagnostics and posterior analysis
 - Effective Sample Size (ESS), 129, 142
 - Monte Carlo Standard Error (MCSE), 129, 142
 - Parallel plots, 129, 142
 - R-hat statistic, 129, 142
 - Trace plots, 129, 142
- Effective Sample Size (ESS), 129, 142
- Energy conservation measures
 - Hotel RB case study, 167
- Energy Performance Certificates (EPCs), 17
- Energy Performance gap, 2, 22, 152, 174, 188, 194, 206
- Energy Policy making, 2, 10, 97, 152, 155, 159, 160, 162, 194, 195, 200
- Energy Policy measures, 2, 10, 97, 152, 155, 159, 160, 162, 194, 195, 200
- EnergyPlus software, 19, 98, 99, 103, 172
- EPBD 2018 objectives, 39–42
- EPBD cost-optimal method
 - UBEM comparison, 15
 - Cost-optimal plot, 12
 - Handling of uncertainties, 25–29
 - Methodology, 11
 - Policy Uncertainties, 22–24
 - Proposed method update, 29–37
 - Proposed method update flow-chart, 29
 - Risk Analysis, 37
 - Cost-optimal analysis plots, 153
 - Global LCC analysis, 36, 151, 153, 159, 167, 168, 178
 - NZEB EP benchmarking, 36, 151, 175
 - Probabilistic risk analysis, 151, 159, 178
 - Proposed approach versus asset rating NCM methodology, 187–193
 - Proposed NZEB EP benchmarking and risk analysis framework, 153–163
 - Proposed NZEB EP benchmarking and risk analysis framework case study, 163–186
 - Proposed NZEB EP benchmarking and risk analysis framework flowchart, 153
 - Proposed NZEB EP benchmarking approach, 153–159
 - Proposed NZEB EP benchmarking case study, 167–178
 - Proposed probabilistic risk analysis approach, 159–163

- Proposed Risk analysis case study, 178–183
- Risk analysis, 151, 159, 178
- Uncertainties, 22–24
- Factor Analysis of Mixed Data (FAMD), 58, 76
- Gaussian Process Emulator (GPE), 43
 - Introduction, 92
 - RB case study application, 135–136
- Geographic Information system (GIS), 149
- Global LCC analysis, 36, 151, 153, 159, 167, 168, 178
 - Calculation, 153
 - Discount Rate, 151, 153, 159, 167, 168, 178
 - EN 15459, 153, 159, 168, 178
 - Financial perspective, 151, 153, 159, 167, 168, 178
 - Macroeconomic perspective, 151, 153, 159, 167, 168
 - Price Development, 151, 153, 159, 167, 168, 178
 - Sensitivity analysis, 151, 153, 159, 167, 168
- Global LCC risk analysis, 37, 151, 159, 178
- Green Deal objectives, 39–42
- Heterogeneous building stocks, 50
 - EP RB modelling challenges, 51
 - EP analysis challenges, 51
 - Machine Learning data processing challenges to define RBs , 52
 - Studying EP, 50
 - Data processing challenges, 69
 - Defining RBs, 54
 - Defining RBs approach, 54–60
 - Defining RBs approach Flow chart, 54
 - Hierarchical Clustering (AHC), 59, 76
 - Highest Density Interval (HDI), 160
 - Hotel building stock RBs development case study, 63–86
 - Clustering, 76, 82
 - Data collection and preparation, 65
 - Data post-processing, 82
 - Data processing, 69
 - Data reduction, 69, 82
 - Defining RBs flow-chart, 64
 - Final clustering solution, 82
 - Regression, 79
 - Introduction, 1–8
 - Aim and Objectives, 4
 - Background to the research work, 1
 - Dissertation Organisation, 6
 - Research questions, 5
 - Study Significance, 5
 - JEPlus parametric tool, 98, 136, 164, 172, 178
 - K-means clustering, 59, 76
 - k-modes clustering, 59, 76
 - k-prototypes clustering, 59, 76
 - Kennedy and O’Hagan (KOH) framework, 32, 92
 - Life-cycle costs analysis, 151, 153, 159, 167, 168, 178
 - Literature review, 8–48
 - Machine Learning
 - Data processing challenges to define RBs, 52

- Techniques to define RBs, 52
- Meta-models, 21, 43
 - Bayesian Linear Regression, 124
 - Gaussian Process Emulator (GPE), 43, 92, 135
 - Multiple Linear Regression (MLR), 43
- Model dimension reduction, 80
- Monte Carlo Standard Error (MCSE), 129, 142
- Morris Method, 31, 91, 119
- Multi-functional heterogeneous building stocks EP, 50
- Multiple Correspondence Analysis (MCA), 58, 79
- Multiple Linear Regression (MLR), 43, 79, 81
- National Calculation Methodology (NCM), 151, 187
- No-U-Turn Sampler (NUTS), 43, 123
- Normalised Mean Bias Error (NMBE), 35, 114, 131, 144, 166
- NZEB EP benchmarking, 36, 151
 - Ambition levels, 155, 175
 - Hotel RB case study, 167–178
 - Proposed approach, 153–159
 - Visualisation, 157, 175
- NZEB EP benchmarking and risk analysis framework
 - Concept, 153–163
 - Hotel RB case study, 163–186
- Parallel plots, 129, 142
- Predicting RBs EP
 - Dynamic calculations, 19
 - Emulator, 19
 - Hybrid calculations, 19
 - Meta-model, 19
 - Quasi-steady state calculations, 19
- Principal Component Analysis (PCA), 19, 58
- Probabilistic risk analysis
 - EPBD cost-optimal method, 151, 159, 178
 - Highest Density Interval(HDI), 160
 - Hotel RB case study, 178–183
 - Joint plot visualisation, 160
 - Proposed approach, 159–163
 - Robust financial risk calculation, 162
- Python
 - Arviz package, 123, 129, 142
 - Global LCC calculation, 172
 - Risk analysis, 178
 - Sensitivity Analysis Library in Python (SALIB), 98
 - Stan probabilistic programming language, 98, 123
- R-hat statistic, 129, 142
- Reference Buildings (RBs), 15
 - Hotel Probabilistic DHW model, 99
 - Hotel Probabilistic electricity end-uses model, 103
 - Machine learning techniques, 52
 - Parameter uncertainties, 24
 - Technical uncertainties, 24
 - Aggregating RBs EP, 21–22
 - Bayesian calibration, 32
 - Bayesian calibration Diagnostics and analysis, 33
 - Bayesian calibration diagnostics and analysis, 35
 - Bayesian calibration validation, 35
 - Characterisation approaches, 17

- Clustering, 18, 59
- Clustering hotels case study, 76
- Computationally efficiency improvement, 42, 94
- Data dimension reduction, 58
- Defining RBs, 15
- Geographic Information System (GIS), 21
- Heterogeneous building stocks, 54
- Hotel probabilistic RB case study, 98–146
- Hotels case study, 61
- Model dimension reduction, 59
- Predicting RBs EP, 19–21
- Principal Component Analysis (PCA), 19
- Probabilistic RBs, 29, 32
- Probabilistic RBs versus deterministic RBs, 30
- Regression, 19, 60
- Sensitivity Analysis, 31
- Reference Zone approach
 - Application to benchmarking framework, 163–166
 - Concept, 94–97
 - Introduction, 45
 - case study statistical validation, 114
 - Hotel DHW model, 99
 - Hotel electricity end-uses model, 103
- Reference zone approach
 - case study statistical validation, 115
- Regression, 19, 60, 79
 - Degree Days modelling, 173
- Risk analysis
 - Deterministic and robust financial risk comparison, 183–186
 - Deterministic financial risk, 156
 - EPBD cost-optimal method, 151, 159, 178
 - Probabilistic financial risk, 159, 178
 - Robust financial risk calculation, 160
- SBEM-mt, 187
- SBEM-mt software, 151
- Sensitivity Analysis, 31, 91
 - Hotel RB case study, 119–122
 - Computational expense, 91
 - Morris Method, 31, 91, 119
 - Sensitivity Analysis Library in Python (SALIB), 98, 119
- Smartness Indicator, 42
- Stan probabilistic programming language, 98, 123, 124, 129, 131, 142, 144
- Trace plots, 129, 142
- Uncertainties in EPBD and UBEM, 22–24
- Urban Building Energy Modelling (UBEM), 13–46
 - EPBD cost-optimal method comparison, 15